SÃO PAULO STATE UNIVERSITY "JÚLIO DE MESQUITA FILHO"

FACULTY OF PHARMACEUTICAL SCIENCES

and

UNIVERSITY OF AVEIRO

DEPARTMENT OF CHEMISTRY

CASSAMO USSEMANE MUSSAGY

Production of carotenoids by yeast *Rhodotorula glutinis* CCT-2186 and their extraction using alternative solvents

Thesis submitted for the degree of **Doctor of Philosophy**

São Paulo/Aveiro

2021

CASSAMO USSEMANE MUSSAGY

Production of carotenoids by yeast *Rhodotorula glutinis* CCT-2186 and their extraction using alternative solvents

Thesis carried out under “Joint PhD” agreement, presented to the Postgraduate Program in Biosciences and Biotechnology Applied to Pharmacy, Faculty of Pharmaceutical Sciences - UNESP (Brazil) as part of the requirements for the degree of **Doctor in Biosciences and Biotechnology Applied to Pharmacy** and Department of Chemistry - UA (Portugal) for the degree of **Doctor in Chemical Engineering**.

Supervisors: Prof. Dr. Jorge Fernando Brandão Pereira

Prof. Dr. João Araújo Pereira Coutinho

São Paulo/Aveiro

2021

CASSAMO USSEMANE MUSSAGY

Produção de carotenoides pela levedura *Rhodotorula glutinis* CCT-2186 e sua extração empregando solventes alternativos

Tese em regime de cotutela, apresentada ao Programa de Pós-Graduação em Biociências e Biotecnologia aplicadas à Farmácia da Universidade Estadual Paulista "Júlio De Mesquita Filho" para obtenção do grau de **Doutor em Biociências e Biotecnologia Aplicadas á Farmácia** e ao Departamento de Química da Universidade de Aveiro para à obtenção do grau de **Doutor em Engenharia Química**.

Orientadores: Prof. Dr. Jorge Fernando Brandão Pereira

Prof. Dr. João Araújo Pereira Coutinho

São Paulo/Aveiro

2021

Mussagy, Cassamo Ussemane.

M989p Produção de carotenoides pela levedura Rhodotorula glutinis CCT-2186 e sua extração empregando solventes alternativos = Production of carotenoids by yeast Rhodotorula glutinis CCT-2186 and their extraction using alternative solvents / Cassamo Ussemane Mussagy. – Araraquara; Aveiro: [S.n.], 2021.

IX, 298 f. : il.

Tese (Doutorado com dupla titulação) – Unesp, Faculdade de Ciências Farmacêuticas. Programa de Pós Graduação em Biociências e Biotecnologia Aplicadas à Farmácia.

Orientador: Jorge Fernando Brandão Pereira (Brasil)

Tese (Doutorado em Engenharia Química) Universidade de Aveiro, Departamento de Química.

Orientador: João Araújo Pereira Coutinho, Aveiro (Portugal).

1. *Rhodotorula glutinis*. 2. Carotenoides. 3. Lipídios. 4. Líquidos Iônicos. 5. Bio-solventes. 6. Produção. 7. Extração. I. Pereira, Jorge Fernando Brandão, orient. II. Coutinho, João Araújo Pereira, coorient. III. Título.

Diretoria do Serviço Técnico de Biblioteca e Documentação - Faculdade de Ciências Farmacêuticas
UNESP - Campus de Araraquara

CAPES: 33004030081P7

Esta ficha não pode ser modificada

UNIVERSIDADE ESTADUAL PAULISTA

Câmpus de Araraquara

CERTIFICADO DE APROVAÇÃO

TÍTULO DA TESE: Produção de carotenoides pela levedura Rhodotorula glutinis CCT-2186 e sua extração empregando solventes alternativos

AUTOR: CASSAMO USSEMANE MUSSAGY
ORIENTADOR: JORGE FERNANDO BRANDÃO PEREIRA

Aprovado como parte das exigências para obtenção do Título de Doutor em BIOCIÊNCIAS E BIOTECNOLOGIA APLICADAS À FARMÁCIA, área: Análises Clínicas pela Comissão Examinadora:

Prof. Dr. JORGE FERNANDO BRANDÃO PEREIRA (Participaçao Virtual)
Departamento de Engenharia Química / Faculdade de Ciências e Tecnologia, Universidade de Coimbra

Prof. Dr. JOÃO MANUEL DA COSTA E ARAÚJO PEREIRA COUTINHO (Participaçao Virtual)
Departamento de Química / Universidade de Aveiro

Profa. Dra. VALÉRIA DE CARVALHO SANTOS EBINUMA (Participaçao Virtual)
Departamento de Engenharia de Bioprocessos e Biotecnologia / Faculdade de Ciências Farmacêuticas - UNESP - Araraquara

Prof. Dr. MARCOS ROGÉRIO MAFRA (Participaçao Virtual)
Departamento de Engenharia Química / Universidade Federal do Paraná

Profa. Dra. LUCÍLIA MARIA ALVES RIBEIRO DOMINGUES (Participaçao Virtual)
Departamento de Engenharia Biológica / Universidade do Minho

Prof. Dr. PEDRO JORGE MARQUES DE CARVALHO (Participaçao Virtual)
Departamento de Química / Universidade de Aveiro

Araraquara, 21 de janeiro de 2021

Assinado por : **JORGE FERNANDO BRANDÃO PEREIRA**
Num. de Identificação: BI127371052

بسم الله الرحمن الرحيم

To: ***Kylie Glory Mussagy****…*

Acknowledgments

Firstly, I thank Allah for having provided me all the circumstances for carrying out this work and for placed people in my way who direct and indirectly assisted me during this period. I would like to express my deep gratitude to Professor Jorge F. B. Pereira and Professor João A. P. Coutinho, my research supervisors, for their patient guidance, enthusiastic encouragement and useful critiques to perform and improve the research work. I would also like to thank Valéria C. Santos Ebinuma, for her co-supervision and valuable suggestions during the planning and development of this research work. I would like to express my very great appreciation to the colleagues from UNESP-Brazil and Path Group-Portugal. To all the friendship I've made at Brazil and Portugal. The technicians from UNESP and UA laboratories. I am particularly grateful for the assistance given by Prof. Dr. Nivaldo Boralle from Chemistry Institute (UNESP) (allowed me to carry out NMR analyses), Kiki Kurnia (Indonesia) for COSMO-RS analyses, Fabiane Farias and Marcos Mafra from Federal University of Paraná (Brazil). I would like to thank the Brazilian financial agency CAPES-PRINT and Ministry of Science and Technology, High Education and Technical Vocational Training of Mozambique through the HEST Project-World Bank for financial support in Portugal and Brazil during the PhD.

Finally, my special thanks are extended to my family in Mozambique, to my wife and my daughter *Kylie Glory Mussagy* for all love, encouragement throughout my study, patience and support during my years of dedication during the PhD period and also because they accepted the challenge of trust me even during my absence and difficult moments.

To all who directly or indirectly contributed to this work: Thank you very much! Muito obrigado! Gracias! Merci beaucoup! Khanimambo!

Abstract

This thesis consists of the investigation and optimization of sustainable strategies to enhance carotenoids production from yeast *Rhodotorula glutinis* CCT- 2186 (*R. glutinis)* and their extraction by means of ionic liquids (ILs) and bio-based solvents. The interest on carotenoids such as β-carotene, torulene and torularhodin relies on the plethora of relevant properties of these products and their commercial value for food, feed, cosmetic and pharmaceutical industries. However, to make carotenoids more accessible in a sustainable way, their production from microbial sources is of paramount importance. Concerning the production of carotenoids from *R. glutinis* yeast there are still processual challenges, such as the improvement of production yields and development of efficient and sustainable extraction platforms. Initially, different statistical experimental designs were applied to improve carotenoids production and the best bioprocess was scaled-up to a 5 L stirred-tank bioreactor. Since the carotenoids are produced intracellularly, requiring appropriate cell-disrupting and extraction methodologies for their recovery, subsequently, the development of more benign and effective extraction/purification platforms was evaluated. A comprehensive study using aqueous solutions of ionic liquids (ILs) for solid-liquid extraction (SLE) processes was carried out, following the carotenoids purification using a three-phase partitioning system composed of aqueous solutions of ILs and inorganic salts. To gather additional information on the phase separation mechanisms, aqueous biphasic systems (ABS) composed of ILs and inorganic salts were determined and characterized. Afterward, the potential of bio-based solvents was evaluated, with the purpose of designing a more efficient and ecofriendly extraction process for recovery of the intracellular carotenoids from *R. glutinis*. In this study it was designed and optimized an integrated downstream platform using a ternary mixture of bio-based solvents (ethyl acetate/ethanol/water) with isolation and polishing of carotenoids as well as the recycling of the solvents. The overall sustainability of the proposed technology was assessed in terms of solvents recyclability and carotenoids polishing, and the environmental impact of the platform through a life cycle assessment (carbon footprint). This thesis demonstrates the importance of combined organic and inorganic nitrogen sources to supplement the nutritional media for cultivation of *R. glutinis* and production of carotenoids, and that ILs and mixed bio-based solvents can be used to design simple, efficient and sustainable platforms for the recovery of intracellular carotenoids from microbial biomass.

Keywords: *Rhodotorula glutinis*; carotenoids; lipids; ionic liquids, biosolvents; production; extraction.

Resumo

A crescente busca por produtos naturais e os desafios de sua produção industrial, tem motivado pesquisadores a investigar estratégias para o incremento da produção a partir de fontes microbianas e o desenvolvimento de procedimentos sustentáveis e eficientes para a sua extração. Os carotenoides naturais como o β-caroteno, toruleno e torularodina além de serem poderosos antioxidantes naturais, são corantes que vem merecendo destaque devido às suas propriedades biológicas com aplicações relevantes nas indústrias alimentar, cosmética e farmacêutica. No presente trabalho estudou-se um processo integrado que engloba o cultivo da levedura *Rhodotorula glutinis* CCT- 2186 (*R. glutinis*) para o incremento da produção de carotenoides e a extração destes produtos empregando líquidos iónicos (LIs) e bio-solventes como solventes alternativos. Inicialmente, diferentes planejamentos fatoriais foram aplicados para incrementar a produção de carotenoides e para a melhor condição foi realizado um aumento de escala em biorreator de 5 L. Posteriormente, estudos usando soluções aquosas de LIs em processos de extração sólido-líquido foram realizados, seguidos pelo processo de purificação empregando um sistema de partição trifásico composto por soluções aquosas de LIs e sais inorgânicos. Para reunir informações adicionais sobre os mecanismos de separação das fases, sistemas aquosos bifásicos (SAB) compostos por LIs e sais inorgânicos foram determinados e caracterizados. O potencial dos bio-solventes para a recuperação de carotenoides de células de *R. glutinis* foram também avaliados, a fim de se obter um processo de extração/purificação sustentável, mais eficiente e ecologicamente correto. Este último estudo permitiu a compreensão e otimização de uma abordagem *downstream* sustentável para a extração usando misturas ternárias (acetato de etilo/etanol/água) com posterior isolamento e polimento de carotenoides, e reciclagem dos solventes da mistura. A sustentabilidade geral da tecnologia proposta neste trabalho foi avaliada pelo impacto ambiental do processo alternativo em termos de avaliação do ciclo de vida (pegada de carbono). Esta tese revela que o uso combinado de fontes de nitrogênio orgânico e inorgânico é recomendado para a suplementação do meio de cultura para o cultivo de *R. glutinis* e que o uso de LIs e bio-solventes como agentes para o rompimento da parede celular pode ser um procedimento simples, eficiente, sustentável e viável para a recuperação de carotenoides intracelulares da biomassa microbiana.

Palavras-chave: *Rhodotorula glutinis*; carotenoides; lipídios, líquidos iônicos, bio-solventes, produção; extração.

Rights and permissions

The permissions to re-use texts, figures, and tables from previously published articles from the author were secured from:

Publisher: ***Springer Nature and Copyright Clearance Center***

- **Paper 1:** Mussagy CU, Winterburn J, Santos-Ebinuma VC, Pereira JFB (2019) Production and extraction of carotenoids produced by microorganisms, *Appl. Microbiol. Biotechnol.* 103 (3): 1095-1114. doi: 10.1007/s00253-018-9557-5*.*

License number 4920240850449 (Oct 01, 2020).

Publisher: ***American Chemical Society***

- **Paper 2:** Mussagy CU, Santos-Ebinuma VC, Gonzalez-Miquel M, Coutinho JAP, Pereira JFB (2019) Protic ionic liquids as cell-disrupting agents for the recovery of intracellular carotenoids from yeast *Rhodotorula glutinis* CCT-2186, *ACS Sustainable Chem. Eng* 7 (19): 16765-16776. doi: 10.1021/acssuschemeng.9b04247*.*

The author contacted Dr. Rhea M. Williams (Senior Managing Editor of ACS Sustainable Chemistry & Engineering) by e-mail, which granted written permission for use of the respective article.

Publisher: ***Royal Society of Chemistry***

- **Paper 3:** Mussagy CU, Santos-Ebinuma VC, Kurnia KA, Carvalho P, Dias ACR, Coutinho JAP, Pereira JFB (2020) Integrative platform for the selective recovery of intracellular carotenoids and lipids from *Rhodotorula glutinis* CCT-2186 yeast using mixtures of bio-based solvents. *Green Chem*. 22: 8478-8494. doi: 10.1039/D0GC02992K.

RSC have copyright policies that grant automatic permission for re-use the paper in your thesis if you are the author: (…) *you do not need to request permission to reuse your own figures, diagrams, etc, that were originally published in a RSC publication (…), permission should be requested for use of the whole article or chapter except if reusing it in a thesis (...).*

Publisher: *Elsevier*

- **Paper 4:** Mussagy CU, Tabanez NL, Farias FO, Kurnia KA, Mafra MR, Pereira JFB (2020) Determination, characterization and modeling of aqueous biphasic systems composed of propylammonium-based ionic liquids and phosphate salts, *Chem. Phys. Lett.* 754: 137623. doi: 10.1016/j.cplett.2020.137623.
- **Paper 5:** Mussagy CU, Guimarães AA, Rocha LV, Winterburn J, Santos-Ebinuma VC, Pereira JFB (2021), Improvement of carotenoid production from *Rhodotorula glutinis* CCT-2186, *Biochem. Eng. J*. 165: 107827. doi: 10.1016/j.bej.2020.107827.

Elsevier have copyright policies that grant automatic permission for re-use the paper in your thesis if you are the author: *(…) as the author of this Elsevier article, you retain the right to include it in a thesis or dissertation, provided it is not published commercially. Permission is not required, but please ensure that you reference the journal as the original source (…)*

Contents

Notation

List of symbols

%EE	Percentage of extraction efficiency
ΔG_{hyd}	Gibbs free energy of hydration
A	Merchuck correlation constant
B	Merchuck correlation constant
C	Merchuck correlation constant
G^E	Excess free Gibbs energy ($kJ.mol^{-1}$)
H_{VDW}	Van der Waals energy ($kJ.mol^{-1}$)
h^E	Excess enthalpy ($kJ.mol^{-1}$)
H_{HB}	Hydrogen bonding energy ($kJ.mol^{-1}$)
H_{MF}	Electrostatic - misfit energy ($kJ.mol^{-1}$)
K	Partition coefficient
K_{ow}	Octanol-water partition coefficient
pKa	Acid constant dissociation
T	Temperature (ºC, K)
δ	Root mean-square deviation
η	Dynamic viscosity (mPa.s)
λ_{max}	Maximum absorption
ρ	Density ($g.cm^{-3}$)
σ	Charge distribution

List of abbreviations

[BMIM][BF_4]	1-butyl-3-methylimidazolium tetrafluoroborate
[BMIM][PF_6]	1-butyl-3-methylimidazolium hexafluorophosphate
[DEAPA][Ac]	3-diethylamino propylammonium acetate
[DEAPA][But]	3-diethylamino-propylammonium butanoate
[DEAPA][Hex]	3-diethylamino-propylammonium hexanoate
[DEAPA][Pro]	3-diethylamino propylammonium propanoate
[DMAPA][Ac]	3-dimethylamino-1-propylammonium acetate
[DMAPA][But]	3-dimethylamino-1-propylammonium butanoate
[DMAPA][Hex]	3-dimethylamino-1-propylammonium hexanoate
[DMAPA][Pro]	3-dimethylamino-1-propylammonium propanoate
[Emim][DBP]	1-ethyl-3-methylimidazolium dibutyl-phosphate
$[Emim]^+$	1-ethyl-3-methylimidazolium
[PA][Ac]	Propylammonium acetate
[PA][But]	Propylammonium butanoate
[PA][Hex]	Propylammonium hexanoate
[PA][Pro]	Propylammonium propanoate
2-MeTHF	2-methyl tetrahydrofuran
AA	Arachidonic acid
ABS	Aqueous biphasic systems
Ac	Acetic acid
AILs	Aprotic ionic liquids
ANOVA	Analysis of variance
But	Butyric acid
CAGR	Compound annual growth rate
CH	Cyclohexane
CO_2	Carbon dioxide
EPA	Eicosapentaenoic acid
COSMO-RS	COnductor-like Screening MOdel for Real Solvent
DCW	Dry cell weight
DEAPA	3-diethylamino-propylamine
DES	Deep Eutectic Solvents

DHA	Docosohexaenoic acid
DMAPA	3-dimethylamino-1-propylamine
DMAPP	Dimethylallyl pyrophosphate
DMSO	Dimethyl sulfoxide
DNS	3,5-dinitrosalicylic acid
EAE	Enzyme-assisted extraction
EFSA	European Food Safety Authority
EtOAc	Ethyl acetate
EtOH	Ethanol
EU	European Union
FDA	Food and Drug Administration
FPP	C_{15}-farnesyl pyrophosphate
GGDP	C_{20}-geranylgeranyl diphosphate
GGPP	Geranylgeranyl pyrophosphate
GPP	C_{10}-geranyl pyrophosphate
H_2O	Water
Hex	Hexanoic acid
HPLC	High-performance liquid chromatography
HSPs	Hansen Solubility Parameters
IBA	3-indole butyric acid
ILs	Ionic liquids
IPA	Isopropanol
IPP	Isopentenyl pyrophosphate
KF	Karl Fischer
LLE	Liquid-liquid equilibria
LLE	Liquid-liquid extraction
MeOH	Methanol
MEP	2-C-methyl-D-erythritol-4-phosphate
MS	Mass spectrometry
MVA	Mevalonic acid
NMR	Nuclear magnetic resonance
NRTL	Non-Random Two-Liquid
OF	Objective function

PA	Propylamine
PILs	Protic ionic liquids
PLE	Pressurized liquid extraction
POME	Palm oil mill effluent
Pro	Propanoic acid
R. *glutinis*	*Rhodotorula glutinis* CCT-2186
RI	Resolution of identity standard
ROS	Reactive oxygen species
RP-HPLC	Reversed-phase high-performance liquid chromatography
SEM	Scanning electron microscopy
SFE	Supercritical fluid extraction
SLR	Solid-liquid ratio
STL	Slope of the tie-line
THF	Tetrahydrofuran
TLC	Thin-layer chromatography
TLs	Tie line
TLL	Tie-line length
TMS	Tetramethylsilane
TPP	Three-phase partitioning
TZVP	Triple- ζ valence polarized basis set
UAE	Ultrasound-assisted extraction
US	United States
VOCs	Volatile organic solvents
VVM	Air volume/medium volume/min
YPD	Yeast Extract-Peptone-Dextrose

List of figures

List of tables

1. MOTIVATION AND THESIS STRUCTURE

1.1 Motivation

Rhodotorula glutinis is capable to synthesize several industrial/commercial high-added value microbial carotenoids, such as β-carotene, torulene and torularhodin. The global market of carotenoids reached US$1.5 billion in 2017 with an expected market of US$2.0 billion by 2022. The growing consumer interest in “natural products”, due to the concerns with synthetic pigments, has made the microbial production of carotenoids more favorable and a sustainable alternative. Often, the production of microbial carotenoids using *R. glutinis* yeast cells uses nitrogen from inorganic sources. In fact, the cultivation conditions are essential to drive the metabolic pathways and maximize the production of carotenoids yields, being still necessary to optimize them, for example, by evaluating how the use of organic nitrogen sources can impact the carotenogenesis. In addition, since carotenoids are produced in the intracellular environment of *R. glutinis* yeast, the design of suitable cell-disruption technologies and integration with further downstream operation are crucial for their recovery in commercial purity requirements. Traditionally, *R. glutinis* yeasts are disrupted by the application of conventional methods using environmentally non-favorable volatile organic solvents (VOCs), which, despite of the high recovery yields of intracellular carotenoids, present health and environmental concerns. The commercial importance of the microbial carotenoids and their growing market, together with the need of sustainable, biocompatible, and optimized platform to obtain carotenoids from microbial sources motivated me to develop this Thesis and to accomplish all the objectives detailed below.

1.2 Objectives

The work done during my PhD aimed to increase the production of carotenoids, namely, β-carotene, torulene and torularhodin, from *R. glutinis* yeast and to design integrated downstream platforms for their recovery using ionic liquids (ILs) and bio-based solvents as environmentally-friendly and biocompatible alternatives.

To fulfill the main objective of the thesis, the following specific objectives have been proposed and successfully achieved:

- To improve the production of β-carotene, torulene and torularhodin using *R. glutinis* CCT 2186 yeast, by applying statistical optimization designs;

- To evaluate the capability of protic ionic liquids to disrupt (permeabilize) the cell wall of *R. glutinis* yeast cells and to increase the recovery of intracellular carotenoids;
- To determine and characterize new ternary phase diagrams of aqueous biphasic systems (ABS) composed of ILs and inorganic salts;
- To evaluate the use of bio-based solvents mixtures as alternative platforms to permeabilize *R. glutinis* yeast cells and to improve the selective recovery of β-carotene, torulene, torularhodin and lipids;
- To develop integrated and circular processes for the recovery and polishing of carotenoids and recycling of the solvents;
- To evaluate the environmental sustainability and impact of the integrated downstream platform.

1.3 Thesis Structure

To contextualize the work of this Thesis project, first, it is important to mention that this research was conducted under the cotutelle agreement between the São Paulo State University (UNESP) and University of Aveiro (UA), and for that reason, during the past four years I developed the experimental work in the two institutions, namely, 3 years at UNESP and 1 year at UA. The obtained results were already published in a significant amount of different international scientific journals, namely, one review and four original articles. Thus, this thesis is divided in five main chapters, each one corresponding to a different published manuscript. To elucidate the structure of this Thesis and the association with respective manuscripts a schematic representation is depicted in **Figure 1.1**.

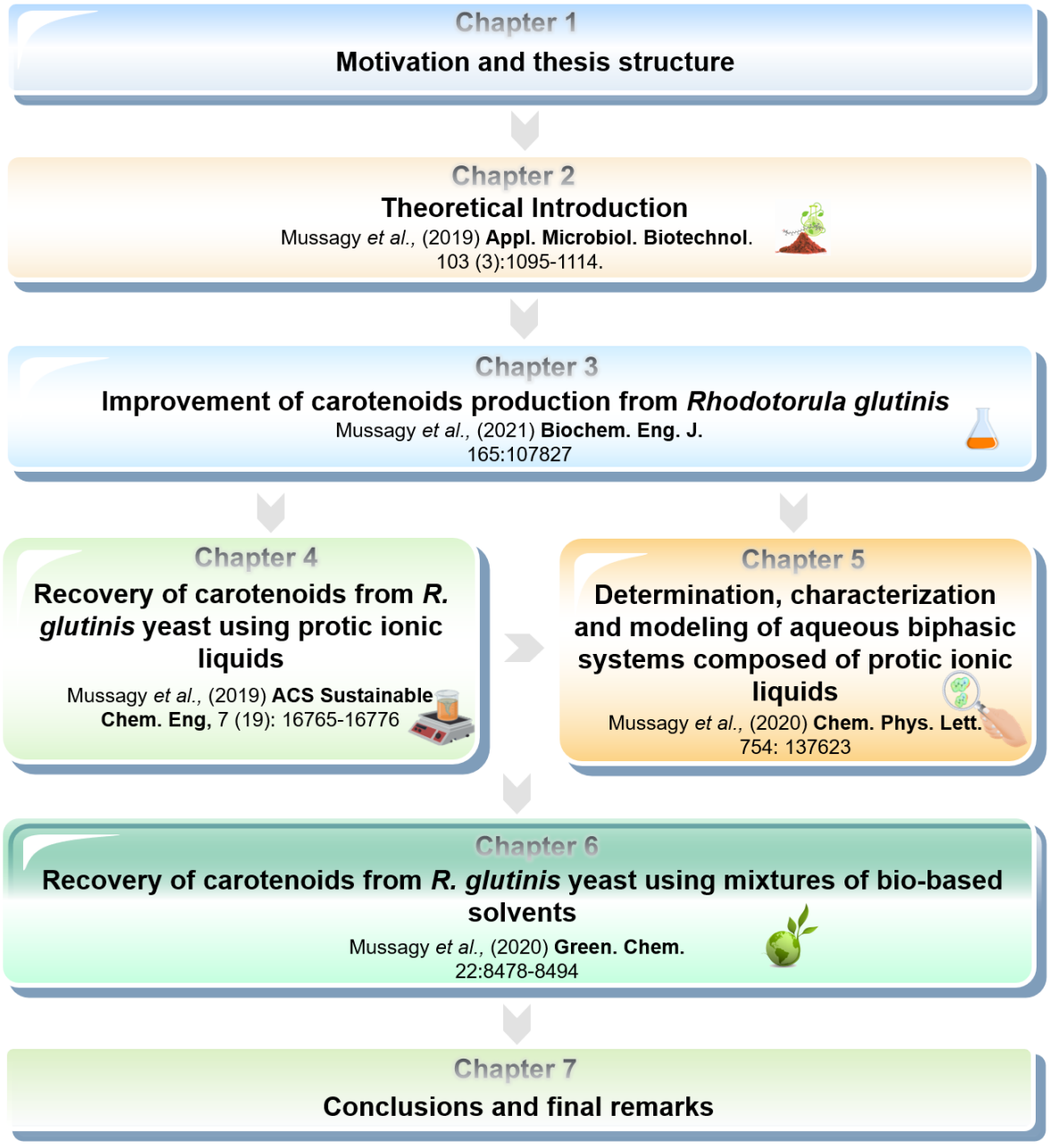

Figure 1.1. Schematic representation of the thesis structure, grouped by chapters and corresponding published manuscripts.

The **Chapter 2 - "Theoretical Introduction"** includes a brief explanation of the main scientific concepts behind the research purposes of this Thesis, followed by a comprehensive overview of the recent biotechnological developments in carotenoid production using microorganisms. A state-of-art of the hot topics in the field are properly addressed, from carotenoid biosynthesis to the current technologies involved in their extraction, and even highlighting the recent advances in the marketing and application of microbial carotenoids. The Chapter 2 is based on the critical review published in the ***Applied Microbiology and Biotechnology*** (Mussagy *et al.*, 2019, doi: 10.1007/s00253-018-9557-5).

After the general introduction, in the **Chapter 3 –** "**Improvement of carotenoids production from *Rhodotorula glutinis*"** the results on the optimization of carotenoid production are presented, in which a response surface methodology was applied to maximize the yield and productivity of carotenoids by *Rhodotorula glutinis* strain CCT-2186 using different nitrogen sources. In that research, two statistical experimental designs were applied to enhance carotenoid production: a first 2^{5-1} fractional factorial design to evaluate the influence of independent variables pH, nitrogen source, glucose, KH_2PO_4 and $MgSO_4$ concentrations; and a second 2^2 central factorial design to optimize the pH and nitrogen sources. After the optimization, the process was scaled-up to a 5 L stirred-tank bioreactor. This chapter is based on the manuscript recently published in the ***Biochemical Engineering Journal*** (Mussagy *et al.,* 2021, doi: 10.1016/j.bej.2020.107827).

Chapter 4: Recovery of carotenoids from *R. glutinis* yeast using protic ionic liquids includes the research published in the renowned ***ACS Sustainable Chemistry & Engineering*** (Mussagy *et al.*, 2019, doi: 10.1021/acssuschemeng.9b04247). This research evaluated the use of protic ionic liquids (PILs) aqueous solutions to permeabilize the yeast cells and to improve the extraction of intracellular carotenoids. Twelve highly concentrated aqueous solutions of ammonium-based PILs were investigated, evaluating the influence of the relative ion's hydrophobicity, PIL concentration, solid-liquid ratio, water content and temperature. In addition, an integrated platform was developed to allow the carotenoids recovery, together with the solvent recycling and carotenoids polishing, by using a three-phase partition system.

From the results obtained in the Chapter 4, and to explore the applications of ammonium-based PILs as potential and alternative solvents for the industrial liquid-liquid extraction (LLE) of other products, their ability to form aqueous biphasic systems (ABS) in the presence of phosphate salts (tripotassium phosphate and dipotassium hydrogen phosphate) was then evaluated. The ternary phase diagrams, tie-lines, and respective tie-line lengths were determined. The compositions of the coexisting phases were experimentally determined and correlated using the Non-Random Two-Liquid (NRTL) model for the activity coefficient. In addition, the predictive model COnductor-like Screening MOdel for Real Solvent (COSMO-RS) was used for a better understanding of the phase separation phenomena, predicting the interaction energy in term of excess enthalpy. The results obtained are presented in the **Chapter 5 – "Determination, characterization and modeling of aqueous biphasic systems composed of protic ionic liquids"**, which is based on the published manuscript Mussagy e*t al.,* 2020**,** doi: 10.1016/j.cplett.2020.137623) in ***Chemical Physical Letters***,

Chapter 6 – "Recovery of carotenoids from *R. glutinis* yeast using mixtures of bio-based solvents" includes all promising results on the development of integrative platform for the recovery of intracellular carotenoids using mixtures of solvents obtained from renewable sources (biosolvents). In fact, this chapter includes the promising research published in the highly recognized ***Green Chemistry*** journal (Mussagy *et al.*, 2020, doi: 10.1039/D0GC02992K). A complete study was carried out, starting with a screening of solid-liquid extractions using pure and solvent mixtures, and further optimization of the best biosolvent mixture (*i.e.,* ethyl acetate/ethanol/water) was carried out, covering the entire ternary phase diagram (*viz.* SLE at monophasic region and liquid-liquid extraction (LLE) at biphasic region). A full understanding of the solvation mechanisms towards carotenoids and lipids extraction using different solvent mixtures compositions was achieved with COnductor-like Screening MOdel for Real Solvent (COSMO-RS), and aiming at the circularity of the entire process, the LLE platform was integrated with following polishing and recycling operations, evaluating the carotenoids and lipids extraction performance from the reuse of mixed solvents in up to three consecutive stages. At the end, the environmental sustainability and the impact of the

proposed technology were addressed by analyzing the carbon footprint of each integrative platform.

Finally, in the **Chapter 7** of this Thesis, I will present the main conclusions, final remarks and future perspectives based on the overall achievements of this research, with a particular emphasis in the high performance of the integrated downstream platforms using ILs and bio-based solvents mixtures.

2. THEORETICAL INTRODUCTION

Based on the manuscript

Production and extraction of carotenoids produced by microorganisms

Mussagy CU, Winterburn J, Santos-Ebinuma VC and Pereira JFB

Applied Microbiology and Biotechnology, 103(3): 1095-1114, **2019**.

Abstract

Carotenoids are a group of isoprenoid pigments naturally synthesized by plants and microorganisms, which are applied industrially in food, cosmetic, and pharmaceutical product formulations. In addition to their use as coloring agents, carotenoids have been proposed as health additives, being able to prevent cancer, macular degradation, and cataracts. Moreover, carotenoids may also protect cells against oxidative damage, acting as an antioxidant agent. Considering the interest in greener and sustainable industrial processing, the search for natural carotenoids has increased over the last few decades. In particular, it has been suggested that the use of bioprocessing technologies can improve carotenoid production yields or, as a minimum, increase the efficiency of currently used production processes. Thus, this review provides a short but comprehensive overview of the recent biotechnological developments in carotenoid production using microorganisms. The hot topics in the field are properly addressed, from carotenoid biosynthesis to the current technologies involved in their extraction, and even highlighting the recent advances in the marketing and application of microbial carotenoids. It is expected that this review will improve the knowledge and understanding of the most appropriate and economic strategies for a biotechnological production of carotenoids.

Keywords: *Carotenoids, microorganisms, production, extraction, biotechnology, market.*

2.1 Introduction

Carotenoids are a group of yellow, orange-red-pigmented polyisoprenoids, synthesized by plants, algae, cyanobacteria, bacteria, and fungi (Heba et al. 2015; Saini and Keum 2017; Rodriguez-Concepcion et al. 2018). These compounds, because of their large structural and functional versatility, are of utmost importance in nature (Esteban et al. 2015). Carotenoids play an important role in light harvesting and energy transfer during photosynthesis and in the protection of the photosynthetic apparatus against photo-oxidative damage (Henríquez et al. 2016), neutralizing free radicals, acting as antioxidant agents, and preventing oxidative damage to cells (Johnson and Schroeder 1996; Vachali et al. 2012). Although carotenoids exhibit a multitude of health beneficial and interesting properties, they are mainly known for their natural coloring characteristics, being the main molecules responsible for the pigmentation and colors of plants and microbial biomass. The presence of bright colors in nature has always captured the interest of scientists. The earliest studies focusing on carotenoids date back to the beginning of the nineteenth century, particularly related to the natural colors of different plants (Takaichi et al. 2006). In 1831, Henrich W.F. Wackenroder isolated β-carotene from carrot juice for the first time (Wackenroder 1831), following which many other carotenoids were discovered, isolated, and properly characterized. In 2017, approximately 1117 natural carotenoids from 683 sources (archaea 8; bacteria 170; and eukaryotes 505) have been described (Yabuzaki 2017).

A large number of carotenoids have been proposed for, or already used in, a wide range of industrial applications, from the most traditional food and cosmetic uses to the more recent pharmaceutical uses. When applied in the food industry, carotenoids are almost exclusively used as additives, in which more than 2500 additives are intentionally added to foods, to maintain and improve organoleptic properties or even to extend their shelf-life (Carocho et al. 2014). The consumption of carotenoids either in foods or as a nutritional supplement can exert positive effects on health, as a precursor of vitamin A, preventing degenerative or age-related diseases as retinoid-dependent signaling, helping with cell communication and regulating gene expression (Sy et al. 2015).

Although widely used in food formulations, many carotenoids used in the industry are artificial (synthetic colorants obtained through chemical synthesis), which are mainly

added to make the food more attractive and, thus, stimulate its consumption. However, the widespread use of synthetic colorants has generated discussions among scientific researchers and world health organizations, regarding the future human health impacts of these compounds. The regulatory agencies, *i.e*., the Food and Drug Administration (FDA) in the United States (US) and the European Food Safety Authority (EFSA) in the European Union (EU), have to approve the color additive before its application in food, drugs, cosmetics, and many medical devices. The tests performed by the regulatory agencies have shown the undesirable characteristics of several synthetic colorants, and as a result, the number of color additives approved by the regulatory agencies has reduced in the last years (Torres et al. 2016). Furthermore, the consumer's conscience has been changing, with concerns about artificial food additives driving a consumer-led need for natural colorants, which may be healthier than synthetic colorants. Consequently, the food industry is replacing artificial coloring agents from their products and focuses on the research and development of most stable and functional natural colorants (Zaccarim et al. 2018).

In addition to synthetic colorants, natural carotenoids are already in commercialization, usually, those extracted from plant sources, as well as some produced via biotechnological routes (Valduga et al. 2009a). Nowadays, the industrial interest for microbial carotenoids has been increasing, particularly due to the low production area requirements (compared to plant sources), processing independent of climatic changes and seasonality, and soil composition (Valduga et al. 2009b). Furthermore, with improvements in biotechnology and bioprocessing technologies, carotenoid microbial bioprocessing can be fully controlled, increasing the production yields and reducing the overall processing costs (for example, using low-cost substrates and reducing the processing losses) (Cardoso et al. 2017a, 2017b).

Because of their lipophilic characteristics, the majority of the microbial carotenoids are intracellular. So, besides upstream processing studies, downstream processing is also of utmost importance. Several studies have been working in the optimization of carotenoid extraction methods, aiming to increase recovery yields. In general, it is observed that the choice of the most efficient method for the extraction of carotenoids is dependent not only on the carotenoid characteristics (mainly its polarity) but also of the producer's characteristics. In general, the chemical methods using organic solvents are the most

applied, but the number of studies regarding the use of alternative and sustainable methods, as for example, using green solvents or supercritical fluids, has been growing (Saini and Keum 2018).

Considering the growing interest in microbial carotenoids, recently, many studies and reviews were published in the field (Gong and Bassi 2016; Markou and Nerantzis 2013; Henríquez et al. 2016; Minhas et al. 2016; Saini and Keum 2018; Ventura et al. 2017). In general, the published reviews always addressed facts, such as their origin, related products, and applications. However, there are several aspects of these biomolecules production, such as the integration of upstream and downstream processing, that have not been highlighted. Thus, in this review, we discuss the important concepts of carotenoid microbial production and extraction as well as their commercialization and market applications.

2.2 Structure, classification, and biosynthesis of carotenoids

Carotenoids are lipophilic isoprenoids that can be classified according to their chemical and nutritional characteristics. Chemically, they are classified as carotenes and xanthophylls. The first class, carotenes, are the most well-known, containing carbon and hydrogen atoms in the chemical structure, as for example, α-carotene, β-carotene, γ-carotene, δ-carotene, and torulene. The second class, xanthophylls, in addition to carbon and hydrogen, also contains oxygen in their chemical structure, such as torularhodin, astaxanthin, and canthaxanthin (Cataldo et al. 2018; Delgado et al. 2016; Colmán et al. 2016; Mata-Gómez et al. 2014; Avalos and Carmen 2005). The chemical structure of the most common carotenoids of each class are depicted in **Figure 2.1**.

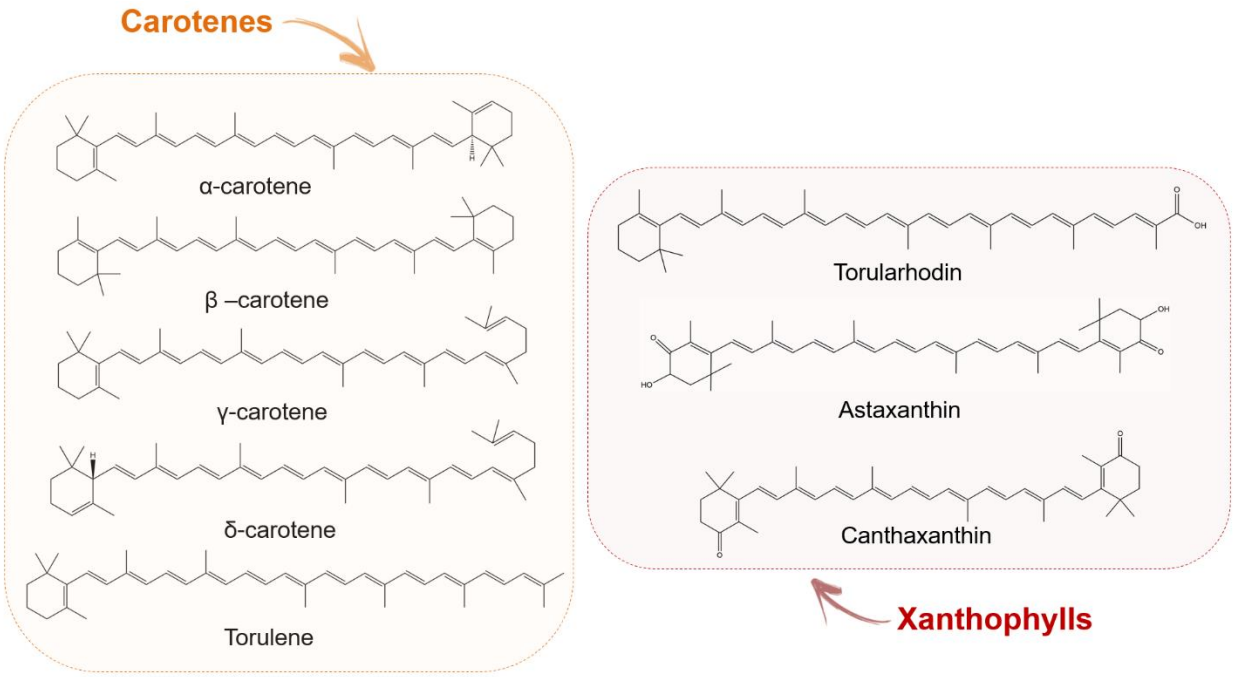

Figure 2.1. Chemical structures of major carotenoids produced by microorganisms

According to its nutritional properties, carotenoids are usually classified as pro-vitamin A, *i.e*., β-carotene, β-cryptoxanthin, and α-carotene, or non-provitamin A, *i.e*., lycopene, lutein, zeaxanthin (Olson 1999; Maldonade et al. 2007; Toti et al. 2018), and ketocarotenoids, such as canthaxanthin and astaxanthin (Jayaraj et al. 2008). The biosynthesis of microbial carotenoids is derived from acetyl CoA, obtained from fatty acids via the β-oxidation pathway in the microorganism mitochondria (Lovisa and Kalluri 2018). Subsequently, the biosynthesis of terpenoids occurs, following the mevalonic acid (MVA) pathway, from which the microorganisms derive C5 isoprenoid precursors isopentenyl pyrophosphate (IPP) and dimethylallyl pyrophosphate (DMAPP) via the MVA, or, depending on the organism, through the 2-C-methyl-D-erythritol-4-phosphate (MEP) pathway (Liang et al. 2017). Then, IPP is condensed with DMAPP, generating C10-geranyl pyrophosphate (GPP), and further elongating to C15-farnesyl pyrophosphate (FPP) and C20-geranylgeranyl diphosphate (GGDP) (Gharibzahedi et al. 2013), as summarized in the top of the scheme depicted in **Figure 2.2**.

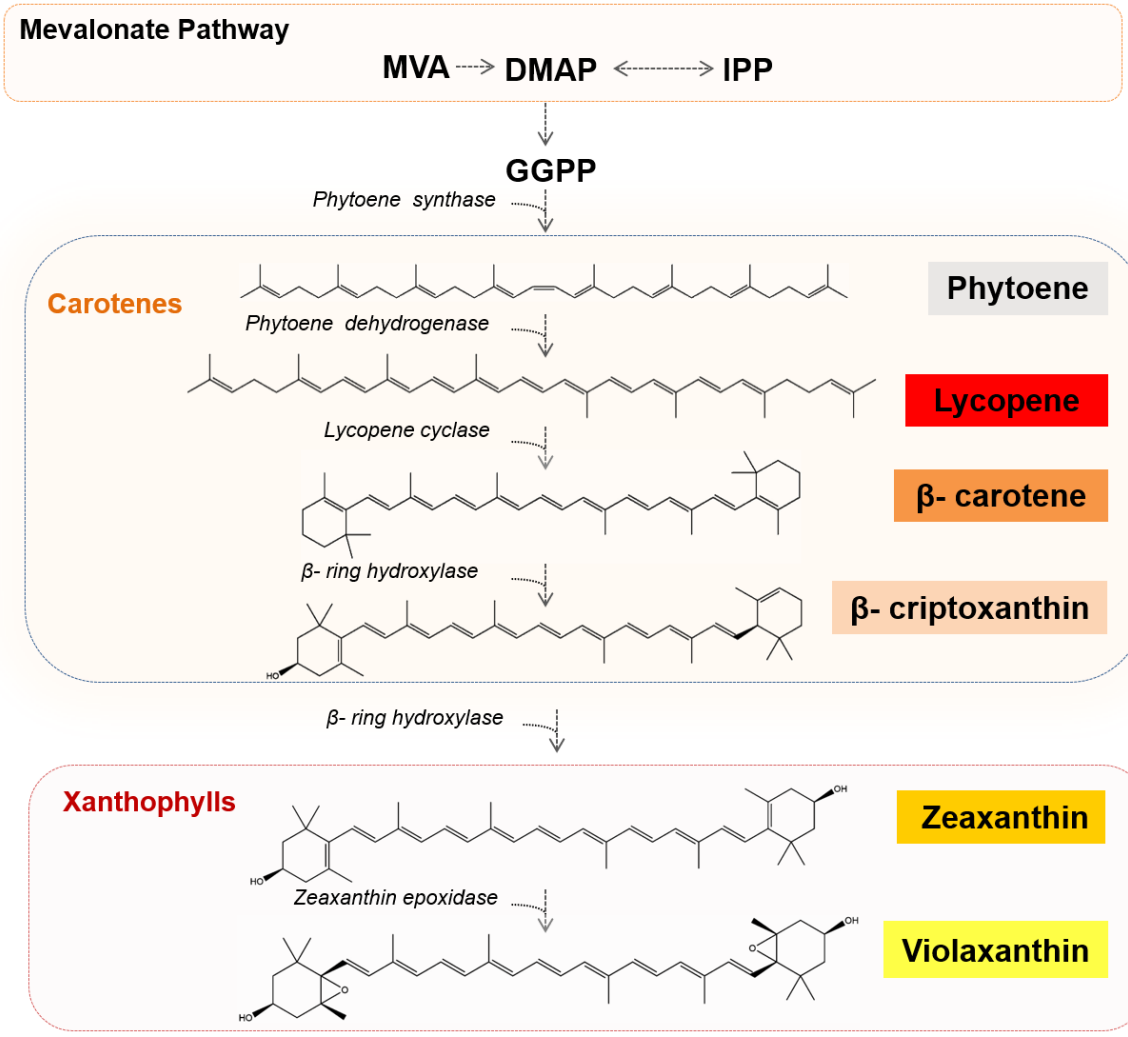

Figure 2.2. Carotenoid biosynthesis through the MVA pathway in microorganisms. Boxes indicate the name of carotenoids and their respective color (adapted from Clotault et al. 2012).

As an example, in the biosynthesis of bacterial carotenoids, the first carotenoid (phytoene) is formed from two geranylgeranyl pyrophosphate (GGPP) molecules catalyzed by phytoene synthase. Therefore, depending on the biocatalytic reactions, *i.e.*, cyclization, substitution, elimination, addition, and rearrangement, the phytoene molecule can result in different molecular structures of carotenoids (Britton et al. 1995). As schematized in **Figure 2.2**, when phytoene is desaturated by phytoene desaturase, the

linear, all-trans lycopene is formed. Through lycopene cyclization, the lycopene β-cyclase introduces two β-ionone end-groups into the chemical structure, forming the well-known β-carotene. Consequently, if the carotene rings of β-carotene undergo hydroxylation reactions, these are converted in xanthophylls, *i.e*., through two enzymatic reactions by β-carotene hydroxylase, the β-carotene is converted in zeaxanthin. Finally, violaxanthin carotenoids can even be formed, through an enzymatic reaction involving zeaxanthin epoxidase (Liang et al. 2017).

2.3 Microbial fermentation processes to produce carotenoids

Recently, the growing interest in natural carotenoids has been forcing their industrial production through the fermentation processes. Particularly, one of the most studied biotechnology fields aims to increase the microbial carotenoids productivity yields, optimizing simply the fermentation processes conditions or through more complex, but efficient, cell engineering and synthetic biology approaches. This section provides a summary of some of the key published works related with the increase of carotenoids productivity yields, through the optimization of the microbial fermentation processes conditions, such as the nutritional composition of the culture medium, pH, temperature, luminosity, aeration rate, and agitation. The choice of the best process conditions is of utmost importance since this affect not only the microbial cell growth but also the specificity of carotenoid biosynthesis (Mezzomo and Ferreira 2016).

As shown in **Table 2.1**, several works studied carotenoid production using different microbial sources, particularly, microalgae, yeast, and bacteria. Independent of the microbial source, a wide array of carotenoids was successfully produced, ranging from the most well-known β-carotene and lutein to the less common astaxanthin and canthaxanthin. The production of a specific type of carotenoid, or a mixture of carotenoids, is a result not only from the microorganism species but also from the different production strategies employed, as briefly summarized in the following paragraphs.

Table 2.1. Examples of "microbial" carotenoids found in nature and their producing sources.

Source	Microorganism	Pigment	References
Microalgae	*Dunaliella salina, Scenedesmus almeriensis, Coelastrella striolata* var. *multistriata*	β-carotene	Rabbani et al.1998; Demming-Adams et al. 2002; Macías-Sánchez et al. 2010; Abe et al. 2005.
	Haematococcus pluvialis, Chlorella vulgaris, Coelastrella striolata var. *multistriata*	Astaxanthin, Cantaxanthin, Lutein	El-Baky et al. 2003; Demming-Adams et al. 2002; El-Baky et al. 2011; Demming-Adams et al. 2002; Abe et al. 2005.
	Undaria pinnatifida, Hijikia fusiformis, Laminaria japónica, Sargassum sp. *and Fucus* sp.	Fucoxanthin	Billakanti et al. 2013; Yan et al. 1999; Xiao et al. 2012; Heo and Jeon 2009; Zaragozá et al. 2008.
	Scenedesmus almeriensis	Lutein	Macías-Sánchez et al. 2010.
Yeast	*Phycomyces blakesleeanus, Blakeslea trispora, Mucor circinelloides, Rhodosporidium* sp., *Sclerotium rolfsii, Sclerotinia sclerotiorum, Sporidiobolus pararoseus, Ustilago maydis, Aspergillus giganteus, Cercospora nicotianae, Penicillium* sp., *Aschersonia aleyroides, Xanthophyllomyces dendrorhous, Rhodotorula glutinis, Rhodotorula rubra* NRRL Y-168	β-carotene	Cerdá-Olmedo 1987; Avalos and Cerdá-Olmedo 2004; Fraser et al. 1996; Navarro et al. 1995; Miguel et al. 1997; Georgiou et al. 2001b; Georgiou et al. 2001a; Han et al. 2012; Estrada et al. 2010; El-Jack et al. 1988; Daub and Payne 1989; Han et al. 2005; Van-Eijk et al. 1979 Johnson 2003; Bhosale and Gadre 2001; Kot et al. 2016; Yoo et al. 2016; Valduga et al. 2009b; Shih and Hang 2006; Malisorn and Suntornsuk 2009; Tinoi et al. 2005.
	Rhodotorula glutinis, Sporobolomyces ruberrimus H110; *Xanthophyllomyces dendrorhous*	Torularhodin, Torulene	Buzzini and Martini 1999; Kot et al. 2016; Yoo et al. 2016; Valduga et al. 2009b; Cardoso et al. 2016; Tinoi et al. 2005; Fang and Wang 2002.
	Phaffia rhodozyma	Astaxanthin	Johnson et al. 1980
Bacteria	*Rhodococcus maris, Mycobacterium brevicaie, Rhodococcus maris*	Cantaxanthin	Valduga et al. 2009b; Johnson and Schroeder 1995.
	Mycobacterium acticola	Astaxanthin	Johnson and Schroeder 1995.
	Arthrobacter glacialis, Arthrobacter sp. M3, A. arilaitensis Re117	Decaprenoxanthin	Giuffrida et al. 2016; Monnet et al. 2010.
	G. alkanivorans strain 1B, *Bacillus circulans*	Astaxanthin, Cantaxanthin, Lutein	Silva et al. 2016; Fang and Wang 2002.

Valduga et al. (2009a) evaluated the effects of various chemical agents, such as acetic acid, mevalonic acid, β-ionone, and diphenylamine, in the increase of the carotenogenesis using yeasts of the *Rhodotorula* genus. It was observed that acetic acid (0.05 to 1% v/v) had no significant influence on the cellular growth and total production of carotenoids (β-carotene, torularhodin, and torulene) from *R. glutinis* and *R. mucilaginosa*. However, the addition of β-ionone (10^{-3} mol/L) after 70 h of fermentation had a negative effect on both yeast cultivations, reducing the cell density from 5.7 to 4.9 g/L, and carotenoid production from 1.98 to 1.70 mg/L. Conversely, the authors have shown that the addition of differing quantities of mevalonic acid (0.05, 0.1, and 0.2% v/v), while having no effect on the microbial growth, enhanced carotenoids production yields around 35 and 120% using *R. glutinis* and *R. mucilaginosa* yeasts, respectively.

More recently, Cardoso et al. (2016) showed that the red yeast *Sporobolomyces ruberrimus* H110 was able to use raw glycerol (from biodiesel production) as a carbon source for carotenoid production, achieving high cellular growth (0.51 g/L) and productivity (0.0064 g/L h). Interestingly, compared to the fermentation process with pure glycerol, the use of raw glycerol increased both carotenoid concentration (approx. 27%) and productivity (1.5-fold). The authors also studied the addition of individual fatty acids (palmitic, stearic, oleic, and linoleic acids) to pure glycerol, observing that these have a favorable effect on carotenoid production, increasing, from 15 to 25%, the maximum carotenoid concentration, and, from 1.6 to 2.0-fold, the productivity rates. Similarly, to the addition of raw glycerol, the presence of palmitic and oleic acids also favored the torularhodin biosynthesis (proportion close to 66%). This is a clear example of the importance of balancing the nutritional content of the fermentation media, which can be properly adjusted, for example adding fatty acids as additives, to direct microbial carotenoid biosynthesis and, consequently, to improve the production yield of a specific carotenoid.

As aforementioned, temperature and pH are also two important parameters for microbial growth and consequent pigment synthesis. For example, Shih and Hang (1996) highlight that acidic pH values, between 3.4 and 4.5, inhibit *R. rubra* cell growth and β-carotene production. However, the authors also observed that through a slight increase of the initial pH to 5.0, even maintaining the media slightly acidic, the maximum cell

concentration (0.131 mg/L) and β-carotene production yield (1041 µg/L) can be enhanced. Regarding the effect of temperature, Malisorn and Suntornsuk (2009) shown that the *R. glutinis* optimal growth is 30 °C, with approximately 2.3 g/L of cells, resulting in a consequent production of 0.178 mg/L of β-carotene.

Although most of the studies focused on the optimization of temperature, pH, and nutritional content of the culture media, other processing parameters have been also studied. Tinoi et al. (2005) evaluated the influence of the shaking rate using shaker flasks to produce carotenoids by *R. glutinis.* It was identified that a balance of the agitation speed is of utmost importance, since at low shaking rates (100 to 150 rpm), the cell growth is reduced, probably because of the low availability of nutrients on the cell surface, while at high agitation rates, some disruption of cells can occur, reducing their viability. In this section, some approaches to improve carotenoid productivity yields or to adjust the production for a specific microorganism were discussed. However, instead of a single strain fermentation process, the production of carotenoids can be performed using consortia or mixtures of two microorganisms. As an example, Fang and Wang (2002) studied the production of astaxanthin, in a 1.5 L bioreactor, using a mixed culture of the yeast *Xanthophyllomyces dendrorhous* (formerly, *Phaffia rhodozyma)* and the bacterium *Bacillus circulans*. The process was carried out in a two-stage batch fermentation, i.e., first stage in which yeast fermentation occurred and a second one in which the bioreactor was subsequently inoculated with *B. circulans*. In the first stage, using solely the *X. dendrorhous* cells, after 72 h, a total of 9.01 mg/L of astaxanthin were produced. The second stage was started with inoculation with *B. circulans* in the bioreactor, and after 144 h of incubation, the production of astaxanthin was slightly increased (10.07 mg/L). Although only a 10% increase after the incubation of the second microbial strain was observed, the use of these consortia is interesting as *B. circulans* has a lytic enzyme activity of the yeast cell walls, providing a highest extraction yield of total carotenoids (over 96%) during the second fermentation stage.

Summing up, a successful production of many carotenoids can be easily attained through the fermentation of several microorganisms. However, to maintain efficient production yields and to conduct a specific biosynthesis pathway, careful control of the

nutritional and processing parameters is essential. Moreover, independently of the upstream bioprocessing, after the fermentation, the carotenoids will remain inside the cells (in the biomass content), requiring proper integration with further downstream processing stages for the efficient extraction and recovery of the microbial carotenoids.

2.4 New genetic engineering approaches to increase carotenoid production yields

One of the strategies to reduce production costs and increase yields is the development of bioengineered hyper-producing strains. Metabolic engineering is the improvement of cellular properties through the modification of specific biochemical reactions, with the use of recombinant DNA technology (Park et al. 2007). Moreover, genetic engineering in non-carotenoid-producing microorganisms is naturally a very useful tool, since it allows the manipulation of "well-known" (*i.e.,* well-defined and understood metabolic pathways) microorganisms to enhance carotenoid productivity yields (Ye and Bhatia 2012).

Since the beginning of this century, several authors have made use of metabolic engineering tools in yeasts, such as *Saccharomyces cerevisiae* and *Candida utilis*, which were successfully modified by inserting carotenogenic genes from *Erwinia uredovora*, *Agrobacterium aurantiacum*, and *Xanthophyllomyces dendrorhus* to produce carotenoids, such as, β-carotene, lycopene, or astaxanthin (Misawa and Shimada 1998; Miura et al. 1998; Bhataya et al. 2009; Ungureanu et al. 2013). Another successful example was the production of lycopene using the yeast *Yarrowia lipolytica*, a natural non-producer of carotenoids, simply by introducing two genes, phytoene synthase and phytoene desaturase. After the integration of the heterologous genes *crtB* and *crtI*, the transformants appeared orange in color, indicating lycopene formation. This transformation increases the specific lycopene content, reaching a yield of 16 mg/g (dry cell weight) (Matthäus et al. 2014). *Pichia pastoris*, another non-carotenogenic yeast, was designed and constructed by adding two plasmids pGAPZA-EBI* and pGAPZA-EBI*L containing the genes encoding lycopene and β-carotene. The results obtained by Araya-Garay and collaborators (2012) showed that the recombinant strain produced both

lycopene and β-carotene, reaching 1.141 and 339 μg/g (dry biomass), respectively (Araya-Garay et al. 2012).

These successful examples demonstrate that the use of genetic engineering can be beneficial for the increase of carotenoid production yields, appearing as effective strategies to improve the production of specific microbial carotenoids and, thus, meeting the world demand for carotenoids in animal feed, cosmetics, food, beverages, and pharmaceutical industries.

2.5 Extraction methods for the recovery of intracellular carotenoids

The microbial production of carotenoids is intracellular, and, like other intracellular bioproducts, after the fermentation, a series of downstream operation units are included for carotenoid recovery and processing. In general, in the first clarification stage, *i.e*., using conventional filtration or centrifugation operations, the cellular biomass, which contains the intracellular carotenoids, is separated from the supernatant. Further, to facilitate the release of intracellular carotenoids, the recovered cells are disrupted, applying at least one of many different physical, chemical, and/or biological cell-disrupting methods. After the partial or total disintegration of the cell structure, the intracellular carotenoids are then extracted and separated from the cell debris. It is important to note that both cell disruption and extraction stages can be integrated into a single operation unit or carried out through different operation units as, for example, combining a chemical pre-treatment of the cells with a further Soxhlet extraction. Afterward, further downstream processing stages for the saponification and separation of a specific carotenoid can also be carried out. Among all the downstream processing steps, the extraction and recovery stages are the critical ones, which are briefly discussed in the next paragraphs. Considering the wide range of carotenoid producers and their cellular variety and complexity, the choice of the most adequate method(s) appears as a key to obtain a complete cell disruption or a selective cell-membrane permeabilization and, consequent, carotenoid release.

Gram-positive cells have an inner membrane and strong cell wall, while Gram-negative cells have both inner and outer membranes (less rigid than Gram-positive cells). These bacterial cells are yet more fragile than yeast and microalgal cells, which are

composed of dynamic, complex, and rigid cell walls. As expected, bacterial cell disruption is easier than the disruption of yeast and microalgal microorganisms. Moreover, as recently highlighted by Saini and Keum (2018), usually carotenoids are strongly associated with other intracellular macromolecules (for example, proteins and fatty acids), hindering their mass transfer process. Therefore, if the intention is to extract intracellular carotenoids from robust cells, most intense methods should be selected, as for example, cell cooking, cryogenic grinding, and/or using chemical agents (acids, base, surfactants, or volatile organic solvents (VOCs)). Conversely, the extraction of an intracellular product from Gram-negative cells can be simply achieved by ultrasonication or a freezing-thawing processes. In addition to the microbial cell characteristics, the relevant carotenoid properties must also be considered, namely, *(a)* the hydrophobic nature of these biomolecules and *(b)* the oxidative properties of carotenoids, which can be reduced in the presence of heat, light, acids, and long extraction times (Saini and Keum 2018).

Further, independent of the cell disruption procedure, the effective disintegration of cells (total or partial) is always a prerequisite for the efficient extraction of intracellular carotenoids, particularly as disruption facilitates the entry of the solvent and the subsequent carotenoid solubilization. Recently, Saini and Keum (2018) have completely revised the conventional and non-conventional extraction procedures applied in the recovery of target carotenoids, as schematized in **Figure 2.3**. Considering the carotenoid characteristics, particularly due to the carotenoid hydrophobicity, most traditional extraction processes use volatile organic solvents (VOCs) as solubilizing agents. Although VOC-based processes allow high extraction yields, they exhibit several human health and environmental risks (Salar-García et al. 2017). Thus, to over-come some of these concerns in the last few years, several researchers have been searching for novel alternative and efficient techniques, particularly, *(a)* replacing the VOCs with greener, biocompatible, and less toxic solvents, such as supercritical fluids, biosolvents, or ionic liquids (Yara-Varón et al. 2016) and *(b)* reducing the amount of solvent required through the combination of the chemical extraction with novel physical (microwave and ultrasound-assisted extractions) or biocatalytic (enzyme-assisted extraction) procedures. As shown in the scheme of **Figure 2.3**, VOCs are mostly used in conventional techniques, such as atmospheric liquid extraction with maceration or Soxhlet extraction, but depending of the

solvent type, they can be associated with some of the non-conventional procedures, such as ultrasound-assisted extraction (UAE) or enzyme-assisted extraction (EAE), while non-conventional solvents are mainly applied in novel processing techniques, since they are more biocompatible, like biosolvents and green solvents, or technique-specific, *i.e*., supercritical fluid extraction (SFE).

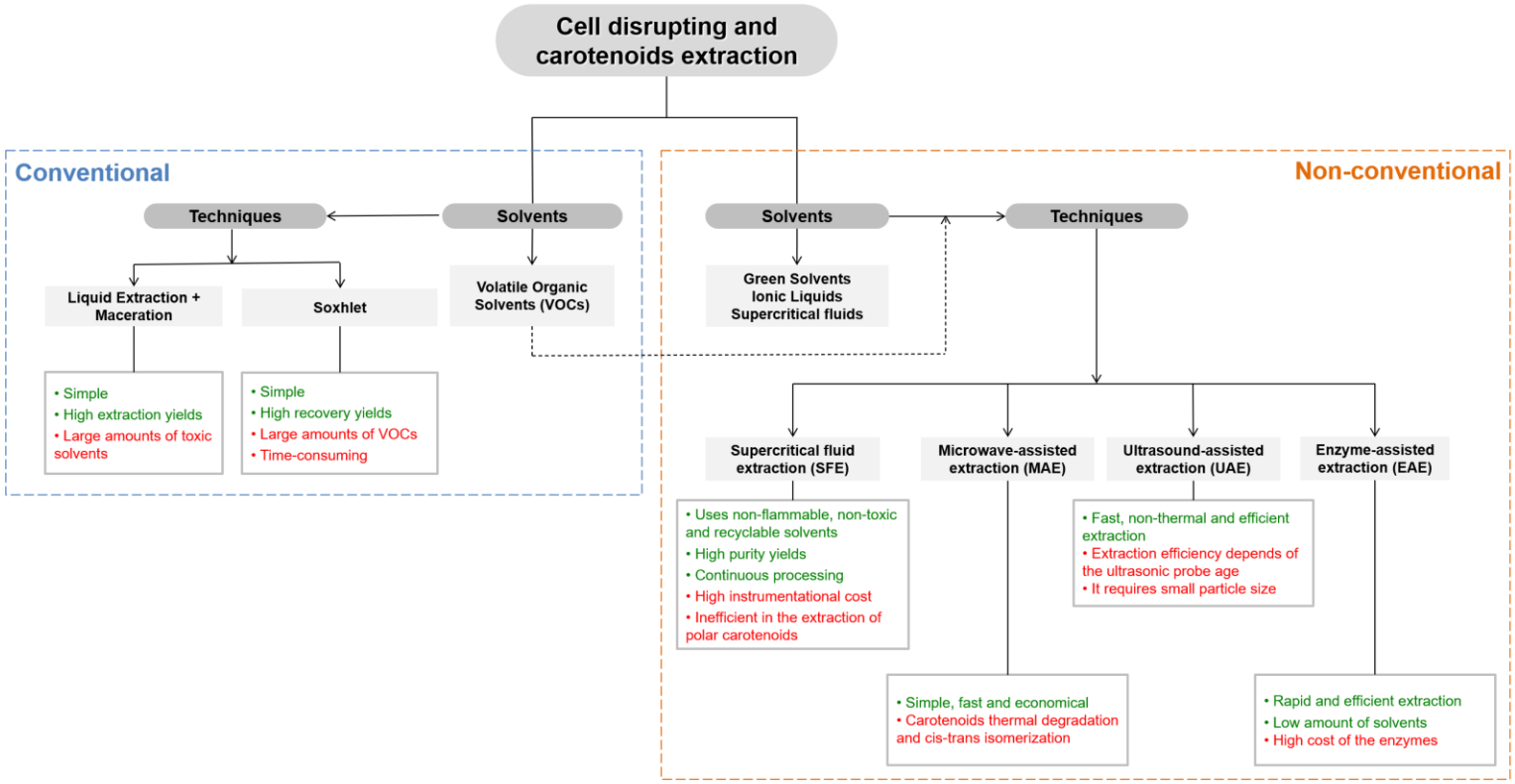

Figure 2.3. Conventional and non-conventional techniques for cell disruption and carotenoid extraction (adapted from Saini and Keum 2017).

As previously highlighted, most of the academic studies and industrial processes use VOCs to extract carotenoid. These solvents are particularly interesting because of their high carotenoid solubilizing potential, as well as their cell-disrupting capability, through permeabilizing walls and membranes. The organic solvent penetrates the microbial cells, dissolving the intracellular carotenoid molecules according to the characteristics of the extractant (or permeabilizing agent). Frequently, non-polar solvents, such as hexane, petroleum ether, or tetrahydrofuran (THF), are excellent choices for the extraction of non-polar carotenoids, whereas polar solvents, like dimethyl sulfoxide (DMSO), acetone, ethanol, and ethyl acetate, are more suitable for the extraction of carotenoids with polar characteristics (Saini and Keum 2018).

The influence of different VOCs on the recovery of carotenoids is being largely studied, for example, Valduga et al. 2009b, evaluated the extraction capability of different combinations of VOCs (acetone, petroleum ether, methanol, hexane, ethyl acetate, DMSO, chloroform) with liquid N_2, through the conventional procedure using VOC atmospheric liquid extraction with successive macerations of cellular biomass from *Sporidiobolus salmonicolor* CBS 2636. Interestingly, the maximum concentration of total carotenoids (253.8 μg/g) was obtained in a combined treatment, using liquid N_2 and DMSO, to disrupt the cell, followed by a liquid extraction with an acetone/methanol (7:3 v/v) organic solution. Similarly, Park et al. (2007) also evaluated the effect of different VOCs (DMSO, petroleum ether, acetone, chloroform, and hexane) in the recovery of carotenoids from *R. glutinis* cells. In their work, instead of maceration, the authors first lyophilized the yeast cells and then added each organic solvent mixture directly to the biomass. The integration of liquid extraction and lyophilization was an effective procedure to recover the total carotenoids produced from *R. glutinis* cells, with the lowest extraction capability obtained with hexane (0.19 mg/g) and the highest recovery yields with both DMSO (0.23 mg/g) and petroleum ether (0.24 mg/g) solvents.

As shown in **Figure 2.3**, some of the most effective and innovative approaches combine conventional VOCs with non-conventional techniques, even at the industrial scale. In several countries, for example, the industrial extraction of

food-based carotenoids involves the use of commercial enzyme preparations in combination with organic solvents, such as hexane and ethyl acetate (Lavecchia and Zuorro 2008). A more complex approach combining conventional Soxhlet extraction using VOCs (with DMSO and acetone) and non-conventional ultrasonication was recently evaluated as an alternative for the extraction of carotenoids from *R. mucilaginosa*. This innovative approach allowed an increase of the concentration of total carotenoids, 317.6 μg/g (*i.e*., equivalent to 91.46 (μg/g) of β-carotene, 152.44 (μg/g) of torulene, and 73.04 (μg/g) of torularhodin) recovered under milder processing conditions (at 25 °C) (Cheng and Yang 2016).

The combination of VOCs and non-conventional techniques proved to be more efficient than the direct application of solvents in the liquid extraction of the carotenoids. Although VOCs are widely used for the extraction of biomolecules due to advantages like high vapor pressures (easily evaporated at room temperature), low cost, and high commercial availability, they exhibit serious disadvantages regarding the bioproducts contamination, low biodegradability, and high atmospheric toxicity ("greenhouse" effect) (Datta and Philip 2018). Therefore, several alternatives have been proposed, varying from the so-called "green" solvents or biosolvents to the supercritical fluids. The search for alternative (non-conventional) solvents intends to minimize the environmental impacts and to increase the sustain-ability and biocompatibility of the overall carotenoid manufacturing process. "Green" solvents are a general classification for more environmentally friendly solvents, *i.e.,* those that comply, at least, with most of the 12 principles of green chemistry (Anastas and Warner 1998). The biosolvents are, in general, obtained from renewable resources, like wood, starch, fruits, and vegetable oils, or from petrochemical products that are non-toxic and biodegradable (Yara-Varón et al. 2016).

Yara-Varón et al. (2016) evaluated the capability of several biosolvents (cyclopentyl methyl ether, dimethyl carbonate, ethyl acetate, isopropyl alcohol, and 2-methyltetrahydrofuran) as possible substitutes for hexane in the extraction of microbial carotenoids, using two predictive models, the solute-solvent Hansen Solubility Parameters (HSPs) and Conductor-like Screening Model for Realistic Solvation (COSMO-RS). The use of predictive methods is a valuable tool to

understand the molecular interaction of solvents with carotenoids, avoiding extensive experimental studies, allowing a solubility scale of different carotenoids in a wide range of solvents to be easily obtained. The “green” solvents were effective for the recovery of β-carotene, particularly cyclopentyl methyl ether and 2-methyltetrahydrofuran, which gave extraction yields higher than those obtained with conventional solid–liquid extraction by maceration using hexane.

Other classes of compounds that have been largely regarded as “green” solvents are ionic liquids (ILs). ILs are commonly defined as salts with a melting point below 100 °C, obtained through the combination of different organic cations and organic or inorganic anions (Chatel et al. 2014). Due to their ionic nature, ILs are wide versatile compounds, exhibiting adjustable solvent properties with an adaptability that is virtually impossible for any other class of other molecular solvents (Feldmann and Ruck 2017). As, for example, through the choice of a cation-anion combination, it is possible to design a suitable solvent, possessing specific conductivity, hydrophobicity, polarity, and solubility, based on the nature of the target solute (Kumar et al. 2017). Moreover, in the last few years, several families of ILs have been classified as eco-friendly in nature, due to the low vapor pressures (negligible volatilities), non-flammability, and high chemical and thermal stabilities (Oliveira et al. 2016). Regarding carotenoids extraction, some studies have already demonstrated the effectiveness of ILs (ILs from the imidazolium-, pyridinium-, and ammonium- based families), as solvents and permeabilizing agents, to extract carotenoids (like astaxanthin) from *Haematococcus pluvialis* microalgae (Praveenkumar et al. 2015) or from non-microbial origin (Saini and Keum 2018).

For example, Praveenkumar et al. (2015) used a series of imidazolium- and pyridinium-based ILs as alternative solvents for the extraction of astaxanthin from *Haematococcus pluvialis* microalgae, using a simple liquid-liquid extraction procedure at room temperature. The addition of ILs damaged and deconstructed the cyst cell wall, facilitating the release of the astaxanthin. The highest extraction capability was obtained (19.5 pg of astaxanthin per cell) with 1-ethyl-3-methylimidazolium ethyl sulfate, in a very short extraction time (1 min of exposure

time); a process 82% more efficient than the conventional procedure using ethyl acetate and French-press-cell homogenization.

As shown, it seems that ILs are promising, highly efficient, and biocompatible alternatives for the extraction of carotenoids. However, only a few studies have reported the extraction of microbial carotenoids using ILs. Additional studies are essential to fully validate the effectiveness of ILs as extractive agents of microbial carotenoids, but it is important to highlight that, because of the wide range of cation–anion combinations, these further studies should focus on ILs with eco-friendlier characteristics, *i.e*., low environmental impact and toxicities, high biodegradability, and those that can be easily obtained from renewable sources.

Similarly, another class of “green” solvents that are of interest to the scientific community are Deep Eutectic Solvents (DES), in particular due to their low toxicities and reduced adverse environmental effects. These characteristics resulted in a rapid increase in the number of applications using DES for the extraction of bioactive compounds (Zainal-Abidin et al. 2017). Very recently, a pioneering work was performed by Cicci et al. (2017), in which intracellular biomolecules were recovered from microalgal biomass of *Scenedesmus dimorphus* by combining DES (composed of 1,2-propanediol, choline chloride, and water, in a 1:1:1 molar ratio) and UAE. DES solvents were effective in extracting a large number of intracellular carotenoids, with approximately 0.11% of carotenoids being recovered, as a proportion of the total biomolecules extracted.

Although the use of DES is quite new, and no further studies have focused on the extraction of microbial carotenoids, DES-based processes were already successfully applied in carotenoid recovery from other sources (animal and vegetal). For example, astaxanthin was obtained from shrimp carotenoids using DES (Zhang et al. 2014). After evaluating different conditions, the combination of ultrasound processing with DES as solvents was established as the most efficient platform for the extraction of astaxanthin, achieving extraction yields (146 g/g), higher than an ultrasound method with ethanol as solvent (102 g/g) (Zhang et al. 2014). Lee and Row (2016) also studied the extraction of astaxanthin from *Portunus trituberculatus* (marine crab) using DES-based processes. The authors observed that the

astaxanthin extraction yields are enhanced 155% using DES (composed of methyl-tri-phenyl-phosphonium bromide and 1,2-butanediol, in 1:4 molar ratio) as additives in an acetone-based extraction procedure (73.49 mg/g), in comparison to the use of IL, 1-ethyl-3-methylimidazolium bromide (47.30 mg/g) as additive (Lee and Row 2016). These examples clearly demonstrate that DES have strong potential to be used as alternative solvents for the recovery of microbial carotenoids. Particularly, natural DES, constituted by amino acids, organic acids, sugars, or choline derivatives, fully accomplish most of the green chemistry principles (Paiva et al. 2014), and we believe that they can be next generation of solvents in biocompatible carotenoid processes.

Contrarily to ILs and DES, supercritical fluids are one of the non-conventional solvents mostly studied in literature for the extraction of microbial carotenoids, with supercritical fluid extraction (SFE) being a widely known and applied technique, even at the industrial scale. This process uses non-flammable, non-toxic, and recyclable solvents under conditions close to the critical point as an extractant of non-polar carotenoids (Saini and Keum 2018). Usually, carbon dioxide (CO_2) or ethanol are used as solvents (Johner and Meireles 2016). SFE is free of toxic waste, does not require post-processing for solvent removal, and does not cause thermal degradation of the biomolecules (Mezzomo and Ferreira 2016).

Lim et al. (2002) compared the extraction efficiency between acetone-based conventional liquid extraction and SFE using carbon dioxide (CO_2) to recover astaxanthin from *Phaffia rhodozyma* red yeasts. The highest astaxanthin extraction yield (90%) was attained using CO_2 (50 g), with the temperature being a key parameter in the extraction. At 40 °C and 500 bar, an increase of the concentration of astaxanthin by about threefold, reaching thirteenfold at 60 °C, was observed, in comparison with a conventional liquid extraction using acetone at same temperature conditions. Another successful example of the use of SFE (using CO_2) for the extraction of microbial carotenoids was reported by Sajilata et al. 2010. In that work, the authors carried out SFE using methanol as an entrainer (*i.e.,* modifier) to extract zeaxanthin from dried bacterial biomass of *Paracoccus zeaxanthinifaciens*, obtaining a maximum recovery of 65% of the total zeaxanthin content using 3 mL of

methanol per gram of lyophilized biomass, at 300 bar and 40 °C. Macías-Sánchez et al. (2005) have also extracted carotenoids from *Nannochloropsis gaditana* microalgae biomass using SFE with CO_2 and methanol, comparing the yields with conventional liquid extraction using methanol as the extractant. SFE was carried out at the micro-scale at 60 °C and 400 mbar, and, after 180 min of processing, approximately, 0.343 μg/mg of the total intracellular carotenoids was recovered. Unfortunately, it was observed that the extraction of total carotenoids with methanol was more efficient than SFE, recovering approximately 0.8 μg/mg of the total carotenoids. This suggests that the non-conventional techniques is not always more effective than the simplest and traditional recovery approaches using VOCs. Therefore, before implementing SFE processing, it is fundamental to balance the eco-friendly and extraction advantages with the non-favorable characteristics, like low efficiencies, carotenoid degradation at the operating conditions required (high temperatures and pressures), equipment cost, and/or high-energy consumption, of the SFE. Here, we highlight that, specifically, CO_2-based SFE has clear biotechnological advantages for the extraction of microbial carotenoids in comparison with the majority of the conventional procedures, which are namely, *(a)* low toxicity of CO_2, *(b)* overall cost–benefit of the SFE, and *(c)* separation and polishing of the recovered carotenoids.

Other non-conventional techniques have been also successfully applied as alternatives for the extraction of microbial carotenoids, such as ultrasound-assisted extraction (UAE) (Dey and Rathod 2013; Goula et al. 2017; Parniakov et al. 2015; Gu et al. 2008; Singh et al. 2015). For example, Gu et al. (2008) evaluated the capability of UAE for the recovery of intracellular carotenoids from *R. sphaeroides* bacteria. In that study, solid-liquid solutions (50 of solvent per g of dried biomass) using acetone as extractant were prepared and then subjected to ultrasonic processing at 500 W. After the sonication, approximately 664 μg/g of the total intracellular carotenoids was recovered. Singh et al. 2015, using response surface methodology, optimized a series of UAE processing parameters [solvent (acetone)/CDW ratio of 67.38 μL/mg, power 27.82% (total power 500 W), pulse length of 19.7 s, and extraction time of 13.48 min], achieving extraction yields of

zeaxanthin (11.2 mg/g) and β-carotene (4.98 mg/g) from the green microalgae *Chlorella saccharophila* (Singh et al. 2015). The UAE methods using VOCs as extractant agents can significantly increase the carotenoid extraction yield when compared to the conventional techniques, but a proper optimization of several factors, such as ultrasonic power, intensity, temperature, and sample/solvent ratio, is of utmost importance.

In summary, several techniques and solvents can be used for breaking cells and extracting intracellular carotenoids, but the efficiency of each method is always dependent on a combination of factors, namely, the microbial biomass, carotenoid nature, and operation conditions. Therefore, the choice of the appropriate method must consider the cost-effectiveness, environmental safety, processing efficiency, and reproducibility. We believe that the use of “green” and biocompatible solvents will overcome some of the environmental and processing drawbacks, particularly, if combined with non-conventional and innovative procedures, appearing thus as more efficient and environmentally friendly platforms for the recovery of a wide range of microbial carotenoids. However, it is essential to create effective and economical integrative platforms for recycling the solvents used in carotenoid extraction. VOCs, for example, are volatile organic solvents that can be easily and efficiently recovered through distillation, but in the case of ILs and DES, the recyclability appears yet as the greatest challenge to be overcome. However, as recently reviewed by Ventura et al. (2017), the development of effective strategies for ILs and DES recycling and carotenoid isolation is already in progress. Particularly, the authors highlight that the integration of the extraction stages with further aqueous biphasic systems (ABS) units can be a promising alternative for solvent recycling or simply by adding anti-solvents, which can allow the carotenoids to crystalize or precipitate (Ventura et al. 2017). In any case, additional studies are up most of the importance to transform these ILs and DES-based extraction processes as realistic environmental and economical sustainable platforms for an industrial recovery of microbial carotenoids.

2.6 Metabolites extracted during the carotenoid extraction

In the previous section, we focused on microbial carotenoid extraction. However, during the extraction processes, other intracellular microbial metabolites, like fatty acids, lipids, proteins, carbohydrates, among others, can also be co-extracted, increasing the complexity of further downstream processing stages required for their separation and subsequent carotenoid purification.

For example, during the extraction of carotenoids, such as astaxanthin or β-carotene, from microalgae using VOCs, other essential fatty acids are simultaneously recovered. In the literature, fatty acid extraction from *Porphyridium cruentum, Isochrysis galbana*, and other microalgae (Medina et al. 1995; Giménez Giménez et al. 1997; Molina Grima et al. 2003) resulted in the simultaneous recovery of fatty acids, such as eicosapentaenoic acid (EPA), docosohexaenoic acid (DHA), and arachidonic acid (AA) (Molina Grima et al. 2003). Likewise, the co-extraction of carotenoids and proteins is widely common, in that case, certain particularities must be considered, such as the use of wet biomass (Román et al. 2002). Powls and Britton extracted a violaxanthin-binding protein from a photosynthetic route using hot methanol obtained from biomass of microalgae Scenedesmus obliquus (Powls and Britton 1977). More recently, Cicci et al. (2017) have shown that DES can be used as biocompatible solvents to extract carotenoids, carbohydrates, proteins, lipids, and pigments (chlorophyll) from *Scenedesmus dimorphus*.

As briefly highlighted, several intracellular metabolites can be recovered during the extraction of the carotenoids. Thus, after the extraction stage, a full characterization of the extract is needed, characterizing not only the target carotenoids but also identifying which metabolites are co-extracted. Consequently, depending on the extract composition, the downstream processing plant should be conveniently designed for the carotenoid purification and polishing, as well depending on the metabolites extracted, the recovery of other added-valued byproducts, as for example, essential fatty acids.

2.7 Analytical techniques for characterization and quantification of carotenoids

After the carotenoid extraction stage, some different analytical procedures can be used to characterize and quantify the microbial carotenoids recovered. Several analytical techniques have been applied for the characterization of carotenoids, with mass spectrometry (MS) being the most frequently employed (Rivera et al. 2014). However, it is important to note that MS techniques do not distinguish stereoisomers and, in that case, nuclear magnetic resonance (NMR) spectroscopy-based procedures must be applied (De Rosso and Mercadante 2007). Another innovative method for the characterization of carotenoids is the use of NIR-FT-Raman spectroscopy, generally regarded as a fast and non-destructive method, characterizing these biomolecules according to the characteristic bands of the most predominant carotenoids. Since this is a non-destructive and relatively simple technique, the use of NIR-FT-Raman spectroscopy is a very important tool for the routine characterization of carotenoids (Schulz et al. 2005).

The characterization of carotenoids is upmost importance, but in general, during the production and extraction processing stages, the proper quantification of the number of carotenoids is more essential, since it determines the global yields of the process. There are several methods for quantification of carotenoids, of which spectrophotometric methods have been mostly used. Although spectrophotometry analytical procedures are commonly applied for the determination of total carotenoid content, these methods are not efficient at differentiating the types of carotenoids or isomers of the same carotene (cis/trans). Therefore, the use of chromatographic techniques, which allows the separation of these compounds, appears as the most convenient procedure for the quantification of a particular carotene molecule (Arvayo-Enríquez et al. 2013). The use of high-performance liquid chromatography (HPLC) in combination with spectrophotometric techniques is thus largely applied in the carotenoid analysis.

HPLC is the most accurate analytical technique for the quantification and identification of microbial carotenoids, but the success of the operation is directly dependent on the processual parameters, such as the type of detector, stationary

and mobile phase, among others. In general, the detectors to quantify and identify carotenoids by HPLC are UV-Vis, but, other detectors using mass spectrometry or photodiode arrangements can also be applied (Schierle et al. 2004). Another important factor is the selection of the appropriate chromatographic column (stationary phase) for the separation of the carotenoids, and for that, it is important to consider factors, such as particle size, shape, and pore degree (Arvayo-Enríquez et al. 2013). Among a large number of chromatographic columns, as carotenoids present a more “hydrophobic” nature, C_{18} and C_{30}-based columns are the most applied in the separation of microbial carotenoids (Jin et al. 2017; Al-Yafeai et al. 2018). Finally, it is also important to mention the importance of the choice of most convenient mobile phase. The solvents commonly used for the quantification of carotenoids by HPLC are water, acetone, methanol, dichloromethane, isopropanol, and acetonitrile, which can be used as pure or mixed solutions. For example, using methanol and isopropanol, it is possible to separate some of the most important carotenoids, except lycopene that cannot be eluted under these conditions (Humayoun Akhtar and Bryan 2008). β-Carotene, torularhodin, γ-carotene, and torulene can be separated using acetone as mobile phase (Lin et al. 2017).

2.8 Carotenoid properties and biological functions

Although the extraction is the key step of carotenoid downstream processing, depending on the application, further purification operations can also be considered in the manufacturing process layout. Independent of the industrial plant design, at the end, the biological properties of the carotenoid should be maintained, since biologically active carotenoids have several interesting properties and functions, playing different but fundamental roles in human health. Several health benefits have been attributed to carotenoids themselves or to carotenoid-rich foods (Xavier and Pérez-Gálvez 2016). Among these health benefits, highlighted roles include as retinoid precursors (as vitamin A), antioxidant potential and free radical scavenging activity, enhancement of the immune function, and sunburn reaction- and cancer-protective effects (Mezzomo and Ferreira 2016). Moreover, considering that carotenoids play a protective role in various reactive oxygen species (ROS), these

are being suggested as protective agents against cardiovascular disorders, various types of cancer, and neurological and photosensitive diseases. However, several factors affecting the bioavailability, absorption, transport, metabolism, or storage of carotenoids and, thus, the exact mechanisms of their functioning in vivo are still far from being fully understood (Fiedor and Burda 2014).

From the wide range of known carotenoids, approximately 50 are precursors (having at least one unsubstituted β-ionone ring with a polyene side chain with a minimum of 11 carbons) of retinoids, such as vitamin A, being the β-carotene most abundant in foods and the one with the highest provitamin A activity (Ambrosio et al. 2006). The liver contains 90% of vitamin A in the human body. Of this, approximately 40% of retinol is readily used, while the remainder is stored. Therefore, once ingested, carotenoids with provitamin A activity are absorbed and converted to retinal in the intestine, which in turn is converted to retinol and transported to the liver, where it is stored (Ambrosio et al. 2006). A schematic overview of the β-carotene cleavage reactions is shown in **Figure 2.4**. Concisely, a central symmetric cleavage divides β-carotene into the central double bond (15–15′), resulting in a retinal molecule, which can be reversibly converted to retinol (vitamin A) and irreversibly to retinoic acid. In asymmetric cleavage, β-apocarotenals are formed, which can be then converted to retinal and, consequently, into retinol and retinoic acid.

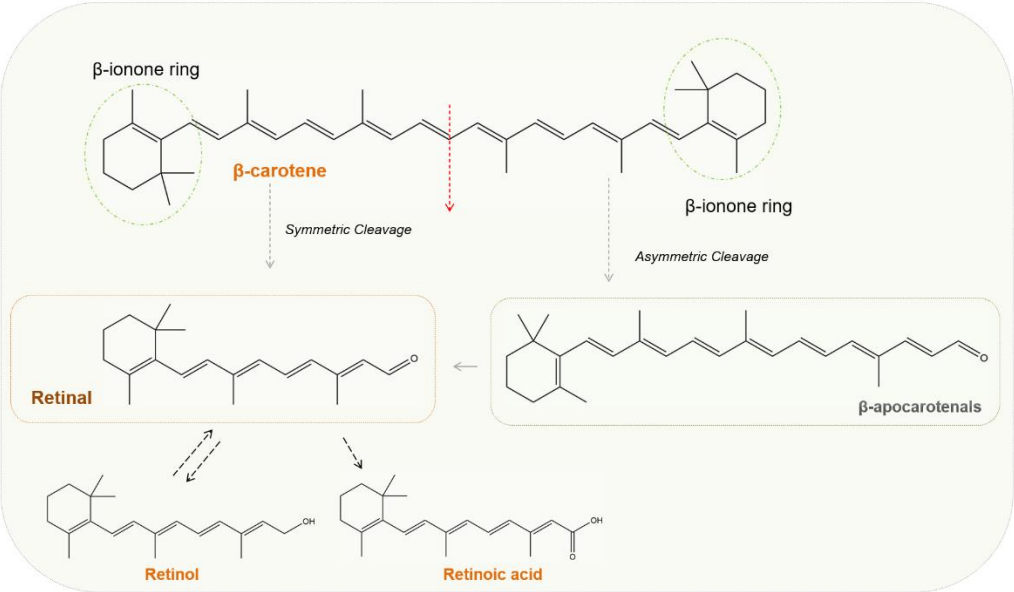

Figure 2.4. Symmetric and asymmetric cleavage of β-carotene (adapted from Ziouzenkova et al. 2007).

In addition to the provitamin A activity, carotenoids have also an important antioxidant action, scavenging free radicals. These radicals are chemical species that have "unpaired electrons," which can react with several biomolecules, damaging human cells (Gammone et al. 2015; Bianchi and Antunes 1999). In general, circa 0.1% of the total oxygen is used in respiration form ROS (Taverne et al. 2018). Therefore, as antioxidants, carotenoids can neutralize the unbeneficial effects of ROS, through physical or chemical mechanisms, as schematized in **Figure 2.5**. Physically, the neutralization of ROS involves an energy transfer, where a singlet oxygen ($^1O_2$) transfers the excitation energy to the carotenoid molecule, forming a carotenoid molecule and triplet (non-reactive) oxygen *(1)*. Then, the excitation energy dissipates through rotational and vibrational interactions, regenerating the original carotenoid molecule *(2)* (**Figure 2.5a**) (Krinsky 1989; Ramel et al. 2012). On the other hand, as shown in **Figure 2.5b**, the chemical neutralization of the ROS effects can be carried out through an electron transfer, allylic hydrogen abstraction, and addition reactions (El-Agamey et al. 2004).

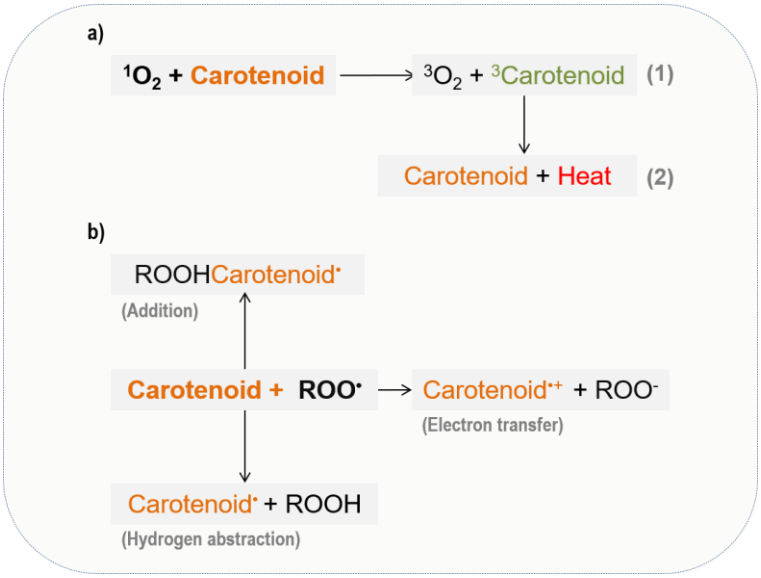

Figure 2.5. a) Physical (adapted from Krinsky 1989) and **b)** chemical (adapted from El-Agamey et al. 2004) mechanisms to neutralize the effects of ROS.

Since carotenoids exhibit a plethora of mechanisms to neutralize the effects of ROS, the antioxidant activity of carotenoids is quite variable. Naguib (2000) performed a comparative study between antioxidant activities of different carotenoids, observing that astaxanthin exhibits higher activity than α-carotene, β-carotene, lutein, and lycopene (Naguib 2000). Carotenoids are also important for the operation and maintenance of biological functions, including vision, reproduction, and immunity (Manimala and Murugesan 2018; Yamagata 2017). For example, β-carotene protects the cells against free radicals, improving immune system functionality and helping the proper functioning of the reproductive system (Pratheeba et al. 2014). The structure of torulene, β-carotene, torularhodin, and lycopene is responsible for both simultaneous pro-vitamin A and antioxidant activities (Maldonade et al. 2007; Kot et al. 2016).

However, it is important to mention that, in certain cases, carotenoids can be non-beneficial to humans. Particularly, as reported by Geoffrey and Felix (1991) and Baker (2001), the excessive and prolonged ingestion of carotenoids, such as canthaxanthin, for both cosmetic skin coloration and dermal photoprotection (*i.e.,* “sunless tanning” products) can cause macular (eye) crystal deposition. Although in

most cases the crystalline deposits did not result in clinical visual disturbances and are reabsorbed after discontinuation of canthaxanthin intake, the use of carotenoids as human health safe substances should be rationally carried out.

2.9 Applications and market

The various beneficial functions of carotenoids have pushed up their commercial value and industrial applications all over the world. Carotenoids are widely used in several industries varying from the most common animal feed and food uses to the most recent nutraceutical and pharmaceutical applications (Jaswir et al. 2011), as schematized in **Figure 2.6**. Commercially, in the most traditional applications, carotenoids are used as food colorants, feed additives, and nutritional supplements. The most innovative purposes resulted particularly from their human health beneficial properties, such as antioxidant, anti-tumoral, provitamin A activities (Cardoso et al. 2017a, 2017b).

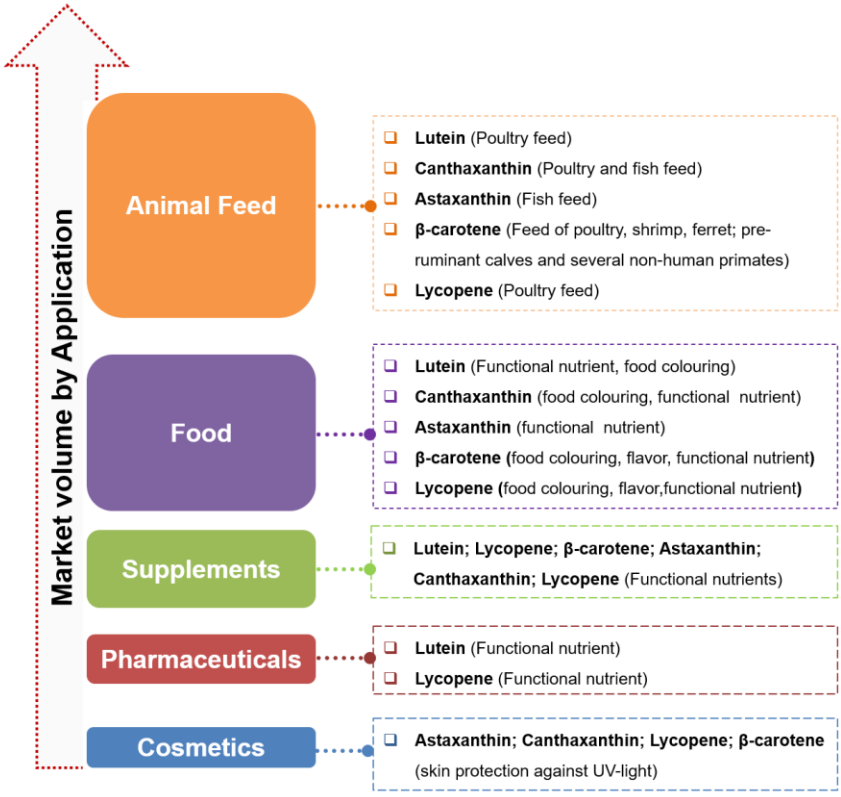

Figure 2.6. Carotenoids and their industrial applications

As schematized in **Figure 2.6**, the carotenoids with highest commercial added-value, *i.e*., a high market volume, are those used in animal and food-feed applications, such as lutein, β-carotene, lycopene, canthaxanthin, and astaxanthin (Langi et al. 2018), although these carotenoids are also largely applied in other industries as well (Martins et al. 2016). In most of the animal feed applications, carotenoids are directly ingested from their natural source, such as fruits and plants, and thus, no extraction or purification processes are required for the recovery of the carotenoids, which is not true in the case of microbial carotenoids (Amaya et al. 2014).

In food, pharmaceutical and nutritional-based purposes for humans, the use of “natural” food colorants (*i.e.,* from the plant and microbial sources) is continually growing, in particular, because of the rising health concerns and the more restrictive regulations for food formulations (Rodriguez-Amaya 2016; Carocho et al. 2015). As an example, microbial β-carotene extracted from *Blakeslea trispora* is being applied

in the manufacturing of butter and margarine, cakes, milk products, and soft drinks (Nabae et al. 2005; Martins et al. 2016). Astaxanthin from *Scenedesmus* sp. and *Xanthophyllomyces dendrorhous* is being used in the feed and nutraceutical industries to the production of salmonids (salmon, rainbow trout) and for the enhancement of egg yolk pigmentation, respectively (Grewe et al. 2007). Another interesting study using microbial carotenoids was carried out by Galaup et al. (2015). They observed that, under certain conditions, the *Brevibacterium linens* can grow on the surface of the well-known Vieux-Pane cheese, producing pigments, which allow for an effective coloring of the cheese.

In addition to their use as food additives or nutritional supplements, microbial carotenoids have been used in nutraceutical formulations as a form of prevention and for treatment of diseases, promoting human life quality. Due to their structure and functional properties, carotenoids can promote chemical reactions, such as oxidation, reduction, and addition in biological membranes, or even act as strong antioxidant, anti-tumoral, and anti-inflammatory agents (Cardoso et al. 2017a, 2017b). Because of these interesting biological properties (such as pro-vitamin A, antioxidant, anti-inflammatory, antitumor), the pharmaceutical and nutraceutical companies have quickly introduced these natural carotenoids, improving both the product quality and consumer health (Shahidi and Ambigaipalan 2015).

In the last few paragraphs, the main industrial applications of microbial carotenoids were discussed. However, it should be highlighted that before their industrial application, as with other chemical and biological compounds, their use should be approved by the respective national regulatory agencies*, e.g.,* the FDA and the EFSA. The use of microbial carotenoids is thus regulated according to the current legislation that specifies the purity, product, source, and quantities that can be added in each formulation or product (Jaswir et al. 2011).

Considering the high number of applications, as expected, the global market of carotenoids is quite impressive. According to the Global Market Carotenoids Report from BBC research (McWilliams 2018), carotenoid commercialization reached a value of US $1.5 billion in 2017, with expectations to achieve a $2.0 billion in 2022, at a compound annual growth rate (CAGR) of 5.7%, as depicted in **Figure**

2.7. Among the carotenoids, the capsanthin market is the largest, with a value of US$ 300.0 million in 2017 and a projection to reach US $385.0 million by 2022 (at a CAGR of 5.1% through 2022). Following closely, astaxanthin, due to its powerful antioxidant activity, appears as the second worldwide high-added value carotenoid, having a market value of US $288.7 million in 2017, with expectations to be the largest market in the future, reaching $426.9 million at a CAGR of 8.1% by 2022 (McWilliams 2018).

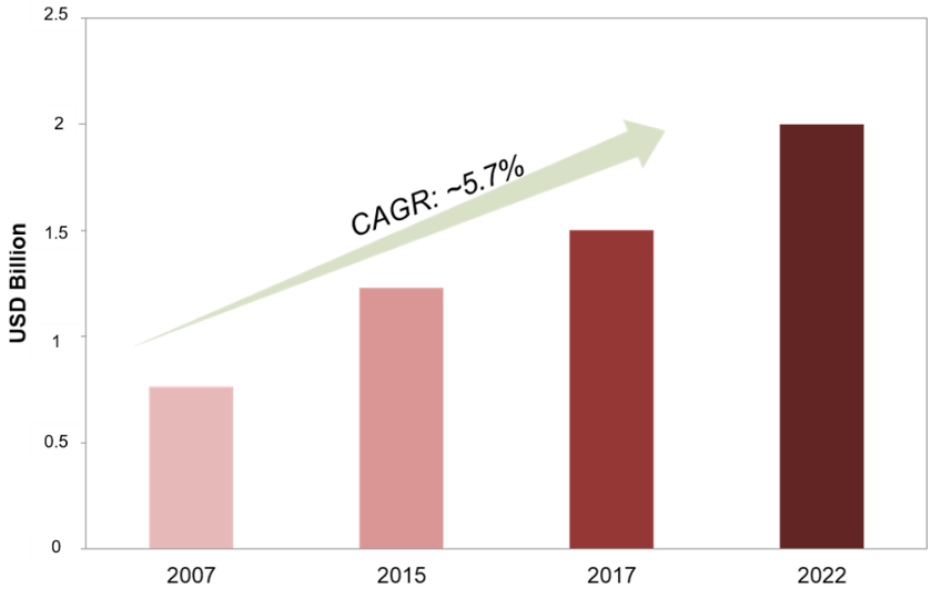

Figure 2.7. Analysis and perspective of global carotenoid market for the period between 2007 and 2022. CAGR, compound annual growth rate (adapted from McWilliams 2018).

Industrially, several companies have been producing carotenoids by biotechnological routes. As detailed in **Table 2.2**, companies from several countries have already invested in the microbial production of natural carotenoids using different sources of production and making different types of carotenoids. For example, astaxanthin is already produced by the cultivation of *Haematococcus pluvialis* or β-carotene from *Dunaliella salina* (Cyanotech 2018; Parry Nutraceuticals 2018).

Table 2.2. Companies producing carotenoids by biotechnological routes.

Company	Source	Commercialized product	Country of production	Reference
BASF Canada Inc.	Microalgae	Betatene® Natural Mixed Carotenoids	Canada	BASF Global 2018
BlueBioTech	Microalgae, *Haematococcus* sp.	Phycocyanin, Astaxanthin, Micro algae powder	German	BlueBioTech 2018
Nutralliance	*Blakeslea trispora*	β-carotene, Beta Caro-gen™	US	Nutralliance 2018
BioExtract	*Dunaliella salina*	β-carotene	India	BioExtract 2018
Cyanotech	*Haematococcus pluvialis*	BioAstin® Hawaiian Astaxanthin®	US	Cyanotech Corporation 2018
Parry Nutraceuticals	*Dunaliella salina*	β-carotene, Natural Mixed Carotenoids	India	Parry Nutraceuticals 2018
AstaReal	*Haematococcus pluvialis*	AstaReal® Astaxanthin	Japan	Asta Real Company 2018
Plankton Australia Pty Limited	*Dunaliella salina*	β-carotene	Australia	Plankton 2018

The main producers responsible for the sale of carotenoids in the global market are the United States (US) and the European countries. However, countries like India, Japan, and Australia will be responsible for significant sales in the future (McWilliams 2018). The global market of biotechnological carotenoids is highly competitive due to the presence of fewer experienced companies in the area. For a long time, this market was dominated by the big company BASF, but companies such as Nutralliance, Parry Nutraceuticals, and others have been adopting strategies for developing new products and collaborating with other industrial partners to gain market. To date, most companies producing biotechnological carotenoids employ microalgae and fungi to obtain them, which may be due to their advantages in large-scale and economical production. Therefore, an integrated approach comparing bioprocessing using microalgae and other microorganisms would be necessary.

2.10 Conclusions

A general overview of the microbial carotenoid state-of-art was herein provided, with the main aspects of the production, extraction, and commercialization stages being discussed. It is evident that the natural carotenoids produced by biotechnological routes have been gaining interest, because of their beneficial health effects and (bio)nature, gradually replacing the synthetic carotenoids in use. Therefore, the production of carotenoids by microorganisms has an excellent potential and space in the future pharmaceutical and food world market, but there are still processing industrial challenges to overcome as, for example, the high cost of the current technologies used for the production and extraction of carotenoids at the industrial scale or the use of large amounts of non-benign solvents as extract agents. We believe that use of integrated upstream and downstream platforms, as well as both the replacement of VOCs by more ecofriendly solvents and development of innovative and low-energy extraction techniques, will overcome some of the current drawbacks, improving the extraction yields and revenues. Developments in scientific research can also improve the quality and added-value of microbial carotenoids, making this an attractive field and market for several biotechnological industries.

2.11 References

Abe K, Hattor H, Hiran M (2005) Accumulation and antioxidant activity of secondary carotenoids in the aerial microalga *Coelastrella striolata* var. *multistriata*. Food Chem 100:656–661.

Al-Yafeai A, Malarski A, Böhm V (2018) Characterization of carotenoids and vitamin E in *R. rugosa* and *R. canina:* comparative analysis. Food Chem 242:435–442.

Amaya E, Becquet P, Carné S, Peris S, Miralles P (2014) Carotenoids in animal nutrition. Fefana Publication. http://fefana.org/publication/ carotenoids-in-animal-nutrition/ Accessed 10 October 2018.

Ambrosio C, Campos F, Faro Z (2006) Carotenoids as an alternative against hypovitaminosis A. Rev Nutr 19:233–243.

Anastas PT, Warner JC (1998) Green chemistry: theory and practice. Oxford University Press, New York, p 30.

Araya-Garay JM, Feijoo-Siota L, Rosa-Dos-Santos F, Veiga-Crespo P, Villa TG (2012) Construction of new *Pichia pastoris* X-33 strains for production of lycopene and β-carotene. Appl Microbiol Biotechnol 93:2483–2492.

Arvayo-Enríquez H, Mondaca-Fernández I, Gortárez-Moroyoqui P, López-Cervantes J, Rodríguez-Ramírez R (2013) Carotenoids ex-traction and quantification: a review. Anal Methods 5:2916.

Asta Real Company (2018). http://www.astareal.com/about-astaxanthin/ source. Accessed 11 July 2018.

Avalos J, Carmen LM (2005) Biological roles of fungal carotenoids. Curr Genet 3:309–324.

Baker RTM (2001) Canthaxanthin in aquafeed applications: is there any risk? Trends Food Sci Technol 12:240–243.

BASF Global (2018). https://worldaccount.basf.com/wa/NAFTA~en_US/Catalog/HumanNutrition/pi/BASF/productgroup/mixed_carotenoids_from_algae. Accessed 11 July 2018.

Bhataya A, Schmidt-Dannert C, Lee PC (2009) Metabolic engineering of *Pichia pastoris* X-33 for lycopene production. Process Biochem 44: 1095–1102.

Bhosale PB, Gadre RV (2001) Production of β-carotene by a mutant of *Rhodotorula glutinis*. Appl Mic Biotechl 55:423–427.

Bianchi LP, Antunes GM (1999) Free radicals and the main dietary anti-oxidants. Nutrition 12:123–130.

Billakanti JM, Catchpole OJ, Fenton TA, Mitchell KA, MacKenzie AD (2013) Enzyme-assisted extraction of fucoxanthin and lipids containing polyunsaturated fatty acids from *Undaria pinnatifida* using dimethyl ether and ethanol. Process Biochem 48:1999–2008.

Bioextract (2018) http://www.bioextract.co.in/contact-us.php Accessed 11 October 2018.

BlueBioTech (2018). https://www.bluebiotech.de/com/uns.htm. Accessed 11 July 2018.

Britton G, Liaaen-Jensen S, Pfander H (1995) Carotenoids. In: Spectroscopy, vol 1B. Birkhauser Verlag, Boston, p 360.

Buzzini P, Martini A (1999) Production of carotenoids by strains of *Rhodotorula glutinis* cultured in raw materials of agro-industrial origin. Bioresour Technol 71:41–44.

Cardoso LAC, Jäckel S, Karp SG, Framboisier X, Chevalot I, Marc I (2016) Improvement of *Sporobolomyces ruberrimus* carotenoids production by the use of raw glycerol. Bioresour Technol 200: 374–379.

Cardoso LAC, Kanno KYF, Karp SG (2017a) Microbial production of carotenoids A review. Afr J Biotechnol 16(4):139–146.

Cardoso LAC, Karp SG, Vendruscolo F, Kanno KY, Zoz LI, Carvalho JC (2017b) Biotechnological production of carotenoids and their appli-cations in food and pharmaceutical products. In: Carotenoids. InTech Open, London, UK.

Carocho M, Barreiro MF, Morales P, Ferreira I (2014) Adding molecules to food, pros and cons: a review on synthetic and natural food addi-tives. Compr Rev Food Sci F 13:377–399.

Carocho M, Morales P, Ferreira ICFR (2015) Natural food additives: Quo vadis? Trends Food Sci Technol 45(2):284–295.

Cataldo V, Arenas N, López J, Camilo C, Agosin E (2018) Sustainable production of β-Xanthophylls in *Saccharomyces cerevisiae*. In Mic Eng. USA.

Cerdá-Olmedo E (1987) Carotene. In: Cerdá-Olmedo E, Lipson ED (eds) Phycomyces. Cold Spring Harbor Laboratory Press, Cold Spring Harbor, pp 199–222.

Chatel G, Pereira JFB, Debbeti V, Wang H, Rogers RD (2014) Mixing ionic liquids-simple mixtures or double salts? Green Chem 16(4):2051.

Cheng YT, Yang CF (2016) Using strain *Rhodotorula mucilaginosa* to produce carotenoids using food wastes. J Taiwan Inst Chem E 61: 270–275.

Cicci A, Sed G, Bravi M (2017) Potential of choline chloride-based natural deep eutectic solvents (NaDES) in the extraction of microalgal metabolites. Chem Eng Trans.

Clotault J, Peltier D, Soufflet-Freslon V, Briard M, Geoffriau E (2012) Differential selection on carotenoid biosynthesis genes as a function of gene position in the metabolic pathway: a study on the carrot and dicots. PLoS One 7(6):38724.

Colmán MM, Martínez-Huélamo M, Miralles E, Estruch R, Lamuela-Raventós R (2016) A new method to simultaneously quantify the antioxidants: carotenes, xanthophylls, and vitamin A in human plasma. Oxidative Med Cell Longev 2016:10.

Cyanotech Corporation (2018). https://www.cyanotech.com/astaxanthin/. Accessed 11 July 2018.

Datta A, Philip L (2018) Biodegradation kinetics of toluene, ethylbenzene, and xylene as a mixture of VOCs. In: Sarma A., Singh V., Bhattacharjya R., Kartha S. (eds) Urban ecology, water quality and climate change. Water Science and Technology Library. 84. Springer.

Daub ME, Payne GA (1989) The role of carotenoids in resistance of fungi to cercosporin. Phytopathology 79:180–185.

De Rosso VV, Mercadante AZ (2007) Identification and quantification of carotenoids, by HPLC-PDA-MS/MS, from Amazonian fruits. J Agric Food Chem 55:5062–5072.

Delgado PR, Gallardo-Guerrero L, Hornero-Méndez D (2016) Carotenoid composition of strawberry tree (*Arbutus unedo* L.) fruits. Food Chem 199:165–175.

Demming-Adams B, Adams WW (2002) Antioxidants in photosynthesis and human nutrition. Sci 298:149–2153.

Dey S, Rathod VK (2013) Ultrasound assisted extraction of β-carotene from *Spirulina platensis*. Ultrason Sonochem 20:271–276.

El-Agamey A, Lowe GM, McGarvey DJ, Mortensen A, Phillip DM, Truscott G, Young AJ (2004) Carotenoid radical chemistry and antioxidant/pro-oxidant properties. Arch Biochem Biophys 430: 37–48.

El-Baky HHA, El-Baz FK, El-Baroty GS (2003) Spirulina species as a source of carotenoids and α-tocopherol and its anticarcinoma fac-tors. Biotech 2:22–240.

El-Jack M, Mackenzie A, Bramley PM (1988) The photoregulation of carotenoid biosynthesis in *Aspergillus giganteus* mut. alba. Planta 174:59–66.

Esteban R, Moran JF, Becerril JM, García-Plazaola JI (2015) Versatility of carotenoids: an integrated view on diversity, evolution, functional roles and environmental interactions. Environ Exp Bot 119:63-75.

Estrada AF, Brefort T, Mengel C, Díaz-Sánchez V, Alder A, Al-Babili S, Avalos J (2010) Ustilago maydis accumulates β-carotene at levels determined by a retinal-forming carotenoid oxygenase. Fungal Genet Biol 46:803–813.

Fang TJ, Wang JM (2002) Extractability of astaxanthin in a mixed culture of a carotenoid over-producing mutant of *Xanthophyllomyces dendrorhous* and *Bacillus circulans* in two-stage batch fermentation. Process Biochem 37:1235–1245.

Feldmann C, Ruck M (2017) Ionic liquids-designer solvents for the synthesis of new compounds and functional materials. Z Anorg Allg Chem 643:2.

Fiedor J, Burda K (2014) Potential role of carotenoids as antioxidants in human health and disease. Nutrition 6(2):466-488.

Fraser PD, Ruiz-Hidalgo MJ, López-Matas MA, Álvarez MI, Eslava AP, Bramley PM (1996) Carotenoid biosynthesis in wild type and mutant strains of *Mucor circinelloides*. Biochim Biophys Acta 1289: 203–208.

Galaup P, Suthiwong N, Leclercq-Perlat MN, Valla A, Caro Y, Fouillaud M, Guérard F, Dufossé L (2015) First isolation of *Brevibacterium* sp. pigments in the rind of an industrial red-smear-ripened soft cheese. Int J Dairy Technol 68:144–147.

Gammone MA, Riccioni G, D'Orazio N (2015) Marine carotenoids against oxidative stress: effects on human health. Marine Mar Drugs 13(10):6226–6246.

Geoffrey BA, Felix MB (1991) Canthaxanthin and the eye: a critical ocular toxicologic assessment. Cutan Ocul Toxicol 10:115–155.

Georgiou CD, Tairis N, Polycratis A (2001a) Production of β-carotene by *Sclerotinia sclerotiorum* and its role in sclerotium differentiation. Mycol Res 105:1110–1115.

Georgiou CD, Zervoudakis G, Tairis N, Kornaros M (2001b) β-Carotene production and its role in sclerotial differentiation of *Sclerotium rolfsii*. Fungal Genet Biol 34:11–20.

Gharibzahedi SMT, Razavi SH, Mousavi SM (2013) Microbial canthaxanthin: perspectives on biochemistry and biotechnological production. Eng Life Sci 13:408–417.

Giménez Giménez A, Ibáñez González MJ, Robles Medina A, Molina Grima E, García Salas S, Esteban Cerdán L (1997) Downstream processing and purification of eicosapentaenoic (20:5n-3) and arachidonic acids (20:4n-6) from the microalga *Porphyridium cruentum*. Bioseparation 7:89–99.

Giuffrida D, Sutthiwong N, Dugo P, Donato P, Cacciola F, Girard-Valenciennes E, Mao YL, Monnet C, Fouillaud M, Caro Y, Dufossé L (2016) Characterisation of the C50 carotenoids produced by strains of the cheese-ripening bacterium *Arthrobacter arilaitensis*. Int Dairy J 55:10–16.

Gong M, Bassi A (2016) Carotenoids from microalgae: a review of recent developments. Biotechnol Adv 34(8):1396–1412.

Goula AM, Ververi M, Adamopoulou A, Kaderides K (2017) Green ultrasound-assisted extraction of carotenoids from pomegranate wastes using vegetable oils. Ultrason Sonochem 34:821–830.

Grewe C, Menge S, Griehl C (2007) Enantioselective separation of all-E-astaxanthin and its determination in microbial sources. J Chromatogr A 1166:97–100.

Gu Z, Deming C, Yongbin H, Zhigang C, Feirong G (2008) Optimization of carotenoids extraction from *Rhodobacters phaeroides*. LWT Food Sci Technol 41:1082–1088.

Han JR, Zhao WJ, Gao YY, Yuan JM (2005) Effect of oxidative stress and exogenous β-carotene on sclerotial differentiation and carotenoid yield of *Penicillium* sp. PT95. Lett Appl Microbiol 40:412–417.

Han M, He Q, Zhang WG (2012) Carotenoids production in different culture conditions by *Sporidiobolus pararoseus*. Prep Biochem Biotechnol 42:293–303.

Heba M, Kanzy NF, Hoida AM (2015) Optimization of carotenoids pro-duction by yeast strains of *Rhodotorula* using salted cheese whey. Int J Curr Microbiol App Sc 4(1):456–469.

Henríquez V, Escobar C, Galarza J, Gimpel J (2016) Carotenoids in microalgae. In: Stange C. (eds) Carotenoids in nature. Subcell biochem.

Heo SJ, Jeon YJ (2009) Protective effect of fucoxanthin isolated from *Sargassum siliquastrum* on UV-B induced cell damage. J Photochem Photobiol B 95:101–107.

Humayoun Akhtar M, Bryan M (2008) Extraction and quantification of major carotenoids in processed foods and supplements by liquid chromatography. Food Chem 111:255–261.

Jaswir I, Noviendri D, Hasrini RF, Octavianti F (2011) Carotenoids: sources, medicinal properties and their application in food and nutraceutical industry. J Med Plant Res 5:33.

Jayaraj J, Devlin R, Punja Z (2008) Metabolic engineering of novel ketocarotenoid production in carrot plants. Transgenic Res 17: 489–501.

Jin H, Lao YM, Zhou J, Zhang HJ, Cai ZH (2017) Simultaneous determination of 13 carotenoids by a simple C18 column-based ultra-high-pressure liquid chromatography method for carotenoid profil-ing in the astaxanthin-accumulating *Haematococcus pluvialis*. J Chromatogr A 1488:93–103.

Johner JCF, Meireles MAA (2016) Construction of a supercritical fluid extraction (SFE) equipment: validation using annatto and fennel and extract analysis by thin layer chromatography coupled to image. LWT Food Sci Technol 36(2):210–247.

Johnson E, Schroeder W (1996) Microbial carotenoids. In: Fiechter A (ed) Advances in biochemical engineering/biotechnology. Springer, Berlin, pp 119–178.

Johnson EA (2003) *Phaffia rhodozyma*: colorful odyssey. Int Microbiol. 6:169–174.

Johnson EA, Schroeder WA (1995) Singlet oxygen and peroxyl radicals regulate carotenoid biosynthesis in *Phaffia rhodozyma*. J Biol Chem 270(31):18374–18379.

Johnson EA, Villa TG, Lewis MJ (1980) *Phaffia rhodozyma* as an astaxanthin source in salmonid diets. Aquaculture 20:123–134.

Kot AM, Błażejak S, Kurcz A (2016) *Rhodotorula glutinis*—potential source of lipids, carotenoids, and enzymes for use in industries. Appl Microbiol Biotechnol 100:6103–6117.

Krinsky NI (1989) Antioxidant functions of carotenoids. Free Radic Biol Med 7:617–635.

Kumar SPJ, Kumar GV, Dash A, Scholz P, Banerjee R (2017) Sustainable green solvents and techniques for lipid extraction from microalgae: a review. Algal Res 21:138–147.

Langi P, Kiokias S, Varzakas T, Proestos C (2018) Carotenoids: from plants to food and feed industries. Methods Mol Biol 1852:57–71.

Lavecchia R, Zuorro A (2008) Improved lycopene extraction from toma-to peels using cell-wall degrading enzymes. Eur Food Res Technol 288:153–158.

Lee YR, Row KH (2016) Comparison of ionic liquids and deep eutectic solvents as additives for the ultrasonic extraction of astaxanthin from marine plants. J Ind Eng Chem 39:87–92.

Liang MH, Zhu J, Jiang JG (2017) Carotenoids biosynthesis and cleavage related genes from bacteria to plants. Crit Rev Food Sci 13:1–20.

Lim GB, Lee SY, Lee EK, Haam SJ, Kim WS (2002) Separation of astaxanthin from red yeast *Phaffia rhodozyma* by supercritical car-bon dioxide extraction. Biochem Eng J 11:181–187.

Lin X, Gao N, Liu S, Zhang S, Song S, Ji C, Dong X, Su Y, Zhao ZK, Zhu B (2017) Characterization the carotenoid productions and profiles of three *Rhodosporidium toruloides* mutants from *Agrobacterium tumefaciens* mediated transformation. Yeast 34:335–342.

Lovisa S, Kalluri R (2018) Fatty acid oxidation regulates the activation of endothelial-to-mesenchymal transition. Trends Mol Med 24:432–434.

Macías-Sánchez MD, Fernandez-Sevill M, Acién-Fernández FG, Cerón-Garcia MC, Molina-Grima E (2010) Supercritical fluid extraction of carotenoids from *Scenedesmus almeriensis*. Food Chem 123:928–935.

Macías-Sánchez MD, Mantell C, Rodríguez M, Martínez de la Ossa E, Lubián LM, Montero O (2005) Supercritical fluid extraction of carotenoids and chlorophyll a from *Nannochloropsis gaditana*. J Food Eng 66(2):245–251.

Maldonade R, Adilma R, Scamparini P, Rodriguez Amaya B (2007) Selection and characterization of carotenoid producing yeasts from Campinas region, Brazil. Braz J Microbiol 38:65–70.

Malisorn C, Suntornsuk W (2009) Improved β-carotene production of *Rhodotorula glutinis* in fermented radish brine by continuous cultivation. Biochem Eng J 43:27–32.

Manimala MRA, Murugesan R (2018) Characterization of carotenoid pigment production from yeast *Sporobolomyces* sp. and their application in food products. J Pharm Phytochem 7:2818–2821.

Markou G, Nerantzis E (2013) Microalgae for high-value compounds and biofuels production: a review with focus on cultivation under stress conditions. Biotech Biotech 31:1532–1542.

Martins N, Roriz CL, Morales P, Barros L, Ferreira I (2016) Food colorants: challenges, opportunities and current desires of agro-industries to ensure consumer expectations and regulatory practices. Trends Food Sci Technol 52:1–15.

Mata-Gómez LC, Montañez JC, Méndez-Zavala A, Aguilar CN (2014) Biotechnological production of carotenoids by yeasts: an overview. Microb Cell Factories 21:13–12.

Matthäus F, Ketelhot M, Gatter M, Barth G (2014) Production of lycopene in the non-carotenoid-producing yeast *Yarrowia lipolytica*. Appl Environ Microbiol 80:1660–1669.

McWilliams A (2018) The global market for carotenoids, report code: FOD025F. BCC Research LLC.

Medina AR, Giménez AG, Camacho FG, Pérez JAS, Grima EM, Gómez AC (1995) Concentration and purification of stearidonic, eicosapentaenoic, and docosahexaenoic acids from cod liver oil and the marine microalga *Isochrysis galbana*. J Am Oil Chem Soc 72:575–583.

Mezzomo N, Ferreira SRS (2016) Carotenoids functionality, sources, and processing by supercritical technology: a review. J Chem-NY 2016: 1–16.

Miguel T, Calo P, Díaz A, Villa TG (1997) The genus *Rhodosporidium*: a potential source of β-carotene. Microbiology 13:67–70.

Minhas AK, Hodgson P, Barrow CJ, Adholeya A (2016) A review on the assessment of stress conditions for simultaneous production of microalgal lipids and carotenoids. Front Microbiol 7:546.

Misawa N, Shimada H (1998) Metabolic engineering for the production of carotenoids in non- carotenogenic bacteria and yeasts. J Biotechnol 59:169–181.

Miura Y, Kondo K, Saito T, Shimada H, Fraser PD, Misawa N (1998) Production of the carotenoids lycopene, β-carotene, and astaxanthin in the food yeast *Candida utilis*. Appl Environ Microbiol 129:178–195.

Molina Grima E, Belarbi EH, Acién Fernández FG, Robles Medina A, Chisti Y (2003) Recovery of microalgal biomass and metabolites: process options and economics. Biotechnol Adv 20:491–515.

Monnet C, Loux V, Gilbrat J, Spinnler H, Barbe V, Vacherie B (2010) The *Arthrobacter arilaitensis* Re117 genome sequence reveals its genetic adaptation to the surface cheese. PLoS One 5:11.

Nabae K, Ichihara T, Hagiwara A, Hirota T, Toda Y, Tamano S, Shirai T (2005) A 90-day oral toxicity study of beta-carotene derived from *Blakeslea trispora*, a natural food colorant, in F344 rats. Food Chem Toxicol 43(7):1127–1133.

Naguib YMA (2000) Antioxidant activities of astaxanthin and related carotenoids. J Agric Food Chem 48(4):1150–1154.

Navarro E, Sandmann G, Torres-Martínez S (1995) Mutants of the carotenoid biosynthetic pathway of *Mucor circinelloides*. Exp Mycol 19: 186–190.

Nutralliance (2018) http://www.nutralliance.com/about_us.html Accessed 11 October 2018.

Oliveira MVS, Vidal BT, Melo CM, Miranda RCM, Soares CMF, Coutinho JAP, Ventura SPM, Mattedi S, Lima AS (2016) (Eco)toxicity and biodegradability of protic ionic liquids. Chembiochem 147:460–466.

Olson JA (1999) Carotenoids and human health. Arch Latinoam Nutr 49:7–11.

Paiva A, Craveiro R, Aroso I, Martins M, Reis RL, Duarte ARC (2014) Natural deep eutectic solvents–solvents for the 21st century. ACS Sustain Chem Eng 2:1063–1071.

Park PK, Kim EY, Chu KH (2007) Chemical disruption of yeast cells for the isolation of carotenoid pigments. Sep Purif Technol 53:148–152.

Parniakov O, Apicella E, Koubaa M, Barba FJ, Grimi N, Lebovka N, Pataro G, Ferrari G, Vorobiev E (2015) Ultrasound-assisted green solvent extraction of high-added value compounds from microalgae *Nannochloropsis* spp. Bioresour Technol 198:262–267.

Parry Nutraceuticals (2018). http://www.parrynutraceuticals.com/ products/natural-mixed-caretenoids/. Accessed 11 July 2018.

Plankton (2018) http://www.planktonaustralia.com/index.php/australian-marine-phytoplankton/ Accessed 11 October 2018.

Powls R, Britton G (1977) A series of mutant strains of *Scenedesmus obliquus* with abnormal carotenoid compositions. Arch Microbiol 113:275–280.

Pratheeba M, Umaa RK, Kotteeswaran R, Thamaraikannan H (2014) Extraction and analysis of beta carotenoid from red yeast *Rhodotorula glutinis*. Intern J Pharm Int Life Sci 2(3):9–29.

Praveenkumar R, Lee K, Lee J, Oh Y (2015) Breaking dormancy: an energy efficient means of recovering astaxanthin from microalgae. Green Chem 17:1226–1234.

Rabbani S, Beyer P, Von LJ, Hugueney P, Kleinig H (1998) Induced β-carotene synthesis driven by triacylglycerol deposition in the unicellular alga *Dunaliella bardawil*. Plant Physiol 116:1239–1248.

Ramel F, Birtic S, Cuiné S, Triantaphylidè C, Ravanat J, Havaux M (2012) Chemical quenching of singlet oxygen by carotenoids in plants. Plant Physiol 158(3):1267–1278.

Rivera SM, Christou P, Canela-Garayoa R (2014) Identification of carotenoids using mass spectrometry. Mass Spectrom Rev 33:353–372.

Rodriguez-Amaya ADB (2016) Natural food pigments and colorants. Curr Opin Food Sci 7:20–26.

Rodriguez-Concepcion M, Avalos J, Bonet ML, Boronat A, Gomez-Gomez L, Hornero-Mendez D, Limon MC, Meléndez-Martínez A, Olmedilla-Alonso B, Palou A, Ribot J, Rodrigo MJ, Zacarias L, Zhu C (2018) A global perspective on carotenoids: metabolism, biotechnology, and benefits for nutrition and health. Prog Lipid Res 70:62–93.

Román RB, Alvárez-Pez JM, Fernández FGA, Grima EM (2002) Recovery of pure b-phycoerythrin from the microalga *Porphyridium cruentum*. J Biotechnol 93:73–85.

Saini RK, Keum YS (2017) Progress in microbial carotenoids production. Indian J Microbiol 57:129–130.

Saini RK, Keum YS (2018) Carotenoid extraction methods: a review of recent developments. Food Chem 240:90–103.

Sajilata MG, Bule MV, Chavan P, Singhal RS, Kamat MY (2010) Development of efficient supercritical carbon dioxide extraction methodology for zeaxanthin from dried biomass of *Paracoccus zeaxanthinifaciens*. Sep Purif Technol 71:173–177.

Salar-García MJ, Ortiz-Martínez VM, Hernández-Fernández FJ (2017) Ionic liquid technology to recover volatile organic compounds (VOCs). J Hazard Mater 321:484–499.

Schierle J, Bernd P, Ceresa A, Fizet C (2004) Journal of AOAC International. J AOAC Int 87:1070–1082.

Schulz H, Baranska M, Baranski R (2005) Potential of NIR-FT-Raman spectroscopy in natural carotenoid analysis. Biopolymers 77:212–221.

Shahidi F, Ambigaipalan P (2015) Novel functional food ingredients from marine sources. Curr Opin Food Sci 2:123–129.

Shih CT, Hang YD (1996) Production of carotenoids by *Rhodotorula rubra* from sauerkraut brine. LWT Food Sci Technol 29(5–6):570–572.

Silva TP, Paixão SM, Alves L (2016) Ability of *Gordonia alkanivorans* strain 1B for high added value carotenoids production. RSC Adv 6: 58055–58063.

Singh D, Gupta A, Wilkens SL, Mathur AS, Tuli DK, Barrow CJ, Puri M (2015) Understanding response surface optimisationoptimization to the modeling of Astaxanthin extraction from a novel strain *Thraustochytrium* sp. Algal Res 11:113–120.

Sy C, Dangles O, Borel P, Caris-Veyrat C (2015) Stability of bacterial carotenoids in the presence of iron in a model of the gastric compartment-comparison with dietary reference carotenoids. Arch Biochem Biophys 572:89–100.

Takaichi S, Mimuro M, Tomita Y (2006) Carotenoids—biological functions and diversity. Shokabo, Tokyo.

Taverne YJ, Merkus D, Bogers AJ, Halliwell B, Duncker DJ, Lyons TW (2018) Reactive oxygen species: radical factors in the evolution of animal life: a molecular timescale from Earth's earliest history to the rise of complex life. BioEssays 40(3):1–9.

Tinoi J, Rakariyatham N, Deming RL (2005) Simplex optimization of carotenoid production by *Rhodotorula glutinis* using hydrolyzed mung bean waste flour as substrate. Process Biochem 40(7):2551- 2557.

Torres FAE, Zaccarim BR, Novaes LCL, Jozala AF, Santos CA, Teixeira MFS, Santos-Ebinuma VC (2016) Natural colorants from filamentous fungi. Appl Microbiol Biotechnol 100(6):2511–2521.

Toti E, Chen CYO, Palmery M, Villaño VD, Peluso I (2018) Non-provitamin A and provitamin A carotenoids as immunomodulators: recommended dietary allowance, therapeutic index, or personalized nutrition? Oxidative Med Cell Longev 1:20.

Ungureanu C, Marchal L, Chirvase AA, Foucault A (2013) Centrifugal partition extraction, a new method for direct metabolites recovery from culture broth: case study of torularhodin recovery from *Rhodotorula rubra*. Bioresour Technol 132:406–409.

Vachali P, Bhosale P, Bernstein PS (2012) Microbial carotenoids. In: Barredo JL. (eds) Microbial carotenoids from fungi. Met in Mol Bio (Methods and Protocols), 898. Humana Press. Totowa, NJ.

Valduga E, Tatsch PO, Tiggemann LT (2009b) Carotenoids production: microorganisms as source of natural dyes. Quim Nova 32(9):2429– 2436.

Valduga E, Valério A, Tatsch PO (2009a) Assessment of cell disruption and carotenoids extraction from *Sporidiobolus salmonicolor* (CBS 2636). Food Bioprocess Technol 2:234–238.

Van-Eijk GW, Mummery RS, Roeymans HJ, Valadon LR (1979) A comparative study of carotenoids of *Aschersonia aleyroides* and *Aspergillus giganteus*. Antonie Van Leeuwenhoek 45:417–422.

Ventura SPM, Silva FA, Quental MV, Mondal D, Freire MG, Coutinho JAP (2017) Ionic-liquid-mediated extraction and separation processes for bioactive compounds: past, present, and future. Trends Chem Rev 117(10):6984–7052.

Wackenroder H (1831) Geiger's pharmacy magazine 33:144–172 Xavier AAO, Pérez-Gálvez A (2016) Carotenoids as a source of antioxidants in the diet. In: Stange C. (eds) Carotenoids in nature. SubcelBiochem. 79.

Xiao X, Si X, Yuan Z, Xu X, Li G (2012) Isolation of fucoxanthin from edible brown algae by microwave-assisted extraction coupled with high-speed countercurrent chromatography. J Sep Sci 35(17):2313– 2317.

Yabuzaki J (2017) Carotenoids database: structures, chemical fingerprints and distribution among organisms.

Yamagata K (2017) Carotenoids regulate endothelial functions and reduce the risk of cardiovascular disease. In: Cvetkovic DJ, Nikolic GS (eds) Carotenoids. InTech, Leskovac, pp 106–121.

Yan X, Chuda Y, Suzuki M, Nagata T (1999) Fucoxanthin as the major antioxidant in *Hijikia fusiformis*, a common edible seaweed. Biosci Biotechnol Biochem 63:605–607.

Yara-Varón E, Fabiano-Tixier AS, Balcells M, Canela-Garayoa R, Bily A, Chemat F (2016) Is it possible to substitute hexane with green solvents for extraction of carotenoids? A theoretical versus experimental solubility study. RSC Adv 6:27750–27759.

Ye VM, Bhatia SK (2012) Pathway engineering strategies for production of beneficial carotenoids in microbial hosts. Biotechnol Lett 34: 1405–1414.

Yoo AY, Alnaeeli M, Park JK (2016) Production control and characterization of antibacterial carotenoids from the yeast *Rhodotorula mucilaginosa* AY-01. Process Biochem 51:463–473.

Zaccarim BR, de Oliveira F, Passarini MRZ, Duarte AWF, Sette LD, Jozala AF, de Carvalho SEV (2018) Sequencing and phylogenetic analyses of *Talaromyces amestolkiae* from the Amazon, a producer of natural colorants. Biotechnol Prog 2:33.

Zainal-Abidin MH, Hayyan M, Hayyan A, Jayakumar NS (2017) New horizons in the extraction of bioactive compounds using deep eutectic solvents: a review. Anal Chim Acta 979:1–23.

Zaragozá MC, López D, Poquet M, Pérez J, PuigParellada P, Màrmol F (2008) Toxicity and antioxidant activity in vitro and in vivo of two *Fucus vesiculosus* extracts. J Agric Food Chem 56:7773–7780.

Zhang H, Tang B, Row KH (2014) A green deep eutectic solvent-based ultrasound-assisted method to extract astaxanthin from shrimp byproducts. Anal Lett 47:742–749.

Ziouzenkova O, Orasanu G, Sukhova G, Lau E, Berger JP, Tang G, Plutzky J (2007) Asymmetric cleavage of β-carotene yields a transcriptional repressor of retinoid X receptor and peroxisome proliferator-activated receptor responses. Mol Endocrinol 21(1): 77–88.

3. IMPROVEMENT OF CAROTENOIDS PRODUCTION FROM *Rhodotorula glutinis*

Based on the manuscript

Improvement of carotenoid production from *Rhodotorula glutinis* CCT-2186

Mussagy CU, Guimarães AA, Rocha LV, Winterburn J, Santos-Ebinuma VC and Pereira JFB

Biochemical Engineering Journal, 165, 107827, **2021**.

Abstract

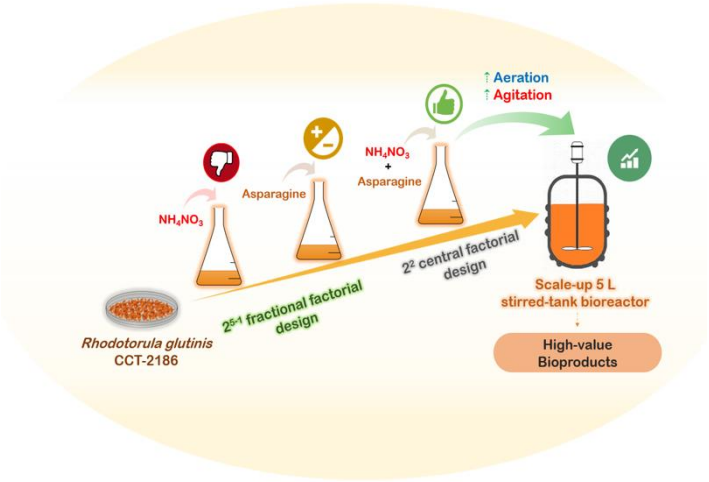

Rhodotorula strains can produce industrial valuable bioproducts. In this work, the production of carotenoids (β-carotene, torularhodin and torulene as main products), and lipids (as side-products) by *Rhodotorula glutinis* using different nitrogen sources was evaluated. Two statistical experimental designs were applied to improve carotenoid production: a first 2^{5-1} fractional factorial design evaluating the influence of independent variables pH, nitrogen source, glucose, KH_2PO_4 and $MgSO_4$ concentrations; a second 2^2 central factorial design to optimize the effect of pH and nitrogen sources. After the optimization using two statistical designs, a culture media composed of (in g/L) glucose (10), asparagine (10), NH_4NO_3 (4), KH_2PO_4 (0.52), $MgSO_4$ (0.52) was found as the best for the production of carotenoids at a pH 5 and 30 ºC, in which 220.93 mg/L of β-carotene, 253.33 mg/L of torularhodin and 28.26 mg/L of torulene were obtained. Under these conditions, 40% (w/w) of lipids were also produced by *R. glutinis* yeast. The best bioprocess was scaled-up to a 5 L stirred-tank bioreactor. The change to a bioreactor allowed to improve aeration and agitation conditions, and

consequently, increasing the production yields (m/v) in, approximately, 25.83%, 11.88%, 24.50% and 10.32% for β-carotene, torularhodin, torulene and lipids, respectively. The combined supplementation of the culture media with both organic (asparagine) and inorganic nitrogen (ammonium nitrate) sources was primordial for enhancing the carotenogenesis. *R. glutinis* are very efficient in the production of valuable carotenoids and lipids, presenting high potential of yeast for the industrial production of more sustainable cosmetic, pharmaceutical, and food products.

Keywords: *Rhodotorula glutinis; production; carotenoids; lipids; yeast.*

3.1 Introduction

Carotenoids are lipid-soluble pigments responsible for the yellow, orange and red colors (Cabral et al. 2011). These are widespread substances with important physiological roles, for example, as high-quality food color and feed additives, antioxidants, as well as an alleged role in the prevention of breast, cervical, ovarian, colorectal cancers and cardiovascular and eye diseases (Milani et al. 2017; Cerón García et al. 2018). The global market for carotenoids reached $1.5 billion in 2017 with an expected market of $2.0 billion by 2022 (Mussagy et al. 2018). The growing consumer interest in “more natural products”, due to the concern with synthetic pigments, has made the microbial production of carotenoids more favorable and sustainable alternative (Das et al. 2007; Ye and Bhatia 2012). Several studies have been demonstrating the biotechnological potential of *Rhodotorula* yeast, suggesting it as one of the most promising microorganisms for industrial food, feed and pharmaceutical processes (Squina and Mercadante 2005; Tinoi et al. 2005; Jeevaratnam and Latha 2010; Kot et al. 2016).

The yeast-based processes for obtaining carotenoids and lipids have been extensively studied and, as demonstrated for other microorganisms, with a strict dependence on production yields and growing conditions (*e.g*., nutritional content, pH, and temperature) (Valduga et al. 2009). The efficiency of carotenoids’ biosynthesis using *R. glutinis* is achieved by adjusting the composition of the cultivation medium (Malisorn and Suntornsuk 2009), commonly, through the evaluation of individual effect of different carbon (*e.g*., such as sucrose and glucose) (Buzzini and Martini 2000; Maldonade et al. 2007) or inorganic nitrogen sources (Aksu and Eren 2007; Saenge et al. 2011). However, the number of studies distinguishing the effect of inorganic and organic nitrogen sources on yeast carotenogenesis are scarce, particularly, when used cultivation medium with reduced carbon supplementation.

In any case, if the development of industrial processes for the production of microbial carotenoids is foreseen, compositional cultivation conditions are a minor part and other operational costs must also be considered for commercial viability (Yen et al. 2015). For that purpose, scale-up studies using bench-scale bioreactors

bring further advantages, such as simple operation and low energy consumption, appearing as a low-expensive solution to validate the best conditions for the production of microbial carotenoids using *R. glutinis (Malisorn and Suntornsuk 2009; Yen et al. 2015)*, as previously demonstrated (Mondala et al. 2012; Yen et al. 2015; Harith et al. 2020).

Considering that the optimization of cultivation conditions is of upmost importance to maximize the biomass, carotenoids and lipids production yields, in this work, two-statistical optimization designs were applied to improve the production of carotenoids (β-carotene, torularhodin, and torulene) using *R. glutinis* CCT 2186 yeast, namely: a first 2^{5-1} fractional factorial design - to evaluate the influence of independent variables pH, nitrogen source (organic or inorganic), glucose, KH_2PO_4 and $MgSO_4$; and a second 2^2 central factorial design - to optimize the pH and nitrogen sources. As a final test to validate the industrial potential of *R. glutinis* in producing carotenoids and lipids, the condition optimized after the second statistical design was scaled-up in a 5 L stirred-tank bioreactor.

3.2 Experimental section

3.2.1 Materials

β-carotene and torularhodin standards were acquired from Carbosynth (San Diego, CA, U.S.A). Dimethyl sulfoxide (DMSO) (P.A) was acquired from Exodo Científica (Sumaré, SP, Brazil); peptone (bacteriological) and yeast extract were obtained from Kasvi (Sao Jose dos Pinhais, PR, Brazil), glucose (P.A) from Synth (Diadema, SP, Brazil); 3,5-dinitrosalicylic acid (DNS), potassium dihydrogen phosphate (KH_2PO_4) from Vetec (Rio de Janeiro, RJ, Brazil), magnesium sulfate ($MgSO_4$) and ammonium nitrate (NH_4NO_3) from Dinâmica (Indaiatuba, SP, Brazil) and asparagine (P.A) from Inlab (Sao Paulo, SP, Brazil). All the other reagents were of analytical grade and purchased from Exodo Científica (Sumaré, SP, Brazil).

3.2.2 Microorganism and growth conditions

Rhodotorula glutinis CCT 2186 yeast was acquired from the Tropical Culture Collection André Tosello (Campinas, SP, Brazil), isolated from the leaves of a kaki

fruit (Diospyros). The inoculum was prepared by the activation of yeast *R. glutinis* CCT-2186 in Yeast Extract-Peptone-Dextrose (YPD) medium, with the following composition (g/L in deionized water): peptone (bacteriological) (20); yeast extract (10); glucose (20). The inoculum culture was prepared in Erlenmeyer® type (100 mL) flasks containing 25 mL of the YPD medium. Cells were then grown for 48 h at 30 °C and 150 rpm using a temperature-controlled orbital shaker (Tecnal, model TE-421, Piracicaba, SP, Brazil).

For the production of carotenoids and lipids, it was used a basal medium composed of (g/L in deionized water): glucose (10); KH_2PO_4 (0.52); $MgSO_4$ (0.52); NH_4NO_3 (4); and asparagine (10). The initial pH of the medium was adjusted to 5.0 by adding 2 mol/L of HCl or NaOH solution, before autoclaving. Erlenmeyer® type flasks (500 mL) containing 100 mL of the basal medium were sterilized at 121 ºC for 15 min in an autoclave (Tecnal®, model AV 30 (Piracicaba, SP, Brazil)). Afterwards, the flasks were inoculated with 5% v/v of a preculture (yeast in YPD medium) and incubated at 30 °C, 170 rpm for 72 h. Since carotenoids are intracellular, after cellular growth, the cells were then separated from the supernatant by centrifugation at 2500x*g* for 10 min at 4º C using a Hitachi CR-22N (Tokio, Japan) centrifuge. The supernatant was used to determine the residual glucose content, while cell pellets were used to quantify biomass content, *i.e.* cellular growth, carotenoid and lipid production. All the production assays using shake flasks were performed in duplicate. To optimize the production of carotenoids, the culture nutritional conditions were changed according the experimental design described in section 3.2.3.

3.2.3 Experimental design to optimize the production of carotenoids

A statistical design tool was used to improve the production of carotenoids by employing two statistical design approaches. In the first step, two 2^{5-1} fractional factorial (16 experimental runs plus 4 central points) designs were used to determine the influence of (A) glucose, (B) KH_2PO_4, (C) $MgSO_4$, (D) nitrogen source and (E) pH on the production of carotenoids, *i.e.* considering as response variables β-carotene, torularhodin and torulene, respectively. Although both biomass and lipid content were also determined in all experimental conditions, these were not the

focus of the work, and were therefore not considered as response variables in the statistical design. In the first fractional factorial design the effect of NH_4NO_3 as inorganic nitrogen source was evaluated, whilst in the second experimental design the effect of an organic nitrogen source was considered, namely asparagine as a nitrogen source. The range and levels of the components used are detailed in **Table 3.1**.

From the results of the 2^{5-1} statistical design a second statistical design was performed, where the effects of pH and asparagine (most significant parameters in the first experimental design) for the production of β-carotene, torularhodin and torulene (response variables) were optimized in a 2^2 central composite design (the range and levels of the components detailed in **Table 3.2**). In these experiments NH_4NO_3 (at 4 g/L) was added and maintained constant in the cultivation media. All the experiments were performed in an orbital shaker at 30 °C and 170 rpm for 72 h, as detailed in the previous section.

Table 3.1. Variables and factor levels employed in the two 2^{5-1} fractional factorial designs for studying β-carotene, torularhodin and torulene production by *R. glutinis*, at 30 °C, 170 rpm for 72 h.

Factor	Symbol	Range and levels		
		-	0	+
Glucose (g/L)	A	5.0	12.5	20.0
KH_2PO_4 (g/L)	B	0.5	1.0	1.5
$MgSO_4$ (g/L)	C	0.5	1.0	1.5
Nitrogen source (g/L)	D	2.0	4.0	6.0
pH	E	4	5.5	7.0

Table 3.2. Variables and factor levels used in the 2^2 central composite design for studying β-carotene, torularhodin and torulene production by *R. glutinis*, at 30 °C, 170 rpm for 72 h.

Factor	Range and levels				
	Axial (-1.41)	Lower (-1)	Center (0)	Higher (+1)	Axial (+1.41)
pH	2.2	3.0	7.0	5.0	7.8
Asparagine (g/L)	0.0	5.0	10.0	20.0	20.6

* Fixed variables (g/L): Glucose (10), KH_2PO_4 (0.52), $MgSO_4$ (0.52), NH_4NO_3 (4)

Statistica® software Version 10.0 (StatSoft, Tulsa, OK, USA) was used for the regression analysis of experimental data and to estimate the corresponding regression coefficients. The quality of the fit of the polynomial model was expressed by determination of the correlation coefficient, R^2, and statistical significance was validated by an F-test at a significance level of (p) ≤ 0.05 (in this work a confidence level of 95% was considered, considering the independent variables with p values lower than 0.05 as significant).

3.2.4 Production of carotenoids using a 5 L stirred-tank bioreactor

After the two optimizations of the production in orbital shaker, a 5 L bioreactor fermentation was performed to scale-up carotenoid production. The inoculum was prepared in Erlenmeyer® type (500 mL) flasks containing 100 mL of the YPD medium at 30 °C, 170 rpm for 48 h. Afterwards, an inoculum with a cell concentration of 0.2 mg/mL was transferred to a 5 L stirred-tank bioreactor (Tecnal®, model Tec-Bio-Flex (Piracicaba, SP, Brazil), equipped with a disc impeller, oxygen and pH electrodes) containing 4 L of the optimized cultivation medium from the 2^2 central factorial design, which was composed of (g/L in deionized water): glucose (10); asparagine (10); KH_2PO_4 (0.52); $MgSO_4$ (0.52); NH_4NO_3 (4). The cultivation medium was previously sterilized at 121 ºC for 15 min. The pH of the medium was adjusted to 5.0 at beginning of the fermentation, remaining constant throughout all the process. The fermentation was then conducted at 30 °C, 300 rpm and 1 vvm (air volume/medium volume/min) for 72 h. Antifoam was added as necessary. Samples were collected every 6 h for determination of glucose concentration, dry cell weight, lipids, β-carotene, torularhodin and torulene content.

3.2.5 Analytical methods

3.2.5.1 Determination of residual sugars and dry cell weight

Total reducing sugars were determined spectrophotometrically with 3,5-dinitrosalicylic acid (DNS) method, as described by Miller (Miller 1959), using a standard glucose calibration curve. Dry cell weight (DCW) of each sample was determined according to the method described by Buzzini and Martini (Buzzini and Martini 2000). Briefly, each sample of fermented broth was centrifuged at 2500 x*g*

for 5 min, washed twice with the same volume of distilled water, dried in petri dishes at 50 °C for 48 h, and then weighed in an analytical balance (Shimadzu, model AUY220, Sao Paulo, SP, Brazil) ($\pm 10^{-4}$ g) for determination of the DCW.

3.2.5.2 Determination of lipid content

To determine the lipid content of the yeast cells, lipids were extracted, dried and weighed by using a method adapted from Bligh and Dyer (Bligh and Dyer 1959). Briefly, the cells were harvested by centrifugation (2500 *xg* for 10 min at 10 °C), washed and dried to obtain constant weight. The weight of the dry pellet was measured in an analytical balance. The dry pellet was then resuspended in 30 mL of a chloroform/methanol (2:1 v/v) mixture and vortexed for 15 min at room temperature. Further, 10 mL of a NaCl aqueous solution (2 mol/L) was added, and the mixture centrifuged at 2500 x*g* for 15 min to separate the aqueous and organic phase. The organic phase was transferred to rotary evaporator flasks (previously weighed, w_1), which were dried under vacuum (at 300 mbar for 30 min) until the organic phase was fully evaporated, and the final weight of the flask measured (w_2). Lipid content, expressed as % dry cell weight *per* initial weight of the pellet (*w*) was determined according to **Equation 3.1**, expressed as % dry cell weight (*w* = weight of the cell pellet).

$$\text{Lipid content } (\%) = \frac{W_2 - W_1}{W} \times 100 \qquad (3.1)$$

In 5 L stirred-tank bioreactor, for comparison purposes the lipid concentration was evaluated in g/L.

3.2.5.3 Carotenoids isolation and characterization

Carotenoids from *R. glutinis* yeast were first isolated by using a conventional method described by Mussagy et al (Mussagy et al. 2019). Briefly, *R. glutinis* wet biomass was subjected to chemical treatment with successive solvent extractions using DMSO. After the extraction, the samples were centrifuged at 2500 *xg* at 4 °C for 10 min and the supernatants containing carotenoids carefully recovered and lyophilized. Lyophilized carotenoids-rich extracts were solubilized in acetone (1 mL) and separated by liquid chromatography in a column filled with silica gel 60 (Merck,

Pinheiros, SP, Brazil) and a mixture of hexane/ethyl ether/acetic acid (70:29:1 v/v/v) as mobile phase. A qualitative analysis of the extracts by thin-layer chromatography (TLC) using pre-coated TLC sheets ALUGRAM (silica gel 60, Macherey-Nagel, Germany) was also carried out (a mixture of hexane/ethyl ether/acetic acid (70:29:1 v/v/v) used as mobile phase). The three fractions of the carotenoid lyophilized extracts separated in the column liquid chromatography were collected in different glass test tubes and then identified by reversed-phase high-performance liquid chromatography, RP-HPLC (using column chromatograph Shimadzu Shim-pack C_{18} (Japan), 4.6 mm x 250 mm and methanol/acetonitrile/dichloromethane (60:10:30, v/v/v) as the mobile phase). The chemical structures and purities of the three fractions of carotenoids were confirmed by proton nuclear magnetic resonance (^{1}H NMR) using a Bruker Avance III HD 600 (14.1T) (Massachusetts, USA).

After the identification and characterization of the chemical structures of carotenoids produced by *R. glutinis* yeast, the respective visible-light absorption spectra were determined using a Thermo Scientific (Genesis10S) UV−Vis spectrophotometer (accuracy: ± 0.005 AU at 1.0 AU) (China). The visible-light spectra from 380 to 600 nm were obtained, and the respective carotenoids calibration curves established at 450 nm (β-carotene), 480 nm (torulene), and 500 nm (torularhodin). The carotenoid concentrations (mg/L) were determined according to the pre-established calibration curves obtained from pure β-carotene and torularhodin standards, and from the purified fraction of torulene.

3.2.5.4 Extraction and determination of Carotenoids

Carotenoid extraction was carried out according to the modified method of Mussagy et al (Mussagy et al. 2019). After lipid extraction, the cell pellets were mixed with 5 mL of DMSO and disrupted by maceration (5 min ON/15 min OFF for a total 1 h). After the procedure the supernatant was recovered, and the procedure repeated until the cells become fully bleached. The supernatant recovered from the cell disruption was mixed with 10 mL of 20 % (w/v) of NaCl aqueous solution and 10 mL of petroleum ether. After the formation of both phases, the nonpolar phase was collected and excess water was removed with sodium sulfate (Na_2SO_4), the carotenoid-rich extracts were then dissolved in acetone (1 mL), filtered with

Polytetrafluoroethylene (PTFE) membrane of 0.22 µm pore size, and quantified using external calibration curves in a Thermo Scientific® UV-Vis spectrophotometer (model Genesis 10S, China). Since carotenoids are light-sensitive, all assays were performed by using sealed vials covered with aluminum foil to protect carotenoids from oxidation, photodegradation and isomerization.

3.3 Results and discussion

3.3.1 Optimization of the production of carotenoids by statistical design

The production of a microbial metabolite is largely influenced by the components of the growth medium, particularly, carbon, nitrogen and mineral sources, pH and temperature (de Oliveira et al. 2019; de Oliveira et al. 2020). The use of experimental design methodology allows a reduction of the number of experiments and assess the interaction among the independent variables (Park et al. 2007). In the present work, two 2^{5-1} fractional factorial designs and one 2^2 central factorial design were applied to improve the production of three intracellular carotenoids (β-carotene, torularhodin and torulene) by *R. glutinis* CCT 2186.

In the first set of experiments, a 2^{5-1} design was applied to assess the significance of the following independent variables on carotenoid production, *i.e.*: glucose (A); KH_2PO_4 (B); $MgSO_4$ (C); NH_4NO_3 (D); pH (E). The 2^{5-1} design strategy is adequate for initial screenings, since it decreases the number of experiments (in comparison to the full factorial design), as well as it elucidates the main effects in the microbial processes, and allows the adjustment of the next statistical optimization strategy (Rodrigues and Lemma 2014). The matrix of the first 2^{5-1} fractional factorial design and corresponding experimental results of biomass, lipid and carotenoid production by *R. glutinis* are shown in **Table 3.3**.

Table 3.3. Matrix of 2^{5-1} fractional factorial design for study of β-carotene, torularhodin and torulene production by *R. glutinis* using NH_4NO_3 as nitrogen source, at 30 °C, 170 rpm for 72 h.*

Run	Design matrix					Experimental results				
	A	B	C	D	E	DCW (g/L)	Lipid content (% w/w)	β- carotene (mg/L)	Torularhodin (mg/L)	Torulene (mg/L)
1	-	-	-	-	+	2.71	42.04	106.30	135.84	11.55
2	-	-	-	+	-	6.06	21.75	111.55	141.98	11.74
3	-	-	+	-	-	3.96	4.95	80.30	101.79	8.41
4	-	+	-	-	-	5.58	13.66	157.05	187.07	15.60
5	+	-	-	-	-	2.67	29.78	73.80	92.59	7.64
6	-	-	+	+	+	3.13	18.05	123.30	153.94	12.81
7	-	+	-	+	+	3.06	24.08	119.30	157.62	13.50
8	-	+	+	-	+	5.02	20.33	140.80	178.79	15.07
9	-	+	+	+	-	2.33	26.45	117.55	143.20	11.12
10	+	+	+	-	-	4.84	3.46	88.55	113.45	9.40
11	+	+	-	+	-	4.32	21.13	103.05	134.31	11.32
12	+	+	-	-	+	5.30	10.06	90.80	112.83	9.40
13	+	-	+	-	+	3.70	4.87	106.05	131.24	10.17
14	+	-	+	+	-	3.50	48.99	74.05	92.59	7.64
15	+	-	-	+	+	3.71	37.23	142.30	176.33	14.11
16	+	+	+	+	+	3.60	38.53	88.05	107.62	8.90
17	0	0	0	0	0	4.65	9.40	63.55	79.09	5.96
18	0	0	0	0	0	4.68	6.60	67.05	81.85	6.57
19	0	0	0	0	0	4.57	7.24	75.05	90.75	6.84
20	0	0	0	0	0	4.74	8.61	59.80	73.88	5.65

*Glucose (A); KH_2PO_4 (B); $MgSO_4$ (C); NH_4NO_3 (D); pH (E)

From **Table 3.3**, among the 20 runs performed, it was observed that the DCW varied from 2.33 to 6.06 g/L, the lipid content from 3.46 to 48.99 %, whilst the production of carotenoids varied from 59.80 to 157.05 mg/L for β-carotene, 73.88 to 187.07 mg/L for torularhodin and 5.65 to 15.60 mg/L for torulene. The highest DCW concentration (6.06 g/L) was achieved in run 2 [(glucose (5.0 g/L), KH_2PO_4 concentration (1.5 g/L), $MgSO_4$ concentration (0.5 g/L), NH_4NO_3 concentration (0.5 g/L) and pH (4.0)], while the highest production of carotenoids and content of lipids occurred at run 4 [(glucose (5.0 g/L), KH_2PO_4 (1.5 g/L), $MgSO_4$ (0.5) NH_4NO_3 (2.0 g/L), and pH (4.0)] and run 14 [(glucose (20.0 g/L), KH_2PO_4 (0.5 g/L), $MgSO_4$ (1.5 g/L), NH_4NO_3 (6.0 g/L), and pH (4.0)], respectively.

R. glutinis accumulate lipids and carotenoids, in which their biosynthesis share acetyl-CoA as common precursor, although these compounds have distinct metabolic pathways (Perrier et al. 1995). This observation is in line with our results,

since the experimental conditions for obtaining the highest lipid content were different from those where an increase of carotenoid production yields was observed. In fact, while lipids are produced and accumulated during the exponential growth of the microorganism, in which the consumption of carbon source is rapid, the carotenoids are secondary metabolites produced from the beginning of the yeast's stationary phase to the death phase (Singh et al. 2016). Carbon/nitrogen (C/N) ratios of the growth medium influence the production of lipids, specially, affecting the activity of adenosine monophosphate (AMP) dependent isocitrate dehydrogenase in the tricarboxylic acid cycle (TCA) (Ratledge 1993), and thus, channelizing the acetyl CoA for lipid biosynthesis. With the yeast growing, the C/N ratio is altered, with higher levels of nitrogen than carbon, which will activate the precursors for the production of carotenoids, usually, in the deceleration phase of the yeast (*i.e.* between the end of the exponential phase and the beginning of the stationary phase) (Somashekar and Joseph 2000). A medium with a high C/N ratio tends to produce lipids rather than carotenoids, whilst the increase of Nitrogen tends to privilege the carotenogenesis (Somashekar and Joseph 2000).

Although the highest content of carotenoids was achieved in run 4, it is important to note that, among them, torularhodin (187.07 mg/L) was the main carotenoid produced, followed by β-carotene (157.05 mg/L) and with lower torulene content (15.60 mg/L). The low amount of torulene can be explained by a preferential production of torularhodin by the *R. glutinis*, which according to their biosynthesis pathway, torularhodin is always obtained after transformation of the torulene, including, hydroxylation and oxidation (Gribanovski-Sassu and Foppen 1968; Kot et al. 2018).

As the main objective of this work is to evaluate carotenoid production by *R. glutinis,* the analysis of variance (ANOVA) of production of the three carotenoids production as variables response was performed. First order models were fitted to the experimental data in order to evaluate the significance of five factors (pH, NH_4NO_3, glucose, KH_2PO_4 and $MgSO_4$), as detailed in **Table 3.4**.

Table 3.4. Analysis of variance (ANOVA) applied to the regression models according to 2^{5-1} fractional factorial design to evaluate the influence of pH, NH_4NO_3, glucose, KH_2PO_4 and $MgSO_4$ on carotenoid production by *R. glutinis,* at 30 °C, 170 rpm for 72 h.

Factors	β- carotene			Torularhodin			Torulene		
	SS	*F*-ratio	*p*-value	SS	*F*-ratio	*p*-value	SS	*F*-ratio	*p*-value
Glucose	40.64	0.96	0.40	14.73	0.30	0.62	0.47	1.57	0.30
KH_2PO_4	907.52	21.45	0.02*	1435.08	28.79	0.01*	12.67	42.50	0.01*
$MgSO_4$	9.77	0.23	0.66	25.63	0.51	0.53	0.11	0.35	0.59
NH_4NO_3	650.25	15.36	0.03*	1191.11	23.90	0.02*	12.71	42.62	0.01*
pH	228.77	5.40	0.10	409.96	8.23	0.03*	4.12	13.82	0.03*
Pure Error	126.92			149.51			0.89		

*Significant at $p < 0.05$

The ANOVA statistical analysis of the results presented in **Table 3.4** shows that the production of β-carotene was significantly ($p < 0.05$) influenced by the concentration of KH_2PO_4 and NH_4NO_3, while the production of torulene and torularhodin, in addition to the concentration of salts, also were affect by the pH of the cultivation medium (*cf.* Pareto chart from **Figure 3.1-a**). It is important to note that the inorganic source of nitrogen (NH_4NO_3) revealed a significant effect ($p < 0.05$) on the production of the three carotenoids within all the ranges explored in our experiments.

Interestingly, the yields of carotenoid production obtained were higher than those reported in previous studies, using inorganic nitrogen source in the culture medium (Bhosale and Gadre 2001; Saenge et al. 2011). Saenge et al., (Saenge et al. 2011) used different inorganic nitrogen sources to produce carotenoids in a growth medium containing palm oil mill effluent (POME), producing 115.76 mg/L and 105.85 mg/L of carotenoid, with using ammonium sulfate and ammonium nitrate, respectively. Bhosale and Grade (Bhosale and Gadre 2001) also evaluate the influence of different ammonium salts as source of inorganic nitrogen in cultivation media containing molasses to produce carotenoids with *R. glutinis* mutant 32; however, regardless the ammonium-salt added, the concentration of total carotenoid produced were significant lower (*i.e.*, ammonium sulfate ≈ 14.14 mg/L, ammonium nitrate ≈ 8.8 mg/L and ammonium chloride ≈ 17.8 mg/L).

In order to increase the production of carotenoids, and considering that NH_4NO_3 had a significant effect (at a confidence level $p < 0.05$) on the production of the three carotenoids, the next step was to determine whether changing from a source of inorganic nitrogen for an organic (in this case asparagine) has significant influence on the production yields. Asparagine was chosen as organic nitrogen source, based on previous work by our group (Mussagy et al. 2019), where the ability of this amino acid to stimulate the carotenogenesis in *R. glutinis* was observed. Except for the nitrogen source, all other growth conditions were the same as in the first 2^{5-1} factorial design. The main results of the production of biomass, lipids and carotenoids by *R. glutinis* obtained with the second 2^{5-1} fractional factorial design are detailed in **Table 3.5**.

Table 3.5. Matrix of 2^{5-1} fractional factorial design for study of biomass, lipid content, β-carotene, torularhodin and torulene production by *R. glutinis* using asparagine as nitrogen source, at 30 °C, 170 rpm for 72 h.

Run	Design matrix					Experimental results				
	A	B	C	D	E	DCW (g/L)	Lipid content (% w/w)	β-carotene (mg/L)	Torularhodin (mg/L)	Torulene (mg/L)
1	-	-	-	-	+	2.65	26.81	121.91	124.87	14.21
2	-	-	-	+	-	3.57	13.14	190.52	203.31	23.50
3	-	-	+	-	-	2.58	2.62	140.37	161.87	18.42
4	-	+	-	-	-	4.20	17.85	166.54	171.74	19.14
5	+	-	-	-	-	0.27	61.60	124.16	129.87	14.65
6	-	-	+	+	+	4.95	23.04	72.84	71.11	6.03
7	-	+	-	+	+	2.62	27.62	110.87	115.99	13.09
8	-	+	+	-	+	4.90	38.02	130.17	136.25	15.29
9	-	+	+	+	-	2.50	18.03	100.04	104.87	11.65
10	+	+	+	-	-	4.07	15.13	140.17	147.37	16.83
11	+	+	-	+	-	2.80	28.20	132.04	137.00	16.17
12	+	+	-	-	+	3.66	13.69	172.04	176.99	20.30
13	+	-	+	-	+	1.92	13.62	114.04	120.12	14.06
14	+	-	+	+	-	3.32	14.56	177.27	188.37	21.40
15	+	-	-	+	+	3.17	43.19	112.54	121.12	13.81
16	+	+	+	+	+	4.86	6.36	201.92	155.46	9.38
17	0	0	0	0	0	2.22	27.39	137.92	137.37	14.06
18	0	0	0	0	0	2.22	26.83	117.67	118.62	12.90
19	0	0	0	0	0	2.19	26.76	123.42	129.37	14.10
20	0	0	0	0	0	2.36	22.86	126.54	129.49	12.56

*Glucose (A); KH_2PO_4 (B); $MgSO_4$ (C); asparagine (D); pH (E)

As can be seen from **Table 3.5**, the presence of asparagine (D) increased the production of the three intracellular carotenoids compared to the first fractional

factorial design. Interestingly, the highest production rates were not achieved in the same run, *i.e.*, the highest concentration of β-carotene (201.92 mg/L) was obtained in the run 16, while both highest concentration of torularhodin and torulene were obtained in run 2, with 203.31 mg/L and 23.50 mg/L, respectively. Comparing the carotenoid production rates using the source of organic nitrogen (**Table 3.5**) with those using an inorganic one (**Table 3.3**), there was an increase of 22.23%, 7.98% and 31.62% in the production of β-carotene, torularhodin and torulene, respectively. Despite the focus on the production of carotenoid, it is important to note that supplementation with asparagine also favored the production and accumulation of lipids by *R. glutinis*, reaching, in run 5, a production of approximately 61.60% of lipids, which corresponds to an increase of about 20% than in the absence of a source of organic nitrogen (first factorial design).

The experimental results of carotenoid production were subjected to analysis of variance (ANOVA) (**Table 3.6**), in which first order models were used to adjust the experimental data, evaluating the main effects of the five factors (pH, asparagine, glucose, KH_2PO_4 and $MgSO_4$).

Table 3.6. Analysis of variance (ANOVA) applied to the regression models according to 2^{5-1} fractional factorial design that evaluated the influence of pH, asparagine, glucose, K_2HPO_4 and $MgSO_4$ on carotenoid production by *R. glutinis*, at 30 °C, 170 rpm for 72 h.

Factors	β- carotene			Torularhodin			Torulene		
	SS	*F*-ratio	*p*-value	SS	*F*-ratio	*p*-value	SS	*F*-ratio	*p*-value
Glucose	5457.52	75.16	0.00*	3448.33	58.17	0.00*	15.62	24.91	0.02*
KH_2PO_4	985.02	13.57	0.03*	467.97	7.89	0.07	0.67	1.07	0.38
$MgSO_4$	897.30	12.36	0.03*	2249.84	37.95	0.01	66.06	105.35	0.00*
Asparagine	536.85	7.39	0.07	82.31	1.38	0.32	0.03	0.05	0.83
pH	470.67	6.48	0.08	2002.34	33.78	0.01*	56.66	90.37	0.00*
Pure Error	217.82			177.847			1.881		

*Significant at $p < 0.05$

The ANOVA analysis of **Table 3.6** and Pareto chart of **Figure 3.1-b** show that, in the study range, KH_2PO_4, $MgSO_4$ and glucose concentrations had a significant effect (at 95% of confidence level) on the variable response β-carotene. Regarding torularhodin as a variable response, glucose concentrations and pH have significant

effect, while for torulene, glucose, $MgSO_4$ concentrations and pH exhibited a significant effect with 95% of confidence level.

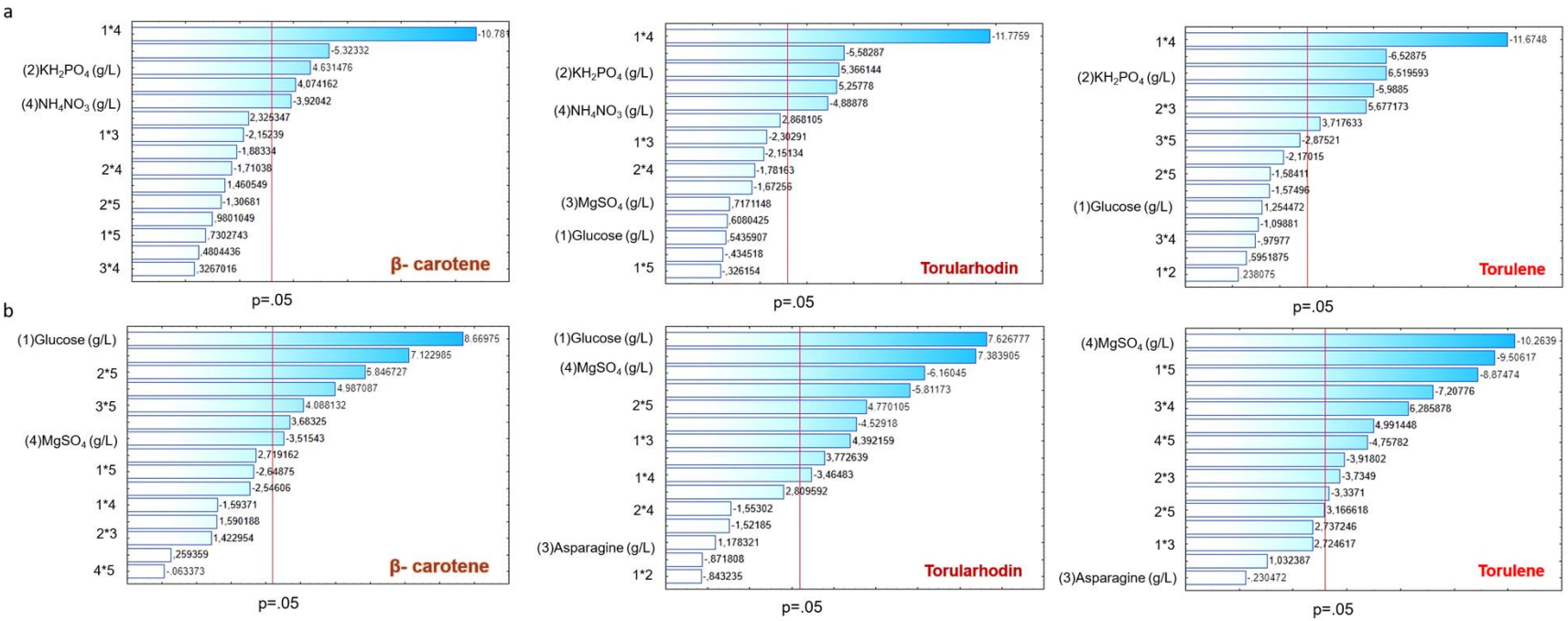

Figure 3.1. Pareto chart for the effects of variables: (1) glucose, (2) KH_2PO_4, (3) $MgSO_4$, (4) nitrogen source (**a:** NH_4NO_3 and **b:** asparagine) and (5) pH under β- carotene, torularhodin and torulene production by *R. glutinis*, at 30 °C, 170 rpm for 72 h, according to the 2^{5-1} fractional factorial design.

The number of studies evaluating the effect of specific amino acids on the production of carotenoid using *R. glutinis* yeast are scarce (Bhosale and Gadre 2001; Mihalcea et al. 2011; Voaides and Dima 2012), and among them with inconclusive results on the effects of amino acids on carotenogenesis. For example, Bhosale and Gadre (Bhosale and Gadre 2001) observed a decrease in the production of carotenoids by *R. glutinis* (mutant 32) with the supplementation of the growth media with amino acids (namely, threonine, glycine, aspartic acid, histidine, lysine, serine, tryptophan and tyrosine), while Voaides and Dima (Voaides and Dima 2012) achieved the highest carotenoid rates by cultivating *R. glutinis* strain Rd3 in amino acid-supplemented media (*i.e.*, using 0.1% (m/v) of glutamic acid ≈ 87.20 µg/g cell dry mass or 0.1% (m/v) of threonine ≈ 63.81 µg/g cell dry mass). Mihalcea et al., (Mihalcea et al. 2011) also obtained a greater accumulation of carotenoids (≈ 1500 µg/L) when *Rhodotorula sp.* yeast were grown in a medium supplemented with threonine (0.2% (m/v)) and alanine (0.1% (m/v)).

Although the asparagine concentration had no significant effect (at 95% confidence level), compared to the first fractional factorial design (which used only NH_4NO_3 as nitrogen source), it was evident that the addition of a source of organic was positive for the carotenoid production, specially torularhodin and torulene, in which asparagine has significance as interaction parameter with the other variables. This is in line with the findings of Alcantara and Sanchez(Alcantara and Sanchez 1999), who stated that the production of zeaxanthin by *Flavobacterium sp.* can be significantly improved (up to 4-fold increase) by combining organic nitrogen and carbon sources, in particular, supplementing the defined culture medium (NaCl; KH_2PO_4; $MgSO_4$ and inorganic salts) with L-asparagine and glucose.

The two initial 2^{5-1} statistical designs demonstrated that both inorganic and organic sources influence the production of carotenoids, but not exclusively, since the other experimental parameters exhibited significance in the three carotenoids as response variables. It is expected because the microbial production of carotenoids is very complex and depends on several factors, *e.g.*, nitrogen and carbon source, presence of microelements in the medium, temperature and pH (Kot et al. 2019).

Based on the results of the two-fractional factorial design, and considering that the use of sources of organic and inorganic nitrogen could allow an improvement in the carotenoids production rates, a 2^2 central factorial design was employed to evaluate the influence of pH and the simultaneous use of inorganic and organic nitrogen sources, as independent variables, in the production of carotenoids (β-carotene, torularhodin and torulene, as response variables). Industrially, high production titers are desired for most microbial-based processes, usually achieved by using high concentration of carbon source (*e.g.*, glucose) in the growth medium. The first optimization, like the previous literature (Bhosale and Gadre 2001), demonstrated that high concentrations of glucose allow high biomass production, but do not necessarily reflect high yields of yeast carotenoid biosynthesis. Therefore, in the second design, low concentrations of glucose (10 g/L) were used, first to reduce some negative effect on carotenogenesis that can occur at high carbon concentration and, second, to clearly elucidate the role of nitrogen in carotenoid production.

For the 2^2 central factorial design, a basal medium composed of (g/L in deionized water) glucose (10), KH_2PO_4 (0.52) and $MgSO_4$ (0.52) was used. All other cultivation parameters were maintained as the previous designs (*i.e.*, temperature at 30 °C and aeration at 170 rpm). This design evaluated the combination level of organic and inorganic nitrogen source, changing the concentration of asparagine (from 5.0 to 20.6 g/L) to a fixed NH_4NO_3 concentration (4 g/L), while the level of pH ranged from 2.2 to 7.8. All the details about the design matrix and corresponding experimental results *i.e.* DCW, lipid and carotenoids content, are detailed in **Table 3.7**.

Table 3.7. Experimental design matrix and experimental results for the 2^2 central factorial design, on carotenoid production by *R. glutinis,* at 30 °C, 170 rpm for 72 h.

Run	Design matrix		Experimental results				
	pH	Nitrogen source (g/L)	DCW (g/L)	Lipid content (% w/w)	β- carotene (mg/L)	Torularhodin (mg/L)	Torulene (mg/L)
1	3.0 (-1)	5.0 (-1)	3.67	38.73	247.63	190.25	28.08
2	3.0 (-1)	20.0 (1)	5.01	44.08	193.15	183.4	21.78
3	7.0(1)	5.0 (-1)	4.63	15.54	223.98	208.49	25.78
4	7.0 (1)	20.0 (1)	5.18	43.46	163.40	156.83	14.47
5	2.2 (-1.41)	10.0 (0)	5.16	41.06	165.05	121.53	18.54
6	7.8 (1.41)	10.0 (0)	5.48	33.92	126.42	118.78	14.53
7	5.0 (0)	0.0 (-1.41)	3.26	25.13	128.55	117.23	14.96
8	5.0 (0)	20.6 (1.41)	5.67	39.18	190.91	183.31	20.95
9 (C)	5.0 (0)	10.0 (0)	4.28	39.75	248.25	216.61	28.26
10	5.0 (0)	10.0 (0)	4.15	34.46	253.33	218.48	28.45
11	5.0 (0)	10.0 (0)	4.08	32.08	249.12	216.09	28.26
12	5.0 (0)	10.0 (0)	4.05	37.53	252.01	220.93	28.20

*Fixed variables (m/v): glucose (10 g/L), KH_2PO_4 (0.52 g/L), $MgSO_4$ (0.52 g/L), NH_4NO_3 (4 g/L). *C- Central point.

As can be seen in **Table 3.7**, regardless of the run, all conditions of the 2^2 experimental design allowed a significant increase in the production of the three carotenoids by *R. glutinis*. The maximum values of β-carotene (from 216.61 to 220.93 mg/L), torularhodin (from 248.25 to 253.33 mg/L) and torulene (from 28.20 to 28.26) concentration were obtained in the center point runs (9, 10, 11 and 12), corresponding to cultures supplemented with 10 g/L of asparagine, 4 g/L of NH_4NO_3 and pH 5. The combination of nitrogen source and pH also influenced the biomass production, especially the first variable, since the largest DCW (5.67 g/L) was achieved with the highest concentration of asparagine (20.6 g/L) - run 8.

Regarding the lipid content, the nitrogen combination (organic and inorganic) increased the lipid production (run 5), which, under same processual conditions, allowed a two-fold increase compared to cultivation with a single inorganic nitrogen source (run 2 from **Table 3.3**), and three-fold compared to the cultivation with an organic source (run 2 from **Table 3.5**). The same positive effect on production of carotenoids was observed for the other equivalent processual conditions, namely, in run 2 (**Table 3.7**) which exhibited an increase of 15.6% and 2.01% compared to cultivations using a single inorganic (run 15 of **Table 3.3**) and organic nitrogen source (run 15 of **Table 3.5**), respectively. Interestingly, the highest production of

lipids was obtained by cultivating *R. glutinis* in a medium rich in nitrogen sources and with minimal concentrations of carbon (10 g/L of glucose).

To obtain further information about the influence of each variable (organic and inorganic nitrogen supplementation and pH), as well as the interaction between both variables in the production of β-carotene, torularhodin and torulene (response variables), the Pareto charts and response surfaces ($p < 0.05$) were prepared, as depicted in **Figs. 3.2 a**, **b** and **c**, respectively.

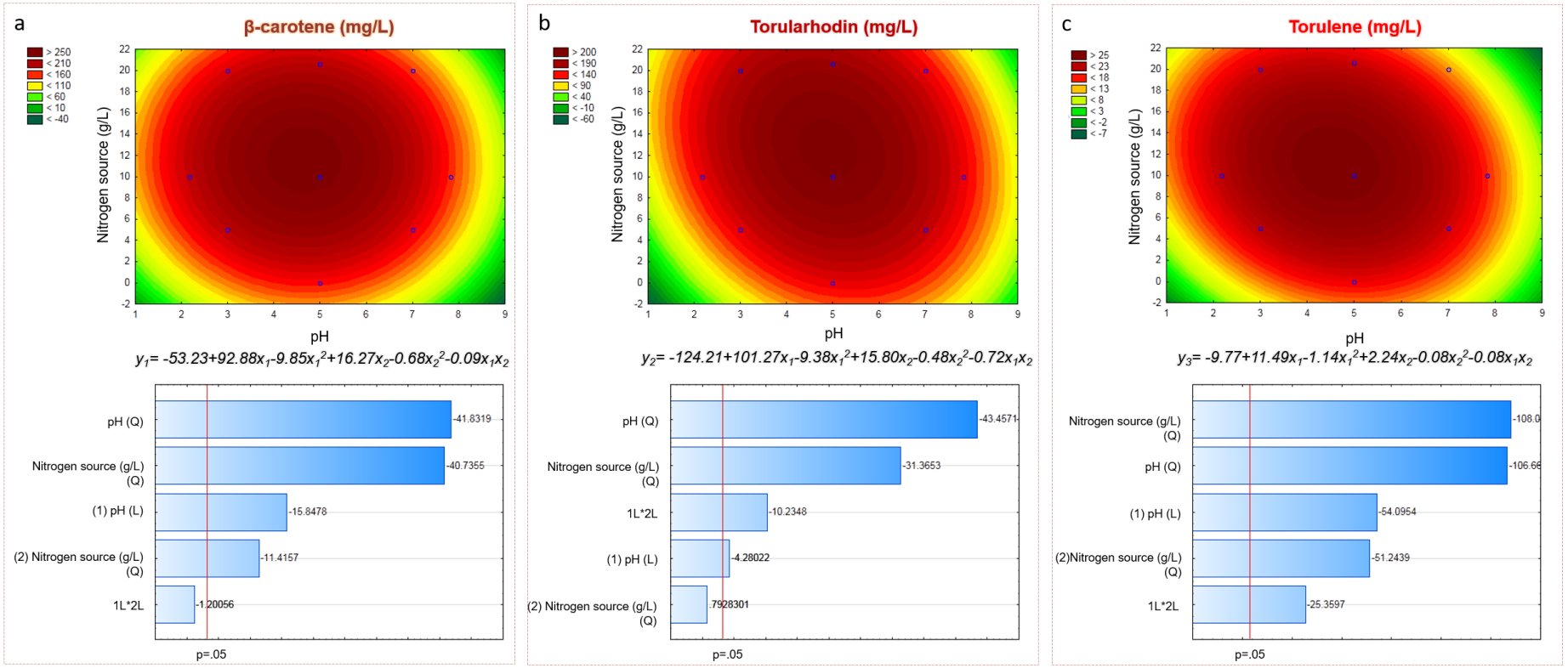

Figure 3.2. Response surface and Pareto Chart for studies of the effects of independent variables x_1: pH and x_2: nitrogen source on y_1: β-carotene (**a**), y_2: torularhodin (**b**) and y_3: torulene (**c**) production by *R. glutinis* CCT-2186 in 72 h in an orbital shaker at 30 °C and 170 rpm.

As shown in **Figs. 3.2 a**, **b** and **c**, for all the response variables, both pH and combined nitrogen source, in linear and quadratic terms, exhibited significant negative effects ($p < 0.05$), *i.e.*, in the study range, the simultaneous increase of organic and inorganic nitrogen concentration and pH caused a reduction in the production of carotenoids. **Table A.1** in the **Appendix A** shows the probability values (*p*) for the β-carotene, torularhodin and torulene. Based on the results of the complete regressions, the models were determined to pH (x_1) and nitrogen combination (x_2) under the production of β-carotene (y_1), torularhodin (y_2) and torulene (y_3), as described by the equations shown in **Figure 3.2.**

The production of secondary metabolites by *R. glutinis* is dependent on both pH and concentrations of nitrogen and carbon sources, which will have a direct impact on microbial carotenogenesis, namely on the type and amount of carotenoids synthesized by yeast cells (Ramel et al. 2012). So, as needed, different conditions can be usefully exploited to maximize the production of carotenoids.

In summary, from the results of **Figure 3.2,** the central runs (*i.e.*, pH 5, 10 g/L of asparagine and 4 g/L of NH_4NO_3) were the best conditions for the simultaneous production of β-carotene (220.93 mg/L), torularhodin (253.33 mg/L) and torulene (28.26 mg/L). Comparing the optimized results from the 2^2 central factorial design (**Table 3.7**) with those from the second 2^{5-1} fractional design (**Table 3.5 -** run 16,), increases of 8.61%, 19.74% and 17.37%, respectively, for the production of β-carotene, torularhodin and torulene were achieved. It is evident that a combined supplementation of the cultivation medium with asparagine and NH_4NO_3 favors the carotenegenesis as well as lipid accumulation by *R. glutinis*. However, together, the optimized results also revealed that at higher pH values the yeast's ability to synthesize lipids is decreased, probably due to the inhibition of yeast growth.

3.3.2 Carotenoid production using a 5 L stirred-tank bioreactor

As shown in the previous section, the use of adequate statistical design approaches allows to find the optimal conditions for the microbial production of biomolecules, in this case intracellular carotenoids. However, mostly of the experiment designs are operated at lab scale, which are far from representative of the bioreactor-based processes at industrial scale. Thus, in order to provide further

information about the ability of *R. glutinis* to produce carotenoids at a larger scale, as final state the optimized culture media was tested in a 5 L stirred-tank bioreactor. After the three experimental designs for the carotenoid production using the orbital shaker, a significance of both independent variables (pH and nitrogen combination) for the biosynthesis of the three carotenoids was demonstrated. Thus, it was found as the optimal conditions for the production of carotenoids, the use of a culture medium composed of 10 g/L of glucose (as carbon source), 10 g/L of asparagine (as organic nitrogen source), 4 g/L of NH_4NO_3 (as inorganic nitrogen source), 0.52 g/L of KH_2PO_4, 0.52 g/L $MgSO_4$, as well as its growth at pH 5. This condition was then used in the cultivation of *R. glutinis* in the 5 L stirred-tank bioreactor. The bioreactor was operated in a batch mode for 72 h, monitoring at each 6 h of cultivation, the pH, DCW, glucose consumption, as well as the lipid and carotenoid (β-carotene, torularhodin and torulene) concentrations, as depicted in **Figure 3.3** (all values are detailed in **Table A.2** in the **Appendix A**).

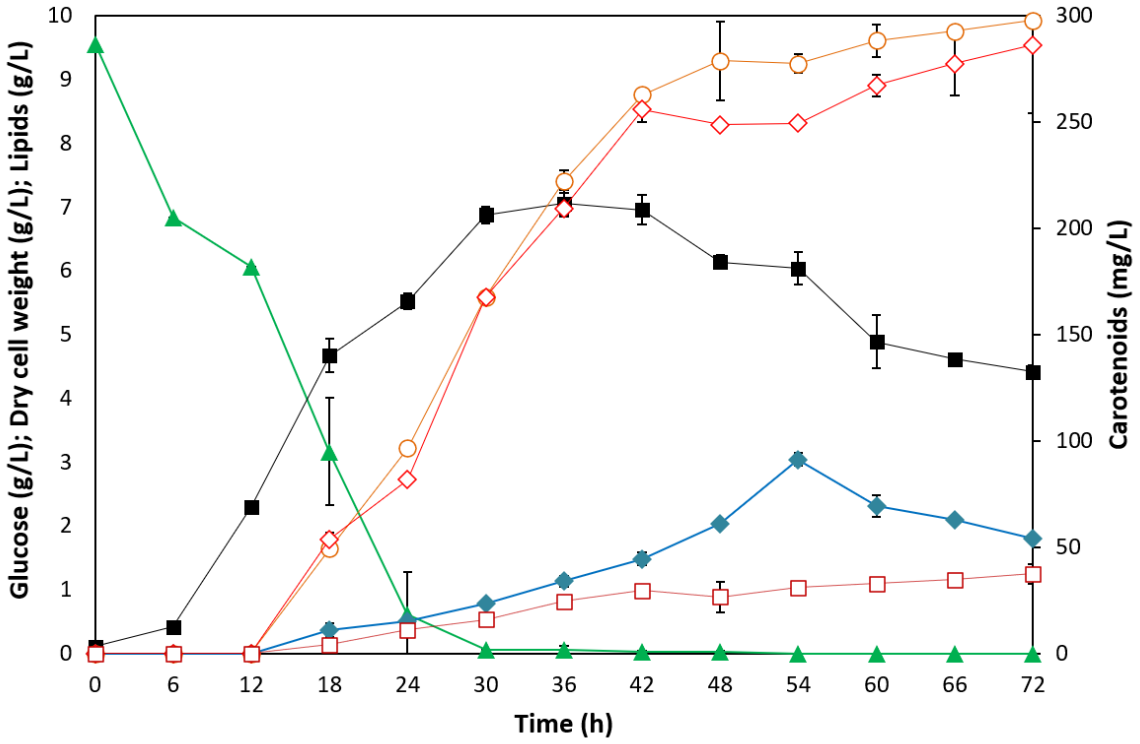

Figure 3.3. Dry cell weight (g/L) (-■-), glucose (g/L) (-▲-), lipids (g/L) (-♦-) and production of β-carotene (-○-), torularhodin (-◇-) and torulene (-□-) by *R. glutinis* CCT-2186 in 5 L stirred-tank bioreactor at 30 °C, 1 vvm, 300 rpm for 72 h. The error bars in some cases, are smaller than the markers.

The cellular biomass is the primary bioproduct of a yeast biorefinery, acting as a key performance indicator in the production lipids and carotenoids by yeast (produced intracellularly). As shown in **Figure 3.3**, the fermentative process started with low cell concentration, with an initial DCW in the bioreactor of 0.09 g/L. After 6 h, exponential cellular growth started, reaching the maximum DCW of 7.14 g/L after 36 h of cultivation. After 42 h, a decrease in DCW occurred, with a final DCW of 4.42 g/L after 72 h of cultivation, a value equivalent to that obtained for the cultivations in the orbital shaker (*cf.* **Table 3.7**-center runs of 2^2 factorial design results). Regarding the DCW decrease, it is a result of both glucose depletion and lipids turnover (as noted by the decrease of lipid content). Maintenance of cell viability and function is highly dependent of the carbon source (in this case glucose). The results from **Figure 3.3** indicate that the DCW decrease occurs in

few hours after the full consumption of the glucose. These results are in accordance with those obtained by: Dai et al [43], using *Rhodotorula glutinis* supplemented with xylose, which also demonstrated a decrease in biomass after the depletion of the carbon source; Yen et al [44], which grown *R. glutinis* in an internal-loop airlift bioreactor by using mixture substrates of rice straw hydrolysate and crude glycerol and found that when the carbon source is depleted, biomass tends to stabilize and then decrease. It is noteworthy that after 30 h, where the maximum DCW concentration was reached, the glucose concentration decreased to 0.04 g/L, corresponding to a consumption of approximately 99.5% of the carbon source, *i.e.*, the glucose was fully consumed during the exponential cell growth phase.

Comparing the production yields obtained in the cultivation in the bioreactor with those obtained with the orbital shaker, a significant increase in the production of the three carotenoids was observed, namely, from 220.93 to 297.84 mg/L for β-carotene (+ 25.83%), from 252.01 to 286.06 mg/L for torularhodin (+ 11.88%) and from 28.20 to 37.35 mg/L for torulene (+ 24.50%). Although the cultivation medium, pH and temperature are the same, in the stirred-tank bioreactor, the agitation rate was increased (from 150 rpm to 350 rpm) and a further aeration source (1 vvm of air) was added. The improvement of cultivation agitation and aeration conditions is beneficial in microbial biosynthesis, mainly because it favors the mass transfer of substrate, product and oxygen, and consequent, all specific metabolic pathways. The influence of aeration on yeast carotenogenesis was previously assessed by Davoli et al. (Davoli et al. 2004), observing that *R. glutinis* yeast produce higher concentrations of carotenoids at higher aeration rates (an increase of approx. 45% in the carotenoids content). Malisorn and Suntornsuk (Malisorn and Suntornsuk 2009) also demonstrated a positive influence of aeration on carotenoid production by *R. glutinis* (DM28) in an 3 L stirred-tank bioreactor, specifically, achieving a maximum of β-carotene (0.21 mg/L after 24 h fermentation) by increasing the oxygen dissolved in the medium from 60% to 80%. Yamane et al. (Yamane et al. 1997) also obtained high astaxanthin production rates by *P. rhodozyma* at high oxygen concentrations.

It has been shown that these microorganisms (*R. glutinis*) do not have a hyperactive fatty acid biosynthesis system, but they are capable of producing in significant quantities, acetyl-CoA, the basic unit of fatty acid biosynthesis (Ratledge 1993; Papanikolaou and Aggelis 2011). *R. glutinis* is one of the oleaginous microorganisms with the greatest potential to synthesize and accumulate lipids intracellularly, for example, in this work it accumulated up to 61.60% (run 5, **Table 3.5**) of its total biomass in lipids (interestingly, obtained under normal, *i.e.,* "stress-free", cultivation conditions). Lipids are preferentially produced (and accumulated) during exponential yeast growth, when the increase in biomass is proportional with the carbon consumption (Singh et al. 2016). In the bioreactor, as shown in **Figure 3.3**, *R. glutinis* achieved a maximum of lipid concentration of 3.04 g/L (50.32% w/w) after 54 h of cultivation, which corresponds to DCW of 6.04 g/L. The lipid content remained above 2.30 g/L until 60 h, but then, decreased to 1.80 g/L after 72 h (end of the cultivation), because of the cell death in consequence of the yeast lipid depletion.

Together with the results of the orbital shaker, the cultivation in the 5 L stirred-tank bioreactor cultivation confirmed that a simple adjustment of the nitrogen sources and pH can significantly increase the production of the three carotenoids by *R. glutinis*, as well as to obtain other valuable by-products, *e.g*., lipids. The performance of the optimal cultivation medium was validated in a 5 L stirred-tank bioreactor, demonstrating that the combined use asparagine and NH_4NO_3 as complex nitrogen source is beneficial for the production of carotenoids (β-carotene, torularhodin and torulene) and lipid accumulation.

This study provides valuable information about the importance of using complex nitrogen source for the production of yeast biomass, from which more than one commercial valuable products can be simultaneously obtained, *i.e., i)* carotenoids from yeast biomass can be used as supplement in functional foods; additive in cosmetics and animal feeds; *ii)* lipids can be used as food additives, diet supplements, substitutions for precious fats, and can also be used as substrates in the third-generation biodiesel production; and *iii)* carotenoids and lipids-free biomass (after the extraction of both

added-value compounds) can be even used as protein and carbohydrate (after carotenoid and lipid extraction) to animal feed or agricultural fertilizers.

3.4 Conclusion

From sequential optimization studies using fractional factorial designs followed by central composite design, a clear effect was found between supplementation with organic and inorganic nitrogen sources and the production of carotenoids (β-carotene, torularhodin and torulene) and lipids from *Rhodotorula glutinis* CCT- 2186. The use of combined sources of organic and inorganic nitrogen is recommended to supplement simple synthetic nutritional media for the cultivation of *R. glutinis*. The performance of the yeast was validated in a 5 L stirred-tank bioreactor, in which, as demonstrated by the improvement in carotenoids production yields, the importance of performing the initial optimization of the nutritional content of cultivation media was confirmed. Despite the promising results using combined sources of inorganic and organic nitrogen sources, additional studies focused in the optimization of C/N balance are recommended, particularly, envisaging the improvement of the *R. glutinis* biomass content and guaranteeing, at same time, the maintenance of high productivity yields for carotenoids and lipids.

3.5 References

Aksu Z, Eren AT (2007) Production of carotenoids by the isolated yeast of *Rhodotorula glutinis*, Biochem. Eng. J. 35:107-113.

Alcantara S, Sanchez S (1999) Influence of carbon and nitrogen sources on Flavobacterium growth and zeaxanthin biosynthesis, J. Ind. Microbiol. Biotechnol. 23:697-700. Bhosale PB, Gadre R V. (2001) Production of β-carotene by a mutant of *Rhodotorula glutinis*, Appl. Microbiol. Biotechnol. 55:423–427.

Bhosale PB, Gadre RV (2001) Production of β-carotene by a mutant of *Rhodotorula glutinis*, Appl. Microbiol. Biotechnol. 55(4), 423-427.

Buzzini P, Martini A (2000) Production of carotenoids by strains of *Rhodotorula glutinis* cultured in raw materials of agro-industrial origin, Bioresour. Technol. 71:41-44.

Cabral MMS, Cence K, Zeni J, et al (2011) Carotenoids production from a newly isolated *Sporidiobolus pararoseus* strain by submerged fermentation, Eur. Food Res. Technol.

Cerón García M del C, González López CV, Fernández Sevilla JM, Molina Grima E (2018) Preparative recovery of carotenoids from microalgal biomass, in: Methods Mol. Biol., 1852:117-115.

Dai C, Tao J, Xie F, Dai Y, and Zhao M (2007) Biodiesel generation from oleaginous yeast *Rhodotorula glutinis* with xylose assimilating capacity." Afr. J. Biotechnol, 6, 2130-2134.

Das A, Yoon SH, Lee SH, Kim JY, Oh DK, Kim SW (2007) An update on microbial carotenoid production: Application of recent metabolic engineering tools, Appl. Microbiol. Biotechnol. 77, 505–512.

Davoli P, Mierau V, Weber RWS (2004) Carotenoids and fatty acids in red yeasts Sporobolomyces roseus and *Rhodotorula glutinis*, Appl. Biochem. Microbiol. 40:392–397.

de Oliveira F, Pedrolli DB, Teixeira MFS, de Carvalho Santos-Ebinuma V (2019) Water-soluble fluorescent red colorant production by *Talaromyces amestolkiae*, Appl. Microbiol. Biotechnol. 103:6529–6541.

Dyer WJ (1959) A rapid method of total lipid extraction and purification., Can. J. Biochem. Physiol. 37.

Gribanovski-Sassu O, Foppen FH (1968) Light and temperature effect on *Epicoccum nigrum*, Phytochemistry. 7:1605-1612.

Harith ZT, Lima MA, Charalampopoulos D, Chatzifragkou A (2020) Optimized production and extraction of astaxanthin from the yeast *Xanthophyllomyces dendrorhous*, Microorganisms. 8. 430.

Jeevaratnam K, Latha B V (2010) Purification and characterization of the pigments from *Rhodotorula glutinis* DFR-PDY Isolated from Natural Source, Glob. J. Biotechnol. Biochem. 5:166-174.

Kot AM, Błazejak S, Gientka I, et al (2018) Torulene and torularhodin: “New” fungal carotenoids for industry? Microb. Cell Fact. 17:49.

Kot AM, Błażejak S, Kieliszek M, et al (2019) Effect of exogenous stress factors on the biosynthesis of carotenoids and lipids by *Rhodotorula* yeast strains in media containing agro-industrial waste, World J. Microbiol. Biotechnol. 35:157.

Kot AM, Błażejak S, Kurcz A, et al (2016) *Rhodotorula glutinis*-potential source of lipids, carotenoids, and enzymes for use in industries, Appl. Microbiol. Biotechnol. 100(14):6103-6117.

Maldonade IR, Scamparini ARP, Rodriguez-Amaya DB (2007) Selection and characterization of carotenoid-producing yeasts from Campinas region, Brazil, Brazilian J. Microbiol. 38:65-70.

Malisorn C, Suntornsuk W (2009) Improved β-carotene production of *Rhodotorula glutinis* in fermented radish brine by continuous cultivation, Biochem. Eng. J. 43:27-32.

Mihalcea A, Ungureanu C, Ferdes M, et al (2011) The influence of operating conditions on the growth of the yeast *Rhodotorula rubra* ICCF 209 and on torularhodin formation, Rev. Chim. 62:659-665.

Milani A, Basirnejad M, Shahbazi S, Bolhassani A (2017) Carotenoids: biochemistry, pharmacology and treatment, Br. J. Pharmacol. 174:1290-1324.

Miller GL (1959) Use of Dinitrosalicylic Acid Reagent for Determination of Reducing Sugar, Anal. Chem. 31:426-428.

Mondala AH, Hernandez R, French T, McFarland L, Santo Domingo JW, Meckes M, Ryu H, Iker B (2012) Enhanced lipid and biodiesel production from glucose-fed activated sludge: Kinetics and microbial community analysis, AIChE J. 58 (4), 1279-1290.

Mussagy CU, Santos Ebinuma V de C, Gonzalez-Miquel M, et al (2019) Protic ionic liquids as cell-disrupting agents for the recovery of intracellular carotenoids from yeast *Rhodotorula glutinis* CCT-2186, ACS Sustain. Chem. Eng. 7:16765–16776.

Mussagy CU, Winterburn J, Santos-Ebinuma VC, Pereira JFB (2019) Production and extraction of carotenoids produced by microorganisms, Appl. Microbiol. Biotechnol. 103:1095-1114.

Papanikolaou S, Aggelis G (2011) Lipids of oleaginous yeasts. Part I: Biochemistry of single cell oil production, Eur. J. Lipid Sci. Technol. 113:1031-1051.

Park PK, Kim EY, Chu KH (2007) Chemical disruption of yeast cells for the isolation of carotenoid pigments, Sep. Purif. Technol. 53:148-152.

Perrier V, Dubreucq E, Galzy P (1995) Fatty acid and carotenoid composition of *Rhodotorula* strains, Arch. Microbiol. 164:173–179.

Ramel F, Birtic S, Cuine S, et al (2012) Chemical Quenching of Singlet Oxygen by Carotenoids in Plants, PLANT Physiol. 158:1267-78.

Ratledge C (1993) Single cell oils - have they a biotechnological future? Trends Biotechnol. 11:278-84.

Rodrigues MI, Iemma AF (2014) Experimental design and process optimization, 1st Ed, CRC Press.

Saenge C, Cheirsilp B, Suksaroge TT, Bourtoom T (2011) Efficient concomitant production of lipids and carotenoids by oleaginous red yeast *Rhodotorula glutinis* cultured in palm oil mill effluent and application of lipids for biodiesel production, Biotechnol. Bioprocess Eng. 16:23-33.

Singh G, Jawed A, Paul D, et al (2016) Concomitant production of lipids and carotenoids in *Rhodosporidium toruloides* under osmotic stress using response surface methodology, Front. Microbiol. 7:1686.

Somashekar D, Joseph R (2000) Inverse relationship between carotenoid and lipid formation in *Rhodotorula gracilis* according to the C/N ratio of the growth medium, World J. Microbiol. Biotechnol. 16:491–493.

Squina FM, Mercadante AZ (2005) Influence of nicotine and diphenylamine on the carotenoid composition of *Rhodotorula* strains, J. Food Biochem. 29:638-652.

Tinoi J, Rakariyatham N, Deming RL (2005) Simplex optimization of carotenoid production by *Rhodotorula glutinis* using hydrolyzed mung bean waste flour as substrate, Process Biochem. 40 (7):2551-2557.

Valduga E, Valério A, Tatsch PO, et al (2009) Assessment of Cell Disruption and Carotenoids Extraction from *Sporidiobolus salmonicolor* (CBS 2636). Food Bioprocess Technol.

Voaides C, Dima R (2012) The effect of nitrogen source on carotenoids production by *Rhodotorula* sp., Rom. Biotechnol. Lett. 17:7570-7576.

Yamane YI, Higashida K, Nakashimada Y, et al (1997) Influence of oxygen and glucose on primary metabolism and astaxanthin production by *Phaffia rhodozyma* in batch and fed-batch cultures: Kinetic and stoichiometric analysis, Appl. Environ. Microbiol. 63:4471–4478.

Ye VM, Bhatia SK (2012) Pathway engineering strategies for production of beneficial carotenoids in microbial hosts, Biotechnol. Lett. 34, 1405–1414.

Yen HW, Chang JT, Chang JS (2015) The growth of oleaginous *Rhodotorula glutinis* in an internal-loop airlift bioreactor by using mixture substrates of rice straw hydrolysate and crude glycerol, Biomass and Bioenergy, 80, 38-43.

Yen HW, Liu YX, Chang JS (2015) The effects of feeding criteria on the growth of oleaginous yeast- *Rhodotorula glutinis* in a pilot-scale airlift bioreactor, J. Taiwan Inst. Chem. Eng. 49, 67-71.

4. RECOVERY OF CAROTENOIDS FROM *R. glutinis* YEAST USING PROTIC IONIC LIQUIDS

Based on the manuscript

Protic Ionic Liquids as cell-disrupting agents for the recovery of intracellular carotenoids from yeast *Rhodotorula glutinis* CCT-2186

Mussagy CU, Santos Ebinuma VC, Gonzalez-Miquel M, Coutinho JAP and Pereira JFB

ACS Sustainable Chemistry & Engineering, 7 (19): 16765-16776, **2019**.

Abstract

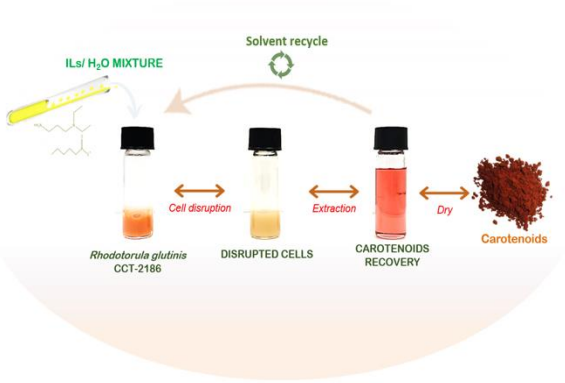

Rhodotorula glutinis (*R*. *glutinis*) yeasts are natural sources of intracellular carotenoids such as β-carotene, torularhodin, and torulene. Since these yeasts are constituted by a rigid cell-wall structure, the use of energy-saving and high-efficiency cell disruption procedures is critical for carotenoids recovery. A new technology using protic ionic liquids (PILs) was here evaluated as an alternative platform to permeabilize the *R*. *glutinis* cells and to improve the extraction of β-carotene, torularhodin, and torulene. The cell disruption ability of 12 highly concentrated aqueous solutions of ammonium-based PILs was determined, evaluating the influence of the relative ion hydrophobicity, solid-liquid ratio, water content, and temperature. Carotenoid extraction yields increased with the hydrophobicity of the PILs (*i.e*., increase of alkyl chain length of the anion or cation), temperature (from 25 to 65 °C), and PIL concentration (from 75 to 90% v/v). Additionally, to demonstrate the potential of PILs in carotenoids recovery, solvent recycling and carotenoids polishing were carried out using a three-phase partitioning system. The results demonstrate that the use of PILs as cell-disrupting agents can be a simple, efficient, sustainable, and feasible method to recover intracellular carotenoids from microbial biomass.

Keywords: *Rhodotorula glutinis*, carotenoids, extraction, protic ionic liquids, β-carotene, torularhodin, torulene.

4.1 Introduction

Carotenoids are a group of yellow, orange, and red polyisoprenoid pigments that can be naturally synthesized by different microorganisms, including microalgae, bacteria, yeasts, and filamentous fungi (Henríquez et al. 2016; Mussagy et al. 2018). These biopigments exhibit a plethora of biological attractive properties, such as antioxidant, antiobesity, antidiabetic, anticancer (particularly those that result from cardiovascular diseases and macular degeneration), and antimicrobial activities (Zoz et al. 2015; Visioli and Artaria 2017; Toti et al. 2018). As a result of their interesting biological properties, natural carotenoids have been attracting great interest from academic and industrial partners for applications in pharmaceuticals, cosmetics, and functional food formulations as well as the most common uses in food industries (Baranskia and Cazzonelli 2016; Mesquita et al. 2017; Dufossé 2018).

Rhodotorula glutinis (*R. glutinis*) is an aerobic yeast able to synthesize in an easy and natural way several industrial high added value metabolites, for example, lipids, carotenoids, and enzymes. Particularly, these yeasts can produce and accumulate approximately 50% of their dried cellular biomass as fractions of carotenoids and lipids (Kot et al. 2016). Among the carotenoids, *R. glutinis* is able to synthesize β-carotene, torulene, and torularhodin, exhibiting variable production yields according to the specific cultivation conditions (Latha et al. 2005) and fast grow (Buzzini and Martini 2000).

However, since the carotenoids from *R. glutinis* yeast are produced intracellularly, appropriate cell-disrupting methodologies are always required for their recovery (Mata-Gómez et al. 2014). A large number of cell disruption techniques, including conventional and nonconventional procedures, have been reported in the literature (Mussagy et al. 2018; Saini and Keum 2018). Traditionally, *R. glutinis* yeasts are disrupted by using conventional solid-liquid extraction procedures with volatile organic solvents (VOCs), such as petroleum ether, dimethyl sulfoxide (DMSO), acetone, chloroform, and hexane (Park et al. 2007). Among the common

VOCs, the use of DMSO, in general, lead to the highest release rates of intracellular carotenoids, but their use in industrial processes is limited by health and environmental concerns (Qi et al. 2008; Galvao et al. 2014).

Therefore, the search for more biocompatible and environmentally friendly solvents, as for example, biosolvents, ionic liquids (ILs), and deep eutectic solvents, is of great importance. Among these, ILs, commonly defined as salts with a melting point lower than 100 °C, (Osada et al. 2016), have been suggested as one of the most interesting classes of alternative solvents, which is mainly due to their unique features like high hydrolytic activity, low volatility, high solvation capacity, and excellent thermal and chemical stabilities (Choi et al. 2019).

Some studies evaluated the capability of different ILs for the extraction of carotenoids (Desai et al. 2016; Vieira et al. 2018; Choi et al. 2019). Choi and collaborators (Choi et al. 2019) extracted astaxanthin and lipids from *Haematococcus pluvialis* cyst cells using 10 1-ethyl-3-methylimidazolium ($[Emim]^+$)-based ILs, obtaining complete astaxanthin recoveries (>99%) and high lipid extraction yields (~82%) at optimum operating conditions, that is, 6.7% (v/v) IL in water, 30 °C of temperature and 60 min of extraction time. Desai and collaborators (Desai et al. 2016) recovered more than 70% of intracellular astaxanthin from intact *H. pluvialis* cells using an aqueous solution of 1-ethyl-3-methylimidazolium dibutyl-phosphate ([Emim][DBP]) (40 wt%). Vieira and collaborators (Vieira et al. 2018) recovered fucoxanthin from *Sargassum muticum* cells using aqueous solutions of different surface-active ILs. These examples demonstrate that ILs are effective solvents to extract carotenoids from natural sources; however, most of these works have been performed using “classic” aprotic ILs (AILs). Recent studies have indicated that AILs are not the most adequate for biologically based applications due to their cytotoxicity, (Egorova et al. 2017), which led to a growing interest in the third generation of more benign and biocompatible ILs, that is, protic ionic liquids (PILs) (Greaves and Drummond 2015).

PILs are a subset of ILs prepared through the stoichiometric neutralization reaction of certain Brønsted acids and Brønsted bases. They have a proton available for hydrogen bonding and differ from the classic AILs in having both cationic and

anionic counterparts formed by low-molecular weight organic compounds, usually substituted (or polysubstituted) amines as cations and organic acids as anions (Greaves and Drummond 2015).

PILs are more favourable than AILs in terms of toxicity and biodegradability (Oliveira et al. 2016). This fact coupled with their low production cost, easier synthesis, and more benign nature (*i.e.,* can be obtained fully or partly from natural raw materials) make them attractive solvents for wider use in industrial bioprocesses (Peric et al. 2013).

Considering these assumptions, the aim of this study was to evaluate the capability of PILs to disrupt (permeabilize) the cell wall of *R. glutinis* yeasts and to increase the recoveries of intracellular carotenoids. Twelve different PILs, obtained from the neutralization of three different propylamines and four different carboxylic acids, were used to assess the effect of the relative hydrophobicity of both cations and anions on cell disruption and carotenoids extraction. The carotenoids extraction efficiencies exposed to different aqueous solutions of the 12 PILs (ranging from 75 to 90% (v/v)) at three different temperatures (25, 45, and 65 °C) and four different solid-liquid ratios (SLRs) (0.05, 0.1, 0.2, and 0.5 g/mL) were determined. To obtain further information about the mechanisms and the disruption ability of the PILs over the *R. glutinis* cell walls, samples of cells after the different treatments were also analyzed by scanning electron microscopy (SEM). The overall sustainability of the proposed technology was assessed in terms of PIL recyclability and carotenoids polishing.

4.2 Experimental section

4.2.1 Materials

β-carotene and torularhodin standards were acquired from Carbosynth (San Diego, CA, U.S.A.). Dimethyl sulfoxide (DMSO) (P.A.), ethyl acetate (P.A.), and glutaraldehyde (25 wt % in water) were acquired from Exodo Cientifica (Sumaré, SP, Brazil) and potassium phosphate tribasic (K_3PO_4) (P.A.) from LS Chemicals (Ribeirao Preto, SP, Brazil). All the amines and carboxylic acids used in the PIL synthesis were purchased from Sigma-Aldrich (St. Louis, MO, U.S.A.), namely,

propylamine (P.A.) (98%), 3-dimethylamino-1-propylamine (DMAPA) (99%), and 3-diethylamino-propylamine (DEAPA) (99%) as cations and hexanoic acid (Hex) (99%), butyric acid (But) (99%), propanoic acid (Pro) (99.5%), and acetic acid (Ac) (99.8%) as anions.

4.2.2 PILs synthesis

PILs were synthesized via a neutralization reaction of the base with the appropriate acid, according to the procedure previously reported (Sintra et al. 2019). Briefly; 1 M of the amine was placed in a 100 mL synthesis-flask, which was cooled to 4 °C, under continuous stirring, using an ice water bath. Then, the corresponding carboxylic acid (1 M) was added. Afterwards, the mixture was left overnight under continuous stirring at room temperature using a magnetic stirrer (IKA® model C-MAG, Staufen, Germany). Before use, all the PILs were purified and dried for 48 h at constant agitation (≈ 100 rpm), at a moderate temperature (≈ 298 K) under vacuum stirring at 300 mbar and 60 °C using a Heidolph (Hei-VAP) rotaevaporator (Schwabach, Germany) coupled with the ultrathermostatic bath Solab-SL 152 (Piracicaba, SP, Brazil). After the synthesis, the structure and purity of all PILs was confirmed by proton nuclear magnetic resonance (^{1}H NMR), using a Bruker Avance III HD 600 (14.1T) NMR spectrometer (Massachusetts, USA) at 600 MHz. The PILs were previously dissolved in D_2O/DMSO-d_6 purchased from Sigma-Aldrich (St. Louis, MO, USA). The corresponding structures and purities obtained from the NMR analysis and further details about the synthesis are presented in **Table B.2** from the **Appendix B**.

The residual water content of the PILs was measured by volumetric titration at 25 °C using a Karl Fischer Metrohm® 803 TI-Stand titrator (Herisau, Switzerland), Hydranal-Methanol Rapid (reagent for accelerated volumetric one-component KF titration), and Hydranal-Composite 5 (reagent for volumetric one-component Karl Fischer titration; methanol free), both supplied by Sigma-Aldrich (St. Louis, MO, USA) as titrants. The pH (± 0.02) of PILs was also determined using a MS Tecnopon® mPA-210 (Piracicaba, SP, Brazil). The calibration of the pH meter was carried out with two buffers (pH values of 4.00 and 7.00). The corresponding pH

values obtained are provided in **Table B.1** from the **Appendix B**. The viscosity was only measured for the PILs yielding the best extractions, *i.e.,* hexanoate-based PILS. For that, the viscosities were determined in a variable temperature range between 25 °C and 70 °C at 5 °C intervals under atmospheric pressure using Anton Paar® SVM 3000 viscometer-densimeter (Graz, Austria). The viscosimeter was previously calibrated using standard solutions.

4.2.3 Microorganism and cultivation conditions

R. glutinis CCT-2186 yeasts, isolated from the leaf of a kaki fruit (Diospyros), were acquired from the Tropical Culture Collection André Tosello (Campinas, SP, Brazil). A stock culture of the microorganism (50% (v/v) glycerol) was maintained at -80 °C. The inoculum was prepared by the activation of yeast *R. glutinis* CCT-2186 in yeast extract-peptone-dextrose (YPD medium), which has the following composition (w/v): bacteriological peptone (2%); yeast extract (1%); glucose (2%). The inoculum culture was prepared in 100 mL Erlenmeyer® type flasks containing 25 mL of the YPD medium. Cells were grown for 48 h at 30 °C and 150 rpm in the orbital shaker Tecnal, TE- 421 (Piracicaba, SP, Brazil). An aliquot of 0.2 mg/mL yeast cells was used as the inoculum. For production, batch fermentations were carried out in 500 mL Erlenmeyer flasks, each one containing 100 mL of modified Czapek-Dox medium, which has the following composition (w/v): glucose (2%), KH_2PO_4 (0.052%), $MgSO_4.7H_2O$ (0.052%), $ZnSO_4$ (0.0001%), NH_4NO_3 (0.4%) and asparagine (1%). For the carotenoids production, Erlenmeyer® type flasks (500 mL) containing 100 mL of autoclaved fresh media were inoculated with 0.2 mg/mL of cell concentration of the 48 h fermented inoculum. The flasks were incubated for 72 h at 30 °C and 150 rpm in rotary orbital shaker (Tecnal, model TE- 421; Piracicaba, SP, Brazil), pH was not adjusted during the process. After 72 h of cultivation a maximum cell biomass concentration of 5.6 g/L was achieved. The fermented medium was then centrifuged in a Hitachi CR-22N (Tokio, Japan) centrifuge, at 2500*xg* for 10 min at 4 °C. The supernatants of all fermented media were then discarded, and the cellular pellets containing carotenoids were collected and stored for the next carotenoid extraction studies.

4.2.4 Conventional methodology for separation and characterization of carotenoids

Intracellular carotenoids were firstly isolated by using a conventional method described by Park and collaborators (Park et al. 2007). Briefly, 1 g of *R. glutinis* wet biomass was subjected to chemical treatment with successive solvent extractions using DMSO. After the extraction with DMSO, the samples were centrifuged at 2500*xg* for 10 min at 4 °C using a Hitachi CR-22 N centrifuge (Tokyo, Japan). The supernatants containing carotenoids were then lyophilized. Lyophilized extracts were solubilized in acetone and separated by liquid chromatography in a column filled with silica gel 60 (Merck, Pinheiros, SP, Brazil), using a mobile phase composed of hexane/ethyl ether/acetic acid (70:29:1 v/v/v). The fractions were collected, evaporated to dryness and then re-suspended in 1 mL of acetone. The acetone-based extracts were firstly qualitatively evaluated by thin-layer chromatography (TLC) using pre-coated TLC sheets ALUGRAM (silica gel 60, Macherey-Nagel, Germany), and hexane/ethyl ether/acetic acid (70:29:1 v/v/v) as the mobile phase. Afterwards, the extracts were analyzed by Reverse Phase High Performance Liquid Chromatography (RP-HPLC) to detect the standard peak of absorbance. The homogeneity and the purity of the different fractions were identified by RP-HPLC on a column chromatography Shimadzu® Shim-pack C_{18} (Japan), 4.6 x 250 mm, using as mobile phase methanol/acetonitrile/dichloromethane (60:10:30, v/v/v) eluting isocratically for 18 min. The flow rate was 1 mL/min, and the column temperature was set at 30 °C. The corresponding carotenoids were detected using UV-Vis detector at λ_{max} 450 nm. The identification of β-carotene and torularhodin (yellow and red fraction respectively) was done by comparison with the standard retention time found (with high purity level) under the same experimental conditions, and for torulene (light red fraction) were compared with data reported in literature (Jeevaratnam and Latha, 2010). The structures of the three purified fractions of carotenoids were confirmed by ^{1}H NMR using a Bruker Avance III HD 600 (14.1T). The fractions of carotenoids were solubilized in DMSO-*d6* and their corresponding ^{1}H NMR spectra acquired, as listed in **Table B.3** from the **Appendix B**.

4.2.5 Carotenoids quantification

After the identification and characterization of the chemical structures of carotenoids produced by *R. glutinis* yeasts, the respective visible-light absorption spectra were obtained using a Thermo Scientific (Genesis 10S) UV−vis spectrophotometer (accuracy: ± 0.005 AU at 1.0 AU) (China) to obtain the maximum absorption (λ_{max}) of β-carotene, torularhodin and torulene. The quantification of carotenoids by UV-Vis spectroscopy is complex due to the choice of solvent system, as the absorption maxima of extracted carotenoids strongly depend on the polarity of the solvent used. For example, with increasing polarity of the solvent*, i.e.,* DMSO, the absorption of isolated carotenoids shows three peaks: 475, 510 and 540 nm; however, when less polar solvents are used, *i.e.,* PILs, the peaks shift to 460, 487 and 532 as shown in **Figure B.1** from the **Appendix B.** Therefore, in that case, the UV-visible spectra for samples were obtained between 380 and 600 nm, and the chromatograms were standardized and processed at λ_{max}= 450nm for β- carotene, λ_{max}= 480nm for torulene and λ_{max}= 500nm for torularhodin. Then the carotenoids were quantified using external calibration curves. The working standard solutions of 0.1, 0.2, 0.4, 0.5 and 1 µg/mL for β-carotene, 0.5,1, 1.5, 2, 2.5 and 3 µg/mL for torulene and 5,10,20,30,40,50 µg/mL for torularhodin were prepared daily using fresh solvent. All solutions were protected against light with aluminum foil and maintained at 4 °C for one month maximum, because longer periods of storage may produce irreproducible results due to degradation or reaction processes.

4.2.6 Carotenoids solid-liquid extraction (SLE) using PILs

Aqueous solutions of the 12 ammonium-based-PILs were prepared and used for the disruption of the *R. glutinis* cells and subsequent carotenoid recovery. For the control, following previous reports that used VOCs as chemical solvents for the extraction of carotenoids from *R. glutinis* cells (Bhosale and Gadre 2001; Aksu and Eren 2007; Park et al. 2007), a conventional method using DMSO was also carried out. All assays were performed according to the following procedures: *(1)* to remove impurities, the *R. glutinis* wet cells were washed three times using 3 mL of a phosphate buffer (pH 7). *(2)* After washing, different amounts of the wet biomass

(0.05, 0.1, 0.2, and 0.5 g) were added in 2 mL Eppendorf tubes. *(3)* The tubes were filled with 1 mL of different aqueous solutions of all ammonium-based PILs (at 75, 80, 85, and 90% (v/v)) or with 1 mL of DMSO for the control assay. *(4)* Samples were homogenized using a rotatory orbital sample shaker (Norte Cientifica, NH 2200, Araraquara, SP, Brazil) for 1 h at 30 rpm. *(5)* After homogenization, all the samples were centrifuged at 2500*xg* and 25 °C for 5 min using an Eppendorf 5415r centrifuge (Willow Springs, NC, U.S.A.). *(6)* After centrifugation, all cell lysate supernatants were filtered using a Millipore filter membrane (0.22 µm) and stored for further quantification of carotenoids, while the pellets containing the cellular debris were stored for further SEM analysis.

4.2.7 Scanning Electron Microscopy (SEM) analysis

Cell samples after the chemical SLE process using DMSO and PILs aqueous solutions were analyzed by SEM. After centrifugation, the samples containing the cell debris were washed 3 times with distilled water to remove the residual solvent content. Washed cell debris were fixed, at 4 ^{o}C for 24 h, with 1 mL of glutaraldehyde aqueous solution (2.5% v/v). The specimens were dehydrated using increasing ethanol solutions (50 to 100% (v/v) of ethanol in water). After the dehydration, samples were coated during 20 seconds with gold layer, at 40 mA and under vacuum $2x10^{-1}$ and then examined using a FEG-SEM JEOL scanning electron microscope, model JSM-7500F (Tokyo, Japan), operating at 2.00 kV.

4.2.8 Recycling of the PILs and carotenoids polishing

The PIL providing the highest purification yield was chosen for the solvent recycling and carotenoids polishing studies. In this stage, samples containing 1 g of the wet biomass were prepared in 15 mL conical centrifuge tubes, which were filled with 10 mL of 90% (v/v) [DEAPA][Hex] in water. The samples were then homogenized in a rotatory orbital sample shaker for 1 h at 30 rpm and 25 °C. After homogenization, all samples were centrifuged at 2500*xg* at 25 °C for 5 min.

After centrifugation, cell lysate supernatants were filtered using a Millipore filter membrane (0.22 µm), and the biomass containing pellets were discarded. Therefore, for the carotenoids polishing and PIL recycling, a three-phase partitioning

(TPP) system composed of 60 wt % [DEAPA][Hex] (with carotenoids), 14 wt % K_3PO_4, and 26 wt % H_2O was prepared. The three-phase system (liquid-solid-liquid) was then centrifuged at 2500*xg* at 25 °C for 10 min. Most of the carotenoids were precipitated as a solid fraction in the interface between both liquid (top and bottom) phases. The solid fraction was carefully removed and both the PIL (top)-rich phase and K_3PO_4 (bottom)-rich phase were reused for consecutive carotenoids extraction steps. The carotenoid-rich solid fraction was then subjected to cold acetone precipitation (5 mL) to remove contaminant proteins. The protein-rich precipitates were removed, and the carotenoids dissolved in the acetone were recovered by evaporation under constant vacuum at 300 mbar and 60 °C for 20 min using a Heidolph (Hei-VAP) rotaevaporator (Schwabach, Germany) coupled to ultrathermostatic bath Solab-SL 152 (Piracicaba, SP, Brazil). The amount and purity of carotenoids were determined according to the above-described methods. The recycling and polishing procedure was repeated three times.

4.2.9 Statistical analysis

Experiments were performed in triplicate, and the results are presented as the mean of three independent assays with the corresponding errors at a 95% confidence level. Statistical analyses were performed using the software R Statistic version 3.5.3 (Vienna, Austria). The results were evaluated by analysis of variance (ANOVA) and Tukey's test in order to verify the existence of significant differences between the groups with a 95% confidence level.

4.3 Results and discussion

4.3.1 Purification and characterization of the carotenoids

Carotenoids from *R. glutinis* were isolated and characterized qualitatively and quantitatively using different chromatographic and spectroscopic analyses. The three purified pigments (red, pink, and yellow) identified as *(1)* torularhodin, *(2)* torulene, and *(3)* β-carotene by NMR spectroscopy were eluted with hexane/ethyl ether/acetic acid (70:29:1 v/v/v) by column liquid chromatography, and the corresponding peaks are determined by RP-HPLC chromatography, as depicted in

Figure 4.1-a. The TLC separation of the carotenoid extracts using the same hexane/ethyl ether/acetic acid (70:29:1 v/v/v) mobile phase confirmed the presence of the three major carotenoids (**Figure 4.1-b**).

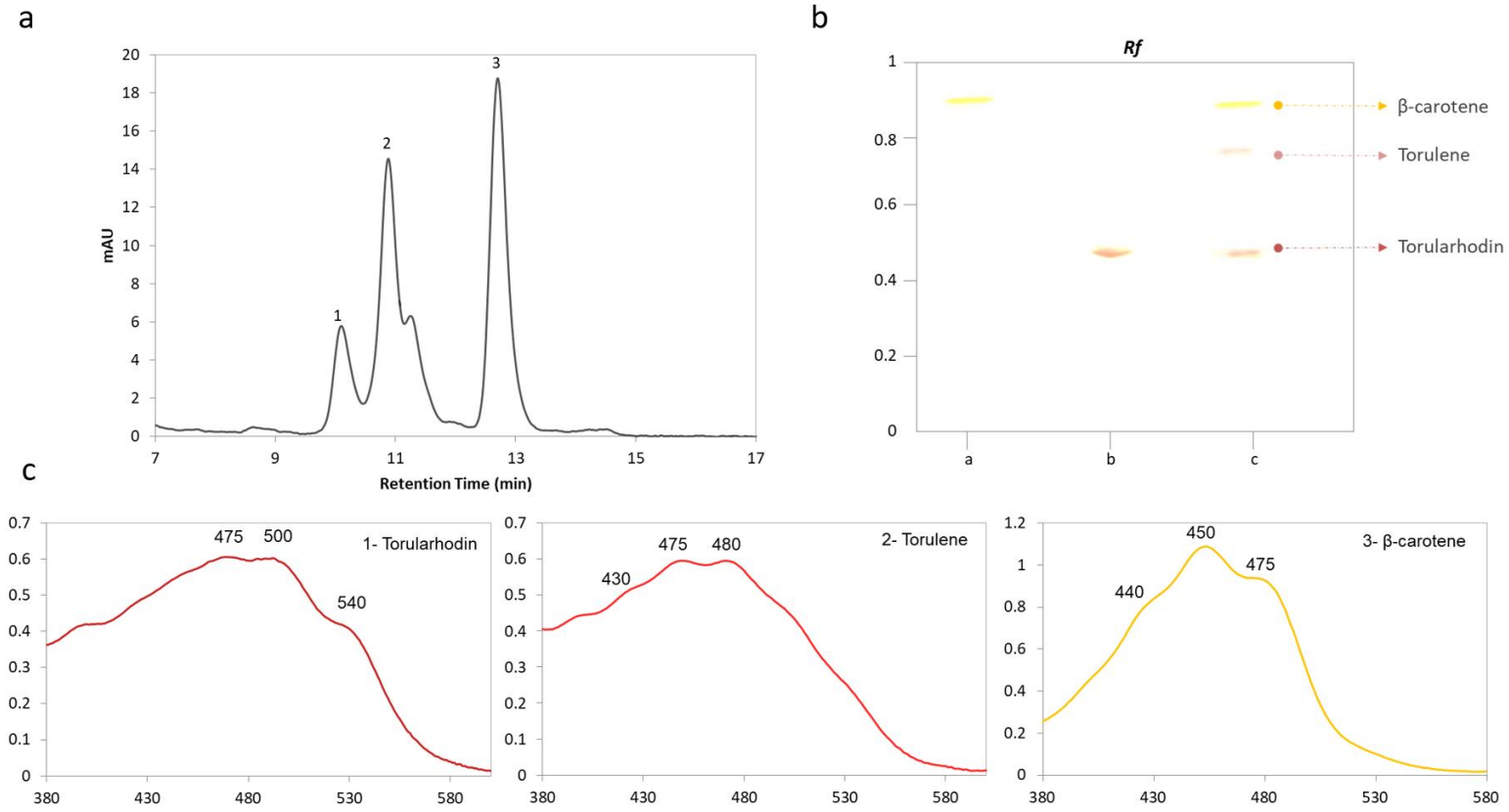

Figure 4.1. **a**- HPLC analysis of the three major carotenoids of *R. glutinis* CCT-2186 (1: torularhodin; 2: torulene; 3: β-carotene). **b**- Analytical TLC of *R. glutinis* cells' extracts: *a*- β-carotene standard, *b*-Torularhodin standard, *c*- Sample (cells' extracts). **c**- UV absorption spectra of the three major pigments of *R. glutinis*.

As shown in **Figure 4.1-b**, β-carotene has the highest mobility (Rf = 0.97) followed by torulene (Rf = 0.80) and lastly torularhodin with half of their mobilities (*Rf*= 0.40). The respective *Rf* values are in accordance with the RP-HPLC chromatogram of the carotenoids (depicted in **Figure 4.1-a**), which eluted the carotenoid fractions in an isocratic reversed-phase mode with retention times following the trend of decreasing polarity of each carotenoid fraction. Carotenoids were also identified according to their visible-light spectra characteristics (**Figure 4.1-c**). Both β-carotene and torulene carotenoids (more apolar) spectra showed a maximum absorbance at wavelengths of 450 nm (λ_{max}= 450 nm) and 480 nm (λ_{max}= 480 nm), respectively. On the other hand, torularhodin, the more polar carotenoid, exhibited a maximum absorbance at 500 nm (λ_{max}= 500 nm). The spectroscopic and chromatographic characteristics of the carotenoids isolated in this work are in agreement with those previously obtained by Jeevaratnam and Latha (Jeevaratnam and Latha 2010) and Park et al. (Park et al. 2007).

4.3.2 Effect of the PILs chemical structure on the extraction of carotenoids

After identifying the major carotenoids produced by *R. glutinis*, these were extracted using different PILs aqueous solutions. In the first set of experiments, the influence of the PIL ion nature on the carotenoid extraction was evaluated, that is, the effect of increasing the anion and cation alkyl chain length. This initial experimental set was carried out at constant concentration of PILs (90% v/v), wet cell concentration of 0.2 g/mL, 1 h of stirring at 30 rpm and 25 °C. The respective values are shown in the **Figure 4.2** and detailed in **Table B.4** in the **Appendix B**.

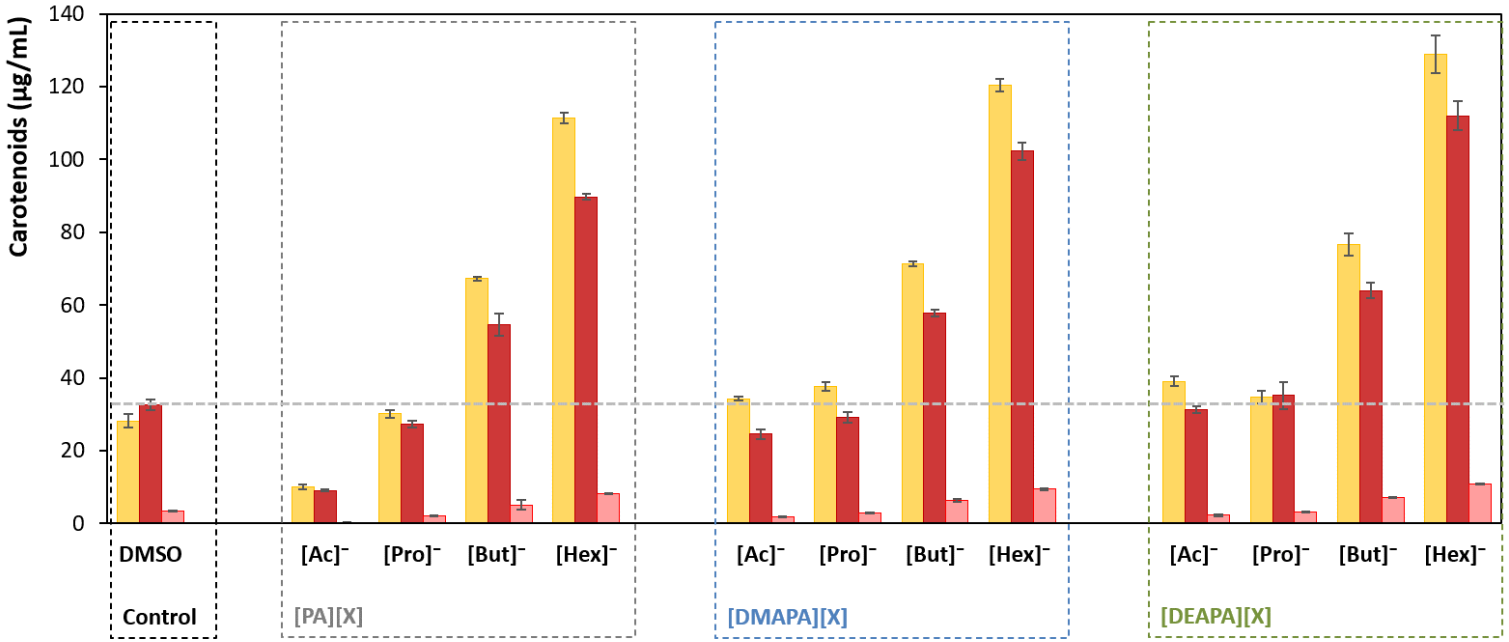

Figure 4.2. Recovery of β-carotene (yellow), torularhodin (red), and torulene (pink) using DMSO and aqueous solutions of PILs (90% v/v) at a wet cell concentration of 0.2 g/mL after 1 h stirring (30 rpm) at 25 °C. The error bars represent 95% confidence levels for the mean of three independent assays.

The results depicted in **Figure 4.2** demonstrate that the PILs exhibit high capacity to extract β-carotene (yellow bars) followed by torularhodin (red bars) and with the lowest recoveries for torulene (pink bars). The lower recovery of torulene is in accordance with the lower abundance of this pigment in the wet biomass. Contrarily to the DMSO control assay that presents a similar aptitude to extract both β-carotene and torularhodin pigments, PILs are more selective toward β-carotene. The selectivity of PILs can be attributed to the highest hydrophobicity found in this pigment that, despite being largely produced by *R. glutinis* cells, was not effectively recovered with DMSO. Interestingly, except [PA][Ac], all the other PILs were able to extract more carotenoids than those of DMSO (in the control assay (28.97 ± 1.86 μg/mL β-carotene, 32.50 ± 1.48 μg/mL torularhodin, and 3.34 ± 0.15 μg/mL torulene were recovered). The highest extraction rates were achieved by using $[Hex]^-$-based PILs, that is, sixfold more carotenoids than those of the control.

Analyzing the effect of PIL anion nature, independent of the target carotenoid, the three families of PILs, that is, [PA][X], [DMAPA][X], and [DEAPA][X], exhibit a similar pattern where increasing the anion alkyl chain length promotes higher carotenoid recovery yields. As shown in **Table B.4** in the **Appendix B**, in general, the extraction aptitude was significantly ($p \leq 0.05$) affected by the anion nature, according to the trend: $[Hex]^- > [But]^- > [Pro]^- > [Ac]^-$. The results from **Figure 4.2** seem to indicate that the hydrophobic character of the PIL anion is a key factor for the extraction of the intracellular carotenoids.

Afterwards, to infer if the anion relative hydrophobicity is governing the carotenoids extraction, the concentration of carotenoids recovered with [PA][X], [DMAPA][X] and [DEAPA][X] were correlated with the logarithmic function of the octanol/water partition coefficient values, log K_{ow}, of the corresponding acids used in the PILs synthesis (**Figure 4.3**), namely: Hex (log K_{ow} = 1.84) > But (log K_{ow} = 0.78) > Pro (log K_{ow} = 0.25) > [Ac] (log K_{ow} = -0.28). The log K_{ow} values (obtained from ChemSpider) correspond to relative measurements of the hydrophobicity of the molecules with higher values indicating higher hydrophobicity of the compounds.

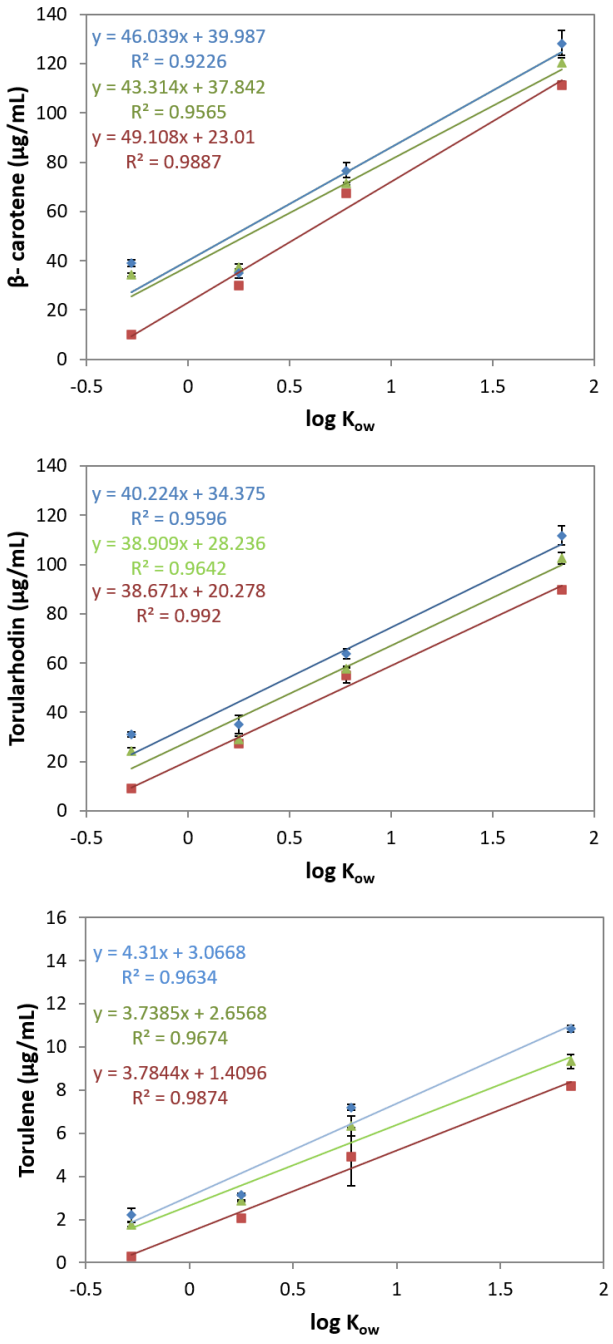

Figure 4.3. Linear relationship between log K_{ow} of the anions versus (**a**) β-carotene, (**b**) torularhodin, and (**c**) torulene recovery at a wet cell concentration of 0.2 g/mL after 1 h of stirring (30 rpm) at 25 °C for different PIL-based cation families: [PA][X] (red square), [DMAPA][X] (green triangle), and [DEAPA][X] (blue diamond).The error bars represent 95% confidence levels for the mean of three independent assays.

As can be seen in **Figure 4.3**, regardless of the cation used, a linear dependency between the relative hydrophobicity of the PIL anion and the carotenoids recovery yields was observed. PILs constituted by $[Ac]^-$ or $[Pro]^-$ anions, the most hydrophilic ones, showed the lowest extraction aptitude (almost equal). The similar positive slopes obtained for the three types of carotenoids confirm the increase of the recovery yields with the hydrophobicity of the PIL anion, as demonstrated by the good correlation of the linear least-squares regression obtained for all the PILs ($R^2 > 0.92$). Although it is not the focus of the work, the slight negative deviation in the linearity observed with $[Pro]^-$-based PILs is probably a result of an odd-even effect previously observed by some authors (Belchior et al. 2018), where the length of the alkyl chain spacer of the anion caused a reduction of the carotenoids recovery. In **Figure 4.3** is also observed a [DEAPA][X] > [DMAPA][X] > [PA][X] trend for the three carotenoids. The influence of the cation in the recovery of carotenoids will be extensively analyzed in the following sections for the $[Hex]^-$-based PILs under different operating conditions.

Figure 4.3 also depicts the following cation trend for the recovery of the three carotenoids: [DEAPA][X] > [DMAPA][X] > [PA][X]. The influence of the cation in the recovery of carotenoids will be extensively analyzed in the following sections for the $[Hex]^-$-based PILs at different operating conditions.

The results of this section demonstrated that the strong hydrophobic character of the anion favors the carotenoid extraction, which is in accordance with previous studies (Absalan, 2008; Mojaat et al. 2008), that defined the hydrophobicity as a good indicator for the choice of the most adequate carotenoids extractants. Mojaat et al. (Mojaat et al. 2008) evaluated the extraction of β-carotene from the microalgae *Dunaliella salina* using organic solvents, observing that only the solvents with the highest log K_{ow} values (log $K_{ow} > 5$) (more hydrophobic) are efficient in the recovery of β-carotene. Absalan et al. (Absalan et al. 2008) studied the aptitude of two hydrophobic ILs (1-butyl-3-methylimidazolium hexafluorophosphate [BMIM][PF_6] and 1-butyl-3-methylimidazolium tetrafluoroborate [BMIM][BF_4]) to recover 3-indole butyric acid (IBA) from pea plants, demonstrating a more affinity of IBA to the hydrophobic ILs. Interestingly, the authors have also shown a predominant effect of

the anionic part of the IL on the extraction of IBA, in comparison with the cationic counterpart.

4.3.3 Effect of temperature on the viscosity of PILs

The previous section supports that the more hydrophobic (more viscous) $[Hex]^-$-based PILs present the highest extraction efficiencies to recover intracellular carotenoids. However, the high viscosity of the PILs is a limitation for their use at the industrial scale, hindering the carotenoids mass transfer process from the intracellular to the extracellular environment as well as increasing the energy-processing requirements in terms of mixing and pumping costs (Marsh et al. 2004). From a thermodynamic point of view, viscosity issues can be simply overcome by increasing the temperature of the process. Therefore, considering that the carotenoids are fairly thermostable (Boon et al. 2010), the second series of experiments evaluated the association between increasing temperature and the solid-liquid extraction using the PIL solutions.

The viscosity dependence with temperature of the $[Hex]^-$-based PIL aqueous solutions (90, 85, 80, and 75% (v/v)) from 25 to 70 °C (defined as the maximum temperature to avoid the thermal degradation of the carotenoids) was assessed. As shown in **Figure 4.4**, the increase of the temperature in $[Hex]^-$-based PILs (90% v/v) significantly decreased the viscosity, namely, from 6.19 to 1.89 mPa·s for [PA][Hex], from 10.08 to 2.64 mPa·s for [DMAPA][Hex], and from 9.79 to 2.51 mPa·s for [DEAPA][Hex]. As previously reported (Kleinert et al. 1998; Ghatee et al. 2010; Ochędzan-Siodłak et al. 2013), the viscosity of the PILs decreases exponentially with the increase of temperature (Ghatee et al. 2010). The viscosities of the PILs are more comparable to those of oils than to those of organic solvents because of the hydrogen bonding and van der Waals interactions (Marsh et al. 2004). Therefore, by increasing the temperature, the intermolecular distances are increased, the attraction forces between the molecules are reduced, and consequently, their viscosities are also reduced (Marsh et al. 2004; Ochędzan-Siodłak et al. 2013).

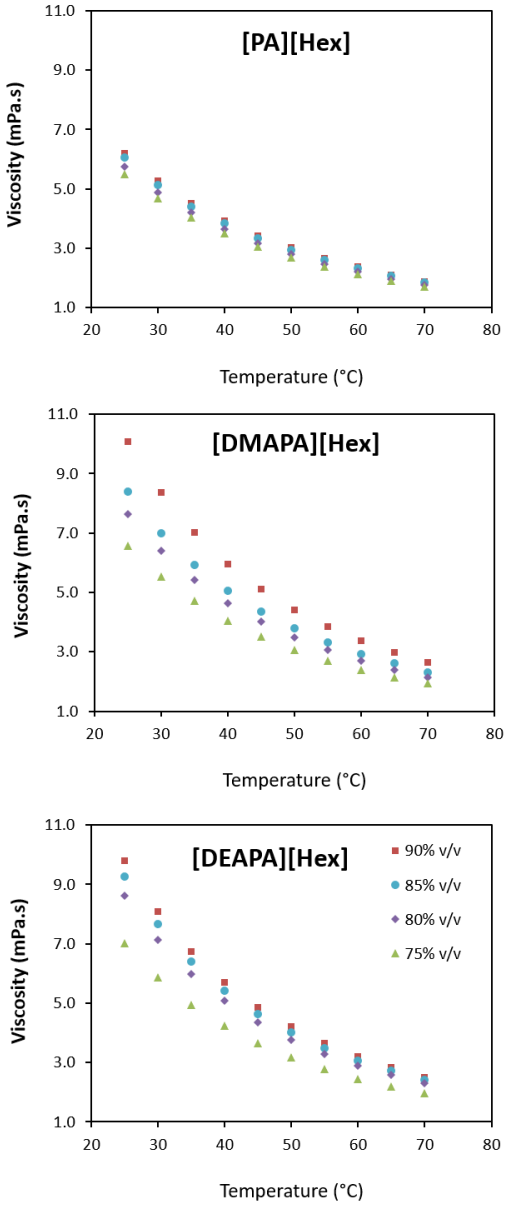

Figure 4.4. Viscosity (mPa.s) of different aqueous solutions of PILs as a function of temperature.

Regarding water influence, the viscosity decreased gradually with the increase of water content for the three PILs, that is, with the highest viscosities at 90% (v/v) of PILs and with the lowest values at 75% (v/v). As expected, the presence of the

water molecules reduced the electrostatic attraction between the ions and thus decreased the cohesive energy of the system and its viscosity (Seddon et al. 2000). Moreover, it was observed that the viscosity is strongly influenced by the chemical structure of the PIL cations with a higher viscosity index for $[DEAPA]^+$ and $[DMAPA]^+$ cations, the bulkier ions. On the other hand, the [PA][Hex] aqueous solutions exhibited the lowest viscosities. Our results are in agreement with those by Zhao et al., (Zhao et al. 2008), which demonstrated a close relation between the diethanolamine-based PILs viscosity and their relative mobility.

4.3.4 Effect of PIL concentration and temperature on the extraction of carotenoids

The previous section illustrates that the temperature increase, high water content, and the use of shorter PIL cations reduced the viscosity index of PILs. However, as shown above, both the water content and PIL cations appeared as key parameters to control the carotenoid extraction yields. Thus, to assess the relative influence of each operating parameter, the extraction of the three carotenoids using [PA][Hex], [DMAPA][Hex], and [DEAPA][Hex] as functions of concentration (v/v) (90, 85, 80, and 75%) and temperature (25, 45, and 65 °C) was performed. The results are depicted in **Figure 4.5** and detailed in **Table B.5** in the **Appendix B**.

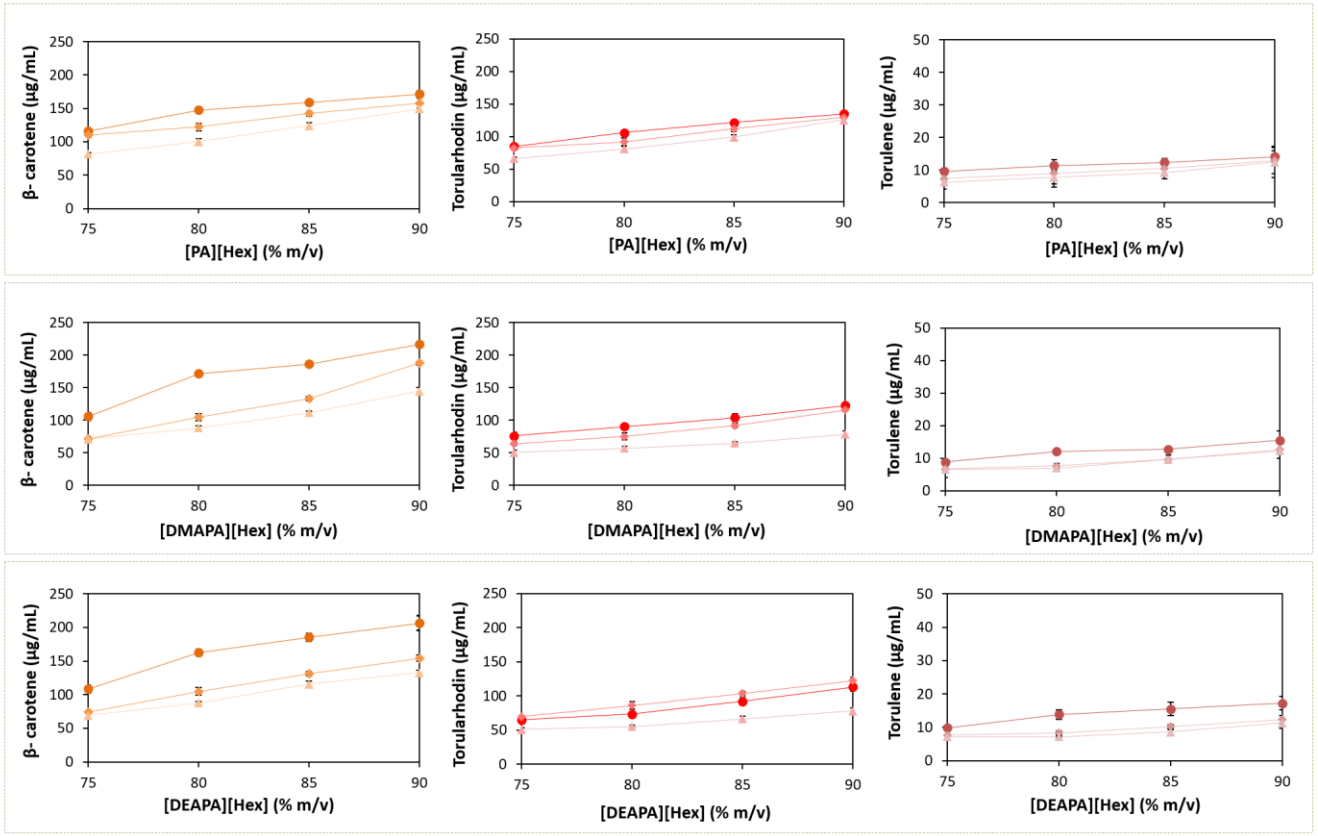

Figure 4.5. Effect of temperature [(triangle) 25 °C, (diamond) 45 °C, and (circle) 65 °C] as a function of PIL concentration [75, 80, 85, and 90% (v/v)] on the release of β-carotene, torularhodin, and torulene from *R. glutinis* wet cells (0.2 g/mL) after 1 h of stirring (30 rpm). The error bars represent 95% confidence levels for the mean of three independent assays but, in some cases, are smaller than the markers.

As shown in **Figure 4.5** the rates of carotenoids recoveries follow the trends [PA][Hex] < [DMAPA][Hex] < [DEAPA][Hex] (from top to bottom) and β-carotene > torularhodin > torulene (from left to right). The increase of temperature and PIL concentration favored significantly ($p \leq 0.05$) the release of β-carotene and torularhodin, but it was not significant for torulene ($p \geq 0.05$) (**Table B.5** from the **Appendix B**). For all the assays, an increase of cell disruption processing temperature favored the carotenoid release, that is, 65 > 45 > 25 °C. For example, the extraction at 25 °C using 90% (v/v) [DEAPA]-[Hex] recovered 133.06 ± 9.74, 78.15 ± 3.83, and 11.25 ± 1.47 μg/mL and, at 65 °C, recovered 206.65 ± 10.75, 112.82 ± 6.09, and 17.21 ± 1.99 μg/mL β-carotene, torularhodin, and torulene, respectively, which correspond to an increase of approximately 35.62, 30.74, and 34.64% of the respective carotenoid concentrations. The increase of temperature reduced the viscosity of the solvents, favoring the diffusion of the solvent into the biomass (Saini and Keum 2018), as well as increasing the carotenoids solubility. The solubility of the material extracted and its diffusivity increased with temperature, and consequently, higher extraction yields were achieved. Furthermore, the temperature can also favor the “destruction” of the cellular structure, (Strati and Oreopoulou 2011), allowing a greater release of the intracellular carotenoid content from the *R. glutinis* yeasts.

Similarly, the increase of PIL concentration from 75 to 90% (v/v) at optimum conditions (*i.e.,* [DEAPA][Hex] at 65 °C), increased the carotenoid concentration from 108.60 ± 5.48 to 206.65 ± 10.75 μg/mL (β-carotene), from 64.83 ± 2.96 to 112.82 ± 6.09 μg/mL (torularhodin), and from 9.84 ± 0.81 to 17.21 ± 1.99 μg/mL (torulene), which correspond to increases of 47.45, 42.54, and 42.83% in the extraction yields, respectively. Note that the increase of carotenoid recoveries is linearly dependent on the increase of PIL concentration. The treatment with concentrated PILs confers a more hydrophobic character to the solvent enhancing the carotenoids solubilization, as well as weakening the cell wall structure and promoting the release of intracellular carotenoids to the extracellular environment.

These results are in agreement with the studies of astaxanthin recovery from intact *H. pluvialis* cells using 1-ethyl-3-methylimidazolium dibutyl-phosphate ([EMIM][DBP]), carried out by Desai et al. (Desai et al. 2016), where it was demonstrated that the extraction yields of astaxanthin increases from ~2% to 18% when the IL concentration increases from 20 to 80%.

The results from this section showed that the decrease of the viscosity by increasing the temperature is beneficial for the recovery of the intracellular carotenoids. However, although more diluted solutions are less viscous, the increase of the PIL concentration is also critical for the cell disruption and the increase of the relative hydrophobicity of the solvent. Therefore, it seems that the balance between both diffusion and solubility parameters is the key for the success on carotenoid recoveries.

4.3.5 Effect of SLR and temperature on the extraction of carotenoids

In the previous section, it was demonstrated that the increase of the extraction of intracellular carotenoids can be enhanced by increasing both the temperature and concentration of the PIL. However, one of the most important processing parameters in the design of cell disrupting/biomass solid-liquid extraction industrial procedures is the solid-liquid ratio (SLR). Therefore, the next set of assays was conducted to find the best SLR (*i.e.,* wet *R. glutinis* cell mass/ PIL solution volume) for the release of the intracellular carotenoids. $[Hex]^-$-based PIL solutions at 90% (v/v) with different SLRs (0.05, 0.1, 0.2, and 0.5 g/mL wet cells) were prepared and used to determine the concentration of the carotenoids released at 25, 45, and 65 °C, as shown in **Figure 4.6** (detailed values are listed in **Table B.6** in the **Appendix B**).

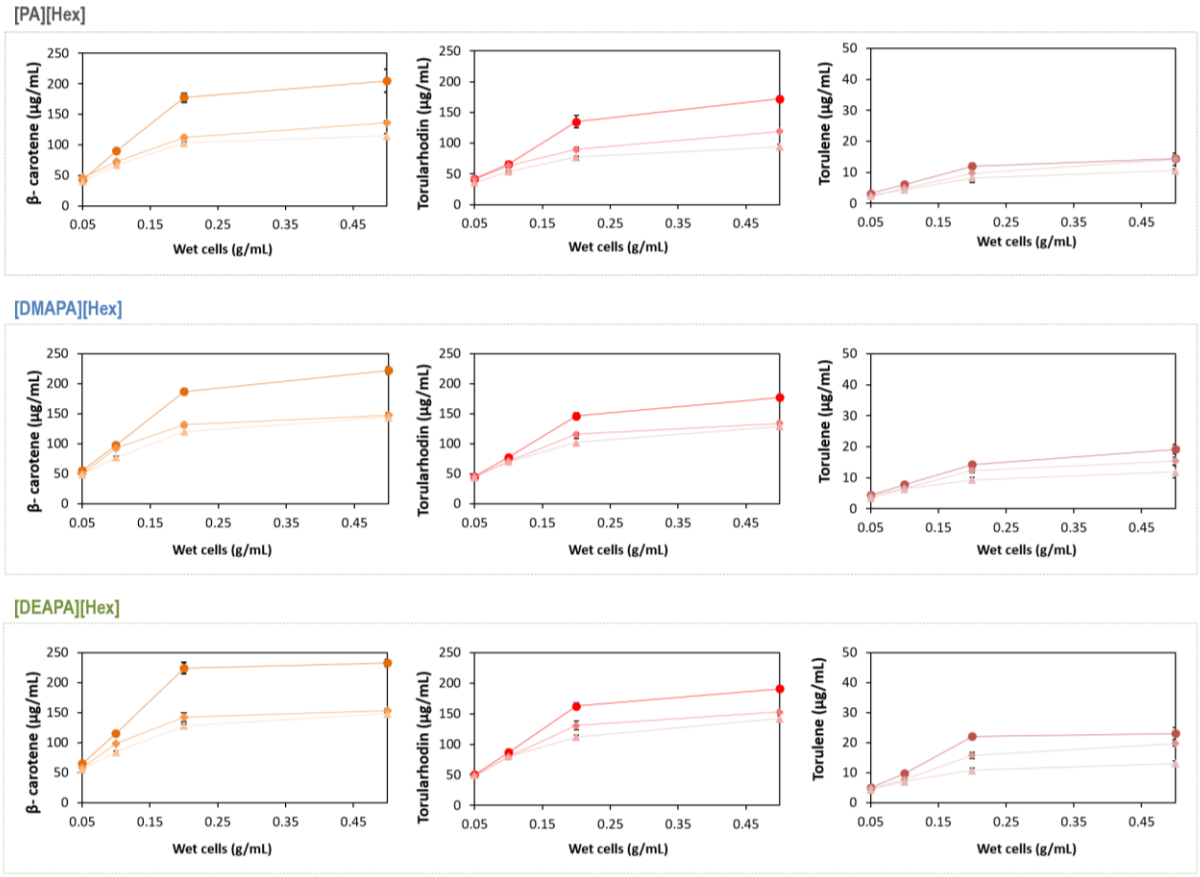

Figure 4.6. Effect of the temperature [(triangle) 25 °C, (diamond) 45 °C, and (circle) 65 °C] as a function of solid-liquid ratio, SLR (0.05, 0.1, 0.2, and 0.5 g/mL wet cells), on the release of β-carotene, torularhodin, and torulene using different solutions of PILs at 90% (v/v) after 1 h of stirring (30 rpm). The error bars represent 95% confidence levels for the mean of three independent assays, but in some cases, they are smaller than the markers.

Figure 4.6 shows a similar pattern between carotenoid concentrations and SLRs for the three $[Hex]^-$-based PILs (top to bottom) and the three carotenoids (left to right) studied. Namely, the concentration of each carotenoid increased linearly with the SLR up to a concentration of 0.2 g/mL *R. glutinis* wet cells. Above that SLR, the carotenoid concentration values remained constant. These results demonstrate that the carotenoid release capacity increases with the increase of the SLR up to a concentration where the solvent is fully saturated with carotenoids. According to Tan et al., (Tan et al. 2011), a higher SLR favors the concentration gradient by increasing the diffusion rate and the biomolecules contact with the solvent, allowing higher solid extraction yields. This is in full agreement with the mass-transfer principle that defines the concentration gradient between the solid and solvent as the driving force of solid/liquid extraction (Norshazila et al. 2017). These previous studies (Tan et al. 2011) also showed that the increase of the SLR only benefited the extraction yields up to the equilibrium concentration, and after which, the concentration of carotenoids remained constant.

Moreover, from **Table B.6** of the **Appendix B**, it is possible to infer the significant effect of temperature as a function of the SLR ($p \leq 0.05$) for both the β-carotene and torularhodin carotenoids. Although the extraction trends are maintained, higher temperatures favored the increase of carotenoid release. The increase of the temperature reduced the viscosity of the PIL solutions, enhancing the permeability of the cell wall for the PILs and consequently increasing the solubility of the carotenoids in the PIL solutions (Kleinert et al. 1998), supporting the results of the previous section.

4.3.6 Comparison and understanding of the PILs effects on the extraction of carotenoids

The main aim of this work was to evaluate and understand the capacity of different PILs for the intracellular recovery of carotenoids (β-carotene, torularhodin, and torulene) from the yeast *R. glutinis.* The experimental assays evaluated several process variables, namely temperature, concentration and type of PIL, and SLR.

Considering the number of parameters and for a better understanding of the PIL characteristics and their effect on the carotenoid release, **Figure 4.7** shows the absolute results obtained for β-carotene, torularhodin, and torulene extractions at 25, 45, and 65 °C at 0.2 g/mL wet cells using aqueous solutions 90% (v/v) different $[Hex]^-$-based PILs (those with the highest extraction capacity) (detailed values are listed in **Table B.5** in the **Appendix B**). As a control, the results were compared with the extraction values obtained with DMSO at similar operating conditions.

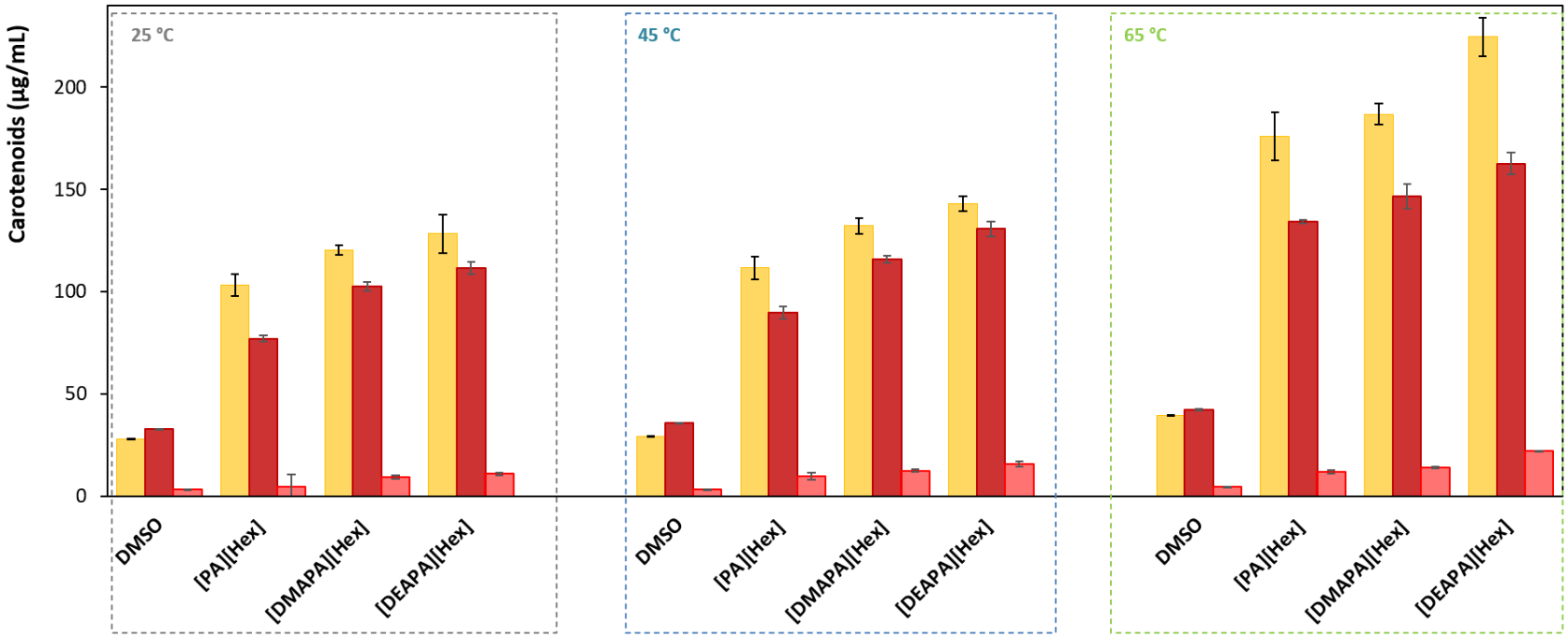

Figure 4.7. Recovery of β-carotene (yellow), torularhodin (red), and torulene (pink) using DMSO (control) and an aqueous solution of [Hex]--based PILs (90% v/v) at a wet cell concentration of 0.2 g/mL after 1 h of stirring (30 rpm) at 25, 45, and 65 °C. The error bars represent 95% confidence levels for the mean of three independent assays.

As shown in **Figure 4.7**, the increase in temperature favored the extraction with the highest yields achieved at 65 °C, exhibiting an increase according to the following trend: [DEAPA][Hex] > [DMAPA][Hex] > [PA][Hex]. Opposite to the PIL aqueous solution, the increase of temperature did not significantly ($p \geq 0.05$) favor the extraction of intracellular carotenoids using DMSO (similar carotenoid concentrations for the three temperatures). All $[Hex]^-$-based ILs were able to recover up to fourfold (25 °C) or sixfold (at 65 °C) more carotenoids than those of the DMSO. The highest carotenoid recoveries were obtained at 65 °C using [DEAPA][Hex] where 206.65 ± 10.75 μg/mL β-carotene, 112.82 ± 6.09 μg/mL torularhodin, and 17.21 ± 1.99 μg/mL torulene were extracted. On the other hand, from **Figure 4.6**, it was possible to confirm that all PILs are more selective for the recovery of β-carotene and torularhodin with a lower capacity to recover torulene. Interestingly, DMSO exhibited a higher aptitude to extract torularhodin than to extract β-carotene. Both PILs and DMSO exhibited a low capability to recover torulene probably because of the low production of *R. glutinis* for this type of carotenoid. To obtain further information about the mechanisms behind the carotenoid extraction as well as PIL effects on the cell structure, some samples of cellular debris undergoing different treatments were analyzed using scanning electron microscopy (SEM) (9000× resolution) and compared with whole yeast *R. glutinis* cells (without any treatment). The morphologies of the cells without any treatment and cell debris after exposure to DMSO (control) and [PA][Hex], [DMAPA][Hex], and [DEAPA][Hex] concentrated (90% v/v) solutions at 25, 45, and 65 °C are compared in **Figure 4.8**.

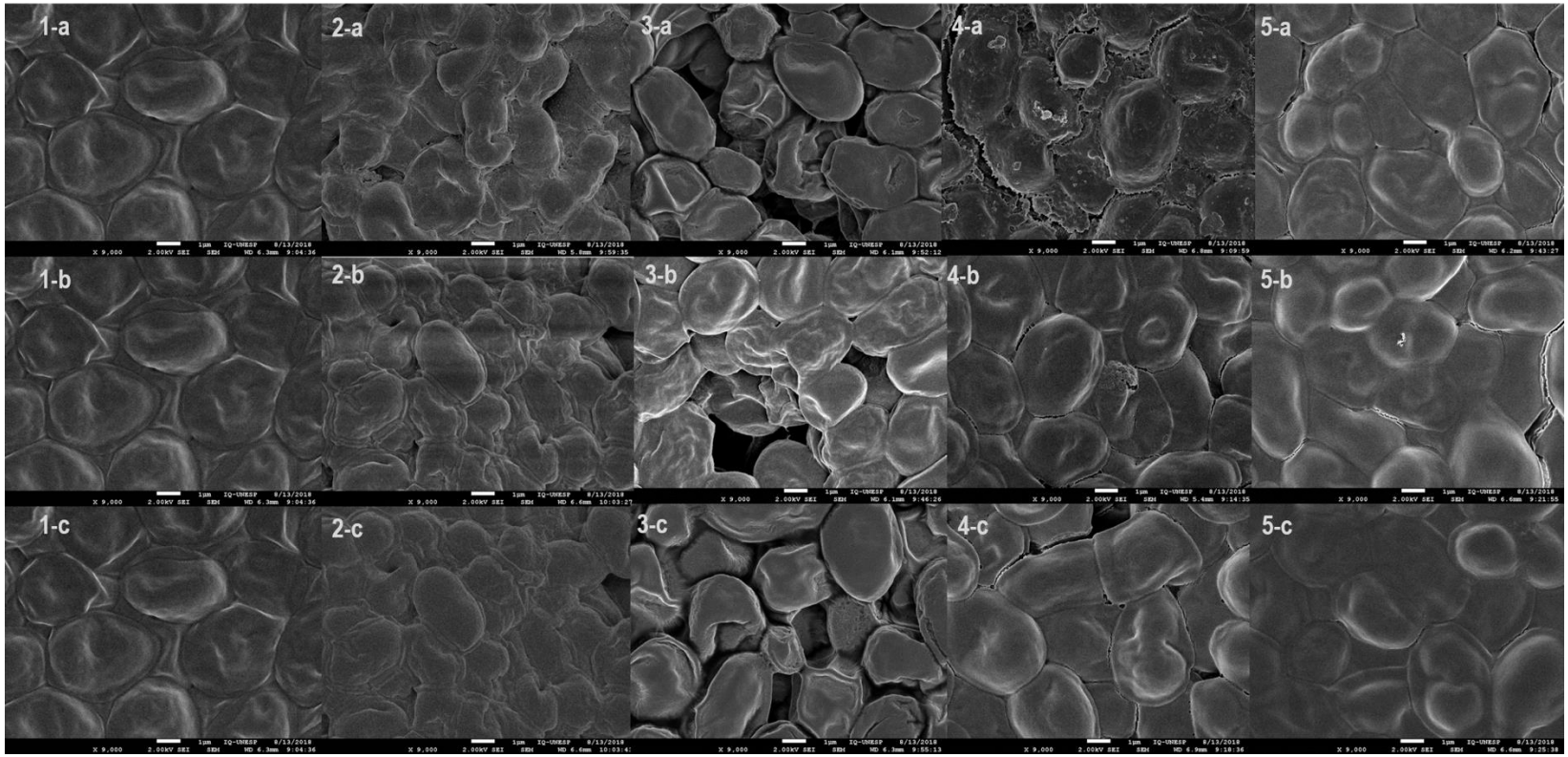

Figure 4.8. Scanning electron microscopy (SEM) images of *R. glutinis* CCT-2186 cells (or cell debris) (×9000) at different conditions: (**a)** 25 °C, (**b**) 45 °C, and (**c**) 65 °C. (**1**) Without treatment and after treatment with (**2**) DMSO, (**3**) [PA][Hex], (**4**) [DMAPA][Hex], and (**5**) [DEAPA][Hex] at 90% (v/v) and 0.2 g/mL wet cells.

As expected, the SEM images of the cells without treatment (**Figure 4.8: 1-a, 1-b** and **1-c**) show the characteristic spherical and oval shape of *R. glutinis* yeast cells (Fell, 1998). After the treatment with DMSO (**Figure 4.8: 2-a, 2-b and 2-c**) no significant cell-wall change was observed, but the cells appear dehydrated. For the cells exposed to the PIL aqueous solutions (**Figure 4.8: 3-5**), it is difficult to distinguish significant changes between the treatments since some cells remained intact and others exhibit a thin coat around the cells, which may be due to some "destruction" (permeabilization) of the cell membrane or the incomplete removal of the PILs after repeated washing with water. Particularly, the cells exposed to both [DMAPA][Hex] and [DEAPA][Hex] treatments at 65 °C seemed to lose the characteristic shape of the cell wall, inducing the permeabilization of the wall as well as a more elongated shape of the cell debris. These results corroborate those described by Desai and collaborators (Desai et al. 2016) where the use of IL permeabilized and/or weakened the cell wall of the microalgae *H. pluvialis*, allowing the recovery of the carotenoid astaxanthin.

From the literature, the carotenoids extraction mechanisms using ILs are still not fully understood (Choi et al. 2019; Desai et al. 2016). Considering the changes of the cell wall structure and the high extraction yields using $[Hex]^-$-based PILs, it is evident that these solvents exhibit a different cell disrupting mechanism than the common organic solvents (such as DMSO). Looking at the yeast cell wall composition, these are constituted by 15-30% proteins, 5-20% lipids, 30-60% polysaccharides, glucans, galactomannan, and with a minor content of chitin (Fell, 1998). Some of the yeast cell components are easily extractable under alkaline conditions, for example, 1,3-β-D-glucan and 1,3-α-D-glucan. Therefore, considering that the pH values of the ammonium-based PIL solutions varied from 7 to 11, it is highly plausible that the alkaline extraction significantly impaired both glucans, leading to a partial exposure of the cell membrane to the PIL solution and consequent permeation of the PILs into the cells. Another hypothesis for the high carotenoid recovery yields can be a mechanism caused by the IL absorption and

bilayer disruption by the addition of relative hydrophobic PIL ions. As previously reported in the simulation studies of Benedetto and Ballone (Benedetto and Ballone 2016) using a few different phosphatidylcholine lipids in water solutions of imidazolium-based ILs, the cations of the imidazolium-based ILs tend to enter the bilayer as a result of preferential attraction with the negative oxygen atoms in the carbonyl group at the matching point of the hydrocarbon tails or by binding to the non-ester oxygen atoms of the phosphonium group. Both authors have clearly shown that the cation absorption is apparently favored by substantial dispersion forces between the IL and phospholipid tails as well as by the hydrophobic character of the hydrocarbon tail of the IL. The simulation results confirmed an increase of both the IL absorption and bilayer disruption with the increase of the alkyl chain length of the cation tail. Other computational studies focused on more hydrophobic anions (I^- > Br^- > Cl^- > F^- ions) also confirmed the tendency to segregate at the lipid/ water interface, in agreement with the experimental evidences for traditional salts (aqueous solutions of alkali halide salts) (Berkowitz and Vácha 2012). Further modelling studies that simulate the interactions/solubility of PILs with the *R. glutinis* cell membrane components will allow us to better understand the main interactions behind the intracellular carotenoid's extraction.

4.3.7 Recycling of the PILs and carotenoids polishing

Due to the current market size and the relatively high cost of ILs, the industrial production of ILs is mainly for lab and pilot-scale applications (Ventura et al. 2017), although a couple of IL technologies have been successfully commercialized (Shubert, 2017). Regarding the current and future IL markets, recently, Shubert (Shubert, 2017) stated that "if the technical performance of an IL is fully demonstrated, it is trivial that, at a certain point also, the price determines the final commercial success of a product", but "to lower costs should never be the only argument that determines the success of technologies". Thus, from an academic point of view, it is important to demonstrate that the IL-based technology is possible even without considering economics. Anyway, to make these technologies

economically viable in comparison to existing industrial ones, ILs regeneration, recycling, and low-purity requirements should be always considered in order to provide technical solutions or answers to reduce the ILs costs in the process.

Therefore, even though no industrial technology is yet available for IL recycling and reusability, most of the academic publications on ILs have been proposing adequate methodologies for the effective reuse and regeneration of the IL solutions (Zhou et al. 2018). Many researchers agree that we are only at the very beginning of understanding the IL recyclability, and the understanding of ILs volatility, purity, stability, biodegradability, and toxicity is still necessary for their recovery since these determine whether an IL can be sustainably applied for a specific application (Ventura et al. 2017; Shubert, 2017; Zhou et al. 2018; Wu et al. 2009).

Therefore, to address the feasibility of the implementation of the proposed technology for future industrial recovery of carotenoids from yeast cells, a method for recycling the PIL solutions and obtaining the recovered carotenoids was attempted. The development of adequate technologies that allow the reuse of solvents is extremely important for increasing the environmental and economic sustainability of the downstream processes. Thus, an integrative approach for the polishing of carotenoids and recycling of the PILs using a three-phase partitioning (TPP) platform is here proposed, as schematized in **Figure 4.9**.

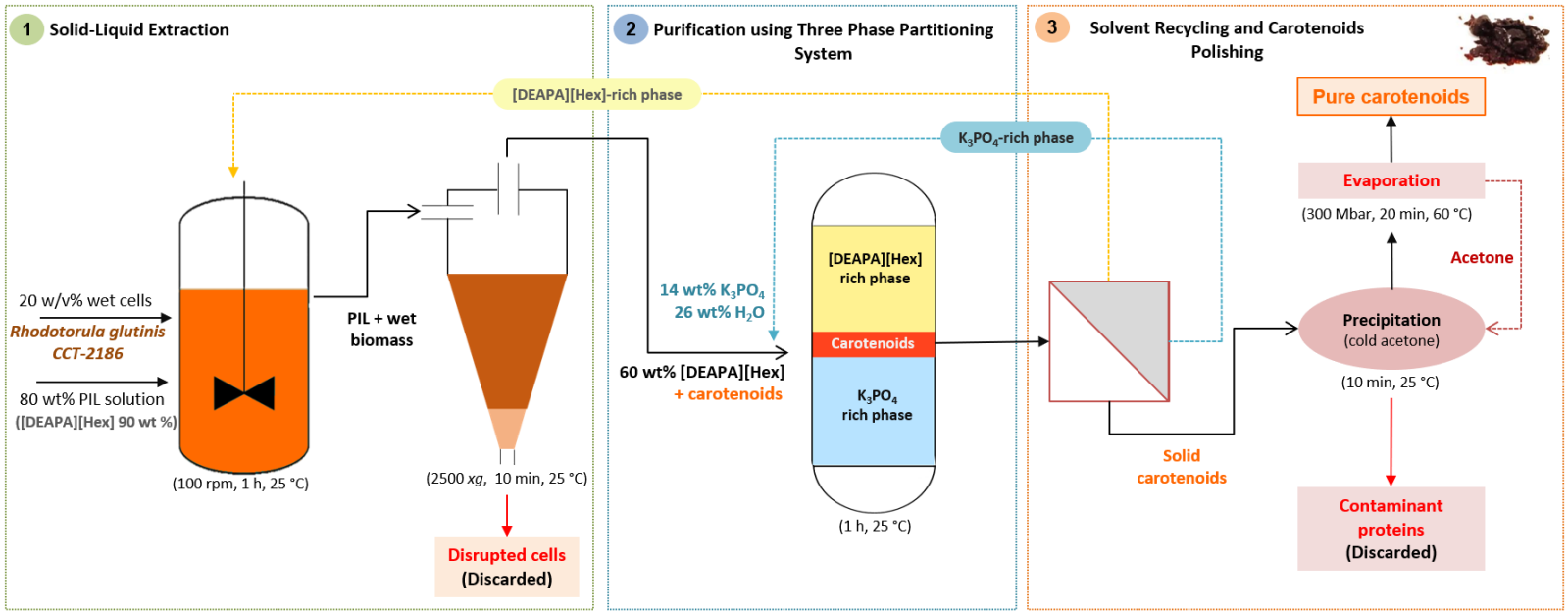

Figure 4.9. Diagram of the integrative process for the extraction of intracellular carotenoids using [DEAPA][Hex] solution (90% v/v), the recycling of the PIL using a three-phase partitioning system (TPP) by adding K_3PO_4 aqueous solution, and the polishing of the carotenoids.

The recycling studies were carried out for the [DEAPA][Hex] concentrated solution (90% v/v), which exhibited the highest recovery yields of carotenoids from *R. glutinis* wet cells. After the extraction, the carotenoid-rich [DEAPA][Hex] solution was separated from the residual *R. glutinis* biomass by centrifugation and subjected to a subsequent TPP extraction by adding K_3PO_4 concentrated aqueous solution at 25 °C. After the addition of the K_3PO_4 aqueous solution, a TPP (liquid-solid-liquid) system was formed with most of the carotenoids being precipitated as a solid fraction in the interface between both liquid (top and bottom) phases. The TPP was filtered, and the carotenoid-rich (solid) fraction was recovered as the concentrate as well as both the PIL (top)-rich phase and K_3PO_4 (bottom)-rich liquid phases (permeate). The PIL-rich phase was recycled for consecutive recovery of intracellular carotenoids from fresh *R. glutinis* cells, and the K_3PO_4-rich phase was recycled in a subsequent TPP procedure. The recycling procedure was repeated three times, and the respective amounts of carotenoids were extracted using the reused PIL solution compared with the fresh PIL (control) (detailed values are listed in **Table 4.1**).

Table 4.1. Recovery of β-Carotene, torularhodin, and torulene using fresh and reused [DEAPA][Hex] solution (90% v/v) at a wet cell concentration of 0.2 g/mL after 1 h of stirring (30 rpm) at 25 °C (Stage 1) and residual carotenoids remaining in the IL solution after the recycling procedure (Stage 3)[a]

PIL solution	Carotenoids recovered (µg/mL)/(%)	Residual carotenoids in IL solution after recycling (µg/mL)/(%)
β-Carotene		
Fresh PIL	187.8 ± 0.5 / 100.0 ± 0.0	18.4 ± 1.4 / 9.8 ± 0.8
1st reuse	206.3 ± 6.5 / 109.7 ± 4.2	37.9 ± 0.1 / 20.2 ± 1.2
2nd reuse	168.8 ± 3.2 / 89.9 ± 0.5	60.6 ± 3.6 / 32.3 ± 1.9
3rd reuse	150.7 ± 1.7 / 80.1 ± 1.9	- / -
Torularhodin		
Fresh PIL	122.6 ± 4.1 / 100.0 ± 0.0	7.5 ± 0.7 / 6.1 ± 0.4
1st reuse	127.7 ± 5.9 / 104.2 ± 1.4	12.3 ± 0.4 / 10.0 ± 0.0
2nd reuse	106.3 ± 4.1 / 86.7 ± 6.2	23.3 ± 0.7 / 19.0 ± 1.2
3rd reuse	91.2 ± 3.9 / 74.4 ± 5.7	- / -
Torulene		
Fresh PIL	22.9 ± 2.6 / 100.0 ± 0.0	9.1 ± 0.8 / 39.7 ± 0.7
1st reuse	27.7 ± 2.8 / 121.1 ± 6.5	17.3 ± 0.5 / 75.7 ± 6.6
2nd reuse	15.5 ± 2.4 / 67.9 ± 8.6	18.3 ± 0.9 / 79.9 ± 13.2
3rd reuse	13.4 ± 1.2 / 58.6 ± 1.6	- / -

[a] The results represent 95% confidence levels for the mean of three independent assays

As can be seen in **Table 4.1**, the PILs can be recycled up to three times without any treatment, guaranteeing the maintenance of good extraction efficiencies (> 58.8%). Particularly, after the third reuse of the PIL solution, the recovery efficiencies of 80.2, 74.4, and 58.8% were achieved for β-carotene, torularhodin, and torulene, respectively. The extraction rates decreased after the second reuse as a result of the solvent saturation, that is, the increase of the residual carotenoids concentration (the fraction that did not precipitate with the TPP procedures) in the PIL solution with the increase of the number of recycling stages (column 2 of **Table 4.1**). However, it is important to note that, in the first reuse, the PIL solution was not saturated, and the residual content of carotenoids caused an increase of the carotenoid recoveries to values higher than 100%.

Anyway, the reusability of the PIL by a simple integration of the initial solid-liquid extraction unit with a subsequent TPP process was demonstrated. However, considering that the recycling and polishing steps were carried out without any treatment, it should be highlighted that the make-up of the solvent (by adding fresh PIL solution) will improve the solvent recycling capacity of this platform.

Simultaneously with the recyclability of the PIL, the carotenoids polishing was performed. Then, the carotenoids-rich solid fraction, obtained after the TPP, was dissolved in acetone and subjected to the next precipitation step. The precipitation using cold acetone allowed the removal of the intracellular proteins also extracted with the [DEAPA][Hex] concentrated solution. After the precipitation, the acetone was removed by evaporation, and the purity of the carotenoids obtained in each recycling step (first, second, and third PIL reuse) was assessed by FTIR-ATR, as shown in **Figure 4.10**.

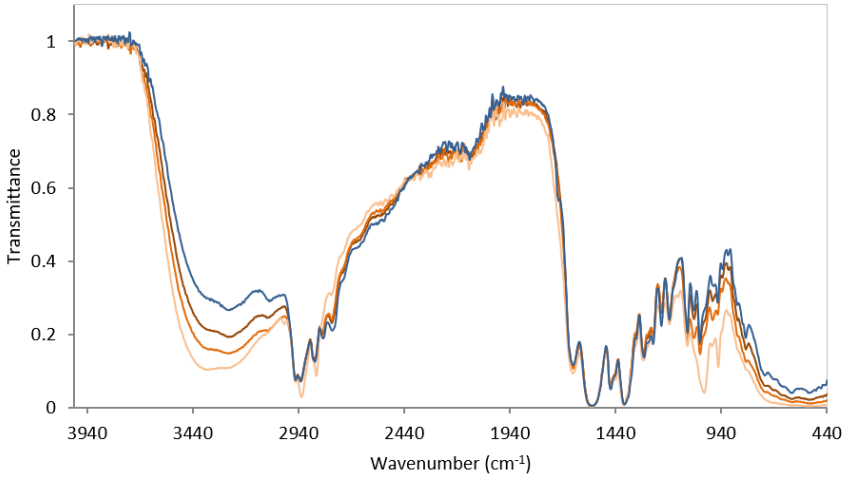

Figure 4.10. Fourier transform infrared spectroscopy with an attenuated total reflectance (FTIR-ATR) of carotenoids with DMSO extraction (control) (—) and reused [DEAPA][Hex]: 1st reuse (—) 2nd reuse (—) and 3rd reuse (—). Wavenumber (cm^{-1}) in the *x* axis and transmittance (%) in the *y* axis.

The FTIR-ATR spectra of the solid carotenoids fractions after the evaporation have a similar profile to that of the original carotenoids extracted with DMSO, confirming the non-degradation and purity of the carotenoids as well as indicating that they can be either used for the formulation of some bioproduct of interest (food or feed purposes) or undergo further biomaterial manufacturing processes.

Summing it up, the results of this work indicate that the integrative approach using PILs is an interesting platform to extract “natural” and valuable carotenoids from *R. glutinis* cells. Furthermore, the recovery of carotenoids and recycling of the PILs are also much easier to accomplish, supporting their use as a more cost-effective purification strategy. Although, for the implementation at the industrial scale, further scaling-up studies are still required, these results indicate that this platform is promising for the recovery of other microbiologically produced molecules.

4.4 Conclusions

In this work, an integrative and effective process for the recovery of intracellular carotenoids from *R. glutinis* CCT-2186 cells was established. All PILs allowed the recovery of the three major carotenoids, that is, β-carotene, torularhodin, and torulene. The increase of the temperature and the hydrophobicity (either by increasing the anionic or cationic alkyl chain length) and concentration of the PILs favored the carotenoids extraction. $[Hex]^-$-based PILs were the most efficient in the recovery of intracellular carotenoids with extraction rates sixfold higher than those of the common volatile organic solvent (DMSO). Additionally, the economic and environmental sustainability of the process was demonstrated by integrating the cell-disruption stage with a subsequent three-phase partitioning unit where the carotenoid extraction yields were maintained after reusing up to three times the [DEAPA][Hex] concentrated solution. This study shows the potential of the use of PILs in the extraction of biologically active molecules (*i.e*., carotenoids) at mild and accessible conditions as an alternative to environmentally nonfavorable volatile organic solvents.

4.5 References

Absalan G, Akhond M, Sheikhian L (2008) Extraction and high-performance liquid chromatographic determination of 3-indole butyric acid in pea plants by using imidazolium-based ionic liquids as extractant. Talanta 77, 407−411.

Aksu Z, Eren AT (2007) Production of carotenoids by the isolated yeast of *Rhodotorula glutinis*. Biochem. Eng. J. 35, 107−113.

Baranskia R, Cazzonelli CI (2016) Carotenoid biosynthesis and regulation in plants. In Carotenoids: Nutrition, Analysis and Technology; Kaczor, A; Baranska, M, Eds.; John Wiley & Sons Ltd; Hoboken 10, 159−189.

Belchior DCV, Almeida MR, Sintra TE,Ventura SPM, Duart IF, Freire MG (2019) Odd-even effect in the formation and extraction performance of ionic-liquid-based aqueous biphasic systems. Ind. Eng. Chem. Res 58, 8323−8331.

Belchior DCV, Sintra TE, Carvalho PJ, Soromenho MRC, Esperanca, JMSS, Ventura SPM, Rogers RD, Coutinho JAP, Freire MG (2018) Odd-even effect on the formation of aqueous biphasic systems formed by 1-alkyl-3-methylimidazolium chloride ionic liquids and salts. J. Chem. Phys 148, 193842.

Benedetto A, Ballone P (2016) Room temperature ionic liquids interacting with biomolecules: An overview of experimental and computational studies. Philos. Mag 96, 870−894.

Berkowitz ML, Vacha R (2012) Aqueous solutions at the interface with phospholipid bilayers. Acc. Chem. Res 45, 74−82.

Bhosale P, Gadre R (2001) Production of β-carotene by a mutant of *Rhodotorula glutinis*. Appl. Microbiol. Biotechnol 55, 423−427.

Boon CS, McClements DJ, Weiss J, Decker EA (2010) Factors influencing the chemical stability of carotenoids in foods. Crit. Rev. Food Sci. Nutr 50, 515−32.

Buzzini P, Martini A (2000) Production of carotenoids by strains of *Rhodotorula glutinis* cultured in raw materials of agro-industrial origin. Bioresour. Technol 71, 41−44.

Chemspider (2019) http://www.chemspider.com/ (accessed June 1st2019).

Choi SA, Oh YK, Lee J, Sim SJ, Hong ME, Park JY, Kim, MS, Kim SW, Lee JS (2019) High-efficiency cell disruption and astaxanthin recovery from *Haematococcus pluvialis* cyst cells using room-temperature imidazolium-based ionic liquid/water mixtures. Bioresour. Technol 274, 120−126.

Desai RK, Streefland M, Wijffels RH, Eppink MHM (2016) Novel astaxanthin extraction from *Haematococcus pluvialis* using cell permeabilising ionic liquids. Green Chem 18, 1261−1267.

Dufosse L (2018) Microbial pigments from bacteria, yeasts, fungi, and microalgae for the food and feed industries. In Natural and Artificial Flavoring Agents and Food Dyes; Academic Press 113−132.

Egorova KS, Gordeev EG, Ananikov VP (2017) Biological activity of ionic liquids and their application in pharmaceutics and medicine. Chem. Rev 117, 7132−7189.

Fell JW, Statzell-Tallman A (1998) The yeast, a taxonomic study; Kurtzman, C., Fell, J. W., Ed.; Elsevier: Amsterdam 800−827.

Galvao J, Davis B, Tilley M, Normando E, Duchen MR, Cordeiro MF (2014) Unexpected low-dose toxicity of the universal solvent DMSO. FASEB J 28, 1317−1330.

Ghatee, MH, Zare M, Moosavi F, Zolghadr AR (2010) Temperature-dependent density and viscosity of the ionic liquids 1-Alkyl-3-Methylimidazolium iodides: Experiment and molecular dynamics simulation. J. Chem. Eng. Data 55, 3084−3088.

Greaves TL, Drummond CJ (2015) Protic ionic liquids: evolving structure-property relationships and expanding applications. Chem. Rev. 115, 11379−11448.

Henríquez V, Escobar C, Galarza J, Gimpel J (2016) Carotenoids in Microalgae. Subcell. Biochem 79, 219−237.

Karpinski TM, Adamczak A (2019) Fucoxanthin An Antibacterial Carotenoid. Antioxidants 8, 239.

Kleinert T, Doster W, Leyser H, Petry W, Schwarz V, Settles M (1998) Solvent composition and viscosity effects on the kinetics of CO binding to horse myoglobin. Biochemistry 37, 717−733.

Kot AM, Błazejak S, Gientka I, Kieliszek M, Brys J (2018) Torulene and torularhodin: “new” fungal carotenoids for industry? Microb. Cell Fact 17, 49.

Kot AM, Błazejak S, Kieliszek M, Gientka I, Brys, J (2019) Simultaneous production of lipids and carotenoids by the red yeast *Rhodotorula* from waste glycerol fraction and potato wastewater. Appl. Biochem. Biotechnol 188, 1−19.

Kot AM, Błazejak S, Kurcz A, Gientkas I, Kieliszek M (2016) *Rhodotorula glutinis* potential source of lipids, carotenoids, and enzymes for use in industries. Appl. Microbiol. Biotechnol 100, 6103.

Latha BV, Jeevaratnam K (2010) Purification and characterization of the pigments from *Rhodotorula glutinis* DFR-PDY isolated from natural source. Global J. Biotechnol. Biochem 5, 166−174.

Marsh KN, Boxall JA, Lichtenthaler R (2004) Room temperature ionic liquids and their mixtures a review. Fluid Phase Equilib 219, 93−98.

Mata-Gomez LC, Montañez JC, Mendeź-Zavala A, Aguilar CN (2014) Biotechnological production of carotenoids by yeasts: an overview. Microb. Cell Fact 13, 12.

Mesquita SDS, Teixeira CMLL, Servulo EFC (2017) Carotenoids: properties, applications and market. Rev. Virtual Quim 9, 672−688.

Mojaat M, Foucault A, Pruvost J, Legrand J (2008) Optimal selection of organic solvents for biocompatible extraction of β-carotene from *Dunaliella salina*. J. Biotechnol 133, 433−441.

Mussagy CU, Winterburn J Santos-Ebinuma VC, Pereira JFB (2019) Production and extraction of carotenoids produced by microorganisms. Appl. Microbiol. Biotechnol 103, 1095−1114.

Norshazila S, Koy CN, Rashidi O, Ho LH, Azrina I, Nurul-Zaizuliana RA, Zarinah Z (2017) The Effect of time, temperature and solid to solvent ratio on pumpkin carotenoids extracted using food grade solvents. Sains Malays 46, 231−237.

Ochedzaņ-Siodłak W, Dziubek K, Siodłak D (2013) Densities and viscosities of imidazolium and pyridinium chloroaluminate ionic liquids. J. Mol. Liq 177, 85−93.

Oliveira MVS, Vidal BT, Melo CM, de Miranda RCM, Soares CMF, Coutinho JAP, Ventura SPM, Mattedi S, Lima AS (2016) (Eco)toxicity and biodegradability of protic ionic liquids. Chemosphere 147, 460−466.

Osada I, de Vries H, Scrosati B, Passerini S (2016) Ionic-liquid-based polymer electrolytes for battery applications. Angew. Chem., Int. Ed 55, 500−513.

Park PK, Kim EY, Chu KH (2007) Chemical disruption of yeast cells for the isolation of carotenoid pigments. Sep. Purif. Technol 53, 148−152.

Peric B, Sierra J, Martí E, Cruanas R, Garau MA, Arning J, Bottin-Weber U, Stolte S (2013) (Eco)toxicity and biodegradability of selected protic and aprotic ionic liquids. J. Hazard. Mater 261, 99−105.

Qi W, Ding D, Salvi RJ (2008) Cytotoxic effects of dimethyl sulphoxide (DMSO) on cochlear organotypic cultures. Hear. Res 236, 52−60.

Saenge C, Cheirsilp B, Suksaroge TT, Bourtoom T (2011) Potential use of oleaginous red yeast *Rhodotorula glutinis* for the bioconversion of crude glycerol from biodiesel plant to lipids and carotenoids. Process Biochem 46, 210−218.

Saini RK, Keum YS (2018) Carotenoid extraction methods: A review of recent developments. Food Chem 240, 90−103.

Seddon KR, Stark A, Torres MJ (2000) Influence of chloride, water, and organic solvents on the physical properties of ionic liquids. Pure Appl. Chem 72, 2275−2287.

Shubert TJS (2017) Current and future ionic liquids markets. ACS Symp. Ser 1250, 35−65.

Sintra TE, Gantman MG, Ventura SPM, Coutinho JAP, Wasserscheid P, Schulz PS (2019) Synthesis and characterization of chiral ionic liquids based on quinine, L-proline and L-valine for enantiomeric recognition. J. Mol. Liq 283, 410−416.

Strati IF, Oreopoulou V (2011) Effect of extraction parameters on the carotenoid recovery from tomato waste. Int. J. Food Sci. Technol 46, 23−29.

Tan PW, Tan CP, Ho CW (2011) Antioxidant properties: Effects of solid-to-solvent ratio on antioxidant compounds and capacities of Pegaga (*Centella asiatica*). Int. Food Res. J 18, 557−562.

Ventura SPM, Silva FA, Quental MV, Mondal D, Freire MG, Coutinho JAP (2017) Ionic-liquid-mediated extraction and separation processes for bioactive compounds: past, present, and future trends. Chem. Rev 117, 6984−7052.

Vieira FA, Guilherme RJR, Neves MC, Rego A, Abreu MH, Coutinho JAP, Ventura SPM (2018) Recovery of carotenoids from brown seaweeds using aqueous solutions of surface-active ionic liquids and anionic surfactants. Sep. Purif. Technol 196, 300−308.

Wu B, Liu W, Zhang Y, Wang H (2009) Do we understand the recyclability of ionic liquids? Chem. − Eur. J 15, 1804-1810.

Zhao C, Burrell G, Torriero AAJ, Separovic F, Dunlop NF, MacFarlane DR, Bond AM (2008) Electrochemistry of room temperature protic ionic liquids. J. Phys. Chem. B 112, 6923− 6936.

Zhou J, Sui H, Jia Z, Yang ZH, Li X (2018) Recovery and purification of ionic liquids from solutions: a review. RSC Adv 8, 32832−32864.

Zoz L, Carvalho JC, Soccol VT, Casagrande TC, Cardoso L (2015) Torularhodin and torulene: bioproduction, properties and prospective applications in food and cosmetics - A Review. Braz. Arch. Biol. Technol 58, 278−288.

5. DETERMINATION, CHARACTERIZATION AND MODELING OF AQUEOUS BIPHASIC SYSTEMS COMPOSED OF PROTIC IONIC LIQUIDS

Based on the manuscript

Determination, characterization and modeling of aqueous biphasic systems composed of propylammonium-based ionic liquids and phosphate salts

Mussagy CU, Tabanez NL, Farias FO, Kurnia KA, Mafra MR and Pereira JFB

Chemical Physics Letters, 754, 137623, **2020**.

Abstract

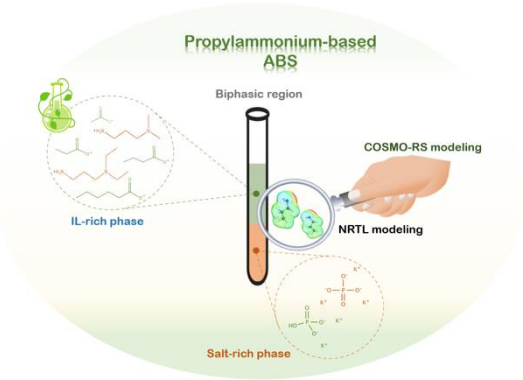

Ionic liquids (ILs)-based aqueous biphasic systems (ABS) are efficient platforms for the extraction and purification of biomolecules. To find more biocompatible ABS, propylammonium-based ILs, phosphate salts and water were mixed at three temperatures, evaluating the influence of IL and temperature on the liquid-liquid equilibria (LLE). The biphasic region increases with the increase of IL' anionic/cationic chain and decreases with the increase of temperature. There is good agreement between the IL' ability to form ABS and the hydrogen bonding interaction predicted by COSMO-RS. The subtle balance of hydrogen bonding between salt anion-water and IL anion-water governs the phase separation.

Keywords: *Aqueous biphasic systems; ionic liquids; liquid-liquid extraction; phase diagrams; COSMO-RS; NRTL.*

5.1 Introduction

Per-Ake Albertsson, in 1956, introduced aqueous biphasic systems (ABS) as a liquid-liquid extraction (LLE) platform to separate proteins (Albertsson 1956). Since then, the partition, extraction and purification of biomolecules using ABS have been extensively studied, mainly because of its high selectivity, low cost, adaptability to continuous processing and biological compatibility (Ventura et al. 2009; Quental et al. 2015a; Neves et al. 2016; Vieira et al. 2018; Mussagy et al. 2019b). ABS consist of two immiscible water-rich phases that can be formed by combining polymer/polymer, polymer/salt or salt/salt aqueous solutions, above certain concentrations (Freire et al. 2012a). In the past decade, after revealing that ionic liquids (ILs) can also be used as phase forming components (Gutowski et al. 2003), the interest in this type of liquid-liquid systems has raised significantly. Comparing with the traditional polymer/salt ABS, the use of ILs as phase forming agents has extra advantages, such as decreasing the phases' viscosity, separation times and emulsification index; to increase of the solvation ability and extraction efficiency (Sintra et al. 2014; Quental et al. 2015a; Marchel et al. 2019). Although most of the previous studies used IL-based ABS due to the more environmentally friendly and sustainable characteristics (in comparison with common volatile organic solvents-based LLE processes (Sintra et al. 2014), its wide tunability is the major advantage of this type of systems (Sintra et al. 2014; Greaves and Drummond 2015; Quental et al. 2015b). In particular, by a proper choice of the cation/anion pair, a careful tailoring of the ABS phases' polarities and solutes' affinities can be achieved, and consequently increasing the selectivity and extraction yields (Marchel et al. 2019).

The influence of the IL' cation (Ventura et al. 2009; Louros et al. 2010; Quental et al. 2015a; Neves et al. 2016; Vieira et al. 2018) and anion nature (Ventura et al. 2009; Sintra et al. 2014; Marchel et al. 2019), or simply the effect of salt type (Asenjo and Andrews 2011; Sintra et al. 2014; Marchel et al. 2019), on the formation of IL/salt ABS have been already studied. However, the number of ABS composed of ammonium-based ILs and inorganic salts are still scarce. Considering that the characterization of ternary phase diagrams is crucial for designing industrial LLE processes, in this work, fourteen novel LLE experimental

data of propylammonium-based ILs/phosphate salts ABS were obtained. First, to investigate the influence of the IL' cation and anion on phase separation, the ability to form ABS in the presence of tripotassium phosphate (K_3PO_4) or dipotassium hydrogen phosphate (K_2HPO_4) aqueous solutions was evaluated for the following ILs: propylammonium propanoate ([PA][Pro]); propylammonium butanoate ([PA][But]); propylammonium hexanoate ([PA][Hex]); 3-dimethylamino-1-propylammonium propanoate ([DMAPA][Pro]); 3-dimethylamino-1-propylammonium butanoate ([DMAPA][But]); 3-dimethylamino-1-propylammonium hexanoate ([DMAPA][Hex]); 3-diethylamino propylammonium propanoate ([DEAPA][Pro]); 3-diethylamino-propylammonium butanoate ([DEAPA][But]); and 3-diethylamino-propylammonium hexanoate ([DEAPA][Hex]). All ABS were determined at 298.15 K and atmospheric pressure, excepting the systems composed of hexanoate-based ILs, for which the LLE was also determined at 308.15 K and 318.15 K. The compositions of the coexisting phases were experimentally determined and correlated using the non-random two-liquid (NRTL) model for the activity coefficient. In addition, the predictive model Conductor-like Screening Model for Real Solvent (COSMO-RS) was used for a better understanding of the phase separation phenomena, predicting the interaction energy in term of excess enthalpy.

5.2 Experimental section

5.2.1 Materials

Tripotassium phosphate (K_3PO_4) (P.A.) and dipotassium hydrogen phosphate (K_2HPO_4) (P.A.) were acquired from LS Chemicals (Ribeirao Preto, SP, Brazil). Propylamines [propylamine (PA) (98%); 3-dimethylamino-1-propylamine (DMAPA) (99 %); 3-diethylamino-propylamine (DEAPA) (99 %)] and carboxylic acids [hexanoic acid (Hex) (99 %); butyric acid (But) (99 %); propanoic acid (Pro) (99.5 %); and acetic acid (Ac) (99.8 %)] used in the ILs synthesis were purchased from Sigma-Aldrich® (St. Louis, MO, USA). All the other reagents were of analytical grade with a minimum purity of 98%. The water used in all the experiments was double distilled, passed through a reverse osmosis system and

then treated with a Milli-Q plus 185 (Massachusetts, USA) water purification equipment.

5.2.2 Ionic Liquids Synthesis

Propylammonium-based ILs (chemical structures in **Table 5.1**) were synthesized *via* neutralization reaction of the base with the appropriate acid, according the procedure previously described (Sintra et al. 2014). Before use, all the ILs were purified and dried for 48 h at constant agitation (≈ 100 rpm), and moderate temperature (≈ 298 K) under vacuum (300 mbar). The purity of each IL was further assessed by proton nuclear magnetic resonance (^{1}H NMR) analysis (Bruker Avance III HD 600 14.1.T, Massachusetts, USA).

Table 5.1. Name, acronym and chemical structure of the ILs and corresponding ability to form ABS with tripotassium phosphate (K_3PO_4) and dipotassium phosphate (K_2HPO_4) aqueous solutions at 298.15 K and atmospheric pressure.

Name	Acronym	Cation	Anion	Ability to Form ABS	
				K_3PO_4	K_2HPO_4
Propylammonium acetate	[PA][Ac]	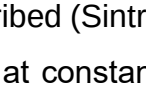		✗	✗
Propylammonium propanoate	[PA][Pro]			✗	✗
Propylammonium butanoate	[PA][But]		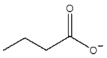	✗	✗
Propylammonium hexanoate	[PA][Hex]		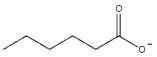	✓	✓
3-dimethylamino-1-propylammonium acetate	[DMAPA][Ac]	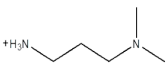		✗	✗
3-dimethylamino-1-propylammonium propanoate	[DMAPA][Pro]			✓	✓
3-dimethylamino-1-propylammonium butanoate	[DMAPA][But]		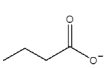	✓	✓
3-dimethylamino-1-propylammonium hexanoate	[DMAPA][Hex]		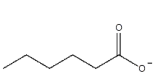	✓	✓
3-diethylamino-propylammonium acetate	[DEAPA][Ac]	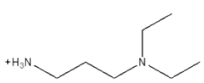		✗	✗
3-diethylamino-propylammonium propanoate	[DEAPA][Pro]			✓	✓
3-diethylamino-propylammonium butanoate	[DEAPA][But]		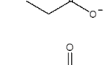	✓	✓
3-diethylamino-propylammonium hexanoate	[DEAPA][Hex]		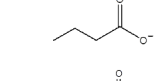	✓	✓

5.2.3 Phase Diagrams Determination

The binodal curve (limit between monophasic and biphasic regimes) of each ternary phase diagram was determined at 298.15 (±1) K and atmospheric pressure through the cloud point titration method (Merchuk et al. 1998). In order to study the effect of temperature, ABS composed of hexanoate-based ILs were also determined at 308.15 K and 318.15 K, and atmospheric pressure. Aqueous solutions of phosphate salts (≈ 40 wt%) and ILs (from 60 to 80 wt%) were used to determine the saturation solubility curves. Briefly, the cloud point method consisted in the repetitive dropwise addition of the salt solution into each IL aqueous solutions until the detection of a cloudy solution (biphasic region), followed by the dropwise addition of ultrapure water until the mixture turns to clear solution (monophasic region). All experimental procedure was performed under constant stirring at controlled temperature. The ternary system compositions were determined by weight quantification of all pure components added, with an uncertainty of $\pm 10^{-4}$ g. The experimental binodal curves were fitted using the equation of the Merchuk (Merchuk et al. 1998) (**Equation 5.1**):

$$Y = A \exp\left[(B \times X^{0.5}) - (C \times X^{3})\right] \qquad (5.1)$$

where *Y* and *X* represent the IL and salt weight fraction percentages, respectively, and *A*, *B*, and *C* are constants obtained by the regression of the experimental binodal data.

5.2.4 Tie-Lines determination

For each ABS, three mixture points in the biphasic region (detailed compositions listed in **Table 5.2** and **5.3**) were chosen and the respective tie-lines (TLs) determined. The ternary systems were gravimetrically ($\pm 10^{-4}$ g) prepared by adding IL, salt, and water in 10 mL graduated centrifuge tubes (a total mass of approximately 10 g). Each system was then vigorously stirred using a vortex mixer Phoenix AP-59 (Araraquara, SP/Brazil) and left to equilibrate in a thermostatic water bath (Solab® model SL-152, Piracicaba, SP, Brazil) for 1 hour

at temperature of interest and atmospheric pressure. The top and bottom phases were carefully separated (using glass Pasteur pipettes) and individually weighed.

The composition of the phases was determined analytically, by combining proton nuclear magnetic resonance (^{1}H NMR) and volumetric Karl Fischer titration method (Farias et al. 2018) (water content). The IL content was quantified by ^{1}H NMR analysis, in a Bruker Avance III (600 MHz) (Massachusetts, USA), using deuterated dimethyl sulfoxide and tetramethylsilane (TMS) as solvent and internal reference, respectively. Karl Fischer titration (Metrohm® 852 Titrando (Herisau, Switzerland) for water quantification was carried out using HYDRANAL™-Methanol Rapid (reagent for accelerated volumetric one-component KF titration) and HYDRANAL™-Composite 5 (reagent for volumetric one-component Karl Fischer titration; methanol free), both supplied by Sigma-Aldrich® (Brazil) as titrants. The composition of phosphate salt in the coexisting phases was obtained by the mass balance of all ABS components, considering the initial mass of each component and the difference between the IL and water amounts in the top and bottom phases, respectively. Tie-line length (TLL), which represents the final concentration of phase components in the top and bottom phases and it is used to express the effect of system composition on the partition (Farias et al. 2018), was calculated for each system according the **equation 5.2**:

$$\mathrm{TLL} = \sqrt{\left([\mathrm{Salt}]_{\mathrm{bottom}} - [\mathrm{Salt}]_{\mathrm{top}}\right)^2 + \left([\mathrm{IL}]_{\mathrm{bottom}} - [\mathrm{IL}]_{\mathrm{top}}\right)^2} \qquad (5.2)$$

where [Salt] and [IL] correspond to salt and IL concentration, respectively, and the subscripts *bottom* and *top* correspond to each of the coexisting phases of the ABS. **Equation 5.3** was applied for the calculation of the slope of the tie-line (*STL*):

$$\mathrm{STL} = \frac{[\mathrm{IL}]_{\mathrm{top}} - [\mathrm{IL}]_{\mathrm{bottom}}}{[\mathrm{Salt}]_{\mathrm{top}} - [\mathrm{Salt}]_{\mathrm{bottom}}} \qquad (5.3)$$

5.2.5 NRTL (non-random two-liquid) model

LLE experimental data was correlated using a local composition non-random two liquid (NRTL) model, applicable to partially miscible systems. The estimation of the new binary interaction parameters was performed using

Matlab®. LLE experimental data were correlated by optimizing the binary interaction parameters, namely A_{0ij} (characteristic energy of interaction between the components) and α_{ij} (non-randomness of the mixture). For this purpose, the LLE equations and the objective function (*OF*) were minimized using a modified Simplex numeric method (Nelder and Mead 1964; Toledo et al. 2019) detailed in **Equation 5.4**:

$$\mathrm{OF} = \sum_{k}^{D}\sum_{j}^{M}\sum_{i}^{N-1}\left(x_{ijk}^{I.exp} - x_{ijk}^{I.calc}\right)^2 + \left(x_{ijk}^{II.exp} - x_{ijk}^{II.calc}\right)^2 \quad (5.4)$$

where weight fraction is represented by *X*, and superscripts *I* and *II* refer to the two liquid phases in thermodynamic equilibrium, *D* is the number of data sets. *M* and *N* are the tie-lines and number of components, respectively. The weight fraction was only used in the *OF* to facilitate the convergence process.

The Root mean-square deviation (δ), **Equation 5.5**, was determined, comparing the experimental and predicted data.

$$\delta = 100.\sqrt{\frac{\sum_{i}^{M}\sum_{j}^{N}\left(x_{ij}^{I.exp} - x_{ij}^{I.calc}\right)^2 + \left(x_{ij}^{II.exp} - x_{ij}^{II.calc}\right)^2}{2MN}} \quad (5.5)$$

5.2.6 Thermodynamic modeling

5.2.6.1 Conductor-like Screening Model for Real Solvent (COSMO-RS)

COSMO-RS has been proven to not only able to predict the thermophysical properties of chemical compound, but also can be used to get an insight into the molecular interactions occurring in the pure and mixture system of interest (Kurnia and Coutinho 2013). The computational modeling consists of two major steps. In the first step, the continuum solvation COSMO calculation of electronic density of IL cation and anion, salt cation and anion, and water molecules were optimized using TURBOMOLE V7.3 2018 software program package using density functional theory level and utilizing the BP functional B88-p86 with a triple- ζ valence polarized basis set (TZVP) and the resolution of identity standard (RI) approximation (Turbomole, 2018). Once the COSMO file is produced, the excess enthalpies of binary and ternary mixtures were determined using COSMO*therm* software using parameter BP_TZVP_C30_1801 (COSMOlogic, Levekusen, Germany) (F. Eckert and A. Klamt, 2018).

The interaction energies in pure ILs, water, and salts, as well as in their binary and ternary mixture were estimated using COSMO-RS. In the molecular approach, COSMO-RS focuses on three specific interaction, namely the electrostatic – misfit energy, H_{MF}, hydrogen bonding energy, H_{HB}, and van der Waals energy, H_{vdW}. These energies are described in **Equations 5.6-5.8**, respectively:

$$H_{MF} = a_{eff}\frac{\alpha}{2}(\sigma + \sigma')^2 \quad (5.6)$$

$$H_{HB} = a_{eff}c_{HB}\left(0; \min(0; \sigma_{donor} + \sigma_{HB}) \times \max\left(0; \sigma_{acceptor} - \sigma_{HB}\right)\right) \quad (5.7)$$

$$H_{vdW} = a_{eff}(\tau_{vdW} + \tau'_{vdW}) \quad (5.8)$$

where a_{eff} is the effective contact area between two surface segments, α'is the interaction parameter, σ_{HB} is the hydrogen bond strength that the threshold for hydrogen bonding, and the last two τ_{vdW} and τ'_{vdW} are elements of specific van der Waals interaction parameters.

The interaction energies that present in the ternary mixture were also estimated by COSMO-RS using the excess enthalpies as the difference in the enthalpy of the studied IL cation, IL anion, salt cation, salt anion or water molecules in its mixture and pure state, according to the **Equation 5.9**:

$$H_{E,i}(\text{interaction}) = H_{i,mixture}(\text{interaction}) - H_{i,pure}(\text{interaction}) \quad (5.9)$$

The $H_{E,i}$ (interaction) in the COSMO-RS model originates from summing the three specific interaction as described in **Equations 5.6-5.8**. Thus, it can be expressed as **Equation 5.10**:

$$H_{E,m} = H_{E,MF} + H_{E,HB} + H_{E,vdW} \quad (5.10)$$

Therefore, the COSMO-RS model could provide the information required for the evaluation of molecular interaction occur of ILs in the pure state, as well as in the aqueous solution, as contribution of IL cation, IL anion, salt cation, salt anion and water molecules.

5.3 Results and discussion

5.3.1 Ternary phase diagrams

In this work, twelve propylammonium-based ILs were combined with two phosphate salts (K_3PO_4 and K_2HPO_4) and water to evaluate the influence of the anion nature, the alkyl side chain length of the cation, salt and temperature effects on the formation of ABS. As shown in **Table 5.1**, amongst the ILs tested, the most hydrophilic ILs, *i.e.* propylammonium acetate ([PA][Ac]), propylammonium propanoate ([PA][Pro]), propylammonium butanoate ([PA][But]), 3-dimethylamino-1-propylammonium acetate ([DMAPA][Ac]) and 3-diethylamino-propylammonium acetate ([DEAPA][Ac]), were not able to form ABS with any of the two phosphate salts. On the other hand, the other seven propylammonium-based ILs were able to promote a biphasic regime with both K_3PO_4 and K_2HPO_4, allowing the formation of fourteen IL/salt ABS at 298 (± 1) K and atmospheric pressure. The detailed binodal experimental weight fraction data for all ABS are provided in **Tables C.1** and **C.2** in the **Appendix C.** All experimental solubility curves were successfully correlated (correlation coefficient > 0.98) using empirical relationship described by Merchuck et al. (Merchuk et al. 1998) (*cf.* **Equation 1**). The fitted parameters, and respective standard deviations, are provided in **Tables C.3** and **C.4** in the **Appendix C**.

5.3.2 Effect of IL cation on the formation of IL/salt ABS

In order to evaluate the effect of IL cation nature on ABS formation, ternary phase diagrams composed of propanoate, butanoate and hexanoate-based ILs, K_3PO_4 and K_2HPO_4, and water, determined at 298 K and atmospheric pressure, were compared in **Figures 5.1a** and **5.1b**, respectively.

From **Figure 5.1**, independently of the phosphate salt and the IL anion, it is observed that the ability of the ILs to promote a biphasic region is as follows: [DEAPA][X] > [DMAPA][X] > [PA][X]. It is noteworthy that, from the propylamine-based ILs, only [PA][Hex] formed ABS when mixed with either K_3PO_4 or K_2HPO_4 (as previously highlighted in **Table 5.1**), although exhibiting the narrowest

biphasic regions. The above trend indicates that ILs with larger cationic alkyl side chains display better performance for the formation of ABS, while shorter cations reduce' the IL ABS phase-forming ability.

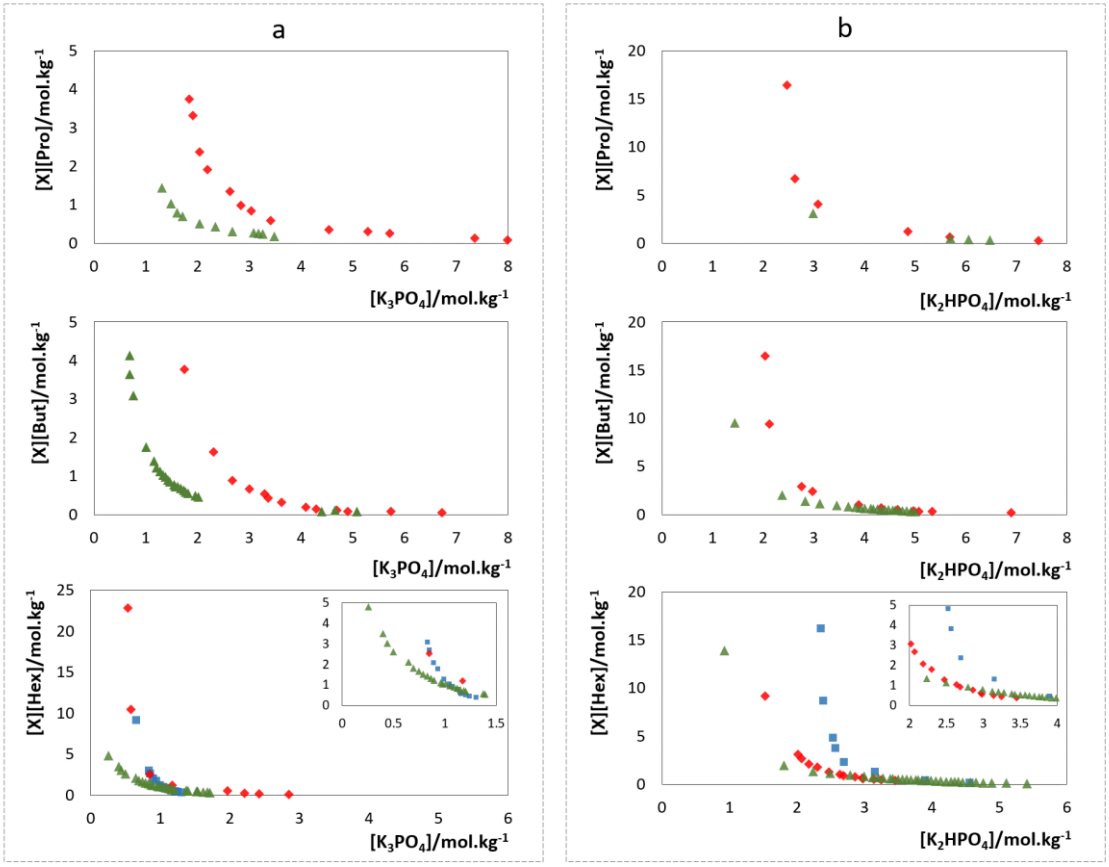

Figure 5.1. Ternary phase diagrams of the systems **a**) IL + K_3PO_4 + H_2O and **b**) IL + K_2HPO_4 + H_2O determined at 298 (± 1) K and atmospheric pressure. [X] corresponds to one of the following cations: $[DEAPA]^+$ (▲); $[DMAPA]^+$ (♦); $[PA]^+$ (■). Note that different scales were employed for clarity of results.

The pattern of ABS formation by the ILs mimics the relative hydrophobicity of the cation, which can be inferred by logarithmic function of the octanol/water partition coefficient values (log K_{ow}) of the starting carboxylic acids used in the ILs synthesis, namely, hexanoate (log K_{ow} = 1.84) > butanoate (log K_{ow} = 0.78) > propanoate (log K_{ow} = 0.25) (values obtained from ChemSpider) (Mussagy et al. 2019). The log K_{ow} values provide a relative measurement of the hydrophobicity, where the higher the value is the more hydrophobic is the compound. As

previously reported (Freire et al. 2007), the increase of the cation alkyl chain length leads to an increase of the relative hydrophobicity of the ILs. Therefore, the increase of the hydrophobic nature reduces its water affinity, making them easier to be salted-out by both phosphate-based salts (strongly hydrated salts), and consequently, facilitating the formation of the IL/salt ABS (Cláudio et al. 2011; Neves et al. 2016). The trend of these propylammonium-based ABS is in agreement with the previous results for systems composed of ILs and different sulphate (Cláudio et al. 2011), phosphate (Bridges et al. 2007) and citrate (Passos et al. 2012) high-melting salts.

5.3.3 Effect of IL anion on the formation of IL/salt ABS

The results from the previous section evidenced a great impact of the IL' cation nature on the formation of IL/salt ABS. However, the significant mechanisms behind the formation salt/salt ABS are commonly associated with the anionic nature of both ILs and salts (Bridges et al. 2007; Du et al. 2007; Ventura et al. 2009; Ventura et al. 2012; Quental et al. 2015b; Pereira et al. 2016; Marchel et al. 2019). Therefore, to assess the effect of increasing alkyl chain length of the IL' anion, ABS composed of [DEAPA][X] (*i.e.* IL with the largest biphasic regions) and both K_3PO_4 and K_2HPO_4 salts are compared as a function of the IL' anion in **Figures 5.2-a** and **5.2-b**, respectively.

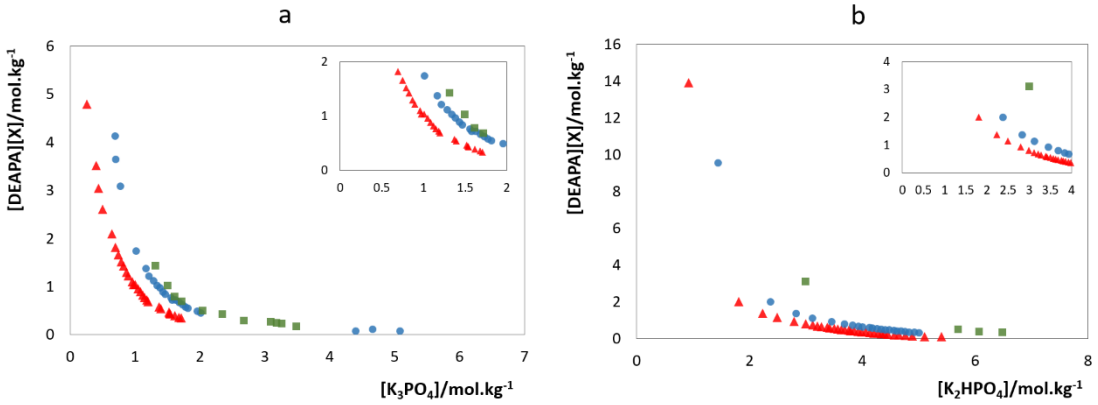

Figure 5.2. Ternary phase diagrams of the systems **a**) [DEAPA][X] + K_3PO_4 + H_2O and **b**) [DEAPA][X] + K_2HPO_4 + H_2O determined at 298 (± 1) K and atmospheric pressure. [X] corresponds to one of the following anions: $[Hex]^-$ (▲), $[But]^-$ (●) and $[Pro]^-$ (■). Note that different scales were employed for clarity of results.

Figure 5.2 shows that, by keeping $[DEAPA]^+$ as common cation, the influence of IL anion to induce liquid-liquid demixing follows the trend: $[Hex]^-$ > $[But]^-$ > $[Pro]^-$. Similar to cation effect, the longer is the alkyl side chain length of the anion the higher is the relative hydrophobicity of the propylammonium-based IL. As previously reported (Bridges et al. 2007; Ventura et al. 2009; Mourão et al. 2012; Dilip et al. 2015), when dealing with high-charge density salts, such as phosphate-based ones, that have enhanced capacity for creating hydration complexes, the formation of IL/salt ABS is always favored by using ILs with weaker affinity for water, with the more hydrophobic ILs easily salted-out into a second aqueous phase.

Both IL cation and salt did not change the sequence of the IL anion to form ABS, that is the anion rank was similar for both K_2HPO_4 and K_3PO_4, as well as for the three cationic IL families ([PA][X], [DMAPA][X] and [DEAPA][X]). However, it can be noted most distinct differences between the binodal curves for the systems constituted by weaker salting-out salt (K_2HPO_4) and more pronounced biphasic regions with K_3PO_4-based ABS with low differences between the different ILs. This agrees with the salting-out mechanisms of the salt/salt ABS (Bridges et al. 2007; Ventura et al. 2009; Louros et al. 2010; Zhang et al. 2010; Mourão et al. 2012; Dilip et al. 2015), since the use of stronger salting out salt, like K_3PO_4 (trivalent salt), reduces the impact of IL anion on the formation of ABS and the binodal curves become to be very close. On the other hand, for the systems composed of K_2HPO_4, a divalent salt with low hydration energies (Marcus 1993), the salting-out effect is reduced and the ILs with higher hydrogen-bond basicity (*i.e.* more hydrophilic) establish stronger interactions with water, decreasing their capacity to undergo phase separation.

5.3.4 Effect of phosphate salt on the formation of IL/salt ABS

A comparison of the different sets of results was carried out aiming to infer the effect of the replacement of a highly basic and charged PO_4^{3-} anion by a less alkaline and charged HPO_4^{2-} on the formation of ABS with propylammonium-based ILs. As illustrated in **Figure 5.3**, both K_2HPO_4 and K_3PO_4 induced the salting-out of propylammonium-based ILs in which a more pronounced effect observed for the ILs with weaker water affinities (longer cationic and/or anionic

alkyl chain lengths). Additionally, independently of the IL, the salt effect on phase separation follows the order, K_3PO_4 > K_2HPO_4. This trend is in accordance with the Hofmeister series (Marcus 1993), which is directly related to the Gibbs free energy of hydration of the ions ($\Delta_{hyd}G$) (Cláudio et al. 2011). The higher salting-out capacity is a result of the a more negative $\Delta_{hyd}G$ of the salt anion, namely, -2765 kJ/mol (PO_4^{3-}) > -1789 kJ/mol (HPO_4^{2-}) (Marcus 1993). Considering that the salt cation is the same, the triple charge and ability of PO_4^{3-} to act as a hydrogen acceptor towards water exerted a higher contribution for the formation of hydration complexes with water than HPO_4^{2-}; the higher competition for water molecules of the trivalent salt anion enhances the dehydration of the IL ions, and consequently, the liquid-liquid demixing (Bridges et al. 2007; Mourão et al. 2012).

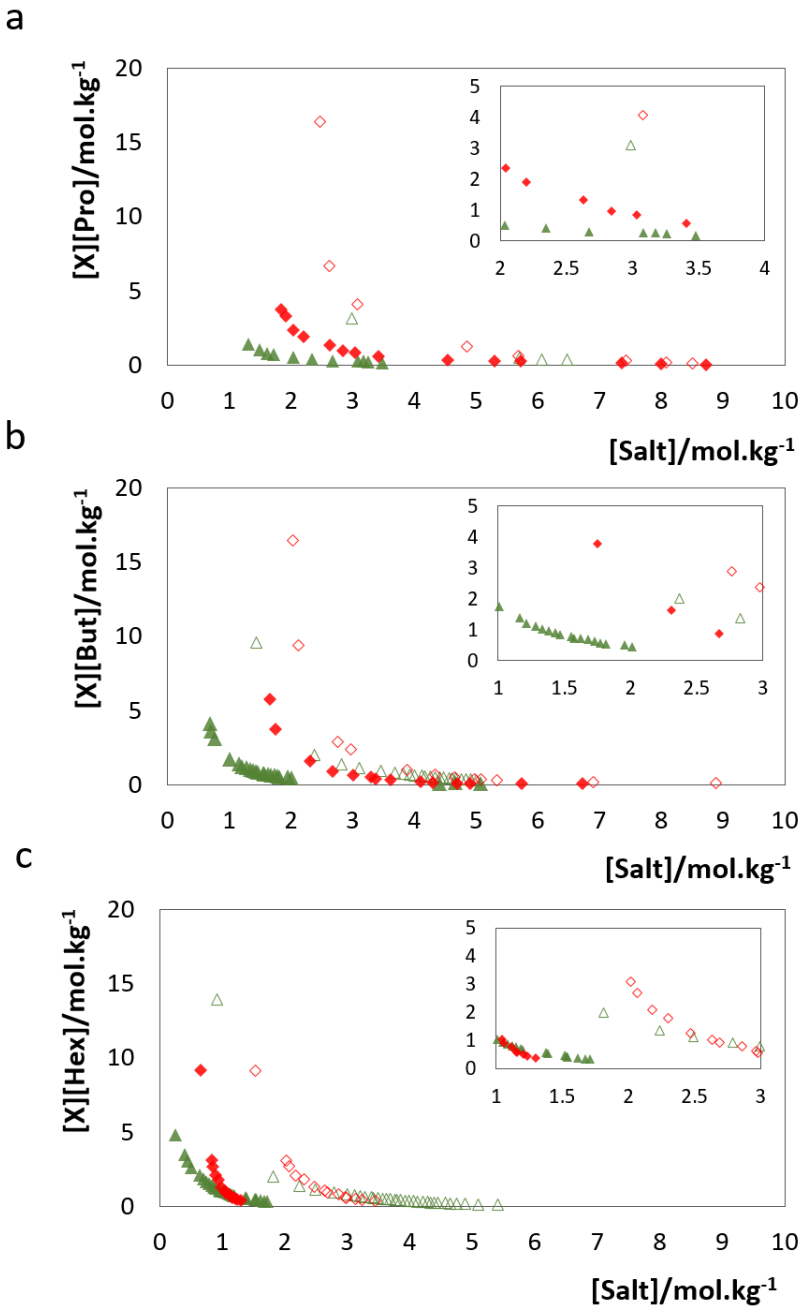

Figure 5.3. Ternary phase diagrams of the systems **a**) [X][Pro] + salt + H_2O, **b**): [X][But] + salt + H_2O and **c**) [X][Hex] + salt + H_2O determined at 298 (± 1) K and atmospheric pressure. The experimental binodal curves of the systems composed of K_3PO_4 are represented by full symbols, and K_2HPO_4 by open symbols. [X] corresponds to $[DEAPA]^+$ (green triangle) or $[DMAPA]^+$ (red diamond) cation.

5.3.5 Effect of the temperature on the formation of [DEAPA][Hex]/salt ABS

In order to better understand the mechanisms that lead the phase separation, the temperature dependency of ABS formation was also determined. The ternary phase diagrams for ABS composed of [DEAPA][Hex] + K_3PO_4 + H_2O and of [DEAPA][Hex] + K_2HPO_4 + H_2O were determined at 298 K, 308 K and 318 K. The respective binodal curves are shown in **Figure 5.4** and the detailed experimental data in **Table C.5** in the **Appendix C**.

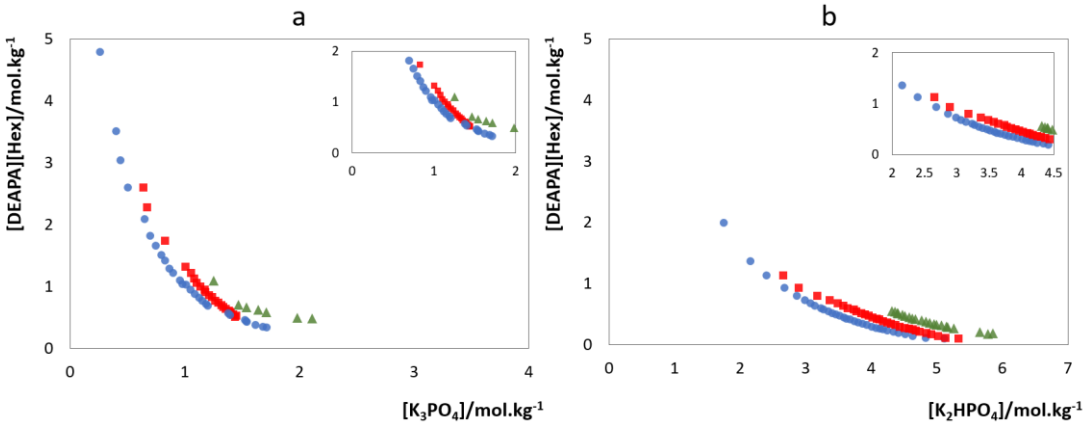

Figure 5.4. Ternary phase diagrams of the systems **a**) [DEAPA][Hex] + K_3PO_4 + H_2O and **b**) [DEAPA][Hex] + K_2HPO_4 + H_2O determined at 298 K (●), 308 K (■) or 318 K (▲), and atmospheric pressure. Note that different scales were employed for clarity of results.

As shown in **Figure 5.4**, in both cases the binodal curves shift towards the left with a decrease in temperature, that is the biphasic region increases with the decrease of temperature. These results implied that, in each type of system, as temperature increases a greater concentration of phosphate salt is need to salt-out propylammonium-based IL. This trend is in close agreement with that observed for other IL/salt ABS (Han et al. 2010; Freire et al. 2012a; Freire et al. 2012b; Dilip et al. 2015). In systems containing ILs and salts, the influence of temperature on the liquid–liquid demixing process is directly related with the decrease or increase of the hydrogen-bonding ability. Considering that the formation of hydration complexes between water and inorganic anions (PO_4^{3-} and HPO_4^{2-}) will lead to dehydration of the ILs, the larger changes with the temperature are observed for the ILs more able to promote hydrogen-bond (more

hydrophilic) (Dilip et al. 2015), while smaller changes are obtained for the ILs with lower hydrogen-bond capability, such as [DEAPA][Hex]. In this way, lower temperatures will be always more favorable for the creation of propylammonium-based IL/salt ABS.

5.3.6 Tie-lines

In this work, three experimental TLs for each IL/salt ABS were determined, along with the respective tie-lines lengths (TLL) and slope of tie-lines (STL). Corresponding TLs values are summarized in **Tables 5.2** and **5.3** and in **Figures C.1** and **C.2** in the **Appendix C**. As an example, in **Figure 5.5** depicts the experimental and fitted binodal curves of the system composed of [DEAPA][Hex] + K_3PO_4 + H_2O along with respective TLs.

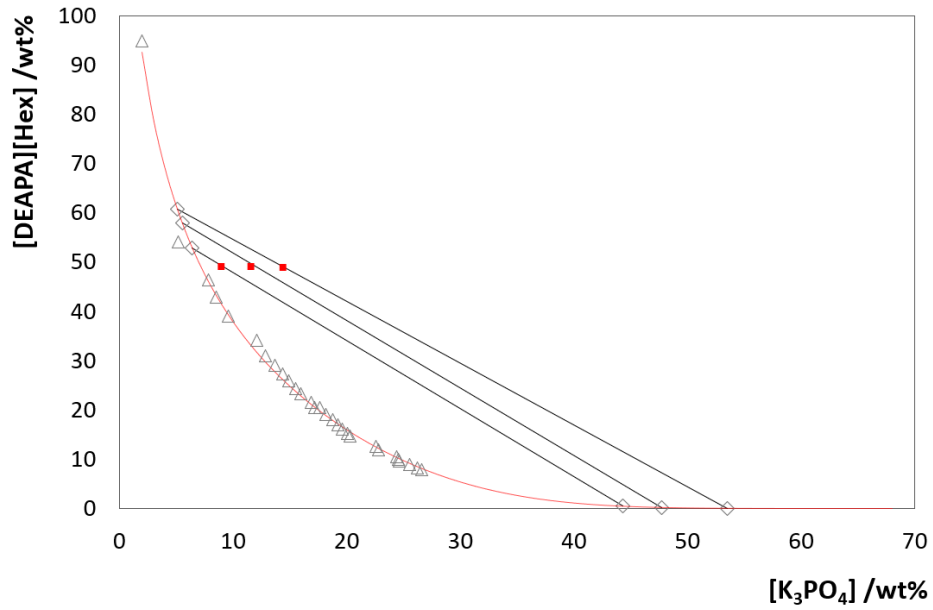

Figure 5.5. Ternary phase diagram of the ABS composed of [DEAPA][Hex] + K_3PO_4 + H_2O, at 298.15 K and atmospheric pressure: binodal curve data (△); tie line experimental data (◊); total composition (■); fitted binodal curve using Equation (5.1) (−).

From the data of **Tables 5.2** and **5.3**, it is observed that for all systems the top phase corresponds to the IL-rich phase, while the bottom phase represents the salt-rich one. Furthermore, it can be observed that the IL concentration in the bottom (salt-rich) phase is very small or even negligible. From the experimental

TL data depicted in **Figures 5.5**, **C.1** and **C.2 (Appendix C),** it is possible to confirm that the proposed analytical procedures for determination coexisting phases' compositions were very accurate, since the analytical TLs are mostly overlapping the fitted binodal curve.

Tables 5.2 and **5.3** also summarizes the STL values, representing the ratio between the difference of IL weight fraction in the top and bottom phases over the difference of the salts weight fraction in the top and bottom phases. Interestingly, independently of the phosphate salt, the ABS composed of the most hydrophobic $[Hex]^-$-based ILs showed the most negative STL, indicating that the more hydrophobic ILs are almost concentrated in the top (IL-rich) phase.

Table 5.2. Equilibrium data of the ABS composed of propylammonium-based IL ($100w_{IL}$) + K_3PO_4 ($100w_s$) + H_2O at 298 K and atmospheric pressure.[a]

		Overall		Top Phase		Bottom Phase			
IL	**TL**	**$100w_{IL}$**	**$100w_s$**	**$100w_{IL}$**	**$100w_s$**	**$100w_{IL}$**	**$100w_s$**	**TLL**	**STL**
[DMAPA][Pro]	1	35.20	38.92	47.82	27.92	1.99	67.64	60.65	-0.84
	2	35.47	40.63	51.70	27.13	1.93	68.04	64.42	-0.82
	3	35.14	42.31	53.61	26.76	1.58	70.87	68.21	-0.76
[DMAPA][But]	1	40.92	34.11	40.92	34.11	43.06	14.01	53.27	-1.13
	2	39.57	36.64	39.57	36.64	47.34	13.11	57.81	-1.04
	3	39.70	38.13	39.70	38.13	50.43	12.52	63.47	-0.94
[DMAPA][Hex]	1	48.84	15.28	52.45	13.80	2.70	48.46	60.64	-1.33
	2	49.06	17.44	55.11	13.52	1.19	52.63	66.60	-1.22
	3	50.15	19.93	58.48	13.19	0.63	56.53	72.28	-1.14
[DEAPA][Pro]	1	39.89	22.08	45.51	17.36	4.58	47.98	51.12	-1.15
	2	39.49	26.87	52.04	16.42	4.49	52.00	59.38	-0.98
	3	40.04	30.02	59.43	15.53	4.61	54.71	67.38	-0.90
[DEAPA][But]	1	39.96	16.47	38.99	15.95	16.91	41.43	33.72	-0.90
	2	39.29	19.57	37.58	16.21	11.60	33.54	31.23	-1.60
	3	40.14	20.85	40.32	15.72	19.52	42.92	34.24	-0.76
[DEAPA][Hex]	1	43.53	13.51	52.96	6.41	0.46	44.30	64.74	-1.14
	2	43.05	16.02	57.91	5.55	0.21	47.69	71.45	-1.02
	3	43.36	18.73	60.76	5.11	0.04	53.50	77.64	-0.90

[a]The standard uncertainty for the weight fraction u (w) is 0.05 and the standard uncertainty for the temperature u (T) is 0.20 K.

Table 5.3. Equilibrium data of the ABS composed of propylammonium-based IL ($100w_{IL}$) + K_2HPO_4 ($100w_s$) + H_2O at 298 K and atmospheric pressure.[a]

		Overall		Top Phase		Bottom Phase			
IL	**TL**	**$100w_{IL}$**	**$100w_s$**	**$100w_{IL}$**	**$100w_s$**	**$100w_{IL}$**	**$100w_s$**	**TLL**	**STL**
[DMAPA][Pro]	1	44.17	37.75	51.72	34.67	6.49	56.69	50.31	-1.71
	2	45.24	39.72	55.08	33.92	2.08	66.26	62.09	-1.33
	3	44.55	41.97	61.96	32.50	1.53	68.62	70.40	-1.19
[DMAPA][But]	1	49.00	34.04	52.74	30.22	0.81	64.09	62.00	-1.42
	2	49.69	36.30	58.28	29.20	0.72	64.80	67.69	-1.38
	3	50.00	37.59	64.46	28.16	0.52	66.66	74.63	-1.29
[DMAPA][Hex]	1	38.60	28.73	41.63	26.03	0.01	60.78	54.22	-1.11
	2	38.50	30.40	44.25	25.50	0.00	65.82	59.87	-0.95
	3	39.01	32.06	46.63	25.03	0.00	70.00	64.78	-0.87
[DEAPA][Pro]	1	40.44	38.27	50.26	32.24	3.92	59.07	53.55	-1.36
	2	40.10	40.17	56.66	30.66	1.50	66.38	65.72	-1.08
	3	39.33	42.08	60.78	29.72	1.08	68.67	71.29	-0.98
[DEAPA][But]	1	40.31	30.04	48.96	24.19	5.87	50.50	50.49	-1.31
	2	39.89	32.70	52.75	23.19	2.73	58.03	60.95	-1.07
	3	38.44	34.70	57.11	22.13	1.95	61.04	67.50	-0.94
[DEAPA][Hex]	1	40.31	23.04	40.51	22.29	2.64	50.89	47.46	-1.32
	2	39.89	25.70	46.51	20.44	1.10	57.16	58.40	-1.06
	3	38.44	29.70	50.29	19.39	0.66	60.37	64.36	-0.92

[a]The standard uncertainty for the weight fraction u (w) is 0.05 and the standard uncertainty for the temperature u (T) is 0.20 K.

Considering that the propylammonium-based ILs are based on an acid-base reaction, unlike aprotic ILs, it is fundamental to be attentive for the stability of these protic ILs on very alkaline aqueous media. Therefore, to infer on the final stoichiometry of the base (corresponding propylamine) and acid (corresponding carboxylic acid) in each ABS, the acid:base molar ratio of the IL-rich phase (top) was calculated for all the mixtures points under study, as well the pH values of both coexisting phases. The acid:base molar ratios are depicted in **Figure 5.6**, being detailed together with phases' pH values in **Table C.6** in the **Appendix C**. Due to very low IL concentration in the salt (bottom)-rich phase, as can be confirmed by the ^{1}H NMR spectra depicted in **Figure C.5** in **Appendix C**, the acid:base molar ratios in the bottom phase were not determined.

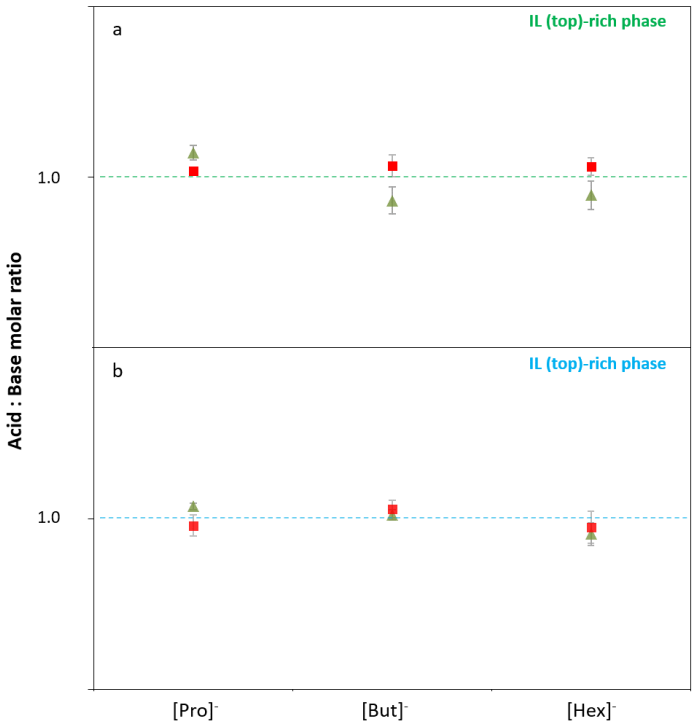

Figure 5.6. Acid:Base molar ratio between the IL forming carboxylic acid ([Pro]$^{-}$, [But]$^{-}$ and [Hex]) and propylamine (■ - [DMAPA]$^{+}$; ▲ - [DEAPA]$^{+}$) on the initial mixture composition (dashed lines) and in the IL (top)-rich phase of ABS composed of K_2HPO_4 (**a**) or K_3PO_4 (**b**) + IL + H_2O.

Interestingly, the acid:base stoichiometry of all propylammonium-based is maintained in the top phase for both IL/phosphate salts ABS. As illustrated in **Figure 5.6**, the initial acid:base molar ratio (dashed lines) are very close with the molar ratio in the IL-rich phase after the phase separation, with values close to 1 for all the systems.

The maintenance of the stoichiometry between IL forming acid and base is very important, particularly, because at the alkaline pH values of these phosphate-based ABS, which have pH values from 8 to 11 (**Table C.6** in the **Appendix C**) part of the starting propylamines are in non-speciated (neutral) form. Remarkably, even considering that approximately 50% of the IL-rich phase is actually rich on the neutral amine (according the pKa values of diethylpropylamine and dimethylpropylamine of 10.38 and 9.87, respectively – values obtained from ChemSpider chemical database (Mussagy et al. 2019a; Chemspider 2020)), the strong salting-out effects of both phosphate salts guarantee the maintenance of the acid:base molar ratio in the IL-rich phase, and consequently, that these systems still behave as *de facto* ternary systems.

5.3.7 Correlation of experimental tie-lines using NRTL Model

The non-random two-liquid model (NRTL model), proposed by Renon and Prausnitz (Renon and Prausnitz 1968), is an activity coefficient model that correlated the activity coefficients of a compound with its mole fraction in the liquid phase concerned. This model, based on the local composition concept, is applicable to partially miscible systems to calculate corresponding phase equilibria. The previous experimental phase diagrams, were then correlated with the NRTL model and the experimental and calculated data compared according the root mean square deviations (δ). **Tables 5.4** and **5.5** detail all binary parameters of the NRTL model obtained for ABS under study, as well as the corresponding values.

Table 5.4. Data binary interaction parameters of NRTL model and root mean square deviations (δ) for systems composed by K_3PO_4 (1) + IL (2) + water (3) at 298 K.

IL	*i*	*j*	*Aij (K)*	*Aji (K)*	*δ (%)*
[DMAPA][Pro]	1	2	0.8140	0.4292	0.0019
	1	3	0.8984	0.5966	
	2	3	0.3343	0.9020	
[DMAPA][But]	1	2	0.5860	0.6664	0.3300
	1	3	0.2467	0.6260	
	2	3	0.0835	0.6609	
[DMAPA][Hex]	1	2	0.9880	0.3889	0.8533
	1	3	0.8641	0.2467	
	2	3	0.4547	0.7844	
[DEAPA][Pro]	1	2	0.4899	0.9787	0.0034
	1	3	0.1679	0.5005	
	2	3	0.7127	0.4711	
[DEAPA][But]	1	2	0.1842	0.2999	0.0010
	1	3	0.5972	0.2126	
	2	3	0.1341	0.8949	
[DEAPA][Hex]	1	2	0.6671	0.6751	0.0033
	1	3	0.5864	0.6203	
	2	3	0.3610	0.8112	

Table 5.5. Data binary interaction parameters of NRTL model and root mean square deviations (δ) for systems composed by K_2HPO_4 (1) + IL (2) + water (3) at 298 K.

IL	*i*	*j*	*Aij (K)*	*Aji (K)*	*δ (%)*
[DMAPA][Pro]	1	2	0.3258	0.7475	0.0335
	1	3	0.0959	0.5433	
	2	3	0.7485	0.3381	
[DMAPA][But]	1	2	0.4195	0.4890	0.0017
	1	3	0.3581	0.9292	
	2	3	0.2560	0.4668	
[DMAPA][Hex]	1	2	0.1233	0.2400	0.0033
	1	3	0.1839	0.0497	
	2	3	0.4173	0.9027	
[DEAPA][Pro]	1	2	0.1233	0.2400	0.0026
	1	3	0.1839	0.0497	
	2	3	0.4173	0.9027	
[DEAPA][But]	1	2	0.5860	0.6664	0.0047
	1	3	0.2467	0.6260	
	2	3	0.0835	0.6609	
[DEAPA][Hex]	1	2	0.4362	0.3945	0.0037
	1	3	0.8266	0.8186	
	2	3	0.6135	0.8862	

In addition, to infer the efficiency of the fitting, a graphical analysis was also performed through the overlapping analysis of the experimental and calculated TLs. **Figure 5.7** illustrates an example of experimental and predicted TLs (by NRTL model) for the systems composed of $[Hex]^-$-based ILs. All the other graphical comparisons are presented in **Figures C.3** and **C.4** in the **Appendix C**.

NTRL model provides a good representation of the experimental data for all ILs/salt ABS. The low δ values (δ ≤ 0.85%) (**Tables 5.4** and **5.5**), as well as the overlapping between experimental and calculated TLs (**Figure 5.7, Figures C.3** and **C.4** in the **Appendix C**), confirm the potential of NRTL model to represent the phase behavior of

propylammonium-based IL/phosphate salt ABS over the entire range of compositions analyzed.

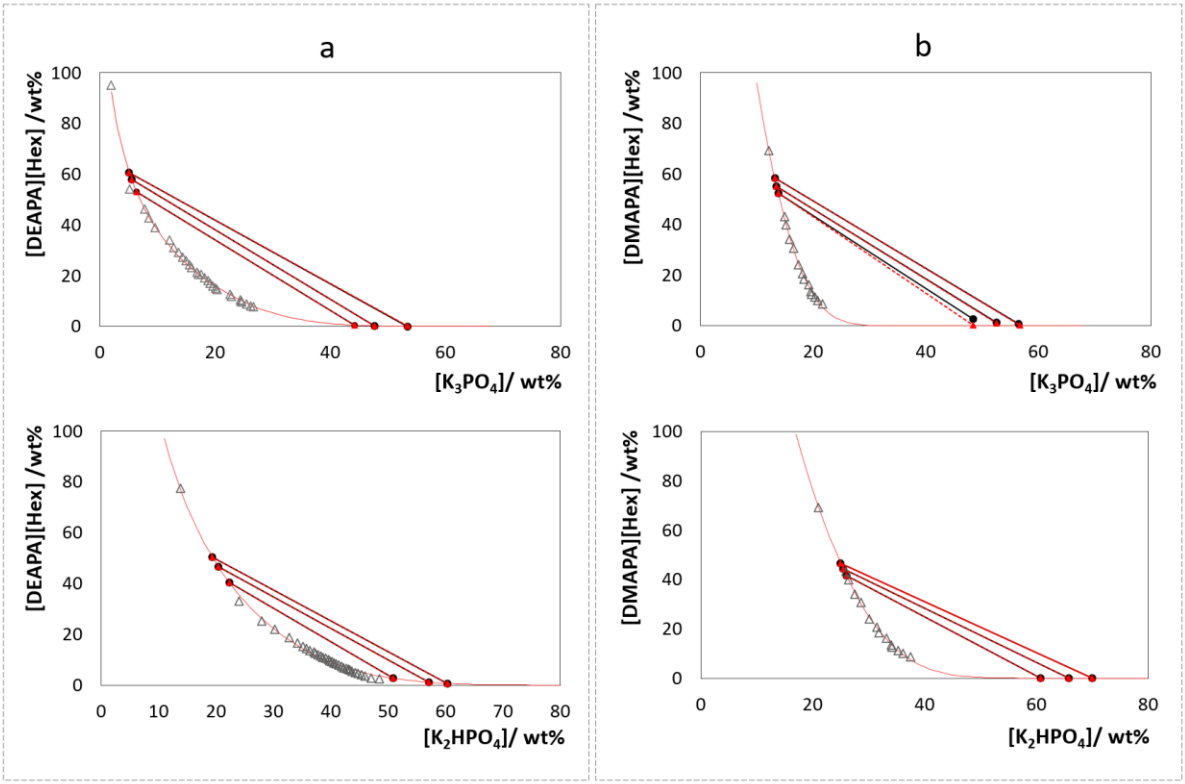

Figure 5.7. Experimental and calculated (by NRTL model) tie-lines of systems composed of **a**) [DEAPA][Hex] + Salt + H_2O and **b**) [DMAPA][Hex] + Salt+ H_2O systems at T= 298 (± 1) K and atmospheric pressure.

5.3.8 Thermodynamic Modeling using COSMO-RS

One advantage of using COSMO-RS is the model allows the study of a molecule behavior in both pure and mixture state. In this context, COSMO-RS model provides the charge distribution, σ, of the specific polarity on the molecular surface that simply visualized by the σ-profile histogram. Qualitative analysis of σ-profile of the component of a mixture could give some important information about the molecule and consequently, can be used to predict possible interactions in the fluid phase. **Figure 5.8** show the σ-profile of the studied inorganic salts, ILs cations, and ILs anions, respectively. In general,

the *σ*-profile qualitatively divided into three main regions as follow (*i*) hydrogen bond donor with the region of $\sigma < -1$ e·nm^{-2}, (*ii*) nonpolar region that located between $-1 < \sigma < 1$ e·nm^{-2}, and (*iii*) hydrogen bond acceptor with the region of $\sigma < 1$ e·nm^{-2}.

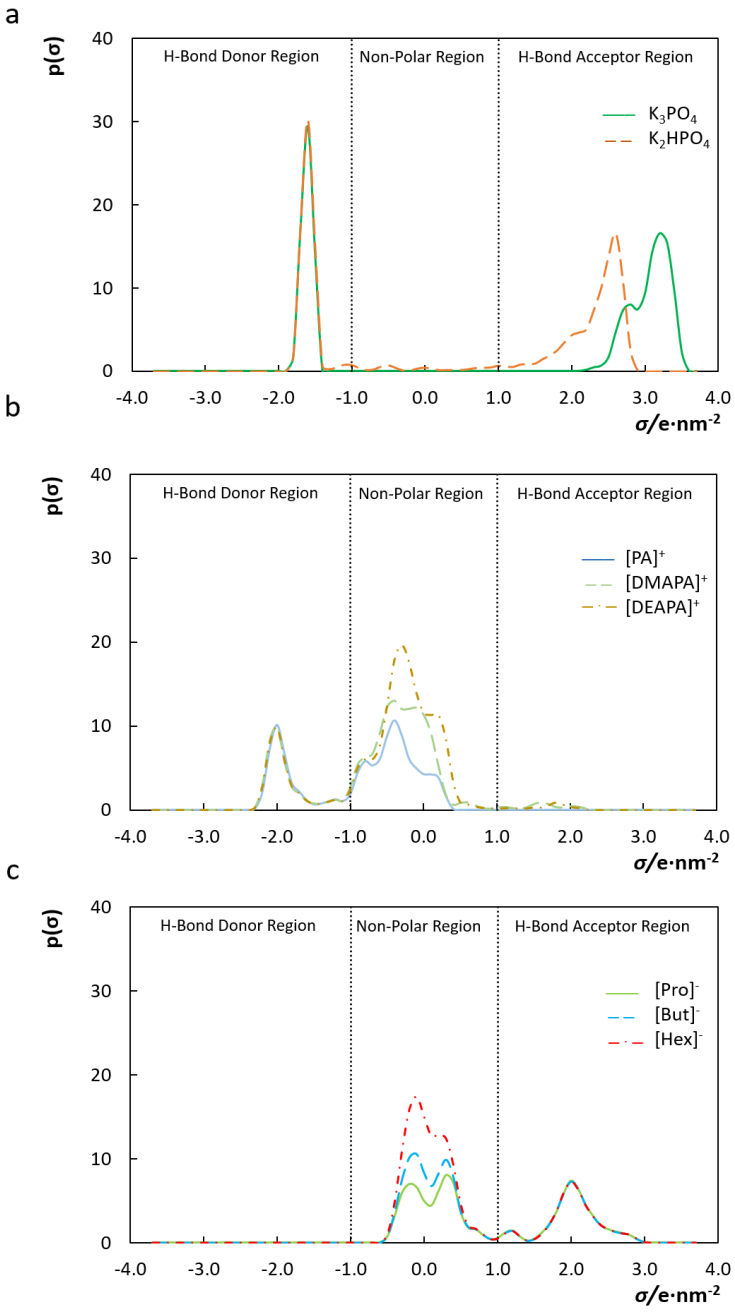

Figure 5.8. Representation of σ-profiles for: **a**- phosphate salts (K_3PO_4 and K_2HPO_4); **b**- ILs cations ($[PA]^+$, $[DMAPA]^+$ and $[DEAPA]^+$) and **c**- ILs anions ($[Pro]^-$, $[But]^-$, and $[Hex]^-$).

As can be seen from **Figure 5.8-a**, the σ-profile K_3PO_4 shows peak within polar region at 3.2 e·nm^{-2} and -1.6 e·nm^{-2}. The peak at 3.2 e·nm^{-2} assigns to the highly electronegative charge phosphate anion (PO_4^{3-}) that have strong ability as hydrogen bond acceptor. Whereas the peak at -1.6 e·nm^{-2} indicates the electropositive charge arise from the ion potassium (K^+) of the salt. The σ-profile K_2HPO_4 also show similar profile with K_3PO_4; however, it is observed that the peak is shifting to less electronegative area at 3.2 e·nm^{-2}. It shows that HPO_4^{2-} is less negative than PO_4^{3-} and consequently, the latter anion will form stronger hydrogen bond. Thus, the stronger ability of PO_4^{3-} to form ABS when compare to HPO_4^{2-} can be attributed to the stronger capacity of the former to form hydrogen bond with either water or ILs anion.

On regards to ILs cation (**Figure 5.8-b**), the σ-profile shows peak at polar region at -2.9 e·nm^{-2} that can be attributed to the hydrogen bond donor group of ammonium cation, whereas multiple peaks at nonpolar region circa -0.3 e·nm^{-2} could be assigned to the nonpolar group of the ILs cation. Interestingly, while the peak intensity at -2.9 e·nm^{-2} remain constant for all studied ILs cation, it is observed the increase of peak intensity at -0.3 e·nm^{-2} from $[PA]^+$ to $[DMAPA]^+$ and the highest for $[DEAPA]^+$. This indicates that the three cations has the same strength to form hydrogen bond, and therefore, their capability to form ABS is influenced by the nonpolar character. Accordingly, it can be projected that the strength of the studied ILs to form ABS can be rank as follow: $[PA]^+ < [DMAPA]^+ < [DEAPA]^+$.

Moving to ILs anion (**Figure 5.8-c**), the σ-profile shows peak within polar region at 2.0 e·nm^{-2} that correspond to carboxylate head group and within nonpolar region at circa -0.2 e·nm^{-2}. It is worth to note that the peak intensity at 2.0 e·nm^{-2} is similar for three studied anion that indicate their comparable capability to form hydrogen bond. Meanwhile, it is observed an increase of peak intensity at nonpolar region, with $[Pro]^-$ is the lowest, followed by $[But]^-$ and the highest is $[Hex]^-$. Therefore, the capability of ILs anion to form ABS is also influenced by their nonpolar character and can be ranked as follow: $[Pro]^- < [But]^- < [Hex]^-$.

Aiming to get further insight into the molecular mechanism that govern the phase separation in the propylammonium-based ABS, COSMO-RS was finally used to explore the excess enthalpies of binary pairs of IL-water, salt-water, and IL-salt according to the aforementioned procedure. In previous work, some of us have showed that COSMO-RS could provide a novel understanding on the molecular level interaction that play role on the phase separation of ABS composed by polymer and ionic liquid/salt (Pereira et al. 2014). The model also capable to differentiate the impact of PEG polymer end groups in the formation of ionic liquid-based ABS (Pereira et al. 2015). Both previous studies support the reliability of the COSMO-RS used here to infer upon the main molecular mechanism ruling the phase separations.

The interaction energy in the pure system, as well as in the binary and ternary systems are given in **Table C.7** in the **Appendix C**. In the binary as well as ternary mixture, in general, hydrogen bonding is the dominant interaction occurring in the salt' anion with water and IL' anion with water, while electrostatic-misfit and van der Waals forces are just marginal. It is apparent that both salt and IL anions have high attraction toward water molecules. However, in the ternary molecules, there seem that is a competition between these two different anions towards water molecules that lead to the phase separation, as will be discussed below.

The estimated partial molar excess enthalpies (h^E) for salt anion in the ternary system as a function of molar fraction of ILs shows that, indeed, the hydrogen bonding interaction of salt' anion with water molecule contributes highly to the exothermicity of the system. Meanwhile, the hydrogen bonding interaction between IL' anion with water molecules play secondary role. The more favorable interaction of water with salt' anion could be addressed due to high localized negative charged of both PO_4^{3-} and HPO_4^{2-} when compare to carboxylic anion of each propylammonium-based IL. For the system with the same salt, for example K_2HPO_4, as depicted in **Figure 5.9**, the hydrogen bond strength of IL with water molecule can be ranked as follow: [DEAPA][Hex] < [DEAPA][But] < [DMAPA][Hex] < [DEAPA][Pro] < [DMAPA][But] < [DMAPA][Pro] < [PA][Hex]. This sequence closely follows the ability trend of the propylammonium-based ILs to induce the

phase separation. It should be noted that the excess enthalpies of the mixture increase with the temperature, indicating a less favorable interaction at high temperature. Consequently, the system has lower capability to form ABS at higher temperature, as observed experimentally (**Figure 5.4**). This effect of temperature in the excess enthalpies has also been observed in other binary mixtures containing ILs (Kurnia and Coutinho, 2013).

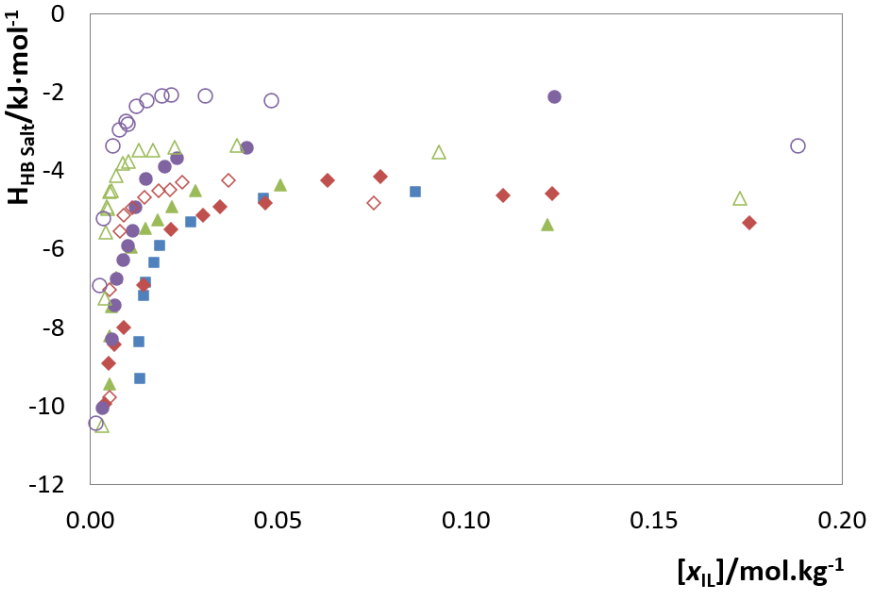

Figure 5.9. Partial molar excess enthalpies of salt anion in the ternary system of K_2HPO_4 (1) + IL (2) + H_2O (3) at 298.15 K predicted using COSMO-RS. [X] corresponds to [PA][HEX] (■), [DMAPA][Pro] (♦), [DMAPA][But] (▲), [DMAPA][Hex] (◊), [DEAPA][Pro] (●), [DEAPA][But] (△), and [DEAPA][Hex] (○).

In the studied ternary mixtures, as previously mentioned, there is a competition between the salt anion and the IL anion for the solvation by water molecules. The COSMO-RS model showed that hydrogen bonding between salt anion with water is highly negative, an indicative of more spontaneous solvation of salt anion by water molecules. Therefore, it is here confirmed that the salt anion preferentially forms hydration complexes, and as a result, the water molecules are removed from the IL-solvation environment. The

extend of this exchange process depends on the affinity of each IL toward water molecules. IL with strong affinity toward water molecules, for example [PA][Hex], which have the highest negative h^E values, are less capable of inducing phase separation in IL/salt ABS. On the other hand, [DEAPA][Hex] have the weakest interactions with water molecules as reflected by the lowest negative h^E values and, ultimately, it has the highest abilities to induce the ABS formation. The gathered results confirm that the hydrogen bond capability of salt' anion and IL' anion with water play significant role in the formation of ABS.

5.4 Conclusions

In this work, fourteen novel ternary phase diagrams for ABS composed of propylammonium-based ILs were reported. Considering the ternary phase diagram behaviors, it was concluded that the ability to form IL/phosphate salt ABS increases with the increase of cation and anion alkyl chain length. The effect of the cation and anion nature of the propylammonium-based ILs on their capacity to promote ABS is directly controlled by their relative hydrophobicity, and consequent stronger/weaker water affinity. The effect of phosphate-based salts to form ABS with propylammonium-based ILs results directly of their salting-out aptitude. Additionally, the aptitude to form IL/salt ABS decreased with the increase of the temperature. The experimental data were successfully correlated using the NRTL activity coefficient model. COSMO-RS calculations confirmed that is the ability of salt anion and IL anion to hydrogen bond with water the main mechanism behind the formation of IL/salt ABS, *i.e.* the less is affinity of the IL anion to interact with water molecules, the higher is the ability of the propylammonium-based IL to promote liquid-liquid demixing in the presence of phosphate salt.

5.5 References

Albertsson PA (1956) Chromatography and Partition of Cells and Cell Fragments, Nature. 177, 771-4.

Asenjo JA, Andrews BA (2011) Aqueous two-phase systems for protein separation: A perspective, J. Chromatogr. A. 1218, 8826-8835.

Bridges NJ, Gutowski KE, Rogers RD (2007) Investigation of aqueous biphasic systems formed from solutions of chaotropic salts with kosmotropic salts (salt-salt ABS), Green Chem. 9, 177-183.

Chemspider, The free chemical database, http://www.chemspider.com/. Accessed at 01-10-2019.

Cláudio AFM, Ferreira AM, Shahriari S, Freire MG, Coutinho JAP (2011) Critical assessment of the formation of ionic-liquid-based aqueous two-phase systems in acidic media, J. Phys. Chem. B. 115, 11145−11153.

Dilip M, Bridges NJ, Rodríguez H, Pereira JFB, Rogers RD (2015) Effect of temperature on salt-salt aqueous biphasic systems: Manifestations of upper critical solution temperature, J. Solution Chem. 44.

Du Z, Yu YL, Wang JH (2007) Extraction of proteins from biological fluids by use of an ionic liquid/aqueous two-phase system, Chem. - A Eur. J. 13, 2130-2137.

F. Eckert, A. Klamt. (2018) COSMOtherm Version C30 Release 18 COSMOlogic GmbH & Co. KG, Leverkusen, Germany.

Farias FO, Passos H, Sanglard MG, Igarashi-Mafra L, Coutinho JAP, Mafra MR (2018) Designer solvent ability of alcohols in aqueous biphasic systems composed of deep eutectic solvents and potassium phosphate, Sep. Purif. Technol. 200, 84–93.

Freire MG, Cláudio AFM, Araújo JMM, Coutinho JAP, Marrucho IM, Lopes JNC, Rebelo LPN (2012a) Aqueous biphasic systems: A boost brought about by using ionic liquids, Chem. Soc. Rev. 41, 4966-4995.

Freire MG, Neves CMSS, Carvalho PJ, Gardas RL, Fernandes AM, Marrucho IM, Santos LMNBF, Coutinho JAP (2007) Mutual solubilities of water and hydrophobic ionic liquids, J. Phys. Chem. B. 111, 13082-9

Greaves TL, Drummond CJ (2015) Protic Ionic Liquids: Evolving Structure-Property Relationships and Expanding Applications, Chem. Rev. 108, 206-237.

Gutowski KE, Broker GA, Willauer HD, Huddleston JG, Swatloski RP, Holbrey JD, Rogers RD (2003) Controlling the aqueous miscibility of ionic liquids: Aqueous biphasic systems of water-miscible ionic liquids and water-structuring salts for recycle, metathesis, and separations, J. Am. Chem. Soc. 125, 6632-6633.

Han J, Pan R, Xie X, Wang Y, Yan Y, Yin G, Guan W (2010) Liquid-liquid equilibria of ionic liquid 1-butyl-3-methylimidazolium tetrafluoroborate + sodium and ammonium citrate aqueous two-phase systems at (298.15, 308.15, and 323.15) K, J. Chem. Eng. Data. 55, 3749-3754.

Kurnia KA, Coutinho JAP (2013) Overview of the excess enthalpies of the binary mixtures composed of molecular solvents and ionic liquids and their modeling using COSMO-RS, Ind. Eng. Chem. Res. 52, 13862–13874.

Louros CLS, Cláudio AFM, Neves CMSS, Freire MG, Marrucho IM, Pauly J, Coutinho JAP (2010) Extraction of biomolecules using phosphonium-based ionic liquids + K_3PO_4 aqueous biphasic systems, Int. J. Mol. Sci. 11, 1777-1791.

Marchel M, João KG, Marrucho IM (2019) On the use of ionic liquids as adjuvants in PEG-$(NH_4)_2SO_4$ aqueous biphasic systems: Phase diagrams behavior and the effect of IL concentration on myoglobin partition, Sep. Purif. Technol. 210, 710-718.

Marcus Y (1993) Thermodynamics of solvation of ions, J. Chem. Soc., Faraday Trans. 87, 2995-2999.

Merchuk JC, Andrews B a, Asenjo J a (1998) Aqueous two-phase systems for protein separation, J. Chromatogr. B Biomed. Sci. Appl. 711, 285–293.

Mourão T, Cláudio AFM, Boal-Palheiros I, Freire MG, Coutinho JAP (2012) Evaluation of the impact of phosphate salts on the formation of ionic-liquid-based aqueous biphasic systems, J. Chem. Thermodyn. 54, 398-405.

Mussagy CU, Santos Ebinuma V de C, Gonzalez-Miquel M, Coutinho JAP, Pereira JFB (2019a) Protic ionic liquids as cell disrupting agents for the recovery of intracellular

carotenoids from yeast *Rhodotorula glutinis* CCT-2186, ACS Sustain. Chem. Eng. 7, 16765-16776.

Mussagy CU, Winterburn J, Santos-Ebinuma VC, Pereira JFB (2019b) Production and extraction of carotenoids produced by microorganisms, Appl. Microbiol. Biotechnol. 103, 1095-1114.

Nelder JA, Mead R (1964) A simplex method for function minimization, Comput. J. 7, 308–313.

Neves CMSS, Shahriari S, Lemus J, Pereira JFB, Freire MG, Coutinho JAP (2016) Aqueous biphasic systems composed of ionic liquids and polypropylene glycol: insights into their liquid-liquid demixing mechanisms, Phys. Chem. Chem. Phys. 18, 20571-20582.

Passos H, Ferreira AR, Cláudio AFM, Coutinho JAP, Freire MG (2012) Characterization of aqueous biphasic systems composed of ionic liquids and a citrate-based biodegradable salt, Biochem. Eng. J. 67, 68−76.

Pereira JFB, Kurnia K a, Cojocaru OA, Gurau G, Rebelo LPN, Rogers RD, Freire MG, Coutinho J a P (2014) Molecular interactions in aqueous biphasic systems composed of polyethylene glycol and crystalline vs. liquid cholinium-based salts., Phys. Chem. Chem. Phys. 16, 5723–31.

Pereira JFB, Kurnia K a., Freire MG, Coutinho J a. P, Rogers RD (2015) Controlling the Formation of Ionic-Liquid-based Aqueous Biphasic Systems by Changing the Hydrogen-Bonding Ability of Polyethylene Glycol End Groups, Chem. Phys. Chem. 16, 2219–2225.

Pereira MM, Coutinho JAP, Freire MG (2016) CHAPTER 8: Ionic liquids as efficient tools for the purification of biomolecules and bioproducts from natural sources, in: RSC Green Chem.

Quental M V., Caban M, Pereira MM, Stepnowski P, Coutinho JAP, Freire MG (2015a) Enhanced extraction of proteins using cholinium-based ionic liquids as phase-forming components of aqueous biphasic systems, Biotechnol. J. 10 (2015), 1457-1466.

Quental M V., Passos H, Kurnia KA, Coutinho JAP, Freire MG (2015b) Aqueous Biphasic Systems Composed of Ionic Liquids and Acetate-Based Salts: Phase Diagrams, Densities, and Viscosities, J. Chem. Eng. Data. 60, 1674-1682.

Renon H, Prausnitz JM (1968) Local compositions in thermodynamic excess functions for liquid mixtures, AIChE J., 135-144.

Sintra TE, Cruz R, Ventura SPM, Coutinho JAP (2014) Phase diagrams of ionic liquids-based aqueous biphasic systems as a platform for extraction processes, J. Chem. Thermodyn. 77, 206-213.

Toledo MO, Farias FO, Igarashi-Mafra L, Mafra MR (2019) Salt Effect on Ethanol-Based Aqueous Biphasic Systems Applied to Alkaloids Partition: An Experimental and Theoretical Approach, J. Chem. Eng. Data. 64, 2018-2026.

TURBOMOLE V7.3. 2018. available from http://www.turbomole.com.

Ventura SPM, Neves CMSS, Freire MG, Marrucho IM, Oliveira J, Coutinho JAP (2009) Evaluation of anion influence on the formation and extraction capacity of ionic-liquid-based aqueous biphasic systems, J. Phys. Chem. B. 113, 9304-9310.

Ventura SPM, Sousa SG, Serafim LS, Lima ÁS, Freire MG, Coutinho JAP (2012) Ionic-liquid-based aqueous biphasic systems with controlled pH: The ionic liquid anion Effect, J. Chem. Eng. Data.57, 507-512.

Vieira FA, Guilherme RJR, Neves MC, Rego A, Abreu MH, Coutinho JAP, Ventura SPM (2018) Recovery of carotenoids from brown seaweeds using aqueous solutions of surface-active ionic liquids and anionic surfactants, Sep. Purif. Technol. 196, 300-308.

Zhang D, Deng Y, Chen J (2010) Enrichment of aromatic compounds using ionic liquid and ionic liquid-based aqueous biphasic systems, Sep. Sci. Technol. 45, 663-669.

6. RECOVERY OF CAROTENOIDS FROM *R. glutinis* YEAST USING MIXTURES OF BIO-BASED SOLVENTS

Based on the manuscript

Integrative platform for the selective recovery of intracellular carotenoids and lipids from *Rhodotorula glutinis* CCT-2186 yeast using mixtures of bio-based solvents

Mussagy CU, Santos-Ebinuma VC, Kurnia KA, Dias ACR, Carvalho P, Coutinho JAP and Pereira JFB

Green Chemistry, 22: 8478-8494, **2020**.

Abstract

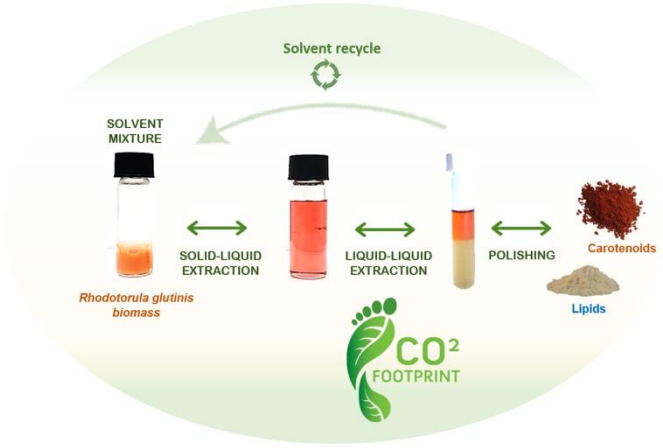

Natural bioactive compounds have been attracting a growing interest from industry as a “greener” alternative to synthetic raw materials/products. *Rhodotorula glutinis* yeast naturally synthesize added value compounds like lipids and carotenoids, commonly used for cosmetic, pharmaceutical, and food applications. *R. glutinis* are constituted by a rigid cell-wall structure, requiring energy-saving and efficient cell disruption methods for a sustainable recovery of the intracellular compounds. A simple and ecofriendly technology using mixed bio-based solvents (biosolvents) was here evaluated as an alternative platform to permeabilize yeast cells and to improve the selective recovery of β-carotene, torularhodin, torulene and lipids. The extraction ability of pure and solvent mixtures (methanol, ethanol, ethyl acetate, isopropanol, cyclohexane and 2-methyl tetrahydrofuran) was initial screened, demonstrating a clear impact of using mixtures to improve the extraction yields (up to three-fold increase). After identifying ethyl

acetate/ethanol/water as the solvent mixture with greater capacity to extract carotenoids and lipids, the selective recovery of carotenoids and lipids was enhanced by optimizing the solvent mixture composition ratio. Envisioning the industrial application, an integrated biosolvents-based downstream platform was designed. Two different strategies were investigated to further isolate of carotenoids and lipids from the *R. glutinis* biomass and to recycle the ethyl acetate/ethanol/water mixture: *i)* precipitation using cold acetone; *ii)* sequential liquid-liquid extraction. The integrated process for each strategy was compared with a conventional extraction procedure in terms of recovery efficiencies and its environmental impact. Regardless of the strategy, it is shown that the mixture of ethyl acetate, ethanol and water (15/27/58% w/w) can be reused up to three consecutive extractive cycles, ensuring high extraction efficiency yields, while decreasing the process carbon footprint by about 75% compared to the conventional method.

Keywords: *Rhodotorula glutinis*; biosolvents; extraction; carotenoid; lipids; sustainability.

6.1 Introduction

Rhodotorula glutinis is a strict aerobic yeast with peculiar metabolic characteristics (Vasconcelos et al. 2018) that allow a simultaneous biosynthesis of lipids (*e.g.*, palmitic acid, margaric acid and stearic acid) (Kot et al. 2019) and carotenoids (*e.g.*, β- carotene, torulene and torularhodin) (Dufossé et al. 2005; Kot et al. 2016; Mussagy et al. 2019b). Lipids (mainly as free fatty acids) produced by *R. glutinis* have a profile similar to some vegetable oils (Kot et al. 2016; Vasconcelos et al. 2018), being thus promising alternatives as food additives, diet supplements, substituents of unhealthy fats, or as raw material in oleochemistry industries (Saxena et al. 1998; Papanikolaou and Aggelis 2011; Lopes et al. 2018). In turn, *R. glutinis* carotenoids are natural pigments (Kirti et al. 2014) widely applied in the food, feed and pharmaceutical industries, due to beneficial properties such as anti-inflammatory, anti-obesity and anti-oxidant properties, provitamin A function, anti-cancer activity, and prevention of age-related health diseases (such as, macular degeneration) (Pinheiro Sant'Ana et al. 1998; Mata-Gómez et al. 2014; Sathasivam and Ki 2018; Toti et al. 2018; Mussagy et al. 2019a).

From a "green" perspective, the microbial production of valuable biomolecules, as is the case of carotenoids and lipids, is preferable to direct extraction from natural plant-based sources, mainly because of being easier, having higher productivity yields, and the energy-saving and environment-friendly nature of their industrial processes (Abdel-Aziz et al. 2018). Despite the recent increase of yeast-based industrial biorefineries (Mussagy et al. 2019a; Choi et al. 2019), the development of efficient, simple and economical downstream processes for the recovery of bioproducts, guaranteeing the maintenance of the biomolecules physicochemical and biological properties, it is still a major challenge (Saini and Keum 2017).

A wide range of microbial metabolites is accumulated intracellularly, such as the carotenoids and lipids in *R. glutinis* cells (Saenge et al. 2011; Kot et al. 2016; Tkáčová et al. 2017), making the design of appropriate cell-disrupting operations critical, in order to allow not only an effective rupture of the cell wall, but also the solubilization and maintenance of biological activities of intracellular solutes (Mata-Gómez et al. 2014; Saini

and Keum 2018; Mussagy et al. 2019b). Amongst the *R. glutinis* cell disruption procedures reported (Gong and Bassi 2016; Saini and Keum 2018; Mussagy et al. 2019a), the most applied for the recovery of intracellular lipids are Soxhlet (Dai et al. 2007; Chuck et al. 2014; Karamerou et al. 2016), Folch (Pan et al. 1986; Cheirsilp et al. 2012; Vasconcelos et al. 2018), and Bligh and Dyer (Kot et al. 2016; Kuan et al. 2018; Santos Ribeiro et al. 2019) methods, which require the use of significant amounts of volatile organic compounds (VOCs) such as hexane, chloroform, and methanol (Kot et al. 2017; Tkáčová et al. 2017). Likewise, the recovery of carotenoids from *R. glutin*is is not environmentally friendly, since conventional techniques using petroleum ether, dimethyl sulfoxide (DMSO), acetone, chloroform and hexane are still the most applied (Aksu and Eren 2007; Valduga et al. 2009; Jeevaratnam and Latha 2010; Cerón-García et al. 2018). From an industrial perspective, the use of conventional VOCs-based solid-liquid extraction (SLE) is probably the simplest and most effective solution for extracting lipophilic carotenoids and lipids from yeast biomass; however, considering that above certain levels of exposure some VOCs are dangerous to human health or harmful to the environment (Hernández-Almanza et al. 2017; Mussagy et al. 2019a), a careful balance between “efficiency” and “greenness” must be always guaranteed.

In order to replace non-ecological and toxic solvents with their benign equivalents, chemical and biotechnological industries have been looking for greener alternatives, in particular bio-based solvents (biosolvents) that can be partially or fully derived from renewable sources (Yara-Varón et al. 2016). Ethanol (Ruen-ngam et al. 2011), ethyl acetate (Gallego et al. 2020), and methanol (Ruen-ngam et al. 2011) are good examples of solvents that can be fully obtained from renewable sources. In reality, there are successful examples of solvents derived from bio-resources for the recovery of biomolecules from microbial sources, although mostly using non-conventional assisted methods (Ruen-ngam et al. 2011; Gallego et al. 2020). These include ultrasound assisted extraction (UAE), and microwave assisted extraction (MAE) to extract astaxanthin from *Haematococcus pluvialis* microalgae (Ruen-ngam et al. 2011), and solvent-based pressurized liquid extraction (PLE) for the recovery of fucoxanthin from marine microalgae

Tisochrysis lutea (Gallego et al. 2020). It should be noted that biosolvents do not always lead to the highest extraction yields for the recovery of lipids (Breil et al. 2017). In general, conventional SLE procedures using pure VOCs do not allow high recovery/extraction yields under mild conditions because the solvent is not able to promote a full lysis of the cell wall structure. Further adjustments of the process conditions are then required, like increase of temperature, processing-times, and/or number of cycles, which will make the process more expensive and less sustainable (Mussagy et al. 2019b).

As noted above, to reduce time, solvent volume and cost and improve recovery yields, assisted non-conventional cell-disruption methods are usually applied, *viz*. combining the use of organic solvents with bead milling, supercritical fluid extraction (SFE), MAE or UAE (Liau et al. 2010; Liu et al. 2011; Gallego et al. 2020). Despite significant enhancement of extraction efficiencies, mechanical-assisted non-conventional methods have a lack of specificity that causes the release of unwanted cell debris and impurities, along with the target-compound(s), negatively affecting the entire process design (Balasundaram et al. 2009). Moreover, either these treatments are only adequate for batch processing mode (*e.g*., bead milling and MAE) or involve highly energy consuming operations (*e.g*., SFE and UAE) (Macías-Sánchez et al. 2010). A representative example of how difficult it is to implement mechanical-assisted solvent extraction methods is SFE, which, in addition to limited separation selectivity between structurally similar biomolecules, it has high implementation and operational costs (Khaw et al. 2017) and process limitations (it requires lyophilized/dry biomass, increasing consequently the energy demand) (Mendes et al. 2003; Cooney et al. 2009; Cheng et al. 2011).

Unlike solvent-assisted extractions, an underexplored but remarkably simple and economic solution is the use of solvent mixtures in conventional SLE processing for the recovery of microbial carotenoids and lipids. Some studies have revealed the potential of mixed solvents in the extraction of astaxanthin from *Haematococcus pluvialis* (Liu et al. 2011), and in the recovery of lipids from *Yarrowia lipolytica* yeast cells (Breil et al. 2017).

Following these promising reports this work provides, for the first time, a very comprehensive study regarding the use of eco-friendly mixed biosolvents as effective alternatives for the selective recovery of three carotenoids (*i.e.* β-carotene, torularhodin, and torulene) and lipids, starting from an initial screening of pure solvents extraction performance up to a final process integration and life-cycle assessment of the best extractive biosolvents-based platforms. The performance of six pure biosolvents {*i.e*., methanol (MeOH), ethanol (EtOH), ethyl acetate (EtOAc), isopropanol (IPA), cyclohexane (CH) and 2-methyl tetrahydrofuran (2-MeTHF)} and their respective mixtures for the recovery of carotenoids and lipids from *R. glutinis* wet biomass at 65 °C was firstly evaluated. Then an optimization of the best biosolvent mixture (*i.e*., ethyl acetate/ethanol/water) was carried out, covering the entire ternary phase diagram (*viz*. SLE at monophasic region and liquid-liquid extraction (LLE) at biphasic region). A full understanding of the solvation mechanisms towards carotenoids and lipids extraction using different solvent mixtures compositions was achieved with COnductor-like Screening MOdel for Real Solvent (COSMO-RS). After selecting the most efficient solvent mixture, namely, ethyl acetate/ethanol/water (15/27/58% w/w in the biphasic region), aiming at the circularity of the entire process, the LLE platform was integrated with following polishing and recycling operations, evaluating the carotenoids and lipids extraction performance from the reuse of solvent mixtures in up to three consecutive stages for two different strategies (precipitation with cold-acetone and sequential liquid-liquid extraction). The environmental sustainability and the impact of the proposed technology were finally addressed by analyzing the carbon footprint of each integrative platform.

6.2 Experimental section

6.2.1 Chemicals

Monoolein, diolein, triolein and Supelco 37 Component FAME mix standards were purchased from Sigma-Aldrich (St. Louis, MO, U.S.A.). β-carotene and torularhodin standards were acquired from Carbosynth (San Diego, CA, U.S.A) while pure torulene

were obtained from *R. glutinis* biomass using a previous purification methodology (Mussagy et al., 2019). All chemicals used in the extraction process are listed in **Table D.1** from the **Appendix D**.

6.2.2 Microorganism and growing conditions

Rhodotorula glutinis CCT 2186 yeast was acquired from the Tropical Culture Collection André Tosello (Campinas, SP, Brazil), which was isolated from the leaf of a kaki fruit (Diospyros). The inoculum was prepared by the activation of *R. glutinis* CCT-2186 in Yeast Extract-Peptone-Dextrose (YPD) medium, which has the following composition (g/L in deionized water): peptone bacteriological (20); yeast extract (10); glucose (20). The inoculum culture was prepared in 100 mL Erlenmeyer® type flasks containing 25 mL of the YPD medium. Cells were then grown for 48 h at 30 °C and 150 rpm in an orbital shaker (Tecnal, model TE- 421 (Piracicaba, SP, Brazil)).

For lipids and carotenoids production, culture medium composed of (g/L in deionized water): glucose (10), KH_2PO_4 (0.52), $MgSO_4$ (0.52), NH_4NO_3 (4) and Asparagine (10) was used. Afterwards, 90 mL of inoculum culture at 0.2 mg/mL of cells were transferred to a 5 L stirred-tank bioreactor (Tecnal®, model Tec-Bio-Flex (Piracicaba, SP, Brazil), equipped with disc impeller, oxygen and pH electrodes) containing 4 L of culture medium. The initial pH of the medium was adjusted to 5.0 by adding 2 mol/L HCl or NaOH before autoclaving. The *R. glutinis* yeast growing was then conducted at 30 ºC, 300 rpm and 1 vvm (air volume/medium volume/minutes) during 96 h. Antifoam was added, as needed. Since the lipids and carotenoids are intracellular, after the cellular growing, the *R. glutinis* cells were then separated from the supernatant by centrifugation at 2500 *xg* for 10 min at 4º C using a Hitachi CR-22N (Tokio, Japan) centrifuge. The supernatants of all fermented media were then discarded, and the cellular pellets (*i.e*., wet biomass) containing carotenoids and lipids were collected and stored for the subsequent extraction studies.

6.2.3 Carotenoids isolation and characterization

Carotenoids from *R. glutinis* wet biomass was subject to chemical treatment with successive solvent extractions using DMSO. The DMSO extracts obtained were lyophilized. Then, these extracts were solubilized in acetone and transferred to a liquid chromatography column separation system, with mobile phase hexane/ethyl ether/etic acid (70:29:1 v/v/v), and major colored fractions of yellow, light red and red were obtained. The yellow, light red and red fractions were collected, evaporated to dryness and then, the carotenoids were re-suspended again in 1 mL of acetone. These acetone-based extracts were first evaluated qualitatively by Thin layer chromatography (TLC) on pre-coated TLC sheets ALUGRAM® (silica gel 60, Macherey-Nagel, Germany) to separate carotenoids and further comparison with literature data using the above-cited mobile phase as eluent. The extracts were also analyzed by Reverse Phase High Performance Liquid Chromatography (RP-HPLC) to detect the standard peak of absorbance. The homogeneity and the purity of the different fractions were identified by RP-HPLC on a column chromatography Shimadzu® Shim-pack C_{18} (Japan), 4.6×250 mm, using as mobile phase methanol/ acetonitrile/dichloromethane (60:10:30, v/v/v) eluting isocratically for 18 min. The flow rate was 1 mL/min, and the column temperature was set at 30 °C. The corresponding carotenoids were detected using UV-vis detector at λ_{max} 450 nm. The identification of β-carotene and torularhodin (yellow and red fraction respectively) was done by comparison with the standards retention time found (with high purity level) under the same experimental conditions, and for torulene (light red fraction) were compared with data reported in literature (Mussagy et al. 2019a, Jeevaratnam and Latha 2010). The structures of three purified fractions of carotenoids were finally confirmed by Proton Nuclear Magnetic Resonance (^{1}H NMR) using a Bruker Avance III HD 600 (14.1T).

6.2.4 Lipids isolation and characterization

Lipids of *R. glutinis* wet biomass were extracted using a mixture of ethanol/ethyl acetate/water. Briefly, the cells were harvested by centrifugation (2500 *xg* for 10 min at 10 °C) and mixed with EtOH/EtOAc/H_2O (55:24:21% w/w/w) and homogenized for 1 h at

300 rpm and 65 °C. Afterwards, EtOAc and H_2O were added to reach a final mass ratio (%) of 27:15:58 (EtOH/EtOAc/ H_2O). The ternary mixture was homogenized for 10 min, centrifuged at 2500 *xg* for 5 min. After the phase separation, the top and bottom phases were carefully separated, filtered with a polyethylene membrane (0.22 µm pore size) to remove residual cellular debris.

After the separation, the bottom phase containing EtOH/H_2O and lipids were collected, transferred to rotary evaporator flasks, which were dried under vacuum (at 100 mbar for 30 min) and dried extracts were solubilized in hexane. These hexane-based extracts were first evaluated qualitatively by Thin layer chromatography (TLC) on pre-coated TLC sheets ALUGRAM® (silica gel 60, Macherey-Nagel, Germany) using hexane/ethyl ether/acetic acid (70:29:1 v/v/v) as mobile phase to separate lipids and further comparison with the standards retention time (with high purity level) under the same experimental conditions using the above-cited mobile phase as eluent. The fatty acids were also analyzed in a gas chromatograph (GC). For that, lipids (50 mg) were methyl esterified using 2 mL of a sodium hydroxide methanolic solution (0.2 M) and heated at 80 °C/15min under vigorous stirring. Then, 2 mL of a methanolic solution of sulfuric acid (1 M) was added, repeating the steps of heating and stirring (once time). 1 mL of a saturated NaCl solution and 2 mL of hexane was added. The solution was vortexed and then kept at rest for phase separation. The upper (organic) phase was removed and the extraction procedure with hexane (2 mL) was repeated. The hexane was removed at 40 °C in the rotavapor and the fatty acids methyl esters were stored at 6 °C for further analysis. The fatty acid composition of the structured lipids was determined by gas chromatography using a Shimadzu gas chromatograph (GC-MS-QP2010) equipped with a flame ionization detector. SH-Stabilwax-DA column (30 m length, 0.25 mm diameter, and 0.25 µm film thickness) was used to separate the fatty acid methyl ester at a flow rate of 1.0 mL/min. The injector temperature was set to 200 °C and the transfer line temperature to 280 °C. The GC oven was programmed as follows: after 2 min at 50 °C, the temperature was increased at 30 °C/min to 150 °C, then at 15 °C/min to 230 °C. The

total run duration was 25 min. The fatty acids were identified on the basis of the peak areas.

6.2.5 Carotenoids and lipids extraction using biosolvents

The solid-liquid extraction (SLE) of carotenoids and lipids was carried out using pure and mixtures of the following biosolvents: methanol (MeOH), ethanol (EtOH), ethyl acetate (EtOAc), isopropanol (IPA), cyclohexane (CH) and 2-methyl tetrahydrofuran (2-MeTHF). The extraction of carotenoids and lipids was carried out according the following sequence: ***1)*** to remove impurities, the *R. glutinis* wet biomass were washed three-times using 10 mL of phosphate buffer (pH 7); ***2)*** after washing, 1 g of wet biomass were added in hermetic Carousel's™ type tubes (50 mL) to prevent solvent evaporation and loss; ***3)*** the tubes were filled with 5 mL of pure or mixed solvents (ratios and acronyms of the different systems are shown in **Table D.2** from the **Appendix D**, and the samples were then homogenized using a Carousel Stirring Hotplate 12 Plus Reaction Station™ (with reaction volume of 5 mL) (Radleys, Germany) for 1 h at 65 °C and 300 rpm; ***4)*** after homogenization, all the samples were centrifuged at 2500 *xg* and 25 ºC for 5 min using an Eppendorf® 5804 centrifuge (Willow Springs, NC, USA); ***5)*** after centrifugation, all cell lysate supernatants were filtered using a Millipore® filter membrane (0.22 µm pore size) and the solvents evaporated at 60 °C and 70 mbar using a rotary evaporator Büchi (R-210, Flawil, Switzerland); ***6)*** carotenoids were re-dissolved in acetone and the lipids remained in the flask dried and weighted; ***7)*** carotenoid-rich extracts were filtered using polyethylene membrane (0.22 µm pore size) and quantified using the methodology described in the section *Determination of carotenoids content*, while the lipids were quantified according the methodology described in the section *Determination of total lipids content.*

For the determination of recovery yields (%), the amount of each carotenoid (β-carotene, torularhodin and torulene) in *R. glutinis* biomass were determined from the total carotenoids obtained from consecutive extractions using DMSO, while the total lipids were determined after the extraction using standard Bligh and Dyer method. The recovery yields (%) of each carotenoids and lipids were defined as the ratio between the amount

(in mass) of each carotenoid or lipids extracted with each biosolvent or mixed biosolvent and the initial amount of each solute accumulated in the *R. glutinis* wet biomass, according to the **Equations 6.1** and **6.2**, respectively:

$$\text{Recovery of carotenoids (\% w/w)} = \frac{\text{Carotenoids extracted}}{\text{Carotenoids in } R.glutinis \text{ wet biomass}} \times 100 \quad (6.1)$$

$$\text{Recovery of lipids \% (w/w)} = \frac{\text{Lipids extracted}}{\text{Lipids in } R.glutinis \text{ wet biomass}} \times 100 \quad (6.2)$$

6.2.6 Determination of total carotenoids content

The carotenoids extraction was carried out according to the method modified by Mussagy et al., (Mussagy et al, 2019). *R. glutinis* wet biomass (1 g) were mixed with 5 mL of DMSO and disrupted by maceration (5 min ON/15 min OFF for a total 1 h). After the procedure, the supernatant was recovered, and the procedure repeated until the cells become fully bleached. The supernatants of the cell lysates were mixed with 10 mL of a NaCl aqueous solution (at 20% (m/v)) and 10 mL of petroleum ether. After the formation of a biphasic system, the non-polar phase was collected and the excess of water removed with sodium sulfate aqueous solutions (Na_2SO_4). The carotenoids-rich extracts were then dissolved in acetone and filtered with a polyethylene membrane (0.22 μm pore size). The quantification of the three carotenoids was obtained from the visible-light absorption spectra using a Microplate reader® UV-vis spectrophotometer (model Biotek, Synergy HT, Germany). The visible-light spectra from 380 to 600 nm were acquired, and the respective carotenoids calibration curves at 450 nm (β-carotene), 480 nm (torulene), and 500 nm (torularhodin) acquired. The carotenoid concentrations (μg/g) were determined according to pre-established standard curve prepared for the β-carotene, torularhodin and torulene (pure torulene standard was obtained from *R. glutinis* biomass using a purification method previously developed by our group) (Mussagy et al, 2019).

6.2.7 Determination of total lipids content

To determine the total lipid content of the yeast cells, lipids were extracted, dried and weighed by using a Bligh and Dyer procedure (Bligh and Dyer 1959). This standard method was also used as control in the subsequent biosolvents-based studies for the recovery of lipids from *R. glutinis* biomass. Briefly, the cells were harvested by centrifugation (2500 *xg* for 10 min at 10 °C), washed and dried (50 °C, 24 h) to obtain constant weight. Dried yeast cells were mixed with chloroform, MeOH and H_2O to reach 1:2:1 ratio (v/v/v) and homogenized for 1 h at 300 rpm and 25 °C. Afterwards, chloroform and H_2O were added to reach a final volume ratio of 2:2:2 (chloroform/MeOH /H_2O). The ternary mixture was homogenized for 10 min, centrifuged at 2500 *xg* for 5 min. After the phase separation, coexisting aqueous and organic phases were carefully separated, and filtered to remove residual cellular debris. After the separation, the bottom phase containing chloroform and lipids was transferred to rotary evaporator flasks (previously weighed, w_1), which were dried under vacuum (at 300 mbar for 30 min) until the organic phase was fully evaporated, and the final weight of the flask measured (w_2). Lipid content, expressed as mg/g dry cell weight per initial weight of the pellet (w) was determined according to the **Equation 6.3**:

$$\text{Total lipids content (mg/g)} = \frac{W_2 - W_1}{\text{W}} \qquad (6.3)$$

6.2.8 Computational Modelling

6.2.8.1 Conductor-like Screening Model for Real Solvent (COSMO-RS)

The computational modelling COnductor-like Screening MOdel for Real Solvent (COSMO-RS) was applied following the standard procedure applied in the two steps. In a first step, the molecular geometry of solutes (β-carotene, torularhodin, torulene, margaric acid, trilinolenin) and glyceryl-1,3-dilinoleate) and solvents (EtOH, H_2O, and EtOAc) were optimized at the density functional theory level and utilizing the BP functional B88-p86

with a triple- ζ valence polarized basis set (TZVP) and the resolution of identity standard (RI) approximation using a quantum chemical TURBOMOLE V7.3 2018 (Turbomole,2018) software program package. Subsequently, the obtained COSMO files were used as input in COSMO*therm* software (COSMOlogic, Levekusen, Germany, using parameter BP_TZVP_C30_1801) (Eckert and Klamt, 2018) to obtain the σ-profile and σ-potential.

In addition, COSMO-RS model was also used to estimate the interaction energy between solvent and solute, in term of excess energy (Kurnia and Coutinho 2013). In this context, the interaction energies in pure solvents as well as in their binary mixture of (solvent + solute) were estimated using COSMO-RS at the parameterization. In the molecular approach, COSMO-RS emphases on three specific interaction, namely the electrostatic - misfit energy (H_{MF}), hydrogen bonding energy (H_{HB}), and van der Waals energy (H_{vdW}). These energies are described in **Equations 6.4-6.6**, respectively:

$$\mathrm{H_{MF}} = \mathrm{a_{eff}}\frac{\alpha}{2}(\sigma + \sigma')^2 \qquad (6.4)$$

$$\mathrm{H_{HB}} = \mathrm{a_{eff}c_{HB}}\left(0; \min(0; \sigma_{\mathrm{donor}} + \sigma_{\mathrm{HB}}) \times \max\left(0; \sigma_{\mathrm{acceptor}} - \sigma_{\mathrm{HB}}\right)\right) \qquad (6.5)$$

$$\mathrm{H_{vdW}} = \mathrm{a_{eff}}(\tau_{\mathrm{vdW}} + \tau'_{\mathrm{vdW}}) \qquad (6.6)$$

where a_{eff} is the effective contact area between two surface segments, *α*'is the interaction parameter, σ_{HB} is the hydrogen bond strength that the threshold for hydrogen bonding, and the last two τ_{vdW} and τ'_{vdW} are elements of specific van der Waals interaction parameters.

The interaction energies that present in the binary mixture were also estimated by COSMO-RS using the excess enthalpies as the difference in the enthalpy of the studied EtOH, EtOAc, H_2O, β-carotene, torularhodin, torulene, linoleic acid and palmitic acid molecules in its mixture and pure state, according to the **Equation 6.7**:

$$H_{\mathrm{E,i}}(\mathrm{interaction}) = H_{\mathrm{i,mixture}}(\mathrm{interaction}) - H_{\mathrm{i,pure}}(\mathrm{interaction}) \qquad (6.7)$$

The $H_{E,i}$ (interaction) in the COSMO-RS model originates from summing the three specific interaction as described in **Equations 6.4 - 6.6**. Thus, it can be expressed as **Equation 6.8**:

$$H_{E,m} = H_{E,MF} + H_{E,HB} + H_{E,vdW} \quad (6.8)$$

Therefore, the COSMO-RS model could provide the information required for the evaluation of molecular interaction occur of solvents in the pure state, as well as in the mixture, as contribution of them in carotenoids and lipids recoveries.

6.2.9 Liquid-liquid extraction of carotenoids and lipids

The liquid-liquid equilibrium (LLE) data for the system with high yields recovery (EtOAc/EtOH/H_2O) were obtained from previous literature (Breil et al. 2017). In order to understand the extraction efficiency (EE%) and partition coefficients (*K*) of carotenoids and lipids in systems, after SLE, further amounts of EtOAc and H_2O were added to the samples to reach the solvents concentrations described in **Table D.6** from the **Appendix D** which are needed to induce a phase separation (*i.e*. formation a biphasic regime). After the solvent's addition, each mixture was then homogenized at 100 rpm, 25 ºC for 10 min and left to equilibrate for 1 h at 25 ºC. The formation of EtOAc/EtOH/H_2O biphasic systems was confirmed by the formation of two coexisting phases, namely, a dark orange-(top) phase (rich in EtOAc and carotenoids) and a clear-(bottom) phase (rich in EtOH/H_2O and lipids). The solvent ratio of all biphasic systems are detailed in **Table D.6** from the **Appendix D**. After the phase separation, the top and bottom phases were carefully separated, filtered with a polyethylene membrane (0.22 µm pore size), and the content of carotenoids and lipids determined according the methods described in the sections *Determination of total carotenoids content* and *Determination of total lipids content,* respectively.

The partition/extraction aptitudes of each system were measured as the extraction efficiency (EE%) and partition coefficient (*K*) of each carotenoid and lipids, which were calculated according the **Equations 6.9**, **6.10** and **6.11**, respectively**:**

$$\mathrm{EE\%} = \frac{C_{rich\ phase}\ x\ V_{rich\ phase}}{C_{top}V_{top} + C_{bottom}V_{bottom}} \quad (6.9)$$

where *C* corresponds to the concentration of β-carotene, torularhodin, torulene or lipids, and V to the volume of the coexisting phase in which the solute was preferentially partitioned (*i.e.*, carotenoids in the top phase, and lipids in the bottom phase). The subscripts 'top', 'bottom' refer to the top and bottom phases, respectively.

$$K_{car} = \frac{[car]_{top}}{[car]_{bottom}} \quad (6.10)$$

$$K_{lip} = \frac{[lip]_{bottom}}{[lip]_{top}} \quad (6.11)$$

K was calculated as the ratio between the concentration of each carotenoid (β-carotene, torularhodin and torulene) in the EtOAc-rich phase ($[car]_{top}$) to that in the EtOH/H_2O-rich phase ($[car]_{bottom}$) (**Equation 6.10**) and concentration of lipids in the EtOH/H_2O-rich phase ($[lip]_{bottom}$) to that in the EtOAc-rich phase ($[lip]_{top}$) (**Equation 6.11**).

6.2.10 Recycling of the bio-based solvents and carotenoids/lipids polishing

The EtOAc/EtOH/H_2O biphasic system that provided the highest *K* and EE% was chosen for the solvent recycling and carotenoids/lipids polishing studies. In this stage, samples containing 20% (w/w) of wet biomass and 80% (w/w) of the mixture EtOAc/EtOH/H_2O (at a weight ratio (%) of 24/22/54) were added in a Caroussel™ type tubes. The samples were then homogenized in a Carousel 12 Plus Reaction Station™ for 1 h, 65 °C at 300 rpm. After homogenization, all samples were centrifuged at 2500 *xg* at 25 ºC for 5 min. Cell lysate supernatants were filtered using a Millipore® filter membrane (0.22 µm pore size) and the biomass solid pellets discarded. Therefore, to separate carotenoids and lipids, 65% (w/w) of EtOAc/H_2O mixture (at a weight ratio (%) of 28/37) was added to the cell lysate supernatant containing carotenoids and lipids. The biphasic mixture (LLE) was homogenized for 10 min and further centrifuged at 2500 *xg* at 25 ºC for 10 min (to achieve the phase separation). The carotenoids were preferentially partitioned in the EtOAc-(top) rich phase, while the lipids were partitioned in the EtOH/H_2O-(bottom) rich phase.

For the recycling of the EtOAc-(top) rich phase, an evaporation unit was introduced after the LLE, from which the solvent evaporated was reused in a consecutive SLE from fresh *R. glutinis* biomass, while the carotenoids were recovered as a solid colored fraction.

On the other hand, two different *scenarios* for the recycling of the bottom phase and further polishing of lipids and proteins were evaluated, namely: *Scenario 1* - EtOH/H_2O-rich phase was evaporated and the mixed solvent reused in extractions; cold acetone (1:1 w/w) were added to solid fraction for the separation of proteins from lipids. *Scenario 2* - EtOH/H_2O-rich phase was used in a second LLE procedure by further addition of pure EtOAc (25% w/w). After the demixing, both phases of the LLE system were filtered, and the EtOAc (top)-rich phase containing lipids was evaporated, with the solvent being recycled into a subsequent LLE, while the lipids-rich (solid) fraction recovered; the EtOH/H_2O-rich phase was also evaporated, and the mixed solvent recycled into a subsequent SLE procedure, with and proteins-rich (solid) fraction also recovered.

These recycling/polishing procedures were repeated for three consecutive times, being the content of carotenoids and lipids recovered (*i.e.,* Recovery yields, %) in each step determined according the methods described in the sections *Determination of carotenoids content* and *Determination of total lipids content*, respectively.

6.2.11 Environmental assessment by determination of carbon footprint

The carbon footprint corresponds to the sum of greenhouse gas (GHG) emissions expressed as carbon dioxide equivalent ($CO_{2\ eq}$) and is calculated for each scenario studied (g $CO_{2\ eq}.\mu g^{-1}_{carotenoids}$ or g $CO_{2\ eq}.g^{-1}_{lipids}$) according to **Equation 6.12**.

$$\text{Carbon footprint} = \frac{\sum(\text{Aj x GHGj})}{\text{p}} \qquad (6.12)$$

where, A_j is the amount of each input *j* presented in **Table D.7** from the **Appendix D** for each scenario (units: g, mL or Wh), GHG*j* is the GHG emission factor for each input *j* presented in **Table D.8** from the **Appendix D** (units: g $CO_{2\ eq}.g^{-1}$, g $CO_{2\ eq}.mL^{-1}$ or g CO_2

$_{eq}$.Wh^{-1}), and p is the amount of extracted carotenoids (β-carotene, torularhodin and torulene) and lipids in each scenario studied (units: µg for carotenoids and mg for lipids).

The values for A*j* in the case of chemicals and water consist in the real quantities consumed during the experiments. The inputs of electricity were estimated based on the time of operation, nominal power of each equipment and fraction of occupancy over capacity of the equipment. The use of the nominal power can lead to an overestimation of the inputs of electricity because the real power may be lower. The values for GHG*j* were sourced from the Ecoinvent 3.6 database. As data for bacteriological peptone, asparagine and KH_2PO_4 are not provided by the Ecoinvent database, data for a similar chemical were adopted instead. However, these chemicals have a negligible contribution to the total carbon footprint.

6.2.12 Statistical analysis

Experiments were performed in triplicate, and the results are presented as the mean of three independent assays with the corresponding errors at a 95% confidence level for each dependent variable (β-carotene, torularhodin, torulene and lipids). Statistical analyses were performed using the R-Studio Software version 3.5.3 (Vienna, Austria). Parametric and non-parametric analysis were performed. For values that showed a normal distribution, one-way analysis of variance (ANOVA) followed by Tukey's multiple-comparison test were performed. The Kruskal-Wallis test, was also used to analyse the values with non-normal distribution. Values of $p \leq 0.05$ were considered statistically significant.

6.3 Results and discussion

6.3.1 Screening of pure biosolvents for the recovery of carotenoids and lipids

The performance of six pure biosolvents for the recovery of intracellular carotenoids from *R. glutinis* biomass was first screened, evaluating the effect of methanol (MeOH), ethanol (EtOH), isopropanol (IPA), ethyl acetate (EtOAc), 2-methyl tetrahydrofuran (2-MeTHF) and cyclohexane (CH) in the simultaneous extraction of β-carotene, torularhodin,

and torulene (**Figure 6.1 Top**) and lipids (**Figure 6.1 Bottom)** from *R. glutinis* biomass (at a concentration of 0.2 g/mL) after 1 h of stirring at 300 rpm and 65 °C. As detailed in **Table D.10** from the **Appendix D**, the choice of each solvent considered both the ability to solubilize the starting *R. glutinis* biomass (*i.e*., solvents that do not solubilize cell pellets were not screened), as well as the biocompatibility and toxicity index of each solvent (from Pfizer solvent selection guide and GSK Solvent Sustainability Guide (Hargreaves 2008)). As noted in **Table D.10** from the **Appendix D**, with exception of chloroform, all the other solvents can be fully (or at least partially) converted from bio-based renewable sources (*e.g*., lignin conversion, agricultural biomasses/wastes conversion, microbial biosynthesis, enzymatic conversion). Regarding biocompatibility and toxicity, from the biosolvents under study, as detailed in **Table D.10** from the **Appendix D**, most are recommended as biocompatible and eco-friendly alternatives, namely, H_2O, EtOH, EtOAc, and IPA. The three exceptions are CH, MeOH and 2-MeTHF, which are ranked as problematic due to some environmental/health issues, like aqueous and air impact and VOC emissions (CH, MeOH and 2-MeTHF), biotreatment (MeOH and 2-MeTHF) and health hazard (MeOH and 2-MeTHF). However, as noted in the next sections these biosolvents are not adequate for the extraction of carotenoid and lipids.

All experimental protocols and detailed values are given in the section Carotenoids and lipids extraction using biosolvents and **Table D.3** from the **Appendix D** respectively. Note that all the results of **Figure 6.1** and **Table D.3** from the **Appendix D** are expressed as the extraction recovery yields (% w/w) relatively to the initial content of carotenoids (*i.e*., β-carotene = 178 $\mu g/g_{wet}$ biomass, torularhodin = 104 $\mu g/g_{wet}$ biomass and torulene = 40 $\mu g/g_{wet}$ biomass) and lipids (221mg/g_{wet} biomass) in the *R. glutinis* wet biomass.

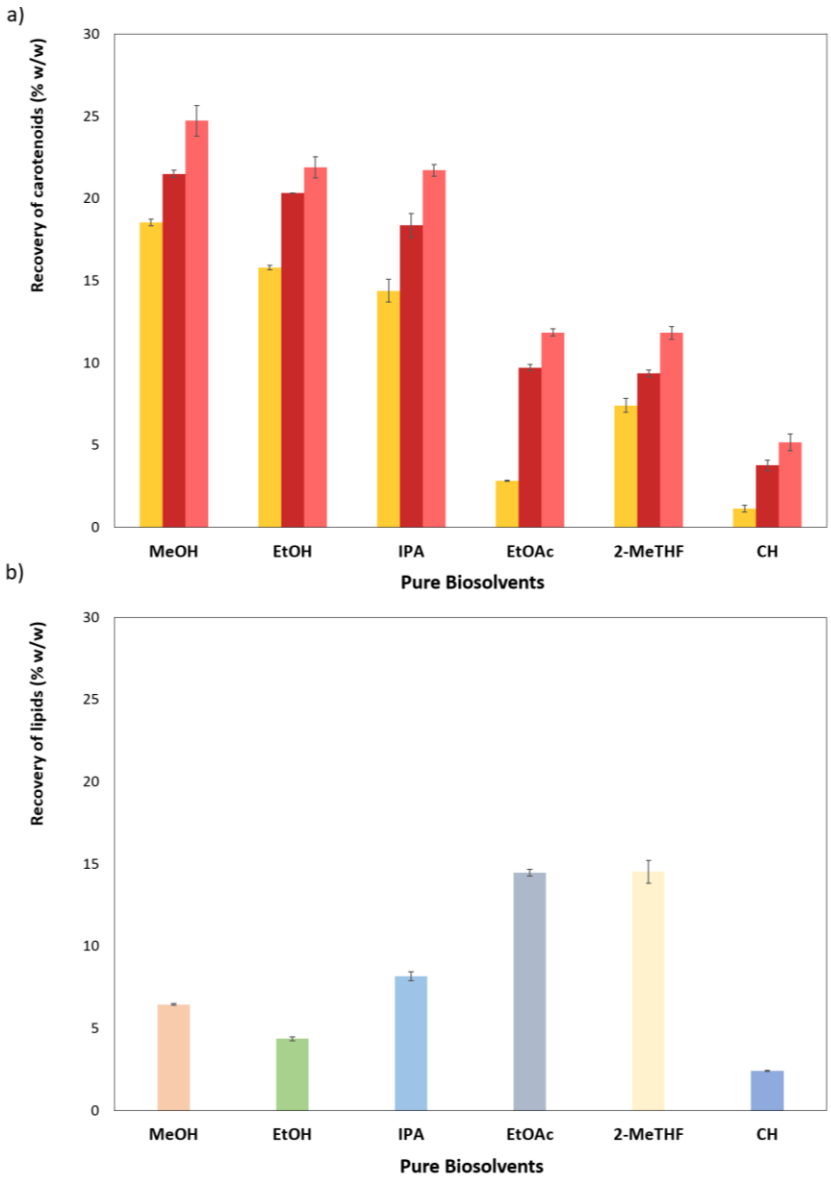

Figure 6.1. Recovery yields (% w/w) of (**a**) carotenoids (β-carotene [yellow], torularhodin [red], and torulene [pink]) and (**b**) lipids using pure biosolvent (MeOH- methanol, EtOH- ethanol, IPA- Isopropanol, EtOAc- ethyl acetate, 2-MeTHF- 2-methyl tetrahydrofuran and CH- cyclohexane) at a *R. glutinis* wet biomass concentration of 0.2 g/mL and after 1 h stirring (300 rpm) at 65 °C. The error bars represent 95% confidence levels for the mean of three independent assays.

The results ($p \leq 0.05$) depicted in **Figure 6.1** demonstrate that all pure biosolvents are able to extract, at 65 °C, some β-carotene (yellow bars), torularhodin (red bars), torulene (pink bars) and lipids. However, depending of their nature, biosolvents are more selective towards carotenoids or lipids. As shown in **Figure 6.1-a** (and **Table D.3** from the **Appendix D**), independently of the target carotenoid, their recovery yields increase as following: CH < 2-MeTHF < EtOAc < IPA < EtOH < MeOH. The carotenoid extraction aptitude of each biosolvent is in close agreement with the solvent polarity scale, as can be confirmed by their octanol/water partition coefficients, log K_{ow}, obtained from ChemSpider (Chemspider 2020): MeOH (log K_{ow} = -0.77) < EtOH (log K_{ow} = -0.31) < IPA (log K_{ow} = 0.05) < EtOAc (log K_{ow} = 0.73) < 2-MeTHF (log K_{ow} = 0.94) < CH (log K_{ow} = 2.67).

The high carotenoid recovery yields can be attributed to greater aptitude of the most polar solvents to solubilize the main constituents of the cell wall (proteins and lipids) (Beard 2011) from a wet yeast biomass. The creation of permeabilization channel in the cell will favor the biosolvents diffusion into intracellular periplasm, and consequent their interaction with carotenoids (and lipids). Since the extraction of carotenoids was carried out directly from a wet *R. glutinis* biomass, the use of more polar and water miscible biosolvents (*i.e*., MeOH, EtOH) is better for the cell wall disruption (Britton 1985; Bassetti and Tramper 1994; Sikkema et al. 1995), facilitating the cells-solvent miscibility. On the opposite, for wet biomass, the solubility of biosolvents with more hydrophobic nature (log K_{ow} values > 0), as is the case of EtOAc, 2-MeTHF and CH, is moderate-to-low, working thus as a diffusion barrier for the recovery of intracellular carotenoids.

In literature, the extraction of lipids is mainly associated with the “like-dissolve-like” principle, where the polarity of the extracts must be similar to the polarity of the target-compound to achieve the highest extraction efficiency (Chisti 2007; Halim et al. 2012). Despite the increasing relative solvent’ hydrophobicity trend, to understand the extraction ability of each biosolvent, we need to consider first their ability to solubilize the wet biomass, and second the profile of intracellular lipids from *R. glutinis*. As depicted in **Figure D.4-a** from the **Appendix D**, the lipids accumulated in *R. glutinis* cells strain CCT-

2186 are mainly free fatty acids (*i.e*., margaric acid (75%), stearic acid (10%) and pentadecylic acid (8%)), cf. **Figure D.4-b** from the **Appendix D**), with a minor traces of triglycerides (TAG) and diglycerides (DAG). Considering that the biosolvent is able of solubilizing properly the wet biomass (which is not the case of CH), it seems that the non-polar character of intracellular lipids accumulated in *R. glutinis* cells favored their recovery using the more hydrophobic biosolvents. Although previous studies focused in the recovery of carotenoids from dry biomass (Breil et al. 2017; Wan Mahmood et al. 2017), similarities with our work can be found. Breil et al., (Breil et al. 2017) recovered almost 63 % (w/w) of lipids from *Yarrowia lipolytica* IFP29 dry biomass using EtOAc, and Mahmood et al., (Wan Mahmood et al. 2017), recovered 59 % (w/w) and 66 % (w/w) of the total lipids from dry biomass of *C. vulgaris* and *Nannochloropsis* sp., respectively, also using EtOAc.

This initial screening using pure biosolvents has shown that, while the more polar compounds are promising for the extraction of intracellular carotenoids, more hydrophobic biosolvents are better candidates for the recovery of lipids. Evidently, if the extraction of both compounds is intended, a balance between diffusion and solubility is required. An adequate miscibility of wet cells with the biosolvent is initially needed, followed by an adequate diffusion of the solvent through the cell wall and penetration into the hydrophilic intracellular environment, and finally the effective solubilization of intracellular hydrophobic carotenoids and lipids.

6.3.2 Screening of mixtures of solvents for simultaneous recovery of carotenoids and lipids

In the previous section, different pure biosolvents were used for the recovery of intracellular carotenoids and lipids from *R. glutinis* biomass, demonstrating that an increase in solvent relative hydrophobicity increases the recovery yields of lipids, but reduces the carotenoids recoveries. Therefore, polar and non-polar solvents must be combined to increase carotenoids and lipid yields. Considering the solvents used in the conventional Bligh and Dyer method (chloroform + MeOH + H_2O), aqueous mixtures of two biosolvents were evaluated, particularly, exploring EtOAc (the solvent with highest aptitude to recover lipids) and CH (the solvent with lowest aptitude to recover lipids) as

potential substitutes of chloroform, and EtOH, IPA and 2-MeTHF as substitutes of MeOH. The conventional Bligh and Dyer mixture was used as control. This experimental stage was carried out at a *R. glutinis* wet cell concentration of 0.2 g/mL, in 1 h of stirring at 300 rpm, and 65 °C. All experimental details and solvent compositions are detailed in **Table D.2** from the **Appendix D**. The respective recovery yields (% w/w) of carotenoids and lipids are shown in **Figure 6.2** and detailed in the **Table D.4** from the **Appendix D**.

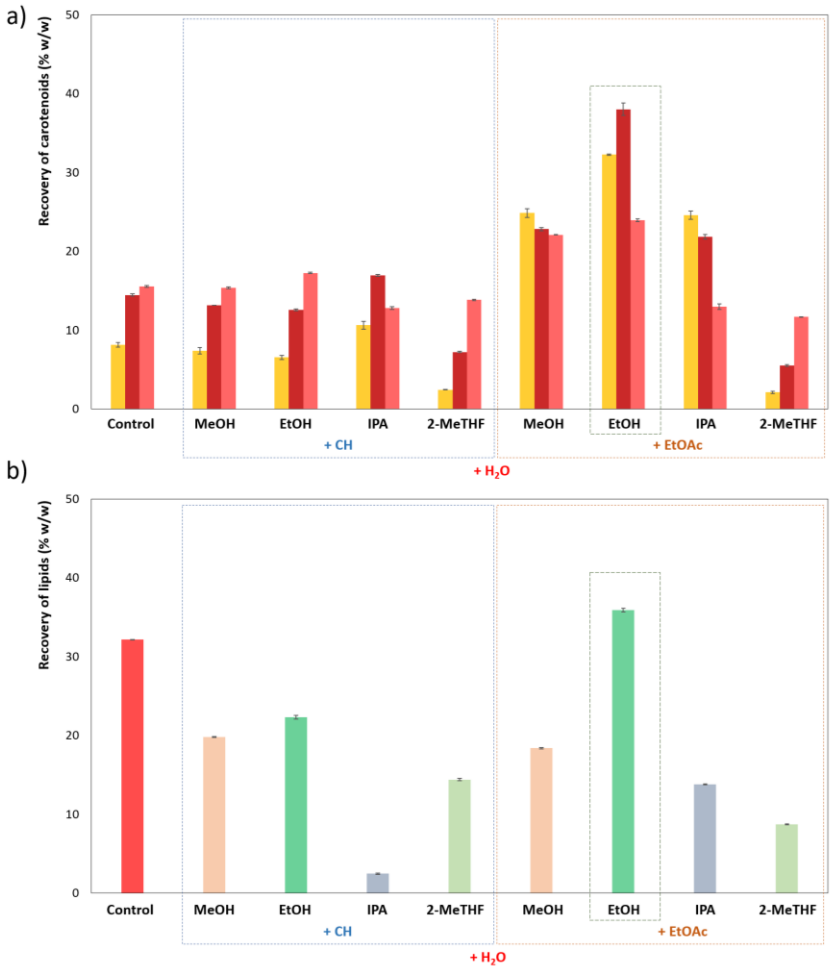

Figure 6.2. Recovery yields (% w/w) of (**a**) carotenoids (β-carotene [yellow], torularhodin [red], and torulene [pink]) and (**b**) lipids using aqueous (25% w/w of H_2O) mixtures of CH (25% w/w) (+ MeOH, EtOH, IPA and 2-Me-THF) (50% w/w) and EtOAc (25% w/w) (+ MeOH, EtOH, IPA and 2-Me-THF) (50% w/w) at *R. glutinis* wet cell concentration of 0.2 g/mL after 1 h stirring (300 rpm) at 65 °C. The conventional Bligh and Dyer mixture of chloroform (25% w/w) + MeOH (50% w/w) +

H_2O (25% w/w) was used as control. The error bars represent 95% confidence levels for the mean of three independent assays.

The results depicted in **Figure 6.2-a** show significant differences ($p < 0.05$) between all aqueous mixtures containing CH and EtOAc for the recovery of β-carotene, torularhodin and torulene. Particularly, while CH-based mixtures allowed carotenoid recovery yields similar or lower than the control, excepting the mixture of EtOAc/2-MeTHF/H_2O, all the EtOAc-based mixtures increased the carotenoid recovery yields. The highest recovery yields (32.25, 38.02 and 23.95% (w/w) of β-carotene, torularhodin and torulene, respectively) were achieved with the ternary system composed of EtOAc (25% w/w) + EtOH (50% w/w) + H_2O (25% w/w), in which three-fold increases in carotenoids recovery where observed when compared with the control. Although the extraction yields using EtOAc-based aqueous mixtures were higher than using the pure EtOAc as extractant, only the mixture of EtOAc/EtOH/H_2O gave significantly ($p < 0.05$) higher carotenoid yields than the third solvent alone (MeOH, IPA and 2-MeTHF). However, it should be highlighted that the capacity to extract each of the carotenoids changed, namely, the extraction of torularhodin (red bars) and β-carotene (yellow bars) with the EtOAc aqueous mixtures was enhanced, while, regardless of the biosolvent, pure solutions exhibited always higher capacity to extract torulene (pink bars) followed by torularhodin, and lowest recoveries for torulene. The change in the selectivity of the EtOAc aqueous mixtures seems to be a result of the decrease in the relative hydrophobicity of the extractant solution.

Carotenoids are poorly soluble (practically insoluble in water) (O'Neil 2001; Mezzomo and Ferreira 2016), and the weak polar organic solvents used as extractants present low cell permeation rates (Saini and Keum 2018). However, as demonstrated by Sachindra et al. (Sachindra et al. 2006), the extraction of carotenoids from wet samples of shrimp waste is enhanced by using a mixture of polar and non-polar solvents (*e.g.*, IPA and hexane) as extractant medium, in which the hydrophilic solvents remove the water in tissues, aiding in the extractability of pigments in the non-polar counterpart (Sachindra et al. 2006). EtOAc is a non-polar to weak polar aprotic solvent soluble in H_2O (6.04 g per

100 g of H_2O at 50 °C) (Glasstone and Pound 1925; Altshuller and Everson 1953), meanwhile EtOH can dissolve both polar and non-polar substances.(Miękus et al. 2019) Thereby, the increase recovery yield of carotenoids by the EtOAc/EtOH/H_2O system may be due to the presence of polar and non-polar characteristics in the mixture, which favored both the miscibility with yeast wet cells, the cell permeabilization, the access to the yeast intracellular matrix and subsequent solubilization of the hydrophobic carotenoids (further discussion about the extraction mechanism will be presented in section *Understanding the solvation in mixed solvents mechanisms using COSMO-RS*).

Figure 6.2-b also shows significant differences ($p < 0.05$) between all aqueous mixtures containing CH and EtOAc for the recovery of lipids. In general, CH and EtOAc-based mixtures recovered less lipids than the control (32.16% w/w of lipids). The exception was the mixture composed of EtOAc (25% w/w) + EtOH (50% w/w) + H_2O (25% w/w), which increased the lipids recovery yield up to 38.84 (% w/w) (a value statistically significant, $p < 0.05$). Regarding the use of pure or mixed solvents, with the exception of CH/IPA/H2O, all the CH-based aqueous mixtures allowed higher recovery yields of lipids than the pure CH. Similarly, the mixtures containing EtOAc/EtOH/H_2O, EtOAc/MeOH/H_2O and EtOAc/IPA/H_2O also increased the lipids' recovery capacity in comparison with the corresponding pure solvents (*i.e*., MeOH, IPA and EtOH).

The extraction and recovery of lipids can be improved by increasing the polarity of the solvent, which can be done by appropriately mixing polar solvents (EtOH + H_2O) to non-polar solvent (EtOAc in this case); this enhancement is due to the ability of polar solvents to release lipids from protein-lipid complexes, facilitating their dissolution in the non-polar solvent (Ghasemi Naghdi et al. 2016).

6.3.3 Solid/liquid extraction of carotenoids and lipids using ternary mixtures of ethyl acetate, ethanol and water

In the *Section 6.3.2*, it was demonstrated that the SLE of intracellular carotenoids and lipids from *R. glutinis* biomass can be enhanced using solvent mixtures composed of EtOAc, EtOH and H_2O. Therefore, this section will be devoted to the optimization of the solvent composition in the recovery of each target compound, as well as in understanding

the intramolecular interactions responsible for their selective recovery, aiming at further optimize the EtOAc/EtOH/H_2O composition and selection.

6.3.3.1 Experimental Optimization

One of the most important processing parameters in the design of biomolecules extraction procedures is to understand the effect of solvent mixture ratio in the selective recovery of the target-compounds. Therefore, the effect of different EtOAc/EtOH/H_2O compositions, detailed in **Table D.2** from the **Appendix D** (mixture points identified in the ternary phase diagram depicted in **Figure 6.3**) in carotenoids and lipids extraction was evaluated. The next set of extractions were carried out at a *R. glutinis* wet biomass concentration of 0.2 g/mL after 1 h of stirring at 300 rpm and 65 °C using different EtOAc/EtOH/H2O mixtures, selecting (randomly) fifteen mixtures points at the monophasic region of EtOAc/EtOH/H_2O phase diagram (points identified as A to R). The respective recovery yields (% w/w) of β-carotene, torularhodin, torulene and lipids are depicted in **Figure 6.3** and in **Table D.5** from the **Appendix D**.

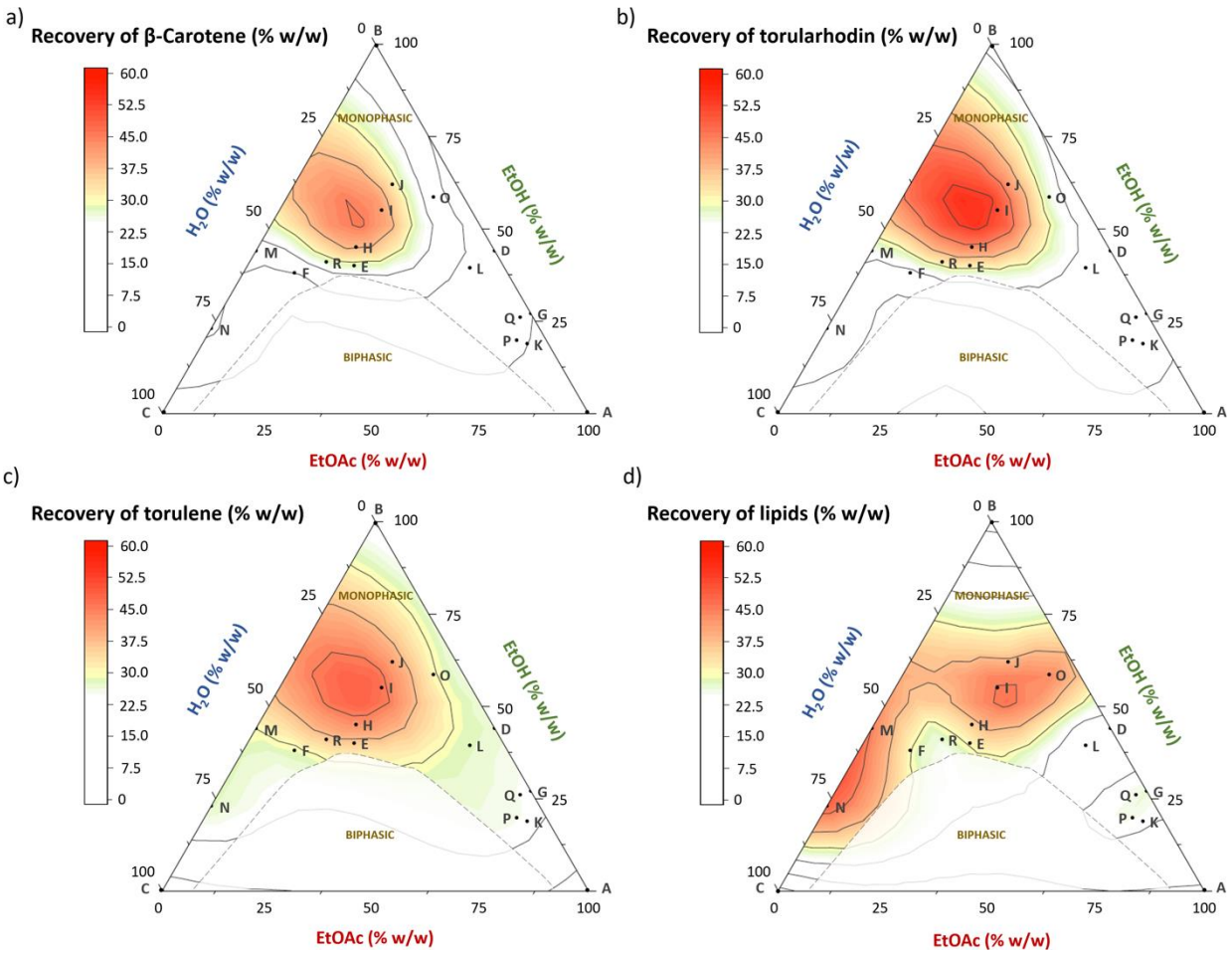

Figure 6.3. Ternary phase diagram of EtOAc/EtOH/H_2O, solvent mixtures composition (% w/w) and respective recovery yields (% w/w) of (**a**) β-carotene, (**b**) torularhodin, (**c**) torulene and (**d**) lipids at a *R. glutinis* wet cell concentration of 0.2 g/mL after 1 h stirring (300 rpm) at 65 °C. The gray curve represents the solubility binodal curve that separates the monophasic (colored zone) and the biphasic region (white zone). The results represent 95% confidence levels for the mean of three independent assays.

To simplify the analysis and discussion of the results, these were grouped according to the impact of solvent (EtOAc, EtOH and H_2O) concentration in the carotenoid and lipids recoveries, either individually or combined. These results are compiled in **Table D.5** from the **Appendix D**. The results plotted in **Figure 6.3-a, b and c** show that high EtOH concentrations (% w/w) (from 45 to 62 %), low concentrations of EtOAc (from 23 to

24%) and H_2O (from 15 to 32%) are the optimal conditions for the recovery of β-carotene, torularhodin and torulene, in which carotenoid recovery yields up to 60% (w/w) are achieved. On the other hand, for the recovery of lipids, ternary (or binary) mixtures with high H_2O (up to 77% w/w) and EtOH (from 23 to 62% w/w) content and low concentration of EtOAc (from 0 to 24% w/w) are preferable. From an overall analysis of **Figure 6.3**, it is possible to find a ternary mixture ratio that maximizes the recovery of all intracellular target-compounds (β-carotene, torularhodin, torulene and lipids), which should have a composition close to the mixture point *I* composed of 24% (w/w) of EtOAc, 55% (w/w) of EtOH and 21% (w/w) of H_2O. In the composition of the point *I,* approximately 46, 60, 51 and 51% (w/w) of the intracellular content of β-carotene, torularhodin, torulene and lipids were extracted, respectively.

Despite the hydrophobic character of the carotenoids and lipids, the presence of H2O in the solvent mixture contributes for the extraction of these biomolecules from the wet yeast oleaginous biomass. It increases the polarity of the solvent mixture, favoring not only the miscibility with the wet biomass, but also contributing to the permeabilization/disintegration of the cell wall (de Jesus et al. 2019), as a result of the formation of a hypotonic environment and increase of the yeast volume by osmosis (Lodish et al. 2000). The yeast cell disintegration facilitates the access of the extractant to the intracellular carotenoids. It should be noted that the addition of short alcohols, also increases the polarity of solvents, contributing to the dissolution of the cell wall membrane. The cell disruption/permeabilization and the dissolution of wet biomass can explain, at least in part, the improvement of carotenoids and lipids yields when polar solvents are added to non-polar solvents. However, as highlighted above, it must be considered that the intracellular compounds are accumulated inside the yeast cells, a very hydrophilic environment, which makes important the solvent polarity, *i.e*., non-polar solvents will not penetrate through the hydrophilic environment that surrounds pigments and lipids (Delgado-Vargas et al. 2000). Anyway, solute and solvent polarities have direct and important influence in the SLE process, *i.e*., “like-dissolve-like” principles, thus, due to predominant non-polar nature of carotenoids and lipids, the mixed solvent extractant

solution should have a relative hydrophobicity to allow their dissolution and extraction, as discussed in the next section.

6.3.3.2 Understanding the solvation mechanisms in mixed solvents using COSMO-RS

In the previous section, it was shown that the increase of the extraction of intracellular carotenoids and lipids can be enhanced by particular compositions of mixed solvents, *i.e.,* EtOAc/EtOH/H_2O. However, more than optimizing the biomolecules extraction procedures, it is essential to understand the effect of the solvent mixture on the recoveries. Therefore, to obtain a better understanding of the impact of the solvent hydrophobic-hydrophilic balance, and the main intramolecular interactions that occur between solvents and solutes for the proposed conceptual process, a computational modelling using COSMO-RS was applied.

The purpose of this COSMO-RS modelling is to clarify the effect of EtOAc/EtOH/H_2O mixtures described in **Table D.5** from the **Appendix D** (points labelled in ternary phase diagram in **Figure 6.3**) on carotenoids and lipids recoveries. One advantage of using COSMO-RS methodology is that the model can estimate thermodynamic properties of both pure fluids and mixtures only using information about the electronic structure of individual molecules. In this context, the molecular interactions in the system of interest (solvent mixture) are obtained from the polarity surfaces (sigma-surfaces) of the individual biomolecules, namely: the three carotenoids - β-carotene, torularhodin, and torulene; and lipids – FFA (margaric acid), TAG: triglyceride (Trilinolenin) and DAG: diglyceride (Glyceryl-1,3-dilinoleate). **Figure D.1** from the **Appendix D** show the sigma profiles for the two data sets of solutes (β-carotene, torularhodin, torulene, and lipids) and the three solvents (EtOAc, EtOH and H_2O). The solutes are divided into two groups: *i)* β-carotene and torulene; *ii)* torularhodin, FFA, TAG and DAG.

The first set, β-carotene and torulene are similar in nature, and the prominent peaks of β-carotene and torulene lie on the non-polar region of the profile that specify their non-polar character. Thus, it can be projected that, due to their non-polar character, β-carotene and torulene will have high interaction towards non-polar solvents. Indeed, the sigma

potential of both β-carotene and tolurene, presented in **Figure D.1-b** from the **Appendix D**, displays negative values within -0.8 $e \cdot nm^{-2} < \sigma < 0.8\ e \cdot nm^{-2}$ showing their likeliness to interact with the non-polar moiety of solvents. In addition, due to absence of peaks within the polar region in their sigma profile, both β-carotene and torulene show poor favourable interactions with polar moieties or polar solvents. Thus, from their sigma profile and potential, it could be projected that a suitable solvent for the recovery of β-carotene and tolurene must be of non-polar character in nature.

The second set of solutes (torularhodin, FFA, TAG and DAG) also show a peak in the non-polar region of the sigma potential (*cf*. **Figure D.1-c** from the **Appendix D**), with additional small peaks at both polar regions. For example, the peak at 1.3 $e \cdot nm^{-2}$ correspond to the oxygen atom of the carboxylic moiety of the compounds that can act as hydrogen bond acceptor. On the other hand, a small peak at circa -1.8 $e \cdot nm^{-2}$ is associated to the hydrogen atom of the carboxylic moiety that have a weak hydrogen bond donor ability. This is predictable as these solutes contain carboxylic acid group. Unlike the first set, the second set of solutes shows not only favorable interactions with non-polar groups, but also with both hydrogen bond donor and acceptors (*cf*. **Figure D.1-c** from the **Appendix D**). It should be stressed that the sigma potentials suggest that their interactions with the polar groups is higher than with the non-polar groups. Therefore, it is expected that the second set of solutes could interact with solvents through hydrogen bond interactions as well dispersive interactions with the non-polar moieties of the solvent.

Concerning the solvent, the **Figure D.1-e-f** from the **Appendix D** shows the sigma profile and potential of EtOAc, EtOH and H_2O. Due to its polar nature, the H_2O molecule shows high attraction towards hydrogen bond donor and acceptor groups, while displaying unfavorable interactions with non-polar groups. Thus, it is expected that H_2O will interact with solutes mainly through hydrogen bonding. Similar with H_2O, EtOH also present remarkable attraction toward hydrogen bond donor and acceptor groups. In addition, the presence of ethyl group of EtOH lead to its likeliness to interact as well with the non-polar moieties of the solutes. Finally, EtOAc displays attraction toward hydrogen bond donor as well as non-polar groups.

To summarize, from the sigma profile and the potential analysis it was revealed that β-carotene and torulene are extremely non-polar compounds in nature, and thus, they display attraction toward solvents with high non-polar character. Whereas, torularhodin and lipids (represented by margaric acid, glyceryl-1,3-dilinoleate and trilinolenin) are not only attracted toward non-polar solvents, but also toward solvents that have the ability to form hydrogen bonding. As can be observed from their sigma profile, there is an enormous difference on the non-polar character between the solute and solvents that lead to low recoveries of solute using single solvent. For example, the recovery values of β-carotene are 2.82, 2.93, and 15.80% by using EtOAc, H_2O, and EtOH, respectively.

The use of a mixture of biosolvents changes the polarity of the final solvent, and consequently improve the recovery of solute. **Figure D.2-a** (from the **Appendix D**) shows the sigma potential of pure and representative of EtOAc/EtOH/H_2O mixtures studied in this work. Unlike the sigma profile, the sigma potential is influenced by the composition and temperature, and thus, can be used to evaluate the likeliness of the mixed solvent to solvate a target compound. The most notable feature presented in **Figure D.2-a (**from the **Appendix D)** is the sigma potential of EtOAc within the region of $\sigma > 1$ e·nm^{-2}, where it shows repulsion towards the hydrogen bonding acceptor. Adding EtOH (50% w/w) into pure EtOAc (50% w/w), as in the case of mixed solvent 4, alters the solvent character from repulsive to attractive interactions toward hydrogen bond acceptors. Furthermore, adding EtOH (30% w/w) and EtOAc (29% w/w) into H_2O (41% w/w), as in the case of mixed solvent 5, shift the repulsive sigma potential to attraction (*cf*. **Figure D.2-a** from the **Appendix D**). In general, all EtOAc/EtOH/H_2O ternary mixtures have varied sigma potential when compare to their original solvent or binary mixtures (*cf*. **Figure D.1-f** from the **Appendix D**), which produce solvent with different character when compare to a pure solvent and, ultimately, increase the recovery of solute.

Afterwards, in order to evaluate the impact of EtOAc/EtOH/H_2O mixtures toward the recovery yields (% w/w) of the different solutes in molecular level, COSMO-RS is used to estimate the excess enthalpies of mixture. The estimation of excess enthalpies with COSMO-RS was performed by taking the sum of the three-contribution associated with

electrostatic-misfit, hydrogen bond, and van der Waals forces. Therefore, the model can be used to analyze the significance of the different intermolecular energies responsible for the recovery of each solute using EtOAc/EtOH/H_2O mixtures. The estimated excess enthalpies are given in **Table D.9** in the **Appendix D**.

In general, for the recovery of β-carotene and torulene, favorable (negative values) contribution arises from the contribution of both EtOH and EtOAc. Whereas, the H_2O molecule contribution is endothermic and is originated from hydrogen bond. In this context, H_2O molecules must break the intermolecular hydrogen bonding between H_2O-H_2O to facilitate the mixing with other solvents and, consequently, the target solute. Remarkably, there is a good correlation between the recovery (% w/w) of β-carotene and the electrostatic-misfit of the solute, as depicted in **Figure 6.4-a**. The electrostatic-misfit arises from the interaction between the non-polar part of solute and the non-polar part of the mixed solvent, as mentioned previously. The same is also observed for the recovery of torulene (**Figure 6.4-b**). This is expected as β-carotene and torulene have similar sigma profiles, and thus, have comparable interactions with the mixed solvent.

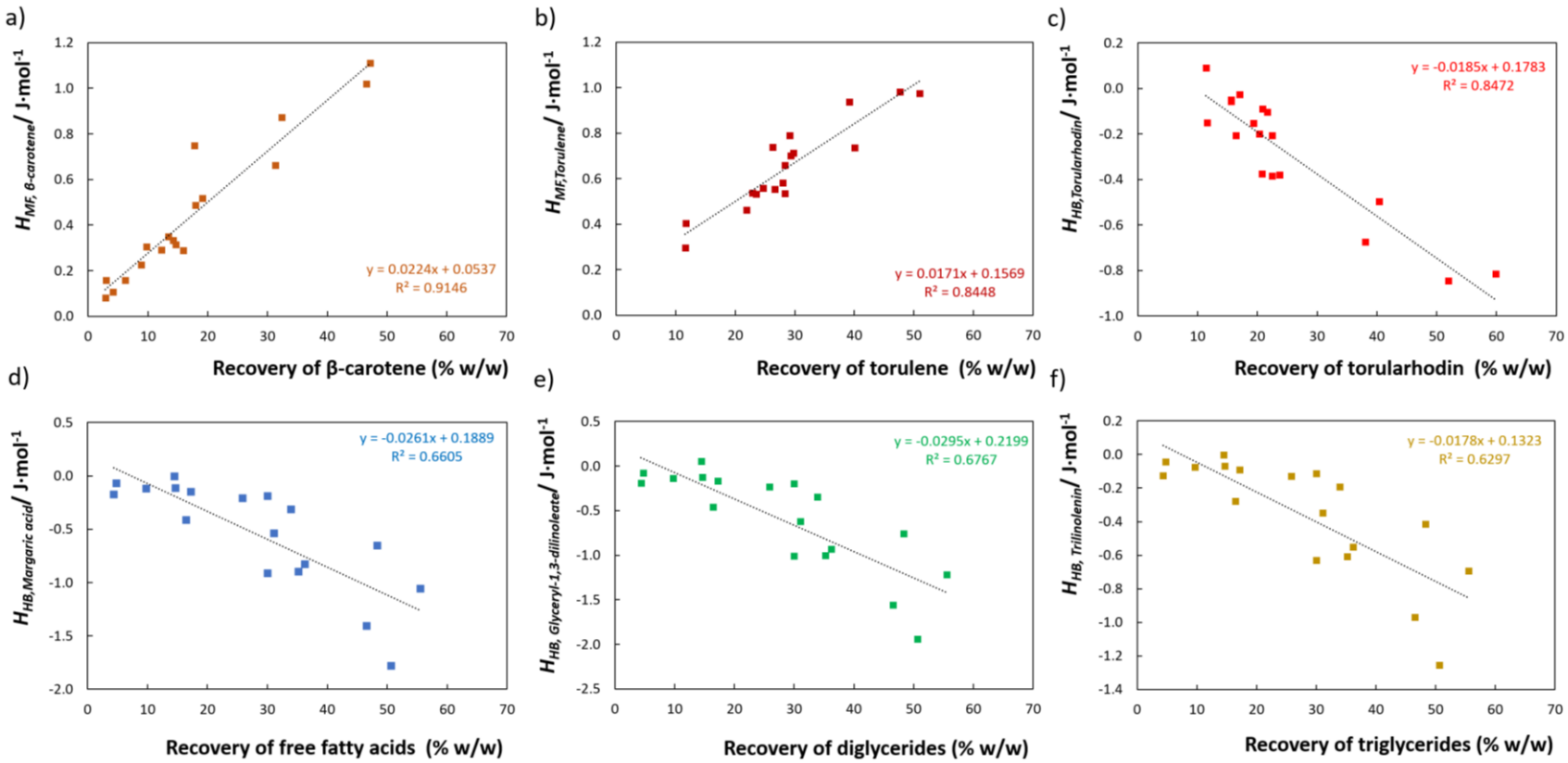

Figure 6.4. Correlation plot between the interaction energies (X-axis) of solvents mixtures and the recoveries (% w/w) of of **a**) (■) β-carotene, **b**) (■) torulene, **c**) (■) torularhodin, **d**) (■) margaric acid, **e**) (■) glyceryl-1,3-dilinoleate and **f**) (■) trilinolein.

For the second set of solutes, the circumstances are quite different. As previously mentioned, these solutes contain carboxylic group that may form hydrogen bond with the mixed solvent. As consequences, the recovery of lipids is highly governed by the two dominant interaction arise from hydrogen bond of solute in the system, as displayed in **Figure 6.4-c-f** and electrostatic misfit of solute in the system (**Figure D.3** from the **Appendix D**). Thus, it seems that the electrostatic misfit and hydrogen bond of solute play a subtle balance in the extraction of lipids. For the lipids, the excess enthalpies were calculated against their main constituent, namely margaric acid, trilinolenin and glyceryl-1,3-dilinoleate. Good correlation between the %recovery and hydrogen bonding interaction and electrostatic misfit originate from the solute is observed. One may question if the hydrogen bond controls the recovery of solute, H_2O should be the best candidate, as it has the strongest hydrogen bond strength, but this is precluded by the H_2O unfavorable interactions with non-polar moieties of the solutes. Thus, the suitable mixture of solvents to enhance the recovery of solute should have the appropriate hydrogen bond strength while possessing the ability to solvate also the non-polar moiety of the solute.

The modelling of the COSMO-RS confirms that the recovery of carotenoids and lipids from *R. glutinis* biomass is enhanced by using mixed solvent instead of a pure solvent. In this regard, a mixture of H_2O, EtOH and EtOAc could provide a suitable extraction medium to recover β-carotene, torulene, torularhodin and lipids. The improvement seems to be a result of the change of hydrophobic-hydrophilic character of the mixed solvent, as result of the nature of each set of solutes, namely: *i*) β-carotene and torulene - interaction between non-polar part of solute and non-polar part of the mixed solvent; *ii*) torularhodin and lipids - hydrogen bond between solute and mixed solvent. It should be emphasized, nevertheless that the modelling using COSMO-RS provides only a molecular view of the solute-solvent interactions. Note that these solvation mechanisms should be considered along with the cell disruption/permeabilization and wet biomass dissolution phenomena discussed in the previous sections.

6.3.4 Liquid-liquid extraction of carotenoids and lipids using ternary mixtures of ethyl acetate, ethanol and water

Envisaging the design of an integrated extraction process for the simultaneous recovery of carotenoids and lipids from *R. glutinis* biomass, and considering the previous optimization study (section *Experimental optimization*), the *point I*, which exhibited the highest recoveries of β-carotene, torularhodin, torulene and lipids, was selected for the following liquid-liquid extraction (LLE) studies. Accordingly, an EtOAc/EtOH/H_2O mixture at initial solvent ratio of 24/55/21 (% w/w) was used for the SLE from wet biomass, and after, the solutes (carotenoids and lipids) extracted were separated through LLE by inducing a phase separation with further addition of EtOAc and H_2O. Six biphasic systems were created, and the corresponding equilibrium phases compositions determined analytically. The mixtures points of each system (identified with the letters *a* to *f*) and respective tie-lines, are represented in the ternary phase diagrams depicted in **Figure 6.5** (detailed values in **Table D.6** from the **Appendix D**). To avoid differences in the volume ratio for each biphasic system and provide a better understanding of the solute separation trends of each system (all the recovery yields and volume ratios are detailed in **Table D.6** from the **Appendix D**), instead recovery yields the extraction abilities are presented in the **Figure (s). 6.5-a, 6.5-b**, and **6.5-c** as the partition coefficient of β-carotene, torularhodin and torulene (K_{car}) between the top (EtOAc-rich) and bottom (EtOH/H_2O-rich) phases, respectively. **Figure 6.5-d** presents the partition coefficient of lipids (K_{lip}), which was defined as the ratio of the concentration of lipids (% w/w) in the EtOH/H_2O-rich (bottom) and EtOAc-rich phases (top).

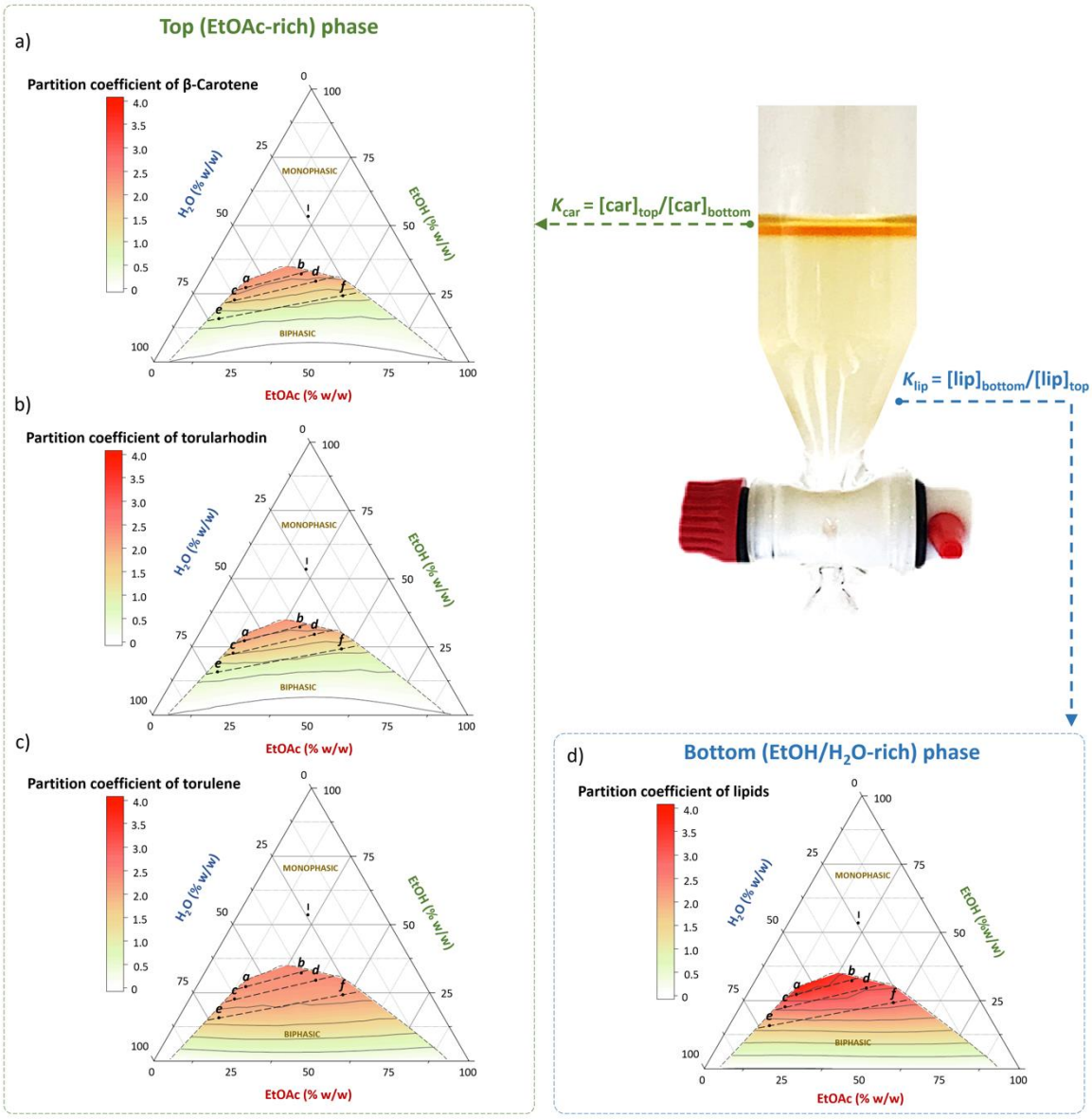

Figure 6.5. Ternary phase diagram of EtOAc/EtOH/H_2O system, mixture points at biphasic regions studied (*a* to *f*), with respective tie-lines (---), and partition coefficient (K_{car}) of (**a**) β-carotene, (**b**) torularhodin, (**c**) torulene and (**d**) partition coefficient of lipids (K_{lip}) at a *R. glutinis* wet cell concentration of 0.2 g/mL after 1 h stirring (300 rpm) at 65 °C. The results represent 95% confidence levels for the mean of three independent assays.

Figure 6.5 shows that the mixture points *a* and *b*, with a composition close to the critical point, present the highest partition coefficients, namely: 2.2 < K_{car} < 2.3, for the three carotenoids (*i.e*., *β*-carotene, torularhodin and torulene); and K_{lip} of approx. 3.7. Note that as the tie-line length increases, all the K_{car} *and* K_{lip} decreased, which means that the closer is the biphasic mixture the critical point, the higher is the partition of the solutes. On the other hand, despite the similar *K* values on the same tie-line (*i.e., a* ≈ *b*; *c* ≈ *d*; *e* ≈ *f*) as result of similar phases' composition, due to the changes of volume ratio of the phases of points on the same tie-line (*cf.* **Table D.6** from the **Appendix D**), an adjustment of the EE (%) of carotenoids (in the EtOAc-rich phase) and lipids (EtOH/H_2O) was achieved. As shown in **Table D.6** from the **Appendix D**, among the mixtures points under study, the highest EE% of *β*-carotene, torularhodin and torulene were obtained for the point *a* (EE > 84%), while the highest EE% of lipids were obtained with points *d*, *e* and *f* (EE > 87%).

As shown in the section *Solid-liquid extraction of carotenoids and lipids using ternary mixtures of ethyl acetate, ethanol and water*, because of the more hydrophobic nature of the EtOAc-rich phase, the non-polar carotenoids are preferentially partitioned into it. On the opposite, lipids are preferentially separated in the EtOH/H_2O-rich phase due to the hydrogen bond interaction of the carboxylic acid group. The strength of free fatty acids interactions toward both hydrogen bond to the polar groups of the EtOH/H_2O (bottom) phase is higher than the dispersive interactions with the non-polar groups of the EtOAc (main constituent of the top phase), favoring thus a preferential partition of the lipids to the bottom phase.

Together, these results confirm that, for the selective separation of carotenoids and lipids, several factors must be considered. In a first stage the choice of an extractant mixture composed of polar and non-polar solvents, which maximizes the SLE extraction of all intracellular targeted solutes. Secondly, the mixture at the biphasic region using optimized systems, with suitable concentrations of the solvent mixtures, allows the selective separation of the solutes, demonstrating that the use of the mixed solvent, unlike the pure solvents, allows not only to enhance cell disruption/permeabilization and

recovery of intracellular carotenoids and lipids, but also facilitates their subsequent separation and purification using simple LLE procedures.

6.3.5 Recycling of the biosolvents and polishing of carotenoids and lipids

In the previous sections, the extraction of β-carotene, torularhodin, torulene and lipids from *R. glutinis* biomass using mixed biosolvents was optimized. In addition, a selective separation of the carotenoids from the lipids was successfully achieved by LLE employing EtOAc/EtOH/H_2O mixtures. It was demonstrated that the use of mixed biosolvents is a feasible, simple, efficient and environmentally friendly solution for the selective recovery of non-polar biomolecules from complex (bio)matrices (like wet biomass). However, from an academic perspective, it is fundamental to demonstrate that the proposed biosolvent-based technology can be, from a technical and sustainable point of view, viable in a future industrial application. Thus, to make these technologies competitive with the existing ones, the design of the solvents recycling/reusability and polishing strategies for the targeted solutes are mandatory (Mussagy et al. 2019a), as well as their proper integration in the processing plant. The development of adequate technologies that allow the reuse of solvents is primordial to guarantee the economic and environmental viability and sustainability of the industrial manufacturing process (Delrue et al. 2012).

Therefore, to address the feasibility of the implementation of the proposed technology for future industrial recovery of carotenoids and lipids from *R. glutinis* biomass, two strategies for recycling the solvent mixtures and obtaining the recovered carotenoids and lipids were attempted. For the recycling studies, the point *I* (w/w), composed of 24% of EtOAc, 55% of EtOH and 21% of H_2O, was selected (**Figure D.5** from the **Appendix D**), since it maximizes the recovery of β-carotene, torularhodin, torulene and lipids (recovery yields > 50% w/w). After the extraction, the biomolecules extracted were separated from the residual *R. glutinis* biomass by centrifugation and then subjected to a LLE (*point a*) at 25 °C, for the selective separation of carotenoids and lipids. With the LLE the carotenoids were preferentially separated into the EtOAc (top)-rich phase, while the lipids partitioned to the EtOH/H_2O (bottom)-rich phase. For recycling of the EtOAc-rich

phase, an evaporation process was introduced after the LLE, from which the solvent evaporated was reused in a consecutive SLE from fresh *R. glutinis* cells and the carotenoids were recovered as a solid-colored fraction. On the other hand, two different *scenarios* for the recycling of the EtOH/H_2O-rich phase and further polishing of lipids and proteins were evaluated, namely:

Scenario 1 –EtOH/H_2O-rich phase was evaporated and the mixed solvent reused in the extraction; cold acetone (1:1 w/w) were added to solid fraction for the separation of proteins from lipids.

Scenario 2 - EtOH/H_2O-rich phase was used in a second LLE procedure by further addition of pure EtOAc (25% w/w). After the demixing, both phases of the LLE system wereas filtered, and the top EtOAc-rich phase containing lipids was evaporated, this solvent being recycled into a subsequent LLE, and the lipids-rich (solid) fraction recovered; the EtOH/H_2O-rich phase was also evaporated, and the mixed solvent recycled into a subsequent SLE procedure, with and proteins-rich (solid) fraction recovered.

These recycling/polishing procedures were repeated three times, and the respective recovery yields (% w/w) of β-carotene, torularhodin, torulene and lipids recoveries determined. All results are listed in **Table 6.1,** including a comparison between using the reused EtOAc/EtOH/H_2O mixture or a fresh EtOAc/EtOH/H_2O solution (control).

Table 6.1. Recovery yields (% w/w) of β-Carotene, torularhodin, torulene and lipids using fresh and reused EtOAc/EtOH/H_2O mixture at a *R. glutinis* wet cell concentration of 0.2 g/mL after 1 h of stirring (30 rpm) at 65 °C.

Solvent	Recovery yields ± σ (% w/w)			
	Lipids[1]	β-carotene[1]	Torularhodin[1]	Torulene[1]
		Scenario 1		
Fresh solvent (control)	48.15 ± 1.32^{a}	45.16 ± 0.19^{a}	59.90 ± 0.08^{a}	43.56 ± 1.08^{a}
First reuse	43.42 ± 0.26^{b}	41.79 ± 0.28^{b}	53.58 ± 1.40^{b}	42.07 ± 0.05^{ab}
Second reuse	41.51 ± 0.17^{c}	40.58 ± 0.97^{bc}	50.42 ± 1.493^{c}	41.79 ± 1.28^{ab}
Third reuse	40.70 ± 0.49^{c}	39.93 ± 0.39^{c}	52.86 ± 0.14^{bc}	41.35 ± 0.19^{b}
		Scenario 2		
Fresh solvent (control)	40.29 ± 0.62^{a}	44.19 ± 1.02^{a}	53.85 ± 0.81^{a}	38.46 ± 0.60^{b}
First reuse	35.81 ± 0.07^{b}	40.45 ± 0.81^{b}	52.43 ± 0.53^{ab}	42.26 ± 1.06^{a}
Second reuse	32.14 ± 0.17^{c}	39.81 ± 0.59^{b}	50.12 ± 0.31^{c}	41.66 ± 0.76^{a}
Third reuse	32.72 ± 0.57^{c}	39.29 ± 0.22^{b}	51.54 ± 0.81^{bc}	42.76 ± 0.46^{a}

[1]Tukey HSD test (α = 0.05) for the mean of three independent assays ± confidence levels; means with the same lowercase letter does not present significant difference (p > 0.05).

As can be seen in **Table 6.1**, regardless of recycling/polishing *Scenario*, the biosolvents (*i.e*., EtOAc-rich and EtOH/H_2O-rich phases) can be recycled up to three times, guaranteeing the maintenance of the good recoveries' efficiencies, namely, losses lower than 10% in comparison with the control (fresh solvent solution). After 3 recycling cycles the recovery yields (%w/w) were higher than 39, 50, 38 and 32 for β- carotene, torularhodin, torulene and lipids, respectively. Nevertheless, even considering the decrease in recovery yields of carotenoids after three cycles, it is important to note that these recoveries are three-fold higher than obtained with Bligh and Dyer method (control of the conventional SLE) and similar for lipids. Regarding the impact of different integrative *Scenarios* in the respective amounts of carotenoids and lipids obtained after polishing procedures, both procedures are adequate for the recovery of the three carotenoids (similar recovery yields for β-carotene, torularhodin and torulene), but for the recovery of lipids and removal of proteins, *Scenario 1* (40.70 % > Recovery yields > 48.15%) is more efficient than *Scenario 2* (32.72 % > Recovery yields > 40.29%). Further details about

efficiency and sustainability of both *Scenarios* are discussed below in the section *Environmental assessment of biosolvents-based platform by determination of carbon footprint*.

These results confirm that the reusability of the solvents and polishing of target biomolecules can be achieved by a simple integration of the initial SLE unit with a subsequent LLE process, and further integration with evaporation, precipitation and/or LLE operation units. To facilitate the understanding of the proposed integrative process for the production of carotenoids and lipids using *R. glutinis* biomass, a schematic representation is presented in **Figure 6**, in which the production, SLE, LLE, recycling and polishing units are properly integrated in a processing platform, including the representation of the two different recycling/polishing *Scenarios*. The use of mixed biosolvents are very promising for the extraction of biomolecules, particularly, due to facilitation of the operation units regarding the polishing of target-solutes and recycling of the solvents, which can make these technologies more cost-effective. Anyway, regardless the potential of these integrative approaches using biosolvents for the industrial production of microbial carotenoids and lipids from *R. glutinis* biomass, within a biorefinery concept, the optimization of other operational processing parameters (*e.g.*, residence times, flow rates, temperature) is still required, in particular if a continuous mode of operation is envisaged. Moreover, the implementation of these platforms at the industrial scale will be also dependent of further scale-up studies.

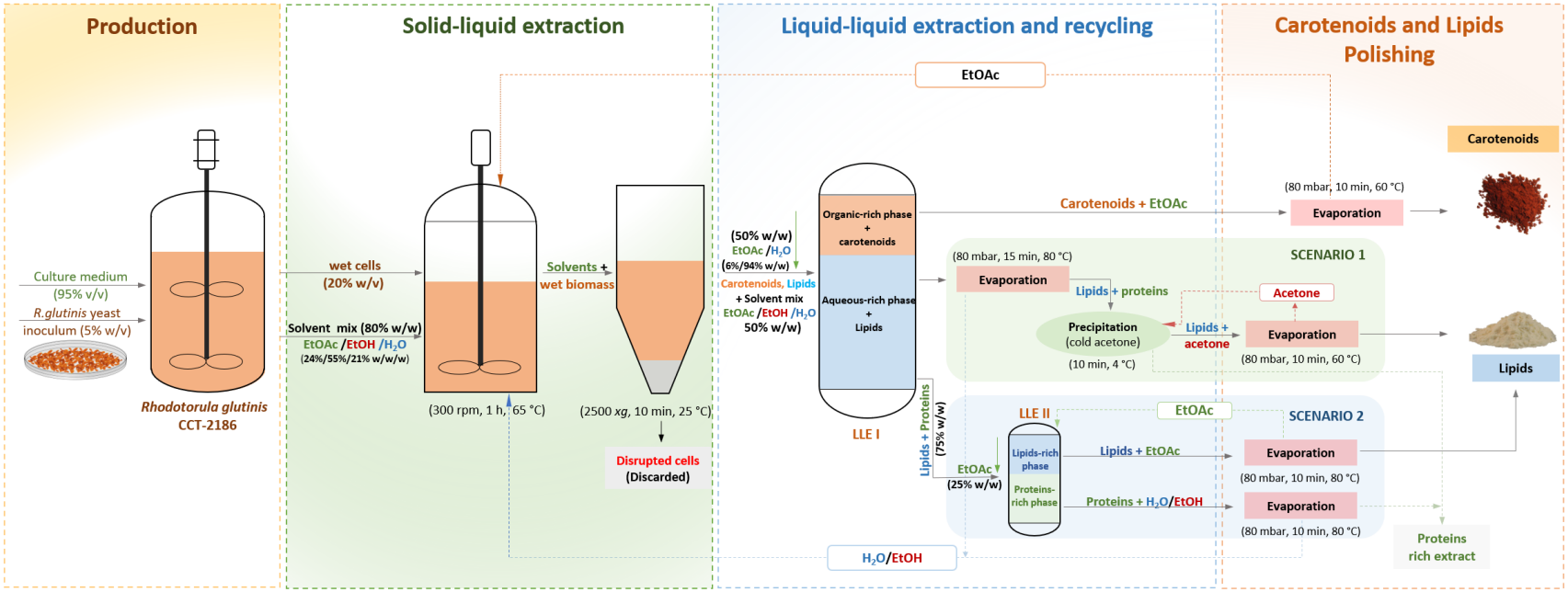

Figure 6.6. Diagram of the integrative process for the production and extraction of intracellular carotenoids and lipids from *R. glutinis* biomass using ethyl EtOAc/EtOH/H_2O mixture, including the recycling of the biosolvents and the polishing of the carotenoids and lipids.

6.3.6 Environmental assessment of biosolvents-based platform by determination of carbon footprint

In the previous section, the potential of two integrative platforms for the extraction of carotenoids and lipids from microbial biomass using mixed biosolvents, namely EtOAc/EtOH/H_2O, was demonstrated. However, considering the current appeal for greener and eco-friendlier processes, the environmental sustainability of the complete biorefinery process was evaluated by a life cycle analysis (LCA). The environmental performance of the integrative platforms applied to obtain the three carotenoids (β-carotene, torularhodin, torulene) and lipids from *R.glutinis* wet biomass was evaluated through the calculation of the carbon footprint of the production, extraction, purification and polishing stages. For that purpose, three different scenarios were investigated, namely: the two *Scenarios* detailed in previous section (*i.e.*, *Scenario 1* – evaporation of EtOAc and EtOH/H_2O-rich phases for polishing the carotenoids and recycling of solvents, and cold acetone precipitation for the separation of proteins from lipids; *Scenario 2* - evaporation of EtOAc-rich phase, and the use of EtOH/H_2O-rich phase in an second LLE procedure for the separation of proteins from lipids), and a *Scenario 3* corresponding to a conventional extraction process using the Bligh and Dyer method (control). Given that the systems studied in each *Scenario* afforded different recovery yields of carotenoids, the results of the carbon footprint for the production, extraction, purification and polishing states are depicted in the **Figure 6.7** (detailed in **Table D.7** from from the **Appendix D**) per µg of carotenoids (β-carotene, torularhodin and torulene) and mg of lipids extracted, allowing a direct comparison between the three *Scenarios*.

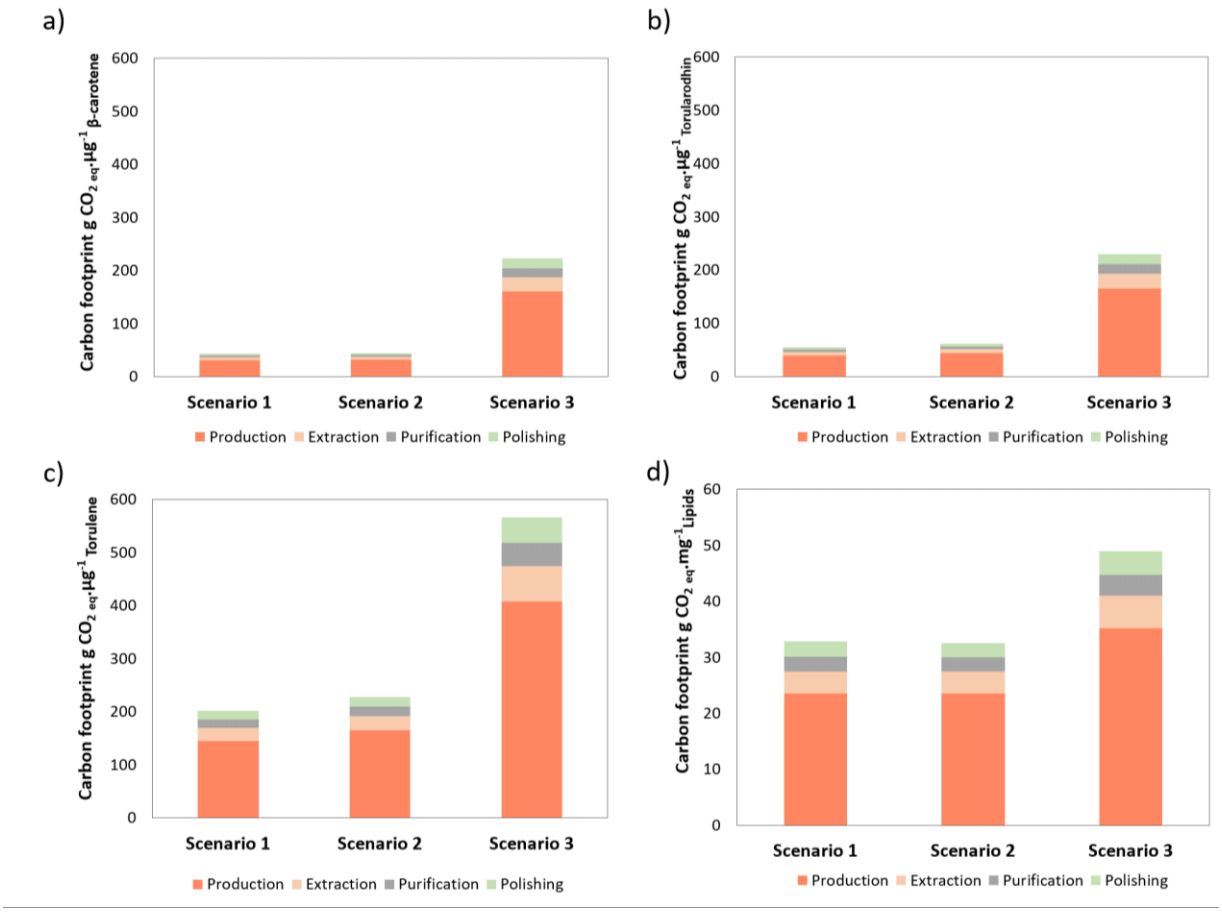

Figure 6.7. The carbon footprint of the integrative platform (production, extraction, purification and polishing stages) for the production of (**a**) β-carotene, (**b**) torularhodin, (**c**) torulene, and (**d**) lipids from *R. glutinis* wet biomass through three different *Scenarios*: *Scenario 1* – evaporation of EtOAc and EtOH/H_2O-rich phases for polishing the carotenoids and recycling of solvents, and cold acetone precipitation for the separation of proteins from lipids; *Scenario 2* - evaporation of EtOAc-rich phase, and the use of EtOH/H_2O-rich phase in an second LLE procedure for the separation of proteins from lipids), and a *Scenario 3* corresponding to a conventional extraction process using the Bligh and Dyer method (control).

Figure 6.7 show that *Scenarios 1* and *2* have significantly lower carbon footprint than the conventional procedure of *Scenario 3*, as a result of the significant improvement in the carotenoids extraction yields of those processes. The best environmental performance for the recovery of carotenoids was achieved with *Scenario 1*, with a carbon

footprint of 43.41, 55.67 and 202.3 g $CO_{2\ eq}.\mu g^{-1}$ of β-carotene, torularhodin and torulene, respectively, with equivalent values for *Scenario 2*. Regarding the recovery of lipids, no significant difference between *Scenarios* 1 and 2 (32.85 and 32.50 g CO_2 eq. mg^{-1} respectively) was found. It is important to note that the conventional Bligh and Dyer method (control, *Scenario 3*) led to the worst environmental performance, with a carbon footprint of 222.90, 230.30 and 565.80 g $CO_{2\ eq}.\mu g^{-1}$ for β-carotene, torularhodin and torulene respectively, and 48.92 g $CO_{2\ eq}.mg^{-1}$ for lipids. These values represent an increase of 80% (β-carotene), 75% (torularhodin), 65% (torulene) and 35% (lipids) in relation to the best environmental process (*Scenario 1*) respectively.

Comparing the environmental impact of the process to obtain each biomolecule, it is found a high carbon footprint for torulene, which is a result of the lower abundance of this pigment in the *R. glutinis* wet biomass. Therefore, it is necessary a higher amount of *inputs* than for the remaining carotenoids to obtain the same amount of carotenoid (1 µg). The major contribution to the carbon footprint, approximately 72%, for all the *Scenarios* is the biomass production stage, mainly due to the high consumption of electricity during the 72-h fermentation in bioreactor, which corresponds to the 96% of the carbon footprint of this stage. It is also possible to observe that in all *Scenarios* about 12% of the carbon footprint is associated with the extraction stage, which is again due to the high electricity consumption of the heating and mixing units used in this stage.

These results suggest that, besides the high recovery yields for β-carotene, torularhodin, torulene, and lipids of the SLE and LLE using EtOAc/EtOH/H_2O mixture, this mixed biosolvent has a much more favorable (compared with the conventional method) environmental impact, further supporting the potential of these biosolvents-based integrative platforms for industrial downstream processing of biomolecules.

6.4 Conclusions

In this work, an integrative and effective process for the recovery of intracellular carotenoids and lipids from *R. glutinis* CCT-2186 biomass using mixed biosolvents was established and optimized. The use of mixtures of polar and non-polar solvents is primordial to enhance the recovery of non-polar carotenoids and lipids from *R. glutinis* wet biomass. The relative hydrophobicity of solvent mixtures allows the dissolution and extraction of carotenoids and lipids. EtOAc/EtOH/H_2O ternary mixtures allowed to obtain recovery yields (carotenoids and lipids) higher than the pure solvents and even than the traditional, widely used, Bligh and Dyer method (solvent mixture of chloroform/MeOH/H_2O), as well as the efficient and selective separation of carotenoids from lipids by further applying LLE (EtOAc/EtOH/H_2O mixtures at the biphasic region). Additionally, the economic and environmental sustainability of the process was achieved by integrating the cell disruption/extraction (the SLE) and separation/purification (LLE) stages with subsequent polishing/recycling process, where the recovery yields were studied and demonstrated up to three consecutive extractions reusing EtOAc/EtOH/H_2O mixtures. The biosolvent-based integrative process allowed a decrease of the carbon footprint by ≈75% for carotenoids and ≈35% for lipids, in comparison with the conventional method, which is further reinforced by the fact that these biosolvents can be obtained from renewable sources. This works demonstrates that biosolvents can be mixed to produce characteristics of the extractant solution, which cannot be obtained when using pure solvents. It is shown that mixed biosolvents can be feasible and environmentally friendly solutions for the development of milder, cost-effective and highly efficient downstream technologies for the recovery of biologically active molecules from biomass sources.

6.5 References

Abdel-Aziz SM, Prasad R, Hamed AA, Abdelraof M (2018) Fungal nanoparticles: A novel tool for a green biotechnology? In: Fungal Nanobionics: Principles and Applications.

Aksu Z, Eren AT (2007) Production of carotenoids by the isolated yeast of *Rhodotorula glutinis*. Biochem Eng J. 107-113.

Altshuller AP, Everson HE (1953) The Solubility of Ethyl Acetate in Water. J. Am. Chem. Soc. 75 (19), 4823-4827.

Balasundaram B, Harrison S, Bracewell DG (2009) Advances in product release strategies and impact on bioprocess design. Trends Biotechnol. 27 (8), 477-85.

Bassetti L, Tramper J (1994) Organic solvent toxicity in *Morinda citrifolia* cell suspensions. Enzyme Microb Technol. 16, 642-648.

Beard JM (2011) Environmental chemistry in society.

Braunwald T, Schwemmlein L, Graeff-Hönninger S, French WT, Hernandez R, Holmes WE, Claupein W (2013) Effect of different C/N ratios on carotenoid and lipid production by *Rhodotorula glutinis*. Appl Microbiol Biotechnol. 97b (14), 6581-8.

Breil C, Abert Vian M, Zemb T, Kunz W, Chemat F (2017) “Bligh and Dyer” and Folch methods for solid–liquid–liquid extraction of lipids from microorganisms. Comprehension of solvatation mechanisms and towards substitution with alternative solvents. Int J Mol Sci. 18 (4), 708.

Britton G (1985) General carotenoid methods. Methods Enzymol. 111, 113-149.

Cerón-García MC, González-López C V., Camacho-Rodríguez J, López-Rosales L, García-Camacho F, Molina-Grima E (2018) Maximizing carotenoid extraction from microalgae used as food additives and determined by liquid chromatography (HPLC). Food Chem. 257, 316-324.

Cheirsilp B, Kitcha S, Torpee S (2012) Co-culture of an oleaginous yeast *Rhodotorula glutinis* and a microalga *Chlorella vulgaris* for biomass and lipid production using pure and crude glycerol as a sole carbon source. Ann Microbiol. 62 (3), 987-993.

Chemspider (2020) The free chemical database, http://www.chemspider.com/. Accessed at 01-04-2020.

Cheng CH, Du TB, Pi HC, Jang SM, Lin YH, Lee HT (2011) Comparative study of lipid extraction from microalgae by organic solvent and supercritical CO_2. Bioresour Technol. 102 (21), 10151-3.

Chisti Y (2007) Biodiesel from microalgae. Biotechnol. Adv. 25 (3), 294-306.

Choi SA, Oh YK, Lee J, Sim SJ, Hong ME, Park JY, Kim MS, Kim SW, Lee JS (2019) High-efficiency cell disruption and astaxanthin recovery from *Haematococcus pluvialis* cyst cells using room-temperature imidazolium-based ionic liquid/water mixtures. Bioresour Technol. 274, 120–126.

Chuck CJ, Lou-Hing D, Dean R, Sargeant LA, Scott RJ, Jenkins RW (2014) Simultaneous microwave extraction and synthesis of fatty acid methyl ester from the oleaginous yeast *Rhodotorula glutinis*. Energy. 69, 446-454.

Cooney M, Young G, Nagle N (2009) Extraction of bio-oils from microalgae. Sep Purif Rev. 38, 291–325.

Dai CC, Tao J, Xie F, Dai YJ, Zhao M (2007) Biodiesel generation from oleaginous yeast *Rhodotorula glutinis* with xylose assimilating capacity. African J Biotechnol. 6 (18), 2130-2134.

de Jesus SS, Ferreira GF, Moreira LS, Wolf Maciel MR, Maciel Filho R (2019) Comparison of several methods for effective lipid extraction from wet microalgae using green solvents. Renew Energy. 143, 130-141.

Delgado-Vargas F, Jiménez AR, Paredes-López O, Francis FJ (2000) Natural pigments: Carotenoids, anthocyanins, and betalains - Characteristics, biosynthesis, processing, and stability. Crit Rev Food Sci Nutr. 173-289.

Delrue F, Setier PA, Sahut C, Cournac L, Roubaud A, Peltier G, Froment AK (2012) An economic, sustainability, and energetic model of biodiesel production from microalgae. Bioresour Technol. 111, 191-200.

Dufossé L, Galaup P, Yaron A, Arad SM, Blanc P, Murthy KNC, Ravishankar GA (2005) Microorganisms and microalgae as sources of pigments for food use: A scientific oddity or an industrial reality? In: Trends in Food Science and Technology. 9, 389-406.

Gallego R, Tardif C, Parreira C, Guerra T, Alves MJ, Ibáñez E, Herrero M (2020) Simultaneous extraction and purification of fucoxanthin from *Tisochrysis lutea* microalgae using compressed fluids. J Sep Sci. 1-11.

Ghasemi Naghdi F, González González LM, Chan W, Schenk PM (2016) Progress on lipid extraction from wet algal biomass for biodiesel production. Microb. Biotechnol. 9 (6), 718-726.

Glasstone S, Pound A (1925) CCCLXIII. - Solubility influences. Part I. the effect of some salts, sugars, and temperature on the solubility of ethyl acetate in water. J Chem Soc Trans. 127, 2660-2667.

Gong M, Bassi A (2016) Carotenoids from microalgae: A review of recent developments. Biotechnol. Adv. 34 (8), 1396-1412.

Halim R, Danquah MK, Webley PA (2012) Extraction of oil from microalgae for biodiesel production: A review. Biotechnol. Adv. 30 (3), 709-732.

Hargreaves CR (2008) Collaboration to deliver a solvent selection guide for the pharmaceutical industry. In: AIChE Annual Meeting, Conference Proceedings.

Hernández-Almanza A, Navarro-Macías V, Aguilar O, Aguilar-González MA, Aguilar CN (2017) Carotenoids extraction from *Rhodotorula glutinis* cells using various techniques: A comparative study. Indian J Exp Biol. 55, 479-484.

Jeevaratnam K, Latha B V (2010) Purification and Characterization of the Pigments from *Rhodotorula glutinis* DFR-PDY Isolated from Natural Source. Glob J Biotechnol Biochem. 5 (3), 166-174.

Karamerou EE, Theodoropoulos C, Webb C (2016) A biorefinery approach to microbial oil production from glycerol by *Rhodotorula glutinis*. Biomass and Bioenergy. 89, 113-122.

Khaw KY, Parat MO, Shaw PN, Falconer JR (2017) Solvent supercritical fluid technologies to extract bioactive compounds from natural sources: A review. Molecules. 22 (7), 1186.

Kirti K, Amita S, Priti S, Mukesh Kumar A, Jyoti S (2014) Colorful World of Microbes: Carotenoids and Their Applications. Adv Biol. 837891.

Kot AM, Błażejak S, Kieliszek M, Gientka I, Bryś J (2019) Simultaneous Production of Lipids and Carotenoids by the Red Yeast *Rhodotorula* from Waste Glycerol Fraction and Potato Wastewater. Appl Biochem Biotechnol. 89, 589–607.

Kot AM, Błażejak S, Kurcz A, Bryś J, Gientka I, Bzducha-Wróbel A, Maliszewska M, Reczek L (2017) Effect of initial pH of medium with potato wastewater and glycerol on protein, lipid and carotenoid biosynthesis by *Rhodotorula glutinis*. Electron J Biotechnol. 27 (2017), 25-31.

Kot AM, Błażejak S, Kurcz A, Gientka I, Kieliszek M (2016) *Rhodotorula glutinis*—potential source of lipids, carotenoids, and enzymes for use in industries. Appl. Microbiol. Biotechnol. 100 (2016) 6103-6117.

Kuan IC, Kao WC, Chen CL, Yu CY (2018) Microbial biodiesel production by direct transesterification of *Rhodotorula glutinis* biomass. Energies. 11 (5) (2018), 1036.

Liau BC, Shen CT, Liang FP, Hong SE, Hsu SL, Jong TT, Chang CMJ (2010) Supercritical fluids extraction and anti-solvent purification of carotenoids from microalgae and associated bioactivity. J Supercrit Fluids. 55, 169-175.

Liu XJ, Wu YH, Zhao LC, Xiao SY, Zhou AM, Liu X (2011) Determination of astaxanthin in *Haematococcus pluvialis* by first-order derivative spectrophotometry. J AOAC Int. 94 (2011), 1752-17577.

Lodish H, Berk A, Zipursky S (2000) Osmosis, Water Channels, and the Regulation of Cell Volume. In: Molecular Cell Biology.

Lopes M, Gomes AS, Silva CM, Belo I (2018) Microbial lipids and added value metabolites production by *Yarrowia lipolytica* from pork lard. J Biotechnol. 265, 76-85.

Macías-Sánchez MD, Fernandez-Sevilla JM, Fernández FGA, García MCC, Grima EM (2010) Supercritical fluid extraction of carotenoids from *Scenedesmus almeriensis*. Food Chem. 123 (3) (2010), 928-935.

Mata-Gómez LC, Montañez JC, Méndez-Zavala A, Aguilar CN (2014) Biotechnological production of carotenoids by yeasts: An overview. Microb. Cell Fact. 13 (2014), 12.

Mendes RL, Nobre BP, Cardoso MT, Pereira AP, Palavra AF (2003) Supercritical carbon dioxide extraction of compounds with pharmaceutical importance from microalgae. Inorganica Chim Acta. 356, 328-334.

Mezzomo N, Ferreira SRS (2016) Carotenoids functionality, sources, and processing by supercritical technology: A review. J. Chem. 3164312.

Miękus N, Iqbal A, Marszałek K, Puchalski C, Świergiel A (2019) Green chemistry extractions of carotenoids from *Daucus carota* L.-Supercritical carbon dioxide and enzyme-assisted methods. Molecules. 24 (23), 4339.

Mussagy CU, Santos Ebinuma V de C, Gonzalez-Miquel M, Coutinho JAP, Pereira JFB (2019a) Protic ionic liquids as cell disrupting agents for the recovery of intracellular carotenoids from yeast *Rhodotorula glutinis* CCT-2186. ACS Sustain Chem Eng. 7 (19), 16765-16776.

Mussagy CU, Winterburn J, Santos-Ebinuma VC, Pereira JFB (2019b) Production and extraction of carotenoids produced by microorganisms. Appl. Microbiol. Biotechnol. 103, 1095-1114.

O'Neil MJ (2001) An Encyclopedia of Chemicals, Drugs, and Biologicals. 13th Edition. Publ 2001 Whitehouse Stn NJ by Merck.

Pan JG, Kwak MY, Rhee JS (1986) High density cell culture of *Rhodotorula glutinis* using oxygen-enriched air. Biotechnol Lett. 8, 715-718.

Papanikolaou S, Aggelis G (2011) Lipids of oleaginous yeasts. Part I: Biochemistry of single cell oil production. Eur. J. Lipid Sci. Technol. 113, 1052-1073.

Pinheiro Sant'Ana HM, Stringheta PC, Cardoso Brandão SC, Cordeiro De Azeredo RM (1998) Carotenoid retention and vitamin A value in carrot (*Daucus carota* L.) prepared by food service. Food Chem. 61, 145-151.

Ruen-ngam D, Shotipruk A, Pavasant P (2011) Comparison of extraction methods for recovery of astaxanthin from *Haematococcus pluvialis*. Sep Sci Technol. 46 , 64-70.

Sachindra NM, Bhaskar N, Mahendrakar NS (2006) Recovery of carotenoids from shrimp waste in organic solvents. Waste Manag. 26 (10), 1092-1098.

Saenge C, Cheirsilp B, Suksaroge TT, Bourtoom T (2011) Potential use of oleaginous red yeast *Rhodotorula glutinis* for the bioconversion of crude glycerol from biodiesel plant to lipids and carotenoids. Process Biochem. 16, 23-33.

Saini RK, Keum YS (2017) Progress in Microbial Carotenoids Production. Indian J Microbiol. 57, 129-130.

Saini RK, Keum YS (2018) Carotenoid extraction methods: A review of recent developments. Food Chem. 240, 90-103.

Santos Ribeiro JE, da Silva Sant'Ana AM, Martini M, Sorce C, Andreucci A, Nóbrega de Melo DJ, Honorato da Silva FL (2019) *Rhodotorula glutinis* cultivation on cassava wastewater for carotenoids and fatty acids generation. Biocatal Agric Biotechnol. 22, 101419.

Sathasivam R, Ki JS (2018) A review of the biological activities of microalgal carotenoids and their potential use in healthcare and cosmetic industries. Mar. Drugs. 16 (1), 26.

Saxena V, Sharma CD, Bhagat SD, Saini VS, Adhikari DK (1998) Lipid and fatty acid biosynthesis by *Rhodotorula minuta*. JAOCS, J Am Oil Chem Soc. 75, 501-505.

Sikkema J, De Bont JAM, Poolman B (1995) Mechanisms of membrane toxicity of hydrocarbons. Microbiol. Rev. 42, 499-507.

Tkáčová J, Čaplová J, Klempová T, Čertík M (2017) Correlation between lipid and carotenoid synthesis in torularhodin-producing *Rhodotorula glutinis*. Ann Microbiol. 67, 541-551.

Toti E, Chen C-YO, Palmery M, Villaño Valencia D, Peluso I (2018) Non-Provitamin A and Provitamin A Carotenoids as Immunomodulators: Recommended Dietary Allowance, Therapeutic Index, or Personalized Nutrition? Oxid Med Cell Longev. 1-20.

Valduga E, Valério A, Tatsch PO, Treichel H, Furigo A, Di Luccio M (2009) Assessment of Cell Disruption and Carotenoids Extraction from *Sporidiobolus salmonicolor* (CBS 2636). Food Bioprocess Technol. 2, 234-238.

Vasconcelos B, Teixeira JC, Dragone G, Teixeira JA (2018) Optimization of lipid extraction from the oleaginous yeasts *Rhodotorula glutinis* and *Lipomyces kononenkoae*. AMB Express. 8, 126.

Wan Mahmood WMA, Theodoropoulos C, Gonzalez-Miquel M (2017) Enhanced microalgal lipid extraction using bio-based solvents for sustainable biofuel production. Green Chem. 19, 5723-5733.

Yara-Varón E, Fabiano-Tixier AS, Balcells M, Canela-Garayoa R, Bily A, Chemat F (2016) Is it possible to substitute hexane with green solvents for extraction of carotenoids? A theoretical versus experimental solubility study. RSC Adv. 6, 27750-27759.

Yoon SH, Rhee JS (1983) Lipid from yeast fermentation: Effects of cultural conditions on lipid production and its characteristics of *Rhodotorula glutinis*. J Am Oil Chem Soc. 60, 1281-1286.

7. FINAL REMARKS AND FUTURE WORK

7.1 Final Remarks

This thesis focused on the development of new strategies to improve the production of carotenoids from *R. glutinis* yeast, in a first stage, by optimizing the nutritional source for microbial growing and production of carotenoids, and second, by enhancing the recovery yields of intracellular carotenoids using aqueous solutions of ionic liquids and bio-based solvents. In fact, all the experimental research developed during my doctorate aimed at designing more sustainable, biocompatible, cost-effective and integrated platforms for the recovery of these added-value compounds from yeast biomass, which I believe was fully achieved.

As presented in Chapter 3, statistical optimization designs were successfully applied to improve the production of carotenoids using *R. glutinis* yeast, from which was confirmed that culture media containing organic and inorganic nitrogen sources represent an attractive alternative to improve the production of microbial pigments instead of lipids (which are also produced by *R. glutinis*). The future industrial use of *R. glutinis* to produce carotenoids was also validated, by implementing the optimized condition in a 5 L stirred-tank bioreactor, with higher carotenoids production yields.

After the optimization of carotenoids production, as detailed in Chapter 4, an integrative and effective process for the recovery of intracellular carotenoids from *R. glutinis* cells using aqueous solutions of ILs was established. The extensive experimental research using 12 highly concentrated aqueous solutions of ammonium-based PILs allowed to conclude that the increase of the temperature and the hydrophobicity (either by increasing the anionic or cationic alkyl chain length) and concentration of the PILs increased the recovery of carotenoids from the intracellular environment of the cells, particularly [DEAPA][Hex] can be recycled up to three times without any treatment, guaranteeing the maintenance of good extraction efficiencies (> 58.8%).

The results presented in Chapter 5 demonstrated that PILs are suitable options to form ABS in the presence of tripotassium phosphate or dipotassium hydrogen phosphate and water. This research confirmed that the PILs aptitude to undergo liquid-liquid demixing is mainly controlled by their relative hydrophobicity, namely, an increase of

biphasic region with the increase of anionic/cationic chain of the IL, as well as by the temperature (a decrease of the demixing region with the increase of temperature).

In Chapter 6, having in mind the increased extraction of carotenoids using simple, and industrial attractive solutions, mixtures of traditional solvents that can be partially or fully derived from renewable sources, *i.e.,* bio-based solvents or biosolvents, were evaluated. In fact, despite being a simple and economic solution, the use of mixed biosolvents is yet underexplored. An integrative and efficient process for the recovery and purification of intracellular carotenoids using biosolvents mixtures was found, particularly, EtOAc/EtOH/H_2O ternary mixtures allowed to obtain recovery yields higher than the pure solvents and even than the conventional method, allowing an efficient and selective separation of carotenoids from the lipids. Interestingly, the results revealed that the use of mixtures of polar and non-polar biosolvents is primordial to enhance the recovery of non-polar carotenoids from *R. glutinis* wet biomass. The bio-based solvent integrated process allowed a decrease of the carbon footprint by ≈75% for carotenoids and ≈35% for lipids, in comparison with the conventional method.

As main conclusion, with this thesis, I believe I have provided significant insights and foundations that support a movement towards the use of eco-friendlier aqueous solutions of ILs and bio-based solvent mixtures for the recovery of intracellular carotenoids from the *R. glutinis* wet biomass, which I hope that will be as a basis to apply these novel approaches as sustainable and biocompatible alternative processes to obtain a plethora of cosmetic, food and pharmaceuticals added-value products.

7.2 Future Work

Despite the significant scientific advances obtained with the research conducted in these last four years, further developments are still required on this field. Considering the promising results detailed in Chapter 3, as future work, it would be interesting to evaluate the C/N balance in culture growing media using combined organic nitrogen sources to improve the simultaneous production of carotenoids and lipids using *R. glutinis* yeast. For

that purpose, further studies regarding the understanding of metabolic pathways are primordial.

Furthermore, concerning the use of ammonium-based PILs as alternative solvents for the recovery of the carotenoids biocompatibility and cytotoxicity/ecotoxicity studies of these compounds are still needed. Likewise, bioactivity assays to evaluate the final application of the carotenoids extracted from *R. glutinis* yeast with ILs and biosolvents are required, in which each bioactivity study should be designed according the carotenoid-target application, namely, food, feed, cosmetics and pharmaceuticals.

Improvement of the solvent recycling steps, scale-up processes and evaluation of techno-economic potential of these technologies should be also investigated.

The experimental results obtained in this work are the first steps towards the development of a circular and integrated process in the biorefinery precepts, which could be extended to a wide variety of microorganisms with potential to biosynthesize carotenoids.

LIST OF PUBLICATIONS AND AWARDS

List of publications in the current thesis

Papers in international scientific periodicals with referees

Mussagy CU, Winterburn J, Santos-Ebinuma VC, Pereira JFB (2019) Production and extraction of carotenoids produced by microorganisms, *Appl. Microbiol. Biotechnol.* 103 (3): 1095-1114. doi: 10.1007/s00253-018-9557-5.

Mussagy CU, Santos-Ebinuma VC, Gonzalez-Miquel M, Coutinho JAP, Pereira JFB (2019) Protic ionic liquids as cell-disrupting agents for the recovery of intracellular carotenoids from yeast *Rhodotorula glutinis* CCT-2186, *ACS Sustainable Chem. Eng* 7 (19): 16765-16776. doi: 10.1021/acssuschemeng.9b04247.

Mussagy CU, Tabanez NL, Farias FO, Kurnia KA, Mafra MR, Pereira JFB (2020) Determination, characterization and modeling of aqueous biphasic systems composed of propylammonium-based ionic liquids and phosphate salts, *Chem. Phys. Lett.* 754: 137623. doi: 10.1016/j.cplett.2020.137623.

Mussagy CU, Guimarães AA, Rocha LV, Winterburn J, Santos-Ebinuma VC, Pereira JFB (2021), Improvement of carotenoid production from *Rhodotorula glutinis* CCT-2186, *Biochem. Eng. J.* 165:107827. doi: 10.1016/j.bej.2020.107827.

Mussagy CU, Santos-Ebinuma VC, Kurnia KA, Carvalho P, Dias ACR, Coutinho JAP, Pereira JFB (2020) Integrative platform for the selective recovery of intracellular carotenoids and lipids from *Rhodotorula glutinis* CCT-2186 yeast using mixtures of bio-based solvents. *Green Chem.* 22: 8478-8494. doi: 10.1039/D0GC02992K.

Kurnik I, **Mussagy CU**, Pereira JFB, Lopes A (2020) Amphiphilic copolymer aqueous solutions with cholinium ionic liquids as adjuvants: new insights into determination of binodal curves and phase separation mechanisms. *J. Mol. Liq.* 318: 114245. doi: 10.1016/j.molliq.2020.114245.

Manuscripts under preparation

Mussagy CU, Remonatto D, Paula AV, Herculano RD, Santos-Ebinuma VC, Coutinho JAP and Pereira JFB, Selective recovery and purification of carotenoids and fatty acids from *Rhodotorula glutinis* using mixtures of biosolvents. Submitted to *Separation and Purification Technology.*

Mussagy CU and Pereira JFB, *Rhodotorula* sp.–based biorefinery: State of the art and challenges to improve sustainability.

Conference papers

Mussagy CU, Santos-Ebinuma VC, Pereira JFB (2019), Microbial carotenoids extraction using aqueous solutions of cholinium-based ionic liquids. Paper presented at the XXII National Bioprocesses Symposium (SINAFERM) XIII Enzymatic Hydrolysis of Biomass Symposium (SHEB).

Vieira SR, Silva JBA, **Mussagy CU**, Santos-Ebinuma VC, Pereira JFB, Druzian JI, Souza CO (2019), Preparation of nanoparticules from cellulose pulp and micro crystalline cellulose using ionic liquid. In: Anais do V Simpósio Internacional de Inovação e Tecnologia. São Paulo: Blucher, 949-955. ISSN 2357-7592. doi: 10.5151/siintec2019-119

Awards

Best work presented as Oral Presentation in the Session Bioproducts Recovery and Purification in XXII National Bioprocesses Symposium (SINAFERM) and XIII Enzymatic Hydrolysis of Biomass Symposium (SHEB) in Uberlandia, Minas Gerais, Brazil (2019).

APPENDIX

Appendix A: *Supporting Information of Chapter 3*

Table A.1. The significance of each response variable effect showed by using F-ratio and p-value tested in the 2^2 central factorial design

Factors	β- carotene			Torularhodin			Torulene		
	SS	*F*-ratio	*p*-value	SS	*F*-ratio	*p*-value	SS	*F*-ratio	*p*-value
(1) pH (L)	1434.07	251.53	0.000*	87.89	18.32	0.02*	34.60	2926.31	0.000*
pH (Q)	9991.89	1749.90	0.000*	9060.16	1888.52	0.000*	134.52	11376.61	0.000*
(2) Nitrogen Source (L)	744.11	130.318	0.001*	3.02	0.62	0.48	31.05	2625.94	0.000*
Nitrogen Source (Q)	9474.99	1659.38	0.000*	4719.67	983.78	0.000*	138.15	11683.50	0.000*
1L by 2L	8.23	1.44	0.316	502.54	104.75	0.001*	7.60	643.11	0.000*
Pure Error	17.13			14.39			0.03		

*Significant at p< 0.05

Table A.2. Kinetics of biomass production, glucose consumption, lipids and production of β-carotene, torularhodin and torulene during fermentation of yeast *R. glutinis* CCT-2186 with optimized medium in 5L Bioreactor at 30 ºC, aeration (1 vvm), 300 rpm for 72 h. The results represent the mean of two independent assays with respective standard deviations.

Time (h)	Biomass (g/L)	Glucose consumption (g/L)	β-carotene (mg/L)	Torularhodin (mg/L)	Torulene (mg/L)	Lipids (g/L)	Lipids content (% CDW)	Lipid productivity (g/L.h)
0	0.10 ± 0.01	9.25 ± 0.00	0.00 ± 0.00	0.00 ± 0.00	0.00 ± 0.00	0.00 ± 0.00	0.00 ± 0.00	0 ± 0.00
6	0.42 ± 0.02	6.49 ± 0.44	0.00 ± 0.00	0.00 ± 0.00	0.00 ± 0.00	0.00 ± 0.00	0.00 ± 0.00	0 ± 0.00
12	2.29 ± 0.01	5.97 ± 0.30	0.00 ± 0.00	0.00 ± 0.00	0.00 ± 0.00	0.00 ± 0.00	0.00 ± 0.00	0 ± 0.00
18	4.67 ± 0.10	2.86 ± 0.84	49.27 ± 2.31	53.75 ± 2.82	4.21 ±0.84	0.37 ± 0.00	7.83 ± 0.98	0.020 ± 0.00
24	5.52 ± 0.00	0.45 ± 0.66	96.40 ± 2.34	81.65 ± 1.02	10.99 ± 0.62	0.50 ± 0.02	9.09 ± 0.37	0.021 ± 0.00
30	6.88 ± 0.00	0.05 ± 0.00	167.69 ± 1.12	167.70 ± 1.15	16.02 ± 2.05	0.78 ± 0.01	11.33 ± 2.11	0.026 ± 0.00
36	7.05 ± 0.10	0.04 ± 0.06	222.05 ± 5.31	209.32 ± 2.78	24.56 ± 2.06	1.13 ± 0.01	16.07 ± 5.23	0.031 ± 0.01
42	6.96 ± 0.10	0.03 ± 0.01	262.75 ± 0.96	255.86 ± 6.05	29.59 ± 1.00	1.48 ± 0.02	21.33 ± 2.86	0.035 ± 0.00
48	6.13 ± 0.14	0.03 ± 0.01	278.64 ± 18.39	248.70 ± 0.94	26.60 ± 7.24	2.04 ± 0.05	33.21 ± 2.48	0.042 ± 0.02
54	6.04 ± 0.03	0.00 ± 0.00	277.44 ± 4.37	249.25 ± 1.77	30.95 ± 0.72	3.04 ± 0.03	50.32 ± 4.60	0.056 ± 0.00
60	4.89 ± 0.17	0.00 ±0.00	288.19 ± 7.49	267.20 ± 5.02	32.82 ± 1.03	2.31 ± 0.01	47.22 ± 2.50	0.038 ± 0.00
66	4.62 ± 0.03	0.00 ± 0.00	292.75 ± 1.53	277.26 ± 14.92	34.64 ± 1.47	2.09 ± 0.02	45.20 ± 2.53	0.032 ± 0.00
72	4.42 ± 0.10	0.00 ± 0.00	297.84 ± 3.66	286.06 ± 32.10	37.35 ± 4.48	1.80 ± 0.01	40.73 ± 1.23	0.025 ± 0.00

Appendix B: *Supporting Information of Chapter 4*

Table B.1. Chemical structure, pH and purity of the studied PILs.

Name	Acronym	Cation	Anion	Residual H_2O (%)	Purity (%)	pH
Propylammonium acetate	[PA][Ac]			3.68	97	6.88
Propylammonium propanoate	[PA][Pro]		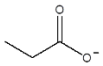	4.27	97.12	6.69
Propylammonium butanoate	[PA][But]		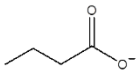	5.10	98.5	6.83
Propylammonium hexanoate	[PA][Hex]		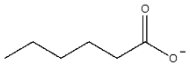	2.54	99.06	7.83
3-Dimethylamino-1- propylammonium acetate	[DMAPA][Ac]			4.21	97.20	10.70
3-Dimethylamino-1- propylammonium propanoate	[DMAPA][Pro]		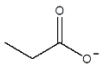	3.95	96.90	10.20
3-Dimethylamino-1- propylammonium butanoate	[DMAPA][But]	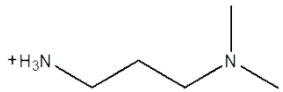	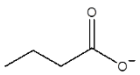	4.21	95.70	10.60
3-Dimethylamino-1- propylammonium hexanoate	[DMAPA][Hex]		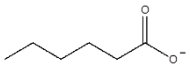	1.52	99.31	11.11
3-Diethylamino-propylammonium acetate	[DEAPA][Ac]			5.23	98.38	9.05
3-Diethylamino-propylammonium propanoate	[DEAPA][Pro]		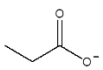	4.65	97.02	8.33
3-Diethylamino-propylammonium butanoate	[DEAPA][But]	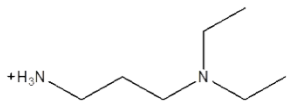	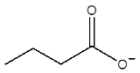	2.15	96.87	8.76
3-Diethylamino-propylammonium hexanoate	[DEAPA][Hex]		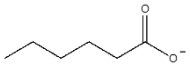	1.24	98.84	9.28

Table B.2. Nuclear Magnetic Resonance (^{1}H NMR) of the studied PILs.

Name		
Propylammonium acetate	[PA][Ac]	^{1}H NMR (600 MHz, D_2O) δ ppm: 0.78 (t, 3H, **C**H_3- COO^-), 1.49 (m, 2H, -**C**H_2-NH_2), 2.77 (t, 2H, -**C**H_2-), 1.79 (s, 3H, **C**H_3-)
Propylammonium propanoate	[PA][Pro]	^{1}H NMR (600 MHz, D_2O) δ ppm: 0.72 (t, 3H, **C**H_3-), 1.42 (m, 2H, -**C**H_2- COO^-), 2.70 (t, 2H, -**C**H_2- NH_2), 0.82 (t, 3H, **C**H_3-), 2.02 (q, 2H, -**C**H_2-)
Propylammonium butanoate	[PA][But]	^{1}H NMR (600 MHz, D_2O) δ ppm: 0.56 (t, 3H, **C**H_3-), 1. 24 (m, 2H, -**C**H_2-), 1.87 (t, 2H, -**C**H_2- NH_2), 0.63 (t, 3H, **C**H_3-), 1.34 (m, 2H, -**C**H_2-), 1.16 (t, 2H, - **C**H_2- COO^-)
Propylammonium hexanoate	[PA][Hex]	^{1}H NMR (600 MHz, DMSO-d6) δ ppm: 0.835 (t, 3H, **C**H_3-), 1.99 (t, 2H, -**C**H_2-),1.45 (m, 2H, -**C**H_2- COO^-), 1.23 (m, 4H, -**C**H_2-), 0.87 (t, 3H, **C**H_3-), 1.57(m, 2H, -**C**H_2-), 2.67(t, 2H, -**C**H_2- NH_2)
3-Dimethylamino-1- propylammonium acetate	[DMAPA][Ac]	^{1}H NMR (600 MHz, D_2O) δ ppm: 2.64 (t, 2H, NH_2-**C**H_2-), 1.58 (m, 2H, -**C**H_2-), 2.34 (m, 2H, -**C**H_2-), 1.73 (s, **C**H_3-COO^-)
3-Dimethylamino-1- propylammonium propanoate	[DMAPA][Pro]	^{1}H NMR (600 MHz, D_2O) δ ppm: 2.56 (t, 2H, NH_2-**C**H_2-), 1.53 (m, 2H, -**C**H_2-), 2.27 (m, 2H, -**C**H_2-), 0.90 (t, 3H **C**H_3-, 7.28 Hz), 2.02 (q, 2H, -**C**H_2- COO^-)
3-Dimethylamino-1- propylammonium butanoate	[DMAPA][But]	^{1}H NMR (600 MHz, D_2O) δ ppm: 2.69 (t, 2H, NH_2-**C**H_2-), 1.63 (m, 2H, -**C**H_2-), 2.39 (m, 2H, -**C**H_2-), 0.75 (t, 3H, **C**H_3-), 1.42 (m, 2H, -**C**H_2-), 2.01 (t, 2H -**C**H_2- COO^-)
3-Dimethylamino-1- propylammonium hexanoate	[DMAPA][Hex]	^{1}H NMR (600 MHz, D_2O) δ ppm: 2.54 (t, 2H, NH_2-**C**H_2-), 1.51 (m, 2H, -**C**H_2-, 2.26 (m, 2H, -**C**H_2-), 0.71 (t, 3H, **C**H_3-), 1.38 (m, 2H, -**C**H_2-), 1.13 (m, 4H -**C**H_2-), 2.01 (t, 2H, -**C**H_2-COO^-)
3-Diethylamino-propylammonium acetate	[DEAPA][Ac]	^{1}H NMR (600 MHz, D_2O) δ ppm: 0.96 (t, 6H, **C**H_3-), 2.72 (m, 6H, NH_2-**C**H_2-), 2.63 (t, 2H, -**C**H_2-), 1.63 (m, 2H, -**C**H_2-), 1.69 (s, 3H, **C**H_3- COO^-)
3-Diethylamino-propylammonium propanoate	[DEAPA][Pro]	^{1}H NMR (600 MHz, DMSO-d6) δ ppm: 0.96 (t, 3H, **C**H_3-), 2.17(q, 2H, -**C**H_2-), 3.43 (q, 2H, -**C**H_2-), 1.03 (m, 2H, -**C**H_2- NH_2), 1.90 (m, 2H, -**C**H_2-COO^-), 0.96 (t,6H, **C**H_3-), 2.17 (q, 4H, **C**H_3-)
3-Diethylamino-propylammonium butanoate	[DEAPA][But]	^{1}H NMR (600 MHz, D_2O) δ ppm: 1.03 (t, 6H, **C**H_3-), 2.88 (m, 6H, NH_2-**C**H_2-), 2.75 (t, 2H, -**C**H_2-), 1.76 (m, 2H, -**C**H_2-), 1.03 (t, 3H, **C**H_3-), 1.55 (m, 3H, -**C**H_2-), 0.69 (t, 3H, **C**H_3-), 1.95 (t, 2H, -**C**H_2- COO^-)
3-Diethylamino-propylammonium hexanoate	[DEAPA][Hex]	^{1}H NMR (600 MHz, D_2O) δ ppm: 1.13 (t, 6H, **C**H_3-), 2.98 (m, 6H, NH_2-**C**H_2-), 2.55 (t, 2H, -**C**H_2-), 1.86 (m, 2H, -**C**H_2-), 1.05 (t, 3H, **C**H_3-), 1.65 (m, 3H, -**C**H_2-), 0.65 (t, 3H, **C**H_3-), 1.75 (t, 2H, -**C**H_2- COO^-), 2.21 (t, 2H, -**C**H_2-)

Table B.3. Nuclear Magnetic Resonance (^{1}H NMR) of the carotenoids from *R.glutinis* CCT-2186.

Carotenoids	^{1}H NMR (600 MHz, DMSO-d6)
β-carotene	δ ppm: 1.23 (s, 6H, CH_3-),1.81 (s, 15H, CH_3-),1.57-2.53 (m, 14H, -CH_2-), 5.61 (t, 1H), 6.51 (s, 14H).
Torulene	δ ppm: 0.90 (s, 6H, CH_3-), 1.79 (s, 15H, CH_3-), 1.50-1.98 (m, 14H, -CH_2-), 5.41 (t, 1H), 6.27 (s, 3H), 6.51 (s, 14H), 9.72 (s, 1H-aldehyde).
Torularhodin	δ ppm:0.90 (s, 6H, CH_3-), 1.79 (s, 15H, CH_3-), 2.40-2.70 (m, 14H, -CH_2-), 5.61 (t, 1H), 6.27 (s, 3H), 6.51 (s 14H), 10.9 (s, 1H-acidic).

Table B.4. Recovery of β-carotene, torularhodin and torulene using DMSO and aqueous solution of PILs (90% v/v) at a concentration of 0.2 g/mL of wet cells after 1 h of stirring (30 rpm) at 25 °C.*****

Solvent	[PIL] 90 %(v/v)	β- carotene (µg/mL)	Torularhodin (µg/mL)	Torulene (µg/mL)
DMSO	-	28.14 ± 1.86	32.70 ± 1.48	3.33 ± 0.15
[PA]	$[Ac]^-$	10.14 ± 0.62^{r}	9.08 ± 0.26^{rst}	0.30 ± 0.04^{x}
	$[Pro]^-$	30.07 ± 1.02^{o}	27.42 ± 0.87^{pq}	2.05 ± 0.09^{wx}
	$[But]^-$	67.38 ± 0.54^{h}	54.97 ± 3.10^{k}	4.92 ± 1.36^{uv}
	$[Hex]^-$	111.64 ± 1.39^{c}	89.80 ± 0.75^{e}	8.17 ± 0.02^{rst}
[DMAPA]	$[Ac]^-$	34.33 ± 0.53^{n}	24.47 ± 1.35^{q}	1.76 ± 0.09^{wx}
	$[Pro]^-$	37.44 ± 1.14^{lm}	29.05 ± 1.42^{op}	2.88 ± 0.03^{vwx}
	$[But]^-$	71.24 ± 0.61^{g}	57.70 ± 0.94^{j}	6.34 ± 0.46^{tu}
	$[Hex]^-$	120.54 ± 1.76^{b}	102.50 ± 2.36^{d}	9.33 ± 0.32^{rs}
[DEAPA]	$[Ac]^-$	39.16 ± 1.36^{l}	31.150 ± 0.94^{o}	2.22 ± 0.31^{wx}
	$[Pro]^-$	34.85 ± 1.76^{n}	35.08 ± 3.73^{mn}	3.15 ± 0.06^{vw}
	$[But]^-$	76.74 ± 3.09^{f}	63.70 ± 2.07^{i}	7.20 ± 0.14^{stu}
	$[Hex]^-$	128.44 ± 5.10^{a}	111.75 ± 3.94^{c}	10.86 ± 0.16^{r}

*Mean of three independent assays ± confidence levels; means with the same lowercase letter does not present significant difference ($p > 0.05$)

Table B.5. Effect of PIL concentration [75%, 80%, 85% and 90% (v/v)] on cell permeability as a function of temperature (25 °C; 45 °C; 65 °C) at a concentration of 0.2 g/mL of wet cells after 1 h of stirring (30 rpm) in the release of β-carotene, torularhodin and torulene.*****

PILs	Temperature	[IL] (v/v)	β- carotene (μg/mL)	Torularhodin (μg/mL)	Torulene (μg/mL)
[PA][Hex]	25 °C	75%	81.38 ± 3.73^{stuvwxyzAB}	66.19 ± 2.10^{zABC}	6.28 ± 2.03^{D}
		80%	100.30 ± 2.19^{pqrstuvwx}	80.89 ± 3.99^{tuvwxyzAB}	7.75 ± 2.02^{D}
		85%	124.14 ± 6.19^{ijklmnop}	98.83 ± 4.27^{pqrstuvwxy}	9.27 ± 2.02^{D}
		90%	149.48 ± 4.55^{efghi}	125.42 ± 4.87^{ijklmnop}	12.48 ± 4.77^{D}
	45 °C	75%	109.79 ± 5.68^{lmnopqrs}	82.40 ± 3.34^{stuvwxyzAB}	7.32 ± 0.93^{D}
		80%	122.45 ± 6.80^{ijklmnop}	91.85 ± 5.76^{qrstuvwxyz}	9.00 ± 4.24^{D}
		85%	142.15 ± 2.94^{fghijk}	112.04 ± 4.20^{lmnopqr}	10.50 ± 1.79^{D}
		90%	158.17 ± 4.03^{defg}	129.36 ± 7.31^{hijklmno}	12.92 ± 4.02^{D}
	65 °C	75%	116.22 ± 3.33^{jklmnopq}	84.78 ± 3.09^{rstuvwxyzA}	9.58 ± 0.91^{D}
		80%	147.72 ± 2.96^{efghi}	106.17 ± 2.10^{mnopqrstu}	11.34 ± 1.03^{D}
		85%	158.92 ± 2.07^{defg}	121.63 ± 3.08^{ijklmnop}	12.39 ± 1.13^{D}
		90%	171.31 ± 5.13^{cde}	134.99 ± 0.46^{fghijkl}	14.17 ± 1.81^{D}
[DMAPA][Hex]	25 °C	75%	71.04 ± 5.48^{yzABC}	63.85 ± 3.56^{zABC}	7.13 ± 2.51^{D}
		80%	87.95 ± 2.52^{qrstuvwxyz}	75.18 ± 3.40^{wxyzABC}	6.88 ± 0.38^{D}
		85%	111.82 ± 4.14^{lmnopqr}	91.50 ± 2.21^{qrstuvwxyz}	8.65 ± 0.38^{D}
		90%	144.61 ± 4.24^{efghij}	115.57 ± 5.26^{klmnopq}	11.26 ± 2.29^{D}
	45 °C	75%	71.15 ± 3.08^{yzABC}	75.85 ± 2.86^{vwxyzABC}	7.25 ± 0.61^{D}
		80%	104.41 ± 1.70^{nopqrstu}	90.28 ± 5.29^{qrstuvwxyz}	8.68 ± 0.66^{D}
		85%	132.84 ± 5.38^{ghijklmn}	104.04 ± 3.45^{opqrstuv}	9.84 ± 1.33^{D}
		90%	187.85 ± 5.51^{abc}	122.56 ± 2.92^{ijklmnop}	12.86 ±0.32^{D}
	65 °C	75%	105.63 ± 6.00^{mnopqrstu}	50.65 ± 5.38^{C}	10.89 ± 0.09^{D}
		80%	171.59 ± 2.51^{cde}	56.98 ± 3.07^{ABC}	14.57 ± 0.50^{D}
		85%	186.14 ± 2.04^{bcd}	64.79 ± 5.75^{zABC}	15.94 ± 0.11^{D}
		90%	216.13 ± 3.34^{a}	78.54 ± 4.97^{uvwxyzABC}	17.98 ± 2.92^{D}
[DEAPA][Hex]	25 °C	75%	69.19 ± 2.00^{zABC}	50.65 ± 2.82^{C}	7.13 ± 0.89^{D}
		80%	87.95 ± 1.14^{qrstuvwxyz}	54.99 ± 1.97^{BC}	7.20 ± 0.12^{D}
		85%	115.83 ± 4.32^{klmnopq}	66.17 ± 4.10^{zABC}	8.62 ± 0.78^{D}
		90%	133.06 ± 9.74^{ghijklm}	78.15 ± 3.83^{uvwxyzABC}	11.25 ± 1.47^{D}
	45 °C	75%	74.69 ± 0.78^{xyzABC}	69.38 ± 2.20^{zABC}	7.61 ± 0.34^{D}
		80%	104.33 ± 7.64^{mnopqrstu}	85.82 ± 5.68^{rstuvwxyz}	8.35 ± 0.56^{D}
		85%	131.05 ± 6.13^{ghijklmno}	103.70 ± 3.08^{opqrstuvw}	10.24 ± 0.58^{D}
		90%	154.42 ± 3.67^{efgh}	122.55 ± 4.99^{ijklmnop}	12.27 ± 1.10^{D}
	65 °C	75%	108.60 ± 5.48^{lmnopqrst}	64.83 ± 2.96^{zABC}	9.84 ± 0.81^{D}
		80%	162.20 ± 4.67^{cdef}	73.44 ± 3.20^{xyzABC}	13.85 ± 1.41^{D}
		85%	185.15 ± 5.48^{bcd}	91.79 ± 5.61^{qrstuvwxyz}	15.51 ± 1.95^{D}
		90%	206.65 ± 10.75^{ab}	112.82 ± 6.09^{lmnopqr}	17.21 ± 1.99^{D}

*Mean of three independent assays ± confidence levels; means with the same lowercase letter present significant difference ($p > 0.05$); means with the same capital letter does not present significant difference ($p > 0.05$).

Table B.6. Effect of SLR (0.05, 0.1, 0.2 and 0.5 g/mL) as a function of the temperature (25 °C; 45 °C and 65 °C) of wet cells after 1 h of stirring (30 rpm) in the release of β-carotene, torularhodin and torulene using different solutions of PILs at 90% (v/v).*****

PILs	Temperature	Wet cells (g/mL)	β- carotene (μg/mL)	Torularhodin (μg/mL)	Torulene (μg/mL)
[PA][Hex]	25 °C	0.05	40.10 ± 1.03^{vwxyzABCDE}	35.81 ± 3.45^{vwxyzABCDE}	2.60 ± 0.74^{E}
		0.1	66.97 ± 4.93^{nopqrstuvwxyzABCDE}	53.93 ± 1.39^{qrstuvwxyzABCDE}	4.4 ± 0.31^{E}
		0.2	103.19 ± 5.47^{hijklmnopqrstuv}	77.15 ± 1.93^{klmnopqrstuvwxyzABCD}	8.17 ± 1.51^{CDE}
		0.5	114.78 ± 6.59^{ghijklmnopqrst}	94.15 ± 3.71^{ijklmnopqrstuvw}	10.53 ± 0.48^{BCDE}
	45 °C	0.05	45.89 ± 6.08^{stuvwxyzABCDE}	41.57 ± 2.28^{uvwxyzABCDE}	2.07 ± 0.36^{E}
		0.1	72.53 ± 4.52^{lmnopqrstuvwxyzABCDE}	63.25 ± 3.28^{opqrstuvwxyzABCDE}	4.95 ± 0.19^{E}
		0.2	111.64 ± 5.69^{ghijklmnopqrstu}	89.80 ± 3.33^{jklmnopqrstuvwxy}	9.71 ± 1.64^{BCDE}
		0.5	136.24 ± 7.32^{defghijklmn}	118.94 ± 2.91^{fghijklmnopqr}	14.23 ± 1.97^{ABCDE}
	65 °C	0.05	42.27 ± 3.72^{uvwxyzABCDE}	41.94 ± 4.53^{uvwxyzABCDE}	3.16 ± 0.66^{E}
		0.1	89.62 ± 2.23^{jklmnopqrstuvwxy}	65.80 ± 4.11^{nopqrstuvwxyzABCDE}	6.04 ± 0.53^{DE}
		0.2	175.50 ± 7.21^{abcdefg}	134.76 ± 9.84^{defghijklmn}	11.96 ± 0.98^{BCDE}
		0.5	204.78 ± 18.66^{abcd}	171.92 ± 5.00^{abcdefgh}	14.45 ± 0.91^{ABCDE}
[DMAPA][Hex]	25 °C	0.05	49.33 ± 2.70^{qrstuvwxyzABCDE}	44.47 ± 2.29^{tuvwxyzABCDE}	3.45 ± 1.02^{E}
		0.1	77.44 ± 2.18^{klmnopqrstuvwxyzABC}	70.20 ± 1.74^{nopqrstuvwxyzABCDE}	6.36 ± 0.73^{CDE}
		0.2	120.54 ± 3.66^{efghijklmnopq}	102.50 ± 6.57^{hijklmnopqrstuv}	9.33 ± 0.78^{BCDE}
		0.5	144.62 ± 5.38^{defghijk}	129.10 ± 3.38^{efghijklmnop}	11.92 ± 2.01^{BCDE}
	45 °C	0.05	49.19 ± 1.53^{qrstuvwxyzABCDE}	44.82 ± 1.16^{stuvwxyzABCDE}	4.13 ± 0.35^{E}
		0.1	93.14 ± 1.86^{ijklmnopqrstuvwx}	71.37 ± 3.20^{mnopqrstuvwxyzABCDE}	6.67 ± 0.45^{CDE}
		0.2	132.22 ± 3.82^{efghijklmno}	115.94 ± 3.15^{fghijklmnopqrs}	12.42 ± 0.68^{BCDE}
		0.5	147.84 ± 5.06^{defghijk}	134.30 ± 3.76^{defghijklmno}	15.41 ± 1.23^{zABCDE}
	65 °C	0.05	55.19 ± 5.47^{qrstuvwxyzABCDE}	45.65 ± 1.85^{stuvwxyzABCDE}	4.39 ± 0.98^{E}
		0.1	97.67 ± 2.61^{ijklmnopqrstuv}	77.66 ± 4.05^{klmnopqrstuvwxyzABC}	7.77 ± 0.27^{CDE}
		0.2	186.80 ± 5.08^{abcdef}	146.49 ± 5.98^{defghijk}	14.25 ± 0.43^{ABCDE}
		0.5	222.12 ± 5.60^{abc}	177.40 ± 5.08^{abcdefg}	19.20 ± 1.49^{yzABCDE}
[DEAPA][Hex]	25 °C	0.05	55.84 ± 3.23^{qrstuvwxyzABCDE}	48.89 ± 3.04^{rstuvwxyzABCDE}	4.36 ± 0.86^{E}
		0.1	84.36 ± 2.25^{jklmnopqrstuvwxyzA}	79.96 ± 2.15^{klmnopqrstuvwxyzAB}	7.07 ± .36^{CDE}
		0.2	128.42 ± 1.13^{efghijklmnop}	111.72 ± 3.24^{ghijklmnopqrstu}	10.86 ± 0.73^{BCDE}
		0.5	148.26 ± 5.14^{defghijk}	142.32 ± 4.18^{defghijklm}	13.12 ± 0.76^{ABCDE}
	45 °C	0.05	58.70 ±2.51^{pqrstuvwxyzABCDE}	48.37 ± 4.06^{rstuvwxyzABCDE}	4.84 ± 0.30^{E}
		0.1	98.16 ± 1.97^{ijklmnopqrstuv}	79.74 ± 1.21^{klmnopqrstuvwxyzAB}	7.83 ± 1.34^{CDE}
		0.2	142.86 ± 3.59^{defghijkl}	130.70 ± 7.11^{efghijklmno}	15.80 ± 1.11^{zABCDE}
		0.5	153.24 ± 5.30^{bcdefghij}	152.78 ± 3.47^{cdefghij}	19.75 ± 0.88^{yzABCDE}
	65 °C	0.05	65.41 ± 4.07^{nopqrstuvwxyzABCDE}	50.15 ± 1.93^{qrstuvwxyzABCDE}	5.08 ± 0.34^{E}
		0.1	115.05 ± 3.16^{ghijklmnopqrst}	86.66 ± 4.32^{jklmnopqrstuvwxyz}	9.79 ± 0.31^{BCDE}
		0.2	224.52 ± 9.54^{ab}	162.67 ± 5.58^{abcdefghi}	22.13 ± 0.23^{xyzABCDE}
		0.5	232.79 ± 6.20^{a}	191.14 ± 5.05^{abcde}	23.13 ± 1.93^{wxyzABCDE}

* Mean of three independent assays ± confidence levels; means with the same lowercase does not present significant difference ($p > 0.05$); means with the same capital letter does not present significant difference ($p > 0.05$).

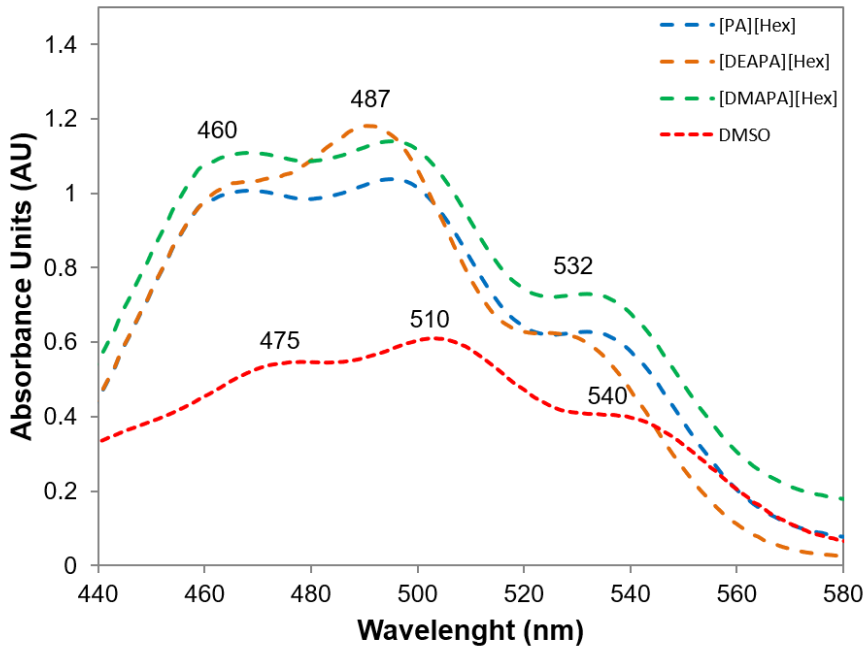

Figure B.1. Absorbance spectra of main carotenoids from *R. glutinis* CCT-2186 extracted using PILs and DMSO (control)

Appendix C: *Supporting Information of Chapter 5*

Table C.1. Experimental weight fraction data for the binodal curves of the systems composed of IL + K_3PO_4 + H_2O T= 298 (± 1) K and atmospheric pressure.

[PA][Hex] *Mw* 175.27 g.mol^{-1}		[DMAPA][Pro] *Mw* 176.26 g.mol^{-1}		[DMAPA][But] *Mw* 190.29 g.mol^{-1}		[DMAPA][Hex] *Mw* 218.34 g.mol^{-1}		[DEAPA][Pro] *Mw* 204.31 g.mol^{-1}		[DEAPA][But] *Mw* 218.34 g.mol^{-1}		[DEAPA][Hex] *Mw* 246.39 g.mol^{-1}	
$100w_{IL}$	$100w_{salt}$	$100w_{IL}$	$100w_{salt}$	$100w_{IL}$	$100w_{salt}$	$100w_{IL}$	$100w_{salt}$	$100w_{IL}$	$100w_{salt}$	$100w_{IL}$	$100w_{salt}$	$100w_{IL}$	$100w_{salt}$
84.89	10.13	47.95	28.03	58.63	26.02	69.30	12.15	26.19	21.71	50.49	12.70	95.00	2.00
72.03	10.90	44.92	28.90	48.16	27.09	43.15	14.99	20.30	24.06	47.32	12.86	54.15	5.16
38.39	15.25	36.80	30.26	28.63	32.91	39.90	15.25	16.41	25.44	43.29	13.98	46.40	7.81
22.65	19.94	31.95	31.81	17.82	36.19	34.06	15.87	14.63	26.65	40.21	14.65	42.85	8.50
11.05	29.46	24.79	35.84	14.01	38.96	30.68	16.50	11.12	30.15	35.69	15.97	39.08	9.60
5.75	31.97	19.47	37.61	11.69	41.12	24.03	17.35	9.60	33.22	30.87	17.27	34.09	12.06
4.21	33.91	17.17	39.19	9.55	41.66	20.58	18.14	7.02	36.18	30.11	17.62	30.98	12.83
1.61	37.69	12.58	41.99	7.15	43.44	18.50	18.38	6.39	39.56	25.43	19.76	29.10	13.68
		8.06	49.04	4.47	46.49	16.27	19.18	5.95	40.26	23.11	20.44	27.21	14.37
		6.98	52.92	3.53	47.68	13.45	19.65	5.51	40.87	21.70	21.36	25.97	14.93
		5.97	54.82	2.72	49.92	12.53	19.71	4.30	42.49	20.30	22.06	24.24	15.52
		3.10	60.95	2.09	51.01	11.26	20.36			19.37	22.67	23.20	15.94
		1.99	62.92	1.97	54.91	10.03	20.82			18.08	23.26	21.43	16.89
		1.32	64.94	1.34	58.81	8.59	21.65			17.30	23.71	20.44	17.16
		0.98	68.94							15.98	24.77	20.39	17.60
										15.25	25.02	19.14	18.20
										15.21	25.60	18.02	18.75
										14.28	26.26	16.88	19.20
										13.44	26.86	16.01	19.63
										12.59	27.34	15.21	20.07
										11.94	27.81	14.60	20.30
										10.89	29.30	12.52	22.58
										10.25	29.92	11.89	22.84
										1.88	48.29	10.43	24.39
										2.81	49.72	10.02	24.56
										1.85	51.86	9.65	24.63
												8.82	25.54
												8.15	26.25
												7.80	26.63

[a] The standard uncertainty for the weight fraction u (w) is 0.05, the standard uncertainty for the temperature u (T) is 0.20 K, and the standard uncertainty for pressure u (P) is 10 kPa.

Table C.2. Experimental weight fraction data for the binodal curves of the systems composed of IL + K_2HPO_4 + H_2O T= 298 (± 1) K and atmospheric pressure.

[PA][Hex] *Mw* 175.27 g.mol^{-1}		[DMAPA][Pro] *Mw* 176.26 g.mol^{-1}		[DMAPA][But] *Mw* 190.29 g.mol^{-1}		[DMAPA][Hex] *Mw* 218.34 g.mol^{-1}		[DEAPA][Pro] *Mw* 204.31 g.mol^{-1}		[DEAPA][But] *Mw* 218.34 g.mol^{-1}		[DEAPA][Hex] *Mw* 246.39 g.mol^{-1}	
$100w_{IL}$	$100w_{salt}$	$100w_{IL}$	$100w_{salt}$	$100w_{IL}$	$100w_{salt}$	$100w_{IL}$	$100w_{salt}$	$100w_{IL}$	$100w_{salt}$	$100w_{IL}$	$100w_{salt}$	$100w_{IL}$	$100w_{salt}$
80.02	29.01	80.17	30.12	80.20	26.18	69.30	21.07	52.88	33.81	70.19	20.00	77.41	13.83
68.23	29.34	62.19	31.36	69.83	26.98	43.15	26.00	43.43	34.22	33.02	29.23	33.02	23.97
54.45	30.53	50.03	34.91	41.59	32.50	39.90	26.45	20.60	39.69	25.20	32.98	25.20	28.03
48.53	30.83	23.36	45.82	36.99	34.13	34.06	27.52	11.10	49.79	21.87	35.16	21.87	30.29
36.89	31.91	13.62	49.73	20.09	40.33	30.68	28.62	8.74	51.35	18.74	37.54	18.74	32.71
24.69	35.39	6.40	56.43	14.28	43.00	24.03	30.08	7.97	53.01	16.63	39.05	16.64	34.26
10.29	40.42	4.19	58.46	10.55	44.76	20.58	31.46	5.43	55.22	15.29	39.98	15.30	35.21
4.68	44.23	2.31	59.71	8.88	46.39	18.50	31.88	3.26	59.67	14.43	40.58	14.44	35.83
				7.98	46.93	16.27	33.26	3.06	60.32	13.70	41.07	13.70	36.34
				6.77	48.19	13.45	34.07			12.96	41.81	12.96	37.08
				4.05	54.57	12.53	34.17			12.49	42.07	12.49	37.35
				2.96	60.76	11.26	35.32			11.93	42.58	11.94	37.86
						10.03	36.11			11.40	43.00	11.40	38.28
						8.59	37.54			10.95	43.42	10.95	38.71
										10.54	43.81	10.54	39.09
										9.95	44.26	9.95	39.55
										9.59	44.50	9.60	39.80
										9.30	44.88	9.30	40.17
										8.71	45.30	8.72	40.60
										8.37	45.68	8.37	40.98
										7.91	46.11	7.91	41.40
										7.42	46.53	7.42	41.83
												6.85	42.30
												6.50	42.71
												6.16	43.03
												5.91	43.32
												5.48	43.71
												5.00	44.31
												4.64	44.74
												4.10	45.31
												3.58	45.96
												2.82	47.04
												2.47	48.49

[a] The standard uncertainty for the weight fraction u (w) is 0.05, the standard uncertainty for the temperature u (T) is 0.20 K, and the standard uncertainty for pressure u (P) is 10 kPa.

Table C.3. Fitted parameters obtained from regression of Equation (1) for the system IL + K_3PO_4 + H_2O at T= 298 (± 1) K and atmospheric pressure.

IL	*A*	*B*	*C*	R^2
[DMAPA][Pro]	11492.80	-1.03	$4.43x10^{-7}$	0.99
[DMAPA][But]	3889.99	-0.78	$1.36 x10^{-5}$	0.99
[DMAPA][Hex]	613.54	-0.52	$2.00 x10^{-4}$	0.99
[DEAPA][Pro]	8109.88	-1.25	$1.12 x10^{-4}$	0.99
[DEAPA][But]	741.91	-0.75	$4.55 x10^{-6}$	0.99
[DEAPA][Hex]	186.01	-0.49	$3.12 x10^{-6}$	0.99

Table C.4. Adjusted parameters obtained from regression of equation (1) for the system IL + K_2HPO_4 + H_2O at T= 298 (± 1) K and atmospheric pressure.

IL	*A*	*B*	*C*	R^2
[DMAPA][Pro]	4529.99	-0.71	$6.43 x10^{-6}$	0.98
[DMAPA][But]	5425.80	-0.79	$9.26 x10^{-6}$	0.98
[DMAPA][Hex]	602.57	-0.39	$3.75 x10^{-5}$	0.98
[DEAPA][Pro]	1352.63	-0.52	$8.82 x10^{-6}$	0.98
[DEAPA][But]	1267.76	-0.63	$6.80 x10^{-6}$	0.97
[DEAPA][Hex]	532.67	-0.52	$12.83 x10^{-6}$	0.98

Table C.5. Experimental binodal data in molality (mol/kg) for the system composed of [DEAPA][Hex] + salt+ H_2O at 298 K, 308 K and 318 (± 1) K and atmospheric pressure.

[DEAPA][Hex] + K_3PO_4 + H_2O						[DEAPA][Hex] + K_2HPO_4 + H_2O					
298 K		308 K		318 K		298 K		308 K		318 K	
m [DEAPA][Hex]	*m* Salt	*m* [DEAPA][Hex]	*m* Salt	*m* [DEAPA][Hex]	*m* Salt	*m* [DEAPA][Hex]	*m* Salt	*m* [DEAPA][Hex]	*m* Salt	*m* [DEAPA][Hex]	*m* Salt
4.79	0.26	7.16	0.37	30.96	0.30	0.89	13.91	1.37	2.65	5.55	2.27
3.51	0.40	2.60	0.64	1.10	1.25	1.74	2.00	1.14	2.89	0.56	4.31
3.04	0.44	2.29	0.67	0.71	1.47	2.15	1.37	0.94	3.17	0.54	4.36
2.60	0.50	1.74	0.83	0.67	1.54	2.39	1.14	0.81	3.36	0.52	4.40
2.10	0.65	1.33	1.01	0.63	1.64	2.67	0.94	0.73	3.48	0.51	4.41
1.82	0.69	1.22	1.05	0.59	1.71	2.86	0.81	0.68	3.56	0.49	4.48
1.67	0.75	1.14	1.08	0.50	1.98	2.98	0.73	0.64	3.63	0.47	4.52
1.52	0.79	1.06	1.10	0.48	2.11	3.06	0.68	0.60	3.73	0.45	4.58
1.42	0.83	1.01	1.13			3.13	0.64	0.58	3.77	0.44	4.63
1.30	0.87	0.95	1.17			3.23	0.60	0.55	3.84	0.42	4.67
1.23	0.89	0.92	1.18			3.27	0.58	0.52	3.90	0.40	4.77
1.11	0.96	0.87	1.21			3.34	0.55	0.50	3.96	0.38	4.83
1.04	0.98	0.83	1.23			3.40	0.52	0.48	4.01	0.36	4.90
1.04	1.01	0.78	1.26			3.46	0.50	0.45	4.08	0.34	4.96
0.96	1.05	0.74	1.29			3.51	0.48	0.43	4.12	0.33	4.99
0.89	1.09	0.71	1.31			3.58	0.45	0.42	4.17	0.32	5.07
0.82	1.12	0.67	1.33			3.62	0.43	0.39	4.24	0.30	5.15
0.77	1.15	0.65	1.35			3.67	0.42	0.37	4.30	0.29	5.17
0.73	1.18	0.62	1.38			3.74	0.39	0.35	4.36	0.27	5.26
0.69	1.20	0.60	1.39			3.80	0.37	0.33	4.43	0.21	5.65
0.58	1.37	0.58	1.40			3.86	0.35	0.30	4.50	0.19	5.85
0.55	1.39	0.56	1.42			3.93	0.33	0.28	4.57	0.18	5.78
0.47	1.52	0.54	1.45			4.00	0.30	0.27	4.62		
0.45	1.53	0.52	1.44			4.07	0.28	0.26	4.67		
0.43	1.54					4.12	0.27	0.24	4.74		
0.39	1.62					4.17	0.26	0.21	4.84		
0.36	1.68					4.24	0.24	0.20	4.91		
0.34	1.71					4.34	0.21	0.17	5.01		
4.79						4.41	0.20	0.15	5.13		
						4.51	0.17	0.12	5.33		
						4.63	0.15	0.10	5.61		
						4.83	0.12				
						5.11	0.10				

[a] The standard uncertainty for the weight fraction u (w) is 0.05, the standard uncertainty for the temperature u (T) is 0.20 K, and the standard uncertainty for pressure u (P) is 10 kPa.

Table C.6. ILs purity, water content (%) and pH values of the ABS' coexisting phases, and Acid:Base molar ratio of the IL (top)-rich phase for the systems composed of IL + salt + H_2O at 298 K and atmospheric pressure.

Name		Water content (%)		pH		Acid:Base molar ratio
	Purity (%)	Top	Bottom	Top	Bottom	IL-rich phase
			K_2HPO_4			
[DMAPA][Pro]	100	35.09	38.56	9.13	9.01	1.03 ± 0.02
[DMAPA][But]	100	30.80	48.46	9.85	9.71	1.07 ± 0.06
[DMAPA][Hex]	100	39.6	32.70	10.01	9.97	1.06 ± 0.05
[DEAPA][Pro]	100	34.39	47.16	10.05	9.89	0.95 ± 0.06
[DEAPA][But]	100	39.59	44.77	10.87	10.63	1.05 ± 0.05
[DEAPA][Hex]	100	40.73	54.76	10.97	10.80	0.95 ± 0.09
			K_3PO_4			
[DMAPA][Pro]	100	40.06	46.66	8.32	8.02	1.14 ± 0.04
[DMAPA][But]	100	32.97	45.12	9.65	9.31	0.86 ± 0.08
[DMAPA][Hex]	100	37.90	49.00	9.97	9.14	0.89 ± 0.08
[DEAPA][Pro]	100	42.85	60.2	9.23	8.92	1.07 ± 0.02
[DEAPA][But]	100	44.73	49.83	10.46	10.41	1.02 ± 0.03
[DEAPA][Hex]	100	31.24	50.01	10.63	9.87	0.91 ± 0.07

Table C.7. Excess enthalpies of ternary mixtures of ionic liquid (1) + salt (2) + H_2O (3) at 298.15 K predicted using COSMO-RS

x_1	x_2	IL cation/kJ·mol^{-1}			IL anion/kJ·mol^{-1}			salt cation/kJ·mol^{-1}			salt anion/kJ·mol^{-1}			water /kJ·mol^{-1}		
		H_{MF}	H_{HB}	H_{VdW}	H_{MF}	H_{HB}	H_{VdW}	H_{MF}	H_{HB}	H_{VdW}	H_{MF}	H_{HB}	H_{VdW}	H_{MF}	H_{HB}	H_{VdW}
[PA][Hex] + K_3PO_4 + H_2O																
0.5042	0.0349	0.21	-0.15	0.04	0.20	-4.21	0.08	-2.26	0.00	0.02	-0.11	-3.93	0.02	0.68	-0.76	-0.36
0.2631	0.0238	0.15	0.69	0.07	0.27	-4.59	0.12	-1.52	0.00	0.02	-0.02	-2.89	0.01	0.72	-1.15	-0.49
0.0726	0.0191	0.08	0.47	0.05	0.17	-1.88	0.08	-1.22	0.00	0.02	0.04	-2.57	0.01	0.56	-1.23	-0.38
0.0358	0.0207	0.05	0.25	0.03	0.10	-0.98	0.05	-1.32	0.00	0.03	0.06	-2.87	0.01	0.56	-1.27	-0.28
0.0172	0.0340	0.04	0.08	0.02	0.07	-0.47	0.02	-2.17	0.00	0.05	0.12	-4.75	0.02	0.86	-1.89	-0.25
0.0087	0.0359	0.02	0.04	0.01	0.04	-0.24	0.01	-2.29	0.00	0.06	0.13	-5.05	0.02	0.92	-2.02	-0.21
0.0064	0.0385	0.02	0.02	0.01	0.03	-0.17	0.01	-2.45	0.00	0.06	0.15	-5.42	0.02	0.99	-2.13	-0.21
0.0055	0.0396	0.01	0.02	0.01	0.02	-0.15	0.01	-2.52	0.00	0.06	0.15	-5.58	0.02	1.02	-2.20	-0.21
0.0035	0.0446	0.01	0.01	0.00	0.02	-0.09	0.00	-2.84	0.00	0.07	0.18	-6.27	0.02	1.16	-2.44	-0.22
0.0023	0.1106	0.02	-0.02	0.00	0.03	-0.04	0.00	-6.91	0.00	0.17	0.49	-14.97	0.06	3.11	-5.30	-0.47
0.0014	0.0524	0.00	0.00	0.00	0.01	-0.03	0.00	-3.33	0.00	0.08	0.22	-7.36	0.03	1.39	-2.85	-0.24
0.0013	0.0669	0.01	0.00	0.00	0.01	-0.03	0.00	-4.24	0.00	0.11	0.28	-9.32	0.04	1.80	-3.52	-0.30
[DMAPA][Pro] + K_3PO_4 + H_2O																
0.3512	0.0186	0.10	0.14	0.10	0.09	-5.09	0.08	-1.21	0.00	0.01	-0.04	-2.20	0.01	0.65	-0.88	-0.42
0.1658	0.0140	0.11	0.41	0.11	0.11	-3.65	0.07	-0.90	0.00	0.01	0.00	-1.78	0.01	0.55	-1.09	-0.44
0.1069	0.0140	0.10	0.36	0.09	0.10	-2.63	0.06	-0.90	0.00	0.01	0.01	-1.84	0.01	0.50	-1.09	-0.40
0.0370	0.0208	0.06	0.12	0.05	0.05	-1.01	0.03	-1.33	0.00	0.03	0.05	-2.86	0.01	0.55	-1.28	-0.27
0.0205	0.0271	0.05	0.04	0.03	0.04	-0.57	0.02	-1.73	0.00	0.04	0.09	-3.78	0.02	0.69	-1.57	-0.23
0.0092	0.0303	0.02	0.01	0.01	0.02	-0.26	0.01	-1.94	0.00	0.05	0.11	-4.28	0.02	0.78	-1.73	-0.19
0.0059	0.0311	0.02	0.01	0.01	0.01	-0.17	0.00	-1.99	0.00	0.05	0.12	-4.40	0.02	0.80	-1.78	-0.17
0.0033	0.0342	0.01	0.00	0.01	0.01	-0.09	0.00	-2.18	0.00	0.05	0.13	-4.84	0.02	0.88	-1.95	-0.17

0.0032	0.0469	0.01	-0.01	0.00	0.01	-0.08	0.00	-2.98	0.00	0.07	0.19	-6.59	0.03	1.22	-2.56	-0.22
0.0025	0.0363	0.01	0.00	0.00	0.01	-0.07	0.00	-2.31	0.00	0.06	0.14	-5.13	0.02	0.94	-2.05	-0.18
0.0023	0.0362	0.01	0.00	0.00	0.01	-0.06	0.00	-2.31	0.00	0.06	0.14	-5.13	0.02	0.94	-2.05	-0.17
0.0024	0.0864	0.02	-0.02	0.00	0.01	-0.05	0.00	-5.44	0.00	0.14	0.37	-11.88	0.05	2.37	-4.36	-0.38
0.0023	0.1072	0.02	-0.03	0.00	0.01	-0.04	0.00	-6.70	0.00	0.17	0.48	-14.54	0.06	3.01	-5.17	-0.46
[DMAPA][But] + K_3PO_4 + H_2O																
0.6872	0.0279	0.17	-0.93	0.03	0.03	-2.87	-0.01	-1.85	0.00	0.02	-0.12	-3.06	0.02	0.46	-0.35	-0.21
0.1887	0.0124	0.11	0.42	0.10	0.14	-4.06	0.08	-0.80	0.00	0.01	-0.01	-1.56	0.01	0.56	-1.02	-0.46
0.0752	0.0134	0.09	0.29	0.08	0.10	-1.99	0.05	-0.86	0.00	0.02	0.02	-1.80	0.01	0.46	-1.03	-0.36
0.0570	0.0162	0.08	0.21	0.07	0.09	-1.54	0.04	-1.04	0.00	0.02	0.03	-2.20	0.01	0.48	-1.11	-0.33
0.0293	0.0239	0.06	0.07	0.04	0.06	-0.81	0.02	-1.52	0.00	0.03	0.07	-3.31	0.01	0.62	-1.41	-0.26
0.0266	0.0260	0.06	0.06	0.04	0.06	-0.74	0.02	-1.66	0.00	0.04	0.08	-3.61	0.01	0.66	-1.50	-0.26
0.0130	0.0289	0.03	0.02	0.02	0.03	-0.37	0.01	-1.85	0.00	0.04	0.10	-4.06	0.02	0.73	-1.64	-0.21
0.0109	0.0325	0.03	0.01	0.02	0.03	-0.30	0.01	-2.07	0.00	0.05	0.12	-4.57	0.02	0.82	-1.82	-0.21
0.0068	0.0352	0.02	0.00	0.01	0.02	-0.19	0.01	-2.24	0.00	0.05	0.13	-4.95	0.02	0.90	-1.97	-0.20
0.0044	0.0583	0.02	-0.02	0.01	0.02	-0.11	0.00	-3.70	0.00	0.09	0.24	-8.14	0.03	1.53	-3.11	-0.28
0.0035	0.0710	0.02	-0.03	0.00	0.02	-0.08	0.00	-4.49	0.00	0.11	0.30	-9.85	0.04	1.90	-3.70	-0.32
0.0039	0.1001	0.04	-0.05	0.00	0.02	-0.07	0.00	-6.28	0.00	0.15	0.43	-13.63	0.06	2.75	-4.87	-0.43
[DMAPA][Hex] + K_3PO_4 + H_2O																
0.3689	0.0072	0.02	0.54	0.09	0.09	-5.57	0.12	-0.47	0.00	0.00	-0.02	-0.85	0.00	0.63	-0.68	-0.43
0.2004	0.0090	0.09	0.56	0.10	0.15	-4.23	0.11	-0.58	0.00	0.01	-0.01	-1.13	0.01	0.55	-0.90	-0.48
0.1004	0.0141	0.10	0.36	0.08	0.15	-2.51	0.09	-0.90	0.00	0.01	0.01	-1.86	0.01	0.50	-1.02	-0.43
0.0426	0.0146	0.06	0.20	0.05	0.09	-1.19	0.05	-0.93	0.00	0.02	0.04	-2.01	0.01	0.43	-0.99	-0.31
0.0238	0.0209	0.05	0.09	0.03	0.07	-0.67	0.03	-1.33	0.00	0.03	0.06	-2.92	0.01	0.54	-1.23	-0.25
0.0121	0.0251	0.03	0.03	0.02	0.04	-0.34	0.02	-1.60	0.00	0.04	0.09	-3.53	0.01	0.64	-1.46	-0.20
0.0096	0.0266	0.03	0.02	0.02	0.03	-0.27	0.01	-1.70	0.00	0.04	0.10	-3.75	0.01	0.67	-1.51	-0.19
0.0085	0.0275	0.02	0.02	0.01	0.03	-0.24	0.01	-1.75	0.00	0.04	0.10	-3.88	0.02	0.70	-1.58	-0.19
0.0052	0.0298	0.02	0.01	0.01	0.02	-0.15	0.01	-1.90	0.00	0.05	0.11	-4.22	0.02	0.76	-1.71	-0.17

0.0043	0.0306	0.01	0.01	0.01	0.02	-0.12	0.01	-1.95	0.00	0.05	0.12	-4.33	0.02	0.78	-1.72	-0.17
0.0032	0.0378	0.01	0.00	0.01	0.01	-0.09	0.00	-2.41	0.00	0.06	0.15	-5.33	0.02	0.97	-2.10	-0.19
0.0031	0.0474	0.01	-0.01	0.00	0.02	-0.08	0.00	-3.02	0.00	0.08	0.19	-6.66	0.03	1.24	-2.61	-0.23
0.0026	0.0339	0.01	0.00	0.00	0.01	-0.07	0.00	-2.16	0.00	0.05	0.13	-4.80	0.02	0.87	-1.92	-0.17
0.0028	0.0533	0.01	-0.01	-0.01	0.02	-0.07	0.00	-3.38	0.00	0.08	0.22	-7.46	0.03	1.39	-2.88	-0.25
0.0029	0.0778	0.02	-0.02	-0.02	0.02	-0.06	0.00	-4.91	0.00	0.12	0.33	-10.75	0.04	2.10	-4.00	-0.35
0.0022	0.0998	0.02	-0.03	-0.03	0.02	-0.04	0.00	-6.26	0.00	0.16	0.44	-13.61	0.06	2.76	-4.88	-0.43
[DEAPA][Pro] + K_3PO_4 + H_2O																
0.5236	0.0295	0.22	-0.54	0.07	0.01	-4.17	0.05	-1.93	0.00	0.02	-0.10	-3.32	0.02	0.64	-0.62	-0.33
0.3161	0.0201	0.20	0.16	0.12	0.08	-4.92	0.07	-1.30	0.00	0.01	-0.04	-2.40	0.01	0.68	-0.95	-0.45
0.1491	0.0135	0.17	0.44	0.12	0.10	-3.40	0.07	-0.87	0.00	0.01	0.00	-1.73	0.01	0.54	-1.06	-0.46
0.1088	0.0115	0.15	0.44	0.11	0.09	-2.70	0.06	-0.74	0.00	0.01	0.01	-1.51	0.01	0.47	-0.99	-0.43
0.0835	0.0118	0.13	0.38	0.10	0.08	-2.17	0.05	-0.75	0.00	0.01	0.02	-1.57	0.01	0.43	-0.95	-0.39
0.0508	0.0161	0.11	0.22	0.08	0.06	-1.38	0.03	-1.02	0.00	0.02	0.04	-2.19	0.01	0.47	-1.07	-0.32
0.0334	0.0199	0.09	0.13	0.06	0.05	-0.93	0.02	-1.27	0.00	0.03	0.06	-2.75	0.01	0.53	-1.23	-0.28
0.0288	0.0217	0.08	0.10	0.05	0.04	-0.80	0.02	-1.38	0.00	0.03	0.06	-3.01	0.01	0.56	-1.29	-0.26
0.0247	0.0237	0.08	0.08	0.04	0.04	-0.69	0.02	-1.51	0.00	0.03	0.07	-3.31	0.01	0.60	-1.38	-0.25
0.0199	0.0269	0.07	0.05	0.04	0.03	-0.55	0.01	-1.72	0.00	0.04	0.09	-3.76	0.02	0.68	-1.53	-0.24
0.0157	0.0324	0.06	0.02	0.03	0.03	-0.43	0.01	-2.06	0.00	0.05	0.11	-4.53	0.02	0.81	-1.81	-0.24
0.0123	0.0338	0.05	0.01	0.02	0.02	-0.34	0.01	-2.15	0.00	0.05	0.12	-4.74	0.02	0.85	-1.90	-0.23
0.0108	0.0367	0.05	0.00	0.02	0.02	-0.29	0.01	-2.34	0.00	0.06	0.13	-5.15	0.02	0.93	-2.05	-0.23
0.0081	0.0394	0.04	0.00	0.00	0.02	-0.22	0.01	-2.51	0.00	0.06	0.15	-5.53	0.02	1.00	-2.16	-0.22
0.0058	0.0447	0.03	-0.01	-0.01	0.01	-0.15	0.00	-2.84	0.00	0.07	0.17	-6.27	0.03	1.15	-2.46	-0.23
0.0058	0.0588	0.04	-0.03	-0.03	0.02	-0.14	0.00	-3.73	0.00	0.09	0.24	-8.19	0.03	1.53	-3.12	-0.29
0.0053	0.0713	0.05	-0.04	-0.04	0.02	-0.12	0.00	-4.51	0.00	0.11	0.29	-9.87	0.04	1.88	-3.67	-0.33
[DEAPA][But] + K_3PO_4 + H_2O																
0.2824	0.0144	0.17	0.40	0.12	0.10	-4.92	0.09	-0.93	0.00	0.01	-0.02	-1.74	0.01	0.64	-0.93	-0.47
0.1890	0.0112	0.16	0.53	0.12	0.11	-4.04	0.09	-0.72	0.00	0.01	0.00	-1.41	0.01	0.56	-0.97	-0.48

0.1092	0.0102	0.14	0.48	0.11	0.10	-2.72	0.07	-0.65	0.00	0.01	0.01	-1.33	0.01	0.45	-0.92	-0.44
0.0429	0.0115	0.09	0.24	0.07	0.06	-1.20	0.04	-0.73	0.00	0.01	0.03	-1.58	0.01	0.37	-0.86	-0.30
0.0239	0.0139	0.06	0.14	0.04	0.04	-0.69	0.02	-0.89	0.00	0.02	0.04	-1.95	0.01	0.39	-0.92	-0.23
0.0161	0.0207	0.05	0.07	0.03	0.03	-0.46	0.02	-1.32	0.00	0.03	0.07	-2.91	0.01	0.53	-1.24	-0.21
0.0065	0.0394	0.03	0.00	0.01	0.02	-0.18	0.01	-2.51	0.00	0.06	0.15	-5.54	0.02	1.01	-2.20	-0.22
0.0054	0.0521	0.03	-0.02	0.01	0.02	-0.14	0.00	-3.31	0.00	0.08	0.21	-7.28	0.03	1.35	-2.80	-0.26
0.0041	0.0734	0.04	-0.03	0.01	0.02	-0.09	0.00	-4.64	0.00	0.11	0.31	-10.16	0.04	1.95	-3.80	-0.34
0.0043	0.0888	0.05	-0.04	0.01	0.02	-0.09	0.00	-5.59	0.00	0.14	0.38	-12.17	0.05	2.39	-4.43	-0.39
[DEAPA][Hex] + K_3PO_4 + H_2O																
0.3096	0.0085	0.11	0.58	0.11	0.10	-5.28	0.11	-0.54	0.00	0.01	-0.02	-1.01	0.00	0.63	-0.76	-0.47
0.1784	0.0057	0.13	0.68	0.11	0.13	-3.99	0.11	-0.36	0.00	0.00	0.00	-0.72	0.00	0.50	-0.80	-0.49
0.0827	0.0071	0.12	0.46	0.09	0.12	-2.19	0.08	-0.45	0.00	0.01	0.01	-0.95	0.00	0.37	-0.75	-0.42
0.0344	0.0101	0.08	0.22	0.06	0.08	-0.99	0.04	-0.64	0.00	0.01	0.03	-1.40	0.01	0.32	-0.73	-0.29
0.0232	0.0108	0.06	0.15	0.04	0.06	-0.68	0.03	-0.69	0.00	0.02	0.03	-1.52	0.01	0.32	-0.74	-0.23
0.0166	0.0131	0.05	0.10	0.03	0.04	-0.49	0.02	-0.84	0.00	0.02	0.04	-1.85	0.01	0.36	-0.84	-0.20
0.0136	0.0147	0.04	0.08	0.03	0.04	-0.40	0.02	-0.94	0.00	0.02	0.05	-2.08	0.01	0.39	-0.92	-0.18
0.0121	0.0162	0.04	0.07	0.02	0.04	-0.35	0.02	-1.03	0.00	0.02	0.06	-2.29	0.01	0.42	-0.97	-0.18
0.0089	0.0206	0.03	0.04	0.02	0.03	-0.26	0.01	-1.31	0.00	0.03	0.07	-2.91	0.01	0.52	-1.19	-0.17
0.0060	0.0271	0.02	0.02	0.01	0.02	-0.17	0.01	-1.73	0.00	0.04	0.10	-3.84	0.02	0.69	-1.56	-0.17
0.0048	0.0300	0.02	0.01	0.01	0.02	-0.13	0.01	-1.91	0.00	0.05	0.11	-4.25	0.02	0.76	-1.70	-0.18
0.0040	0.0310	0.02	0.01	0.01	0.02	-0.11	0.01	-1.98	0.00	0.05	0.12	-4.39	0.02	0.79	-1.77	-0.17
0.0034	0.0325	0.02	0.01	0.01	0.01	-0.10	0.00	-2.08	0.00	0.05	0.13	-4.61	0.02	0.83	-1.83	-0.17
0.0035	0.0446	0.02	0.00	0.00	0.02	-0.09	0.00	-2.84	0.00	0.07	0.18	-6.27	0.03	1.16	-2.47	-0.22
0.0031	0.0373	0.02	0.00	0.00	0.01	-0.08	0.00	-2.38	0.00	0.06	0.15	-5.27	0.02	0.96	-2.08	-0.19
0.0029	0.0611	0.02	-0.01	-0.01	0.02	-0.07	0.00	-3.87	0.00	0.10	0.25	-8.52	0.03	1.61	-3.26	-0.28
0.0029	0.0611	0.02	-0.01	-0.01	0.02	-0.07	0.00	-3.87	0.00	0.10	0.25	-8.52	0.03	1.61	-3.26	-0.28
0.0011	0.0829	0.01	-0.01	-0.01	0.01	-0.02	0.00	-5.23	0.00	0.13	0.36	-11.44	0.05	2.27	-4.22	-0.36

[PA][Hex] + K_2HPO_4 + H_2O

0.7370	0.1762	0.38	-2.19	-0.01	0.27	5.83	-0.13	-4.70	0.00	0.02	-0.57	-10.27	0.09	0.18	-0.16	-0.07
0.0866	0.0473	0.06	0.47	0.05	0.23	-1.94	0.07	-1.19	0.00	0.02	-0.02	-4.53	0.04	0.62	-1.12	-0.42
0.0461	0.0477	0.04	0.29	0.04	0.15	-1.12	0.05	-1.20	0.00	0.03	0.00	-4.71	0.04	0.60	-1.13	-0.34
0.0266	0.0533	0.03	0.16	0.03	0.10	-0.66	0.03	-1.35	0.00	0.04	0.02	-5.32	0.04	0.64	-1.21	-0.29
0.0184	0.0593	0.02	0.11	0.02	0.08	-0.45	0.02	-1.51	0.00	0.05	0.03	-5.92	0.05	0.71	-1.31	-0.26
0.0170	0.0639	0.02	0.09	0.02	0.07	-0.41	0.02	-1.62	0.00	0.05	0.03	-6.35	0.05	0.76	-1.36	-0.27
0.0146	0.0691	0.02	0.07	0.01	0.07	-0.34	0.02	-1.76	0.00	0.05	0.04	-6.84	0.06	0.82	-1.43	-0.27
0.0141	0.0727	0.02	0.06	0.01	0.07	-0.32	0.02	-1.85	0.00	0.06	0.04	-7.17	0.06	0.86	-1.48	-0.27
0.0130	0.0862	0.02	0.04	0.01	0.07	-0.28	0.01	-2.20	0.00	0.07	0.06	-8.36	0.07	1.01	-1.63	-0.30
0.0131	0.0974	0.03	0.03	0.01	0.08	-0.26	0.01	-2.48	0.00	0.08	0.07	-9.29	0.08	1.13	-1.73	-0.32
[DMAPA][Pro] + K_2HPO_4 + H_2O																
0.1754	0.0599	0.12	0.15	0.09	0.18	-2.96	0.05	-1.55	0.00	0.02	-0.07	-5.33	0.04	0.72	-1.10	-0.46
0.1229	0.0493	0.10	0.24	0.09	0.15	-2.50	0.05	-1.26	0.00	0.02	-0.04	-4.60	0.04	0.65	-1.12	-0.43
0.1098	0.0492	0.10	0.23	0.08	0.14	-2.31	0.05	-1.26	0.00	0.02	-0.03	-4.63	0.04	0.64	-1.13	-0.42
0.0771	0.0429	0.08	0.23	0.07	0.11	-1.79	0.04	-1.09	0.00	0.02	-0.02	-4.16	0.03	0.57	-1.10	-0.38
0.0631	0.0436	0.07	0.20	0.07	0.10	-1.51	0.03	-1.11	0.00	0.03	-0.01	-4.26	0.03	0.57	-1.10	-0.36
0.0464	0.0490	0.06	0.14	0.05	0.08	-1.12	0.03	-1.25	0.00	0.03	0.00	-4.82	0.04	0.61	-1.17	-0.32
0.0345	0.0494	0.05	0.11	0.04	0.06	-0.85	0.02	-1.26	0.00	0.04	0.01	-4.92	0.04	0.61	-1.17	-0.29
0.0301	0.0517	0.05	0.09	0.04	0.06	-0.74	0.02	-1.32	0.00	0.04	0.01	-5.15	0.04	0.63	-1.21	-0.28
0.0214	0.0551	0.04	0.06	0.03	0.04	-0.53	0.01	-1.40	0.00	0.04	0.02	-5.51	0.04	0.66	-1.24	-0.26
0.0143	0.0699	0.03	0.03	0.02	0.04	-0.33	0.01	-1.78	0.00	0.06	0.04	-6.91	0.06	0.83	-1.45	-0.26
0.0089	0.0816	0.02	0.01	0.01	0.02	-0.20	0.00	-2.08	0.00	0.07	0.06	-7.99	0.06	0.97	-1.60	-0.27
0.0063	0.0865	0.02	0.00	0.01	0.02	-0.14	0.00	-2.21	0.00	0.07	0.07	-8.43	0.07	1.03	-1.65	-0.27
0.0049	0.0919	0.02	0.00	0.01	0.02	-0.10	0.00	-2.35	0.00	0.08	0.08	-8.90	0.07	1.10	-1.71	-1.71
0.0039	0.1045	0.01	0.00	0.00	0.01	-0.07	0.00	-2.67	0.00	0.09	0.10	-9.94	0.08	1.25	-1.83	-1.83
[DMAPA][But] + K_2HPO_4 + H_2O																
0.2339	0.0817	0.17	-0.15	0.08	0.26	-2.88	0.03	-2.12	0.00	0.02	-0.12	-6.84	0.06	0.81	-1.02	-0.46
0.1216	0.0582	0.12	0.15	0.08	0.19	-2.40	0.05	-1.48	0.00	0.02	-0.04	-5.37	0.04	0.70	-1.17	-0.45

0.0506	0.0443	0.07	0.16	0.06	0.10	-1.25	0.03	-1.12	0.00	0.03	0.00	-4.37	0.04	0.56	-1.10	-0.34
0.0279	0.0449	0.04	0.10	0.04	0.06	-0.72	0.02	-1.14	0.00	0.03	0.01	-4.51	0.04	0.55	-1.10	-0.27
0.0216	0.0488	0.04	0.07	0.03	0.05	-0.56	0.02	-1.24	0.00	0.04	0.02	-4.91	0.04	0.59	-1.15	-0.26
0.0180	0.0523	0.03	0.06	0.03	0.05	-0.46	0.01	-1.33	0.00	0.04	0.02	-5.26	0.04	0.63	-1.21	-0.25
0.0146	0.0544	0.03	0.04	0.02	0.04	-0.37	0.01	-1.39	0.00	0.04	0.02	-5.48	0.04	0.65	-1.24	-0.24
0.0110	0.0594	0.02	0.03	0.02	0.03	-0.28	0.01	-1.51	0.00	0.05	0.03	-5.96	0.05	0.71	-1.31	-0.23
0.0070	0.0675	0.02	0.01	0.01	0.02	-0.17	0.01	-1.72	0.00	0.06	0.04	-6.74	0.05	0.81	-1.42	-0.23
0.0057	0.0754	0.02	0.01	0.01	0.02	-0.13	0.00	-1.92	0.00	0.06	0.05	-7.46	0.06	0.90	-1.52	-0.24
0.0052	0.0839	0.02	0.00	0.01	0.02	-0.12	0.00	-2.14	0.00	0.07	0.06	-8.22	0.07	1.00	-1.62	-0.26
0.0052	0.0986	0.02	0.00	0.01	0.02	-0.11	0.00	-2.52	0.00	0.08	0.08	-9.45	0.08	1.17	-1.78	-0.29
[DMAPA][Hex] + K_2HPO_4 + H_2O																
0.2227	0.0311	0.07	0.45	0.09	0.19	-4.04	0.10	-0.79	0.00	0.01	-0.05	-2.78	0.02	0.62	-0.85	-0.48
0.1235	0.0222	0.07	0.48	0.09	0.17	-2.87	0.09	-0.56	0.00	0.01	-0.02	-2.12	0.02	0.48	-0.85	-0.45
0.0415	0.0339	0.05	0.19	0.05	0.11	-1.08	0.05	-0.86	0.00	0.02	0.00	-3.41	0.03	0.46	-0.92	-0.32
0.0231	0.0360	0.03	0.11	0.03	0.07	-0.62	0.03	-0.91	0.00	0.03	0.01	-3.66	0.03	0.45	-0.93	-0.25
0.0197	0.0381	0.03	0.09	0.03	0.06	-0.53	0.03	-0.97	0.00	0.03	0.01	-3.88	0.03	0.47	-0.97	-0.24
0.0148	0.0413	0.03	0.07	0.02	0.05	-0.40	0.02	-1.05	0.00	0.03	0.01	-4.21	0.03	0.50	-1.01	-0.22
0.0120	0.0484	0.02	0.05	0.02	0.04	-0.32	0.02	-1.23	0.00	0.04	0.02	-4.92	0.04	0.58	-1.14	-0.22
0.0112	0.0549	0.02	0.04	0.02	0.04	-0.28	0.01	-1.40	0.00	0.04	0.03	-5.53	0.04	0.65	-1.24	-0.23
0.0099	0.0588	0.02	0.03	0.01	0.04	-0.25	0.01	-1.50	0.00	0.05	0.03	-5.91	0.05	0.70	-1.29	-0.23
0.0086	0.0624	0.02	0.02	0.01	0.04	-0.21	0.01	-1.59	0.00	0.05	0.04	-6.26	0.05	0.74	-1.34	-0.23
0.0070	0.0675	0.02	0.02	0.01	0.03	-0.17	0.01	-1.72	0.00	0.06	0.04	-6.74	0.05	0.80	-1.42	-0.24
0.0064	0.0751	0.02	0.01	0.01	0.03	-0.15	0.01	-1.92	0.00	0.06	0.05	-7.44	0.06	0.89	-1.51	-0.25
0.0057	0.0847	0.02	0.00	0.01	0.03	-0.12	0.01	-2.16	0.00	0.07	0.07	-8.28	0.07	1.00	-1.63	-1.63
0.0033	0.1059	0.01	0.00	0.00	0.02	-0.06	0.00	-2.70	0.00	0.09	0.10	-10.06	0.08	1.26	-1.84	-1.84
[DEAPA][Pro] + K_2HPO_4 + H_2O																
0.2081	0.0743	0.24	0.01	0.10	0.18	-2.89	0.04	-1.91	0.00	0.02	-0.10	-6.37	0.05	0.78	-1.05	-0.48
0.0755	0.0501	0.15	0.20	0.09	0.11	-1.70	0.04	-1.27	0.00	0.03	-0.02	-4.82	0.04	0.62	-1.14	-0.41

0.0369	0.0425	0.09	0.15	0.06	0.06	-0.94	0.02	-1.08	0.00	0.03	0.00	-4.24	0.03	0.53	-1.06	-0.31
0.0245	0.0425	0.06	0.11	0.04	0.04	-0.64	0.02	-1.08	0.00	0.03	0.01	-4.29	0.03	0.52	-1.06	-0.26
0.0213	0.0445	0.06	0.09	0.04	0.04	-0.55	0.01	-1.13	0.00	0.03	0.01	-4.50	0.04	0.54	-1.08	-0.25
0.0181	0.0445	0.05	0.08	0.03	0.03	-0.48	0.01	-1.13	0.00	0.03	0.01	-4.51	0.04	0.54	-1.07	-0.24
0.0145	0.0461	0.04	0.06	0.03	0.03	-0.38	0.01	-1.17	0.00	0.04	0.02	-4.68	0.04	0.56	-1.10	-0.22
0.0113	0.0488	0.03	0.05	0.02	0.02	-0.29	0.01	-1.24	0.00	0.04	0.02	-4.95	0.04	0.59	-1.15	-0.21
0.0089	0.0505	0.03	0.03	0.02	0.02	-0.23	0.01	-1.29	0.00	0.04	0.03	-5.13	0.04	0.61	-1.17	-0.20
0.0079	0.0548	0.03	0.03	0.02	0.02	-0.20	0.01	-1.39	0.00	0.05	0.03	-5.54	0.05	0.66	-1.23	-0.21
0.0051	0.0707	0.02	0.01	0.01	0.01	-0.12	0.00	-1.80	0.00	0.06	0.05	-7.04	0.06	0.84	-1.47	-0.23
0.0051	0.1026	0.03	0.00	0.01	0.02	-0.10	0.00	-2.62	0.00	0.08	0.09	-9.78	0.08	1.21	-1.81	-0.30
[DEAPA][But] + K_2HPO_4 + H_2O																
0.1728	0.0522	0.19	0.25	0.10	0.18	-3.09	0.06	-1.33	0.00	0.01	-0.06	-4.70	0.04	0.69	-1.03	-0.49
0.0928	0.0366	0.14	0.33	0.09	0.13	-2.16	0.05	-0.92	0.00	0.02	-0.02	-3.52	0.03	0.53	-1.00	-0.43
0.0389	0.0334	0.08	0.19	0.06	0.07	-1.02	0.03	-0.84	0.00	0.02	0.00	-3.36	0.03	0.45	-0.92	-0.31
0.0225	0.0334	0.06	0.12	0.04	0.05	-0.61	0.02	-0.84	0.00	0.03	0.01	-3.41	0.03	0.42	-0.89	-0.24
0.0166	0.0339	0.04	0.09	0.03	0.04	-0.46	0.02	-0.86	0.00	0.03	0.01	-3.48	0.03	0.42	-0.89	-0.22
0.0128	0.0339	0.03	0.07	0.03	0.03	-0.36	0.01	-0.86	0.00	0.03	0.01	-3.49	0.03	0.42	-0.88	-0.19
0.0101	0.0366	0.03	0.05	0.02	0.02	-0.28	0.01	-0.93	0.00	0.03	0.01	-3.76	0.03	0.45	-0.92	-0.18
0.0086	0.0370	0.02	0.05	0.02	0.02	-0.24	0.01	-0.94	0.00	0.03	0.02	-3.81	0.03	0.45	-0.94	-0.17
0.0069	0.0403	0.02	0.04	0.01	0.02	-0.19	0.01	-1.02	0.00	0.03	0.02	-4.14	0.03	0.49	-0.99	-0.17
0.0057	0.0439	0.02	0.03	0.01	0.02	-0.16	0.01	-1.12	0.00	0.04	0.02	-4.51	0.04	0.53	-1.05	-0.17
0.0052	0.0442	0.02	0.02	0.01	0.01	-0.14	0.01	-1.13	0.00	0.04	0.02	-4.54	0.04	0.53	-1.05	-0.17
0.0045	0.0487	0.02	0.02	0.01	0.01	-0.12	0.00	-1.24	0.00	0.04	0.03	-4.98	0.04	0.59	-1.14	-0.18
0.0043	0.0480	0.01	0.02	0.01	0.01	-0.11	0.00	-1.22	0.00	0.04	0.03	-4.91	0.04	0.58	-1.12	-1.12
0.0041	0.0548	0.01	0.01	0.01	0.01	-0.11	0.00	-1.40	0.00	0.05	0.03	-5.57	0.05	0.66	-1.23	-1.23
0.0040	0.0730	0.02	0.01	0.01	0.01	-0.09	0.00	-1.86	0.00	0.06	0.05	-7.26	0.06	0.87	-1.50	-1.50
0.0031	0.1116	0.02	0.00	0.00	0.01	-0.06	0.00	-2.85	0.00	0.09	0.11	-10.50	0.08	1.32	-1.89	-1.89
[DEAPA][Hex] + K_2HPO_4 + H_2O																

0.3527	0.0556	0.15	0.08	0.08	0.18	-3.82	0.07	-1.43	0.00	0.00	-0.12	-4.52	0.04	0.73	-0.68	-0.44
0.1882	0.0372	0.15	0.41	0.10	0.20	-3.56	0.09	-0.93	0.00	0.01	-0.05	-3.36	0.03	0.63	-0.88	-0.50
0.0481	0.0219	0.09	0.28	0.07	0.10	-1.30	0.05	-0.55	0.00	0.01	0.00	-2.21	0.02	0.35	-0.73	-0.35
0.0304	0.0204	0.06	0.20	0.05	0.08	-0.85	0.04	-0.51	0.00	0.01	0.00	-2.09	0.02	0.31	-0.65	-0.28
0.0214	0.0198	0.05	0.15	0.04	0.06	-0.61	0.03	-0.50	0.00	0.02	0.00	-2.05	0.02	0.28	-0.61	-0.23
0.0189	0.0200	0.04	0.13	0.04	0.05	-0.55	0.03	-0.51	0.00	0.02	0.00	-2.07	0.02	0.28	-0.61	-0.22
0.0149	0.0213	0.04	0.10	0.03	0.04	-0.43	0.02	-0.54	0.00	0.02	0.00	-2.22	0.02	0.29	-0.63	-0.19
0.0122	0.0225	0.03	0.08	0.02	0.04	-0.35	0.02	-0.57	0.00	0.02	0.01	-2.34	0.02	0.29	-0.65	-0.17
0.0100	0.0271	0.03	0.06	0.02	0.03	-0.29	0.02	-0.69	0.00	0.02	0.01	-2.81	0.02	0.34	-0.73	-0.17
0.0095	0.0264	0.03	0.06	0.02	0.03	-0.27	0.01	-0.67	0.00	0.02	0.01	-2.74	0.02	0.33	-0.72	-0.16
0.0076	0.0285	0.02	0.05	0.02	0.03	-0.22	0.01	-0.72	0.00	0.02	0.01	-2.96	0.02	0.35	-0.76	-0.15
0.0059	0.0324	0.02	0.04	0.01	0.02	-0.17	0.01	-0.82	0.00	0.03	0.01	-3.36	0.03	0.39	-0.83	-0.15
0.0034	0.0512	0.01	0.01	0.01	0.01	-0.09	0.00	-1.30	0.00	0.04	0.03	-5.22	0.04	0.61	-1.17	-1.17
0.0024	0.0692	0.01	0.01	0.01	0.01	-0.06	0.00	-1.76	0.00	0.06	0.05	-6.92	0.06	0.83	-1.45	-1.45
0.0015	0.1106	0.01	0.00	0.00	0.01	-0.03	0.00	-2.82	0.00	0.09	0.11	-10.44	0.08	1.32	-1.89	-1.89

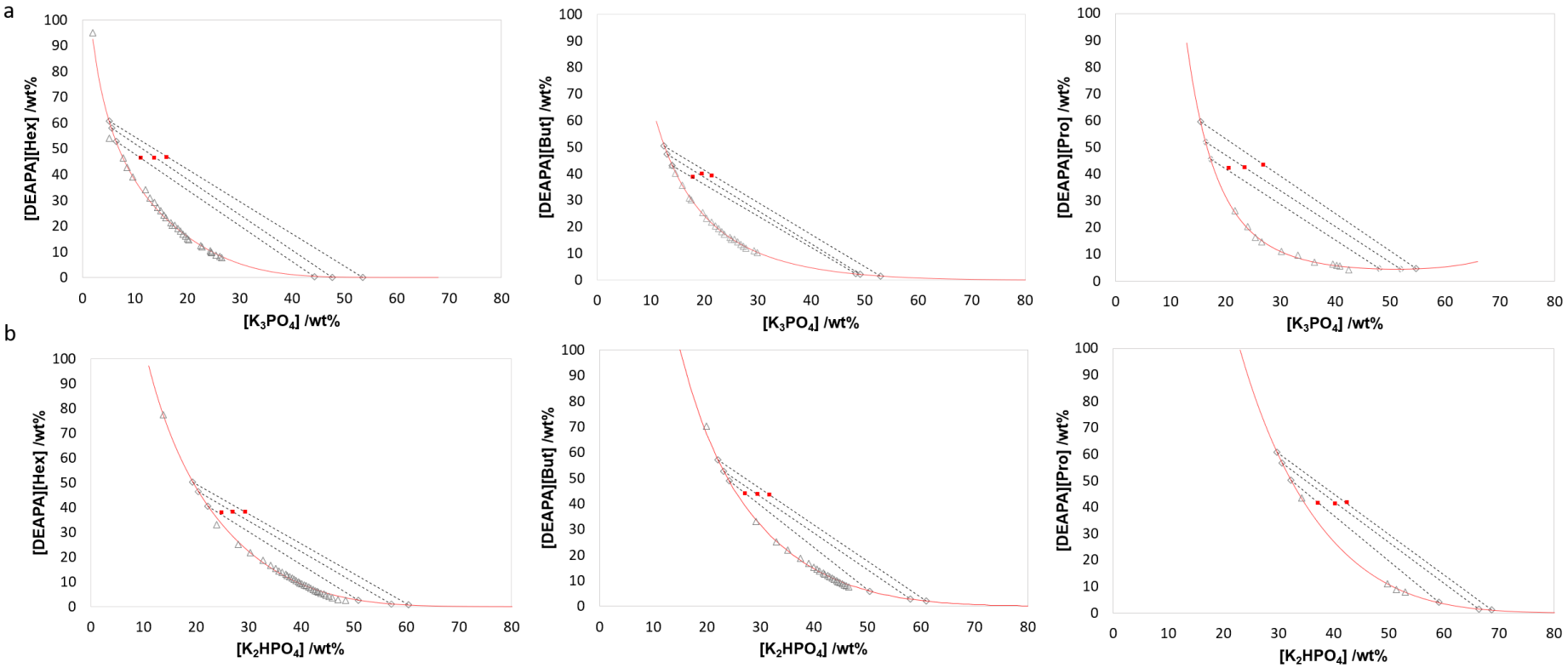

Figure C.1. Ternary phase diagrams for ABS composed of [DEAPA][X] + Salt (**a:** K_3PO_4 and **b:** K_2HPO_4) + H_2O, at T= 298 K and atmospheric pressure. binodal curve data (Δ); tie line experimental data (◊); total composition (■); fitted binodal curve using Equation (5.1) (–).

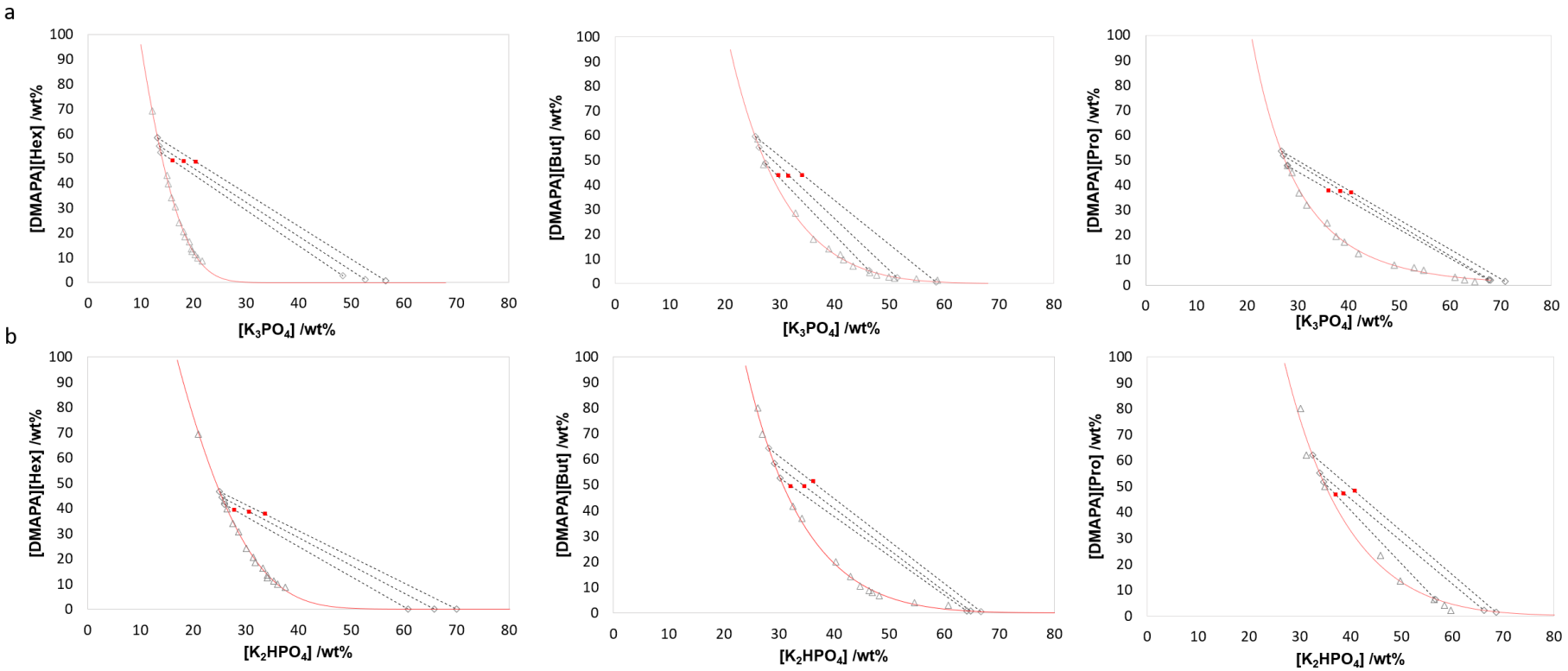

Figure C.2. Ternary phase diagrams for ABS composed of [DMAPA][X] + Salt (**a:** K_3PO_4 and **b:** K_2HPO_4) + H_2O, at T= 298 K and atmospheric pressure. binodal curve data (Δ); tie line experimental data (◊); total composition (■); fitted binodal curve using Equation (5.1) (−).

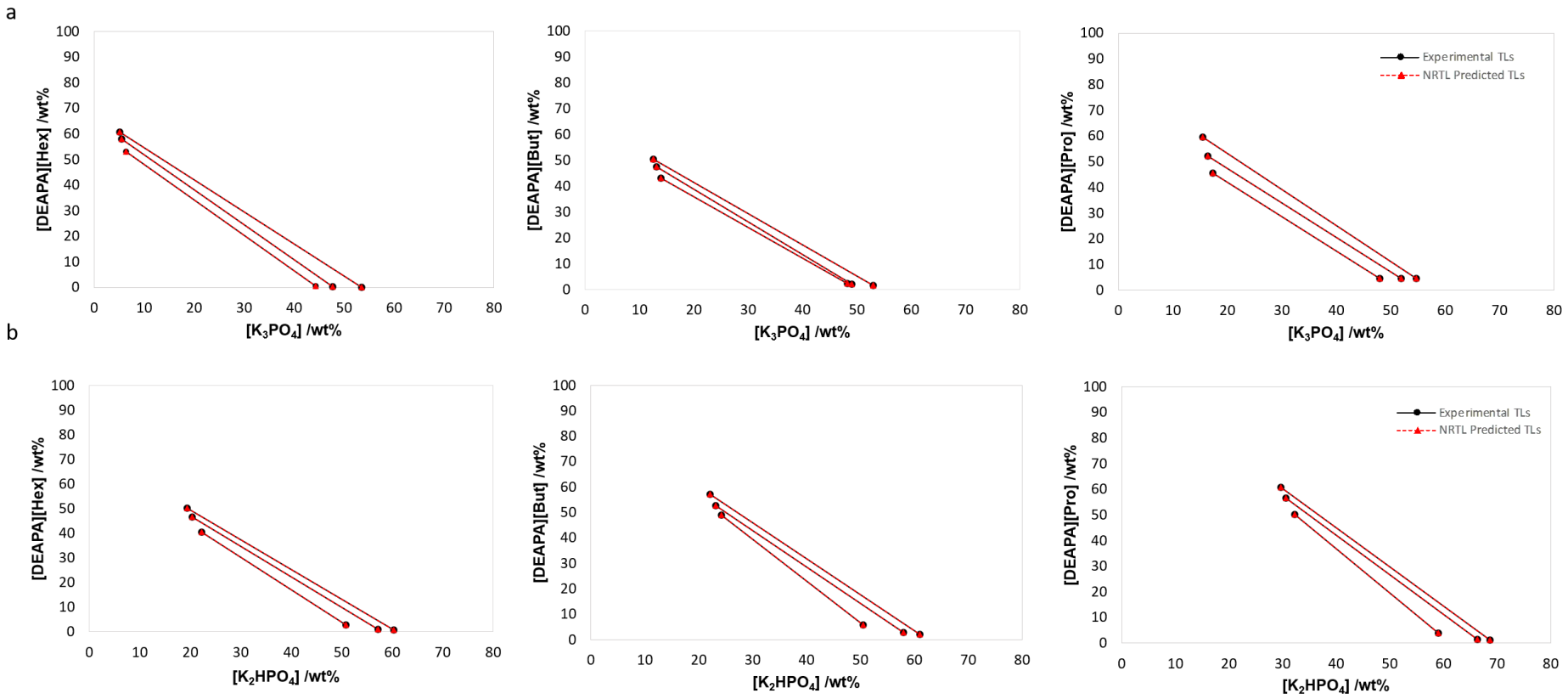

Figure C.3. Experimental and calculated tie-lines (by NRTL model) of the systems composed of DEAPA-based ILs + Salt (**a:** K_3PO_4 and **b:** K_2HPO_4) + H_2O at 298 K and atmospheric pressure.

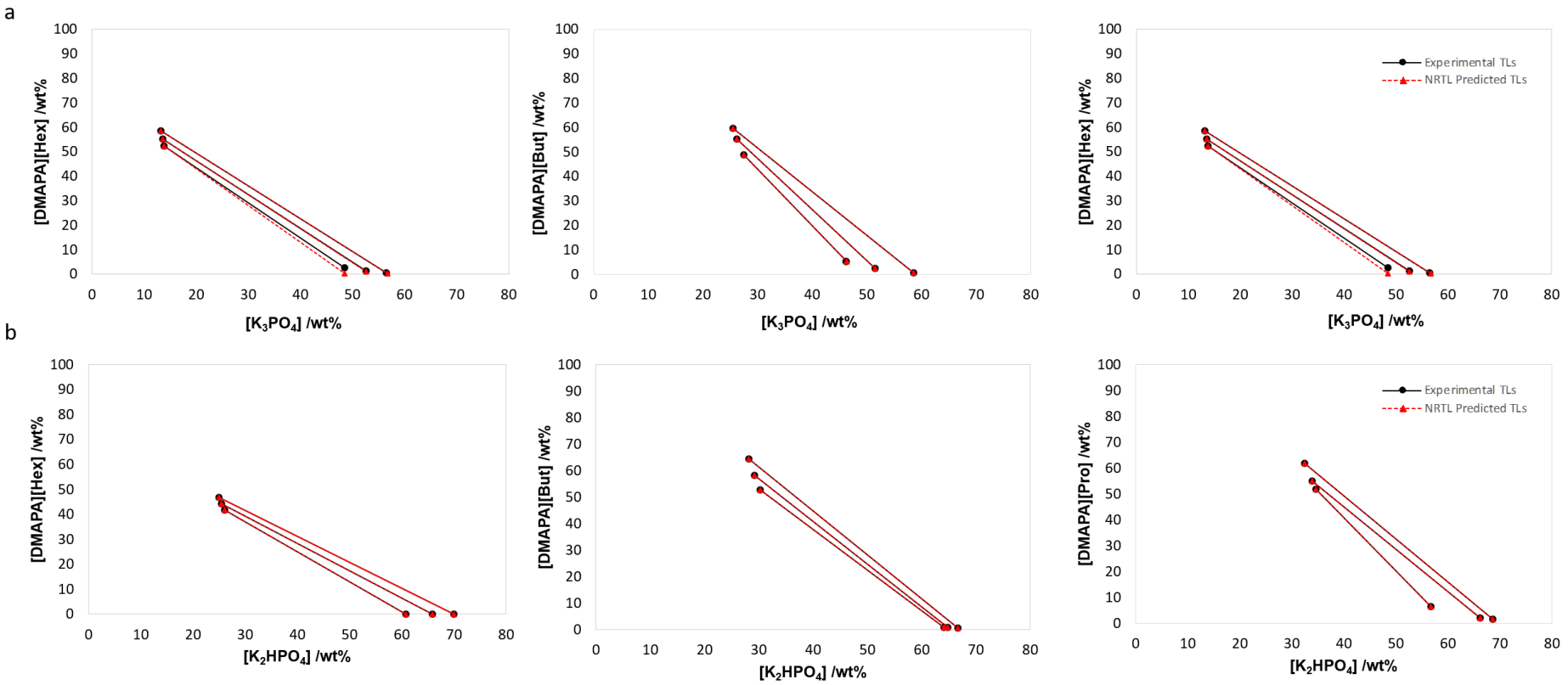

Figure C.4. Experimental and calculated tie-lines (by NRTL model) of the systems composed of DMAPA-based ILs + Salt (**a:** K_3PO_4 and **b:** K_2HPO_4) + H_2O at 298 K and atmospheric pressure.

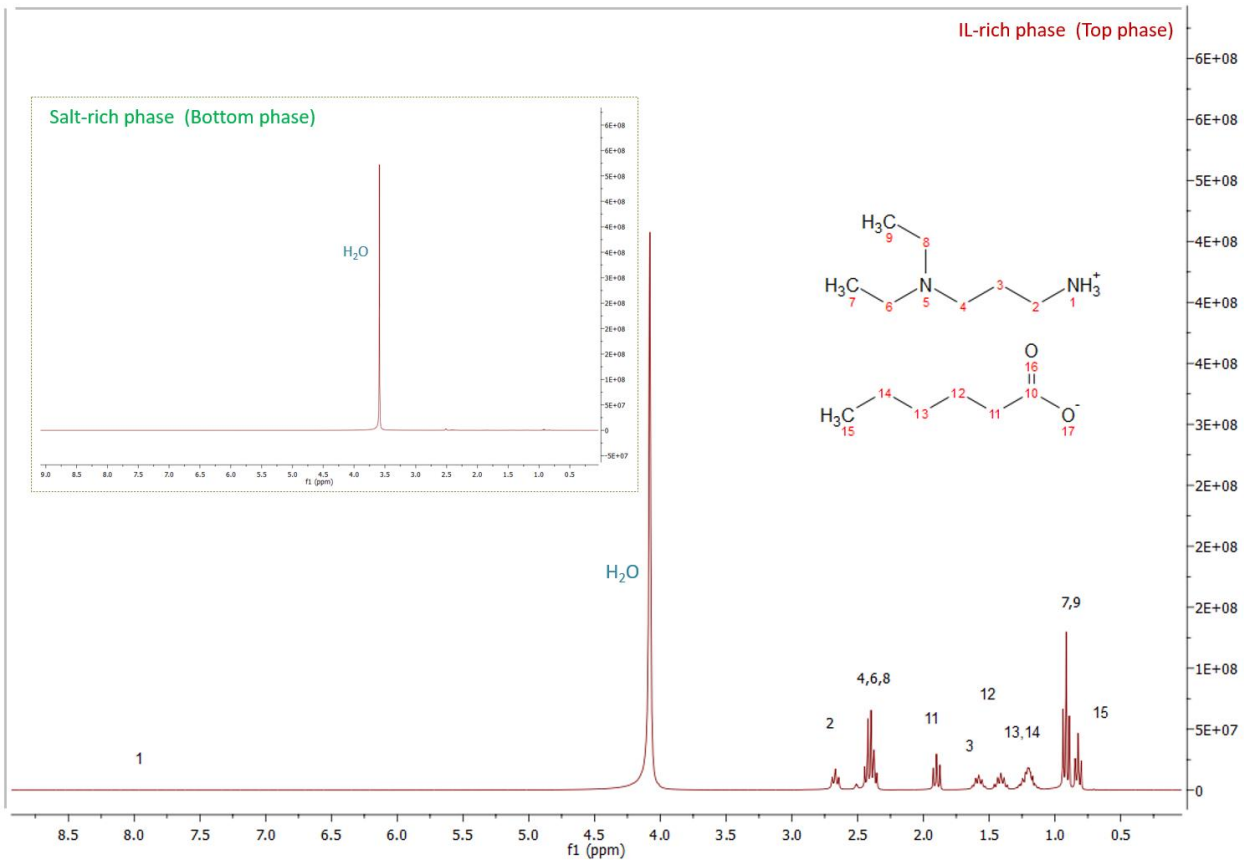

Figure C.5. ^{1}H NMR spectra of the IL (top)-rich phase and salt (bottom)-rich phase of the ABS composed of [DEAPA][Hex] + K_3PO_4 + H_2O at 298 K and atmospheric pressure.

Appendix D: *Supporting Information of Chapter 6*

Table D.1. Solvent properties used in the extraction processes.

Solvent	Formula	Abbr.	CAS Number	Purity (%)	Molecular weight (g/mol)	Density (g/cm^3) (25 °C)	Boiling point (°C)	Octanol/water partition coefficient (log K_{ow})	Supplier
Chloroform	$CHCl_3$	-	67-66-3	99 %	119.38	1.49	61.20	1.80	Fisher Scientific (Portugal)
Cyclohexane	C_6H_{12}	CH	110-82-7	≥99.7%	84.16	0.77	80.74	2.67	Sigma-Aldrich (Portugal)
Ethanol	C_2H_6O	EtOH	64-17-5	Analytical Grade	46.07	0.78	78.37	-0.31	Fisher Scientific (Portugal)
Ethyl acetate	$C_4H_8O_2$	EtOAc	141-78-6	Analytical grade	88.11	0.90	77.10	0.73	Fisher Scientific (Portugal)
Isopropanol	C_3H_8O	IPA	67-63-0	HPLC Grade	60.10	0.78	82.50	0.05	Fisher Scientific (Portugal)
Methanol	CH_4O	MeOH	67-56-1	HPLC grade	32.04	0.79	64.70	-0.77	Fisher Scientific (Portugal)
2-methyltetrahydrofuran	$C_5H_{10}O$	2-MeTHF	96-47-9	99%	86.13	0.85	80.20	0.94	Alfa Aesar (Germany)
Water	H_2O	H_2O	-	Ultrapure	18.01	0.99	100	-	-

Table D.2. Solvent compositions (% w/w) tested during the studies of solid–liquid extraction on carotenoids and lipids extraction from R. *glutinis* biomass at a wet cell concentration of 0.2 g/mL after 1 h stirring (300 rpm) at 65 °C.

Method	Methanol	Ethanol	Isopropanol	Ethyl acetate	2-methyltetrahydrofuran	Cyclohexane	Chloroform	Water
Single-step extraction								
MeOH	100	-	-	-	-	-	-	-
EtOH	-	100	-	-	-	-	-	-
IPA	-	-	100	-	-	-	-	-
EtOAc	-	-	-	100	-	-	-	-
2-MeTHF	-	-	-	-	100	-	-	-
CH	-	-	-	-	-	100	-	-
Solvent mixtures								
Control*	53	-	-	-	-	-	26	21
CH/MeOH	53	-	-	-	-	26	-	21
CH/EtOH	-	53	-	-	-	26	-	21
CH/IPA	-	-	53	-	-	26	-	21
CH/2-MeTHF	-	-	-	-	53	26	-	21
EtOAc/MeOH	53	-	-	26	-	-	-	21
EtOAc/EtOH	-	53	-	26	-	-	-	21
EtOAc/IPA	-	-	53	26	-	-	-	21
EtOAc/2-MeTHF	-	-	-	26	53	-	-	21
EtOAc/EtOH/H_2O optimization								
System A	-	0	-	100	-	-	-	0
System B	-	100	-	0	-	-	-	0
System C	-	0	-	0	-	-	-	100
System D	-	44	-	56	-	-	-	0
System E	-	41	-	18	-	-	-	41
System F	-	38	-	12	-	-	-	50
System G	-	27	-	73	-	-	-	0
System H	-	45	-	23	-	-	-	32
System I	-	55	-	24	-	-	-	21
System J	-	62	-	23	-	-	-	15
System K	-	19	-	77	-	-	-	5
System L		39		52				8
System M	-	44	-	0	-	-	-	56
System N	-	23	-	0	-	-	-	77
System O	-	58	-	34	-	-	-	7
System P	-	20	-	74	-	-	-	7
System Q	-	26	-	71	-	-	-	3
System R	-	40	-	25	-	-	-	35

* Reference system Bligh and Dyer method

Table D.3. Experimental data obtained for the study of carotenoids (β-carotene, torularhodin and torulene) and lipids recoveries using pure solvents at a wet cell concentration of 0.2 g/mL after 1 h stirring (300 rpm) at 65 °C.

Solvent	Recovery ± σ (%)			
	Lipids[1]	β-carotene[2]	Torularhodin[1]	Torulene[1]
MeOH	6.44 ± 0.04^{ab}	18.64 ± 0.19^{a}	24.29 ± 0.20^{b}	28.06 ± 0.35^{ab}
EtOH	4.37 ± 0.11^{ab}	15.85 ± 0.14^{b}	23.18 ± 0.11^{ab}	29.69 ± 0.06^{b}
IPA	8.31 ± 0.26^{ab}	14.39 ± 0.69^{c}	17.98 ± 0.73^{ab}	21.91 ± 0.35^{ab}
EtOAc	14.45 ± 0.20^{a}	2.80 ± 0.03^{e}	9.60 ± 0.20^{ab}	11.82 ± 0.21^{ab}
2-MeTHF	14.66 ± 0.69^{a}	7.41 ± 0.41^{d}	9.25 ± 0.20^{ab}	12.02 ± 0.38^{ab}
CH	2.40 ± 0.04^{b}	1.02 ± 0.19^{f}	3.96 ± 0.01^{a}	11.86 ± 0.50^{a}

[1]Multiple comparison test after Kruskal-Wallis (α = 0.05) and [2]Tukey HSD test (α = 0.05). *Mean of three independent assays ± confidence levels; means with the same lowercase letter does not present significant difference (p > 0.05).

Table D.4. Experimental data obtained for the study of carotenoids (β-carotene, torularhodin and torulene) and lipids recoveries using solvents mixtures at a wet cell concentration of 0.2 g/mL after 1 h stirring (300 rpm) at 65 °C.

Solvent	Recovery ± σ (%)			
	Lipids[2]	β-carotene[2]	Torularhodin[1]	Torulene[2]
Control	32.16 ± 0.03^{b}	8.20 ± 0.29^{d}	14.43 ± 0.15^{abc}	15.59 ± 0.09^{d}
CH-MeOH	19.78 ± 0.08^{d}	7.15 ± 0.39^{e}	13.12 ± 0.00^{abc}	15.42 ± 0.09^{d}
CH-EtOH	22.18 ± 0.23^{c}	6.43 ± 0.27^{e}	12.48 ± 0.11^{abc}	17.20 ± 0.09^{c}
CH-IPA	2.49 ± 0.08^{i}	10.68 ± 0.48^{c}	16.86 ± 0.11^{abc}	12.90 ± 0.19^{f}
CH-2-MeTHF	14.45 ± 0.15^{f}	2.43 ± 0.01^{f}	7.16 ± 0.11^{ab}	13.76 ± 0.19^{e}
EtOAc-MeOH	18.43 ± 0.08^{e}	24.61 ± 0.54^{b}	22.81 ± 0.19^{bc}	22.10 ± 0.09^{b}
EtOAc-EtOH	35.84 ± 0.23^{a}	32.27 ± 0.08^{a}	38.27 ± 0.79^{c}	23.95 ± 0.17^{a}
EtOAc-IPA	13.81 ± 0.04^{g}	24.81 ± 0.51^{b}	21.80 ± 0.29^{abc}	13.08 ± 0.35^{f}
EtOAc-2-MeTHF	8.72 ± 0.05^{h}	2.08 ± 0.13^{f}	5.45 ± 0.11^{a}	11.71 ± 0.02^{g}

[1]Multiple comparison test after Kruskal-Wallis (α = 0.05) and [2]Tukey HSD test (α = 0.05). *Mean of three independent assays ± confidence levels; means with the same lowercase letter does not present significant difference (p > 0.05).

Table D.5. Experimental data obtained for the study of carotenoids (β-carotene, torularhodin and torulene) and lipids recoveries using EtOAc/EtOH/H_2O mixtures at a wet cell concentration of 0.2 g/mL after 1 h stirring (300 rpm) at 65 °C.

System	Recovery ± σ (%)			
	Lipids[2]	β-carotene[1]	Torularhodin[1]	Torulene[2]
A	14.45 ± 0.20^{h}	2.80 ± 0.03^{a}	11.43 ± 0.44^{a}	11.53 ± 0.09^{l}
B	4.96 ± 0.38^{j}	15.85 ± 0.14^{abc}	24. 23 ± 0.11^{abc}	29.69 ± 0.06^{e}
C	4.37 ± 0.11^{j}	2.93 ± 0.00^{ab}	10.77 ± 1.63^{ab}	11.69 ± 0.10^{l}
D	17.04 ± 0.56^{g}	14.05 ± 0.06^{abc}	20.84 ± 0.07^{abc}	28.04 ± 0.17^{g}
E	16.27 ± 0.47^{gh}	32.27 ± 0.08^{abc}	38.27 ± 0.79^{abc}	39.14 ± 0.08^{d}
F	30.13 ± 0.42^{e}	9.65 ± 0.08^{abc}	16.43 ± 0.07^{abc}	26.34 ± 0.16^{h}
G	29.84 ± 0.80^{e}	8.84 ± 0.14^{abc}	17.03 ± 0.07^{abc}	24.59 ± 0.11^{i}
H	35.96 ± 0.64^{d}	46.93 ± 1.39^{c}	51.81 ± 0.28^{bc}	47.60 ± 0.19^{b}
I	55.75 ± 1.06^{a}	46.41 ± 0.27^{bc}	59.82 ± 0.11^{c}	50.99 ± 0.08^{a}
J	31.01 ± 0.32^{e}	31.21 ± 0.11^{abc}	40.28 ± 0.31^{abc}	40.07 ± 0.06^{c}
K	14.62 ± 0.36^{h}	4.07 ± 0.06^{abc}	15.59 ± 0.07^{abc}	22.92 ± 0.11^{k}
L	9.33 ± 0.85^{i}	12.21 ± 0.11^{abc}	19.37 ± 0.04^{abc}	26.60 ± 0.02^{h}
M	46.52 ± 0.38^{c}	17.89 ± 0.05^{abc}	23.73 ± 0.07^{abc}	29.29 ± 0.06^{f}
N	50.84 ± 0.51^{b}	17.82 ± 0.20^{abc}	22.53 ± 0.04^{abc}	29.10 ± 0.04^{f}
O	48.07 ± 2.19^{c}	14.65 ± 0.37^{abc}	22.69 ± 0.43^{abc}	28.34 ± 0.10^{g}
P	33.91 ± 0.02^{d}	13.31 ± 0.05^{abc}	21.67 ± 0.07^{abc}	28.26 ± 0.16^{g}
Q	25.61 ± 0.41^{f}	6.11 ± 0.13^{abc}	15.59 ± 0.76^{abc}	23.46 ± 0.17^{j}
R	35.30 ± 0.66^{d}	19.15 ± 0.20^{abc}	20.73 ± 0.04^{abc}	29.76 ± 0.06^{e}

[1]Multiple comparison test after Kruskal-Wallis (α = 0.05) and [2]Tukey HSD test (α = 0.05). *Mean of three independent assays ± confidence levels; means with the same lowercase letter does not present significant difference (p > 0.05).

Table D.6. Points compositions in the ternary phase diagram and extraction parameters [partition coefficient (K) and extraction efficiency (EE) (%)] of EtOAc/EtOH/H_2O liquid-liquid systems (LLE) used for carotenoids (β-carotene, torularhodin and torulene) and lipids separation at a wet cell concentration of 0.2 g/mL after 1 h stirring (300 rpm) at 65 °C.

System	Points (% w/w)			EE% ± σ (%) / K ± σ			
	EtOAc	EtOH	H_2O	Lipids[1]	β-carotene[2]	Torularhodin[2]	Torulene[2]
a	15	27	58	63.60 ± 0.23^{a}/ 3.70 ± 0.60^{a}	84.73 ± 0.26^{a}/ 2.27 ± 0.04^{a}	84.44 ± 0.27^{a}/ 2.21 ± 0.03^{a}	91.66 ± 0.40^{a}/ 2.51 ± 0.21^{a}
b	33	30	37	81.91 ± 0.05^{ab}/ 3.46 ± 0.00^{a}	60.16 ± 0.38^{c}/ 2.32 ± 0.02^{a}	59.61 ± 0.38^{c}/ 2.26 ± 0.02^{a}	60.41 ± 0.18^{c}/ 2.40 ± 0.11^{a}
c	15	24	61	60.00 ± 3.99^{a}/ 3.77 ± 0.48^{a}	80.67 ± 0.32^{b}/ 2.31 ± 0.02^{a}	80.31 ± 0.32^{b}/ 2.26 ± 0.02^{a}	82.50 ± 0.67^{b}/ 2.31 ± 0.01^{a}
d	35	30	35	88.39 ± 0.01^{ab}/ 3.01 ± 0.01^{a}	51.27 ± 0.25^{d}/ 2.09 ± 0.04^{b}	50.70 ± 0.25^{d}/ 2.04 ± 0.04^{b}	52.51 ± 2.05^{d}/ 2.24 ± 0.08^{a}
e	13	15	72	87.52 ± 0.50^{ab}/ 2.72 ± 0.03^{a}	51.00 ± 0.27^{d}/ 1.22 ± 0.02^{c}	50.43 ± 0.27^{d}/ 1.19 ± 0.02^{c}	50.48 ± 1.04^{e}/ 2.19 ± 0.09^{a}
f	48	24	28	89.56 ± 0.08^{b}/ 2.82 ± 0.11^{a}	33.32 ± 0.32^{e}/ 1.17 ± 0.02^{c}	32.81 ± 0.32^{e}/ 1.14 ± 0.02^{c}	48.57 ± 0.91^{e}/ 2.32 ± 0.12^{a}

[1]Multiple comparison test after Kruskal-Wallis (α = 0.05) and [2]Tukey HSD test (α = 0.05). *Mean of three independent assays ± confidence levels; means with the same lowercase letter does not present significant difference (p > 0.05).

Table D.7. Inputs of chemicals, water and electricity to obtain extracted carotenoids (β-carotene, torularhodin, torulene) and lipids in the three scenarios under study. Scenario 1- EtOAc and EtOH/H_2O-rich phases were evaporated to reuse, and cold acetone were added to the system to separate proteins from lipids; Scenario 2- EtOAc was evaporated, and EtOH/H_2O- rich phase were submitted to an second LLE procedure to separate proteins from lipids; Scenario 3- Control using conventional Bligh and Dyer method.

	Unit	Scenario 1	Scenario 2	Scenario 3
Inputs				
		Biomass Production		
Bacteriological peptone	g	3.48	3.48	3.48
Yeast extract	g	1.74	1.74	1.74
Glucose	g	1.74	1.74	1.74
KH_2PO_4	g	0.09	0.09	0.09
$MgSO_4$	g	0.09	0.09	0.09
NH_4NO_3	g	0.70	0.70	0.70
Asparagine	g	1.74	1.74	1.74
Water - distilled	mL	0.17	0.17	0.17
Electricity	Wh	6201	6201	6201
		Solid-Liquid Extraction		
Ethyl acetate	mL	1.15	1.15	-
Ethanol	mL	2.95	2.95	-
Water - distilled	mL	0.9	0.9	0.8
Chlroform	mL	-	-	1
Methanol		-	-	2
Electricity	Wh	1025	1025	1025
		Purification		
Ethyl acetate	mL	3	3	-
Ethanol	mL	2	2	-
Water - distilled	mL	10	10	1
Chloroform	mL	-	-	1
Electricity	Wh	650		
		Polishing		
Ethyl acetate	mL	-	2.5	
Acetone	mL	15	-	15
Electricity	Wh	652.5	652.5	652.5
Outputs				
β-carotene	μg	80.15	78.44	15.56
Torularhodin	μg	62.50	56.20	15.06
Torulene	μg	17.20	15.16	6.13
Lipids	mg	105.91	106.17	70.90

Table D.8. GHG emission factors used in the calculation of the carbon footprint and name of the processes in Ecoinvent 3.6.

Input	Reference unit	GHG emissions (g $CO_{2\ eq}$/reference unit)[a]	Name of the process in Ecoinvent
Bacteriological Peptone	g	1.917	Chemical production, organic, global
Yeast extract	g	2.961	Ethanol production from whey, rest of the world
Glucose	g	1.095	Glucose production, Europe
KH_2PO_4	g	0.263	Potassium chloride, Europe
$MgSO_4$	g	0.234	Magnesium sulfate production, Europe
NH_4NO_3	g	2.776	Ammonium nitrate production, Europe
Asparagine	g	1.917	Chemical production, organic, global
Ethyl acetate	g	2.572	Ethyl acetate production, Europe
Ethanol	g	1.083	Ethanol, in 95% solution state, from fermentation, rest of the world
Chloroform	g	3.302	Trichloromethane production, Europe
Methanol	g	0.616	Methanol production, global
Acetone	g	2.317	Acetone production, liquid, Europe
Water - distilled	mL	0.300	Not applicable[b]
Electricity	Wh	0.399	Market for electricity, low voltage, Portugal

[a] Considering global warming potentials for converting the mass of each GHG into mass of $CO_{2\ eq}$ from Myhre *at al*. (Myhre at al 2013) for a time horizon of 100 years.

[b] GHG emissions are the sum of GHG emissions from tap water production (Lemos et al 2013) and GHG emissions from electricity consumption during the distillation process.

Table D.9. Excess enthalpies ($J \cdot mol^{-1}$) of (Ethanol + H_2O + Ethyl Acetate + Solute) predicted using COSMO-RS.

	EtOH			H_2O			EtOAc			Solute		
No	H_{MF}	H_{HB}	H_{VdW}	H_{MF}	H_{HB}	H_{VdW}	H_{MF}	H_{HB}	H_{VdW}	H_{MF}	H_{HB}	H_{VdW}
						β-carotene						
1	0.00	0.00	0.00	0.00	0.00	0.00	-0.06	0.00	-0.03	0.08	0.00	0.02
2	-0.16	0.40	-0.11	0.00	0.00	0.00	0.00	0.00	0.00	0.29	-0.00	0.10
3	0.00	0.00	0.00	0.01	0.18	-0.25	0.00	0.00	0.00	0.16	0.00	0.11
4	411.90	1762.20	59.89	0.00	0.00	0.00	-351.81	-1021.79	-51.81	0.33	-0.00	0.10
5	-25.25	-452.28	97.59	106.42	784.75	-334.04	-232.04	-849.45	60.21	0.88	-0.00	0.43
6	-10.40	-382.63	90.88	57.41	497.07	-330.99	-137.00	-572.10	61.83	0.31	0.00	0.17
7	441.61	2060.88	59.08	0.00	0.00	0.00	-361.26	-1151.49	-50.86	0.22	0.00	0.07
8	-78.45	-714.41	119.91	124.22	683.82	-298.47	-167.36	-539.84	20.63	1.11	-0.00	0.52
9	-64.87	-594.63	106.39	133.23	692.51	-235.87	-185.39	-556.79	6.74	1.02	-0.00	0.44
10	-47.06	-470.49	93.47	122.59	609.80	-188.07	-173.08	-498.40	-2.19	0.66	-0.00	0.27
11	249.57	1069.26	56.36	123.34	913.57	-97.21	-400.89	-1411.35	-1.70	0.11	0.00	0.03
12	170.00	520.07	79.76	122.34	765.67	-133.01	-365.83	-1124.35	-9.08	0.29	0.00	0.10
13	-83.69	-871.98	152.06	72.23	298.72	-338.39	0.00	0.00	0.00	0.49	-0.00	0.27
14	0.00	0.00	0.00	10.25	327.83	-226.06	-95.75	-563.62	103.58	0.75	-0.00	0.46
15	110.11	261.46	73.72	91.39	491.22	-106.81	-255.91	-724.76	-17.78	0.32	-0.00	0.11
16	201.62	787.54	59.97	150.44	1107.15	-133.62	-422.91	-1481.19	12.05	0.35	-0.00	0.12
17	306.58	1301.83	64.16	88.71	621.92	-71.26	-396.84	-1306.07	-21.58	0.16	0.00	0.05
18	-28.38	-476.35	100.76	102.88	747.23	-334.89	-217.36	-796.04	57.16	0.52	-0.00	0.26
						Torularhodin						
1	0.00	0.00	0.00	0.00	0.00	0.00	-0.23	-0.17	-0.08	0.20	0.09	0.08
2	-0.09	0.52	-0.09	0.00	0.00	0.00	0.00	0.00	0.00	0.14	-0.19	0.10
3	0.00	0.00	0.00	0.02	0.73	-0.96	0.00	0.00	0.00	0.35	-0.14	0.42
4	411.88	1762.16	59.89	0.00	0.00	0.00	-351.82	-1021.78	-51.81	0.25	-0.08	0.12
5	-25.18	-452.19	97.60	106.40	785.00	-334.02	-231.98	-849.37	60.21	0.43	-0.67	0.45
6	-10.40	-382.57	90.86	57.44	497.37	-331.05	-137.00	-572.06	61.80	0.23	-0.20	0.26

7	441.57	2060.79	59.07	0.00	0.00	0.00	-361.32	-1151.50	-50.88	0.24	-0.02	0.11
8	-78.26	-714.25	119.97	124.19	684.02	-298.44	-167.30	-539.79	20.65	0.46	-0.84	0.50
9	-64.71	-594.32	106.41	133.21	692.74	-235.86	-185.34	-556.73	6.75	0.50	-0.81	0.47
10	-46.95	-470.28	93.49	122.58	609.90	-188.07	-173.05	-498.37	-2.19	0.33	-0.49	0.28
11	249.53	1069.24	56.34	123.34	913.55	-97.21	-401.00	-1411.32	-1.76	0.22	-0.04	0.11
12	170.00	520.11	79.76	122.33	765.68	-133.00	-365.83	-1124.32	-9.08	0.22	-0.15	0.13
13	-83.64	-871.85	152.04	72.24	298.99	-338.39	0.00	0.00	0.00	0.25	-0.38	0.32
14	0.00	0.00	0.00	10.25	328.12	-226.12	-95.73	-563.57	103.56	0.49	-0.38	0.55
15	110.12	261.57	73.71	91.39	491.25	-106.80	-255.91	-724.73	-17.78	0.21	-0.20	0.14
16	201.60	787.52	59.97	150.43	1107.13	-133.62	-422.94	-1481.17	12.03	0.30	-0.10	0.15
17	306.53	1301.81	64.14	88.70	621.91	-71.26	-396.91	-1306.06	-21.61	0.21	-0.05	0.10
18	-28.33	-476.31	100.77	102.87	747.33	-334.88	-217.32	-796.01	57.16	0.23	-0.37	0.25
						Torulene						
1	0.00	0.00	0.00	0.00	0.00	0.00	-0.28	0.00	-0.12	0.30	-0.00	0.10
2	-0.19	0.58	-0.16	0.00	0.00	0.00	0.00	0.00	0.00	0.46	-0.00	0.14
3	0.00	0.00	0.00	0.04	0.81	-1.13	0.00	0.00	0.00	0.41	-0.00	0.45
4	411.79	1762.33	59.83	0.00	0.00	0.00	-351.92	-1021.73	-51.86	0.58	-0.00	0.21
5	-25.26	-452.19	97.55	106.46	784.99	-334.09	-232.06	-849.40	60.17	0.94	-0.00	0.53
6	-10.49	-382.50	90.77	57.54	497.77	-331.21	-137.08	-572.01	61.73	0.74	-0.00	0.47
7	441.51	2060.93	59.03	0.00	0.00	0.00	-361.46	-1151.42	-50.95	0.56	-0.00	0.19
8	-78.40	-714.37	119.91	124.22	683.87	-298.46	-167.35	-539.83	20.63	0.99	-0.00	0.53
9	-64.85	-594.52	106.37	133.23	692.59	-235.87	-185.38	-556.77	6.73	0.98	-0.00	0.48
10	-47.09	-470.29	93.41	122.60	609.89	-188.08	-173.10	-498.38	-2.21	0.74	-0.00	0.35
11	249.48	1069.32	56.31	123.35	913.59	-97.22	-401.16	-1411.24	-1.84	0.54	-0.00	0.19
12	169.90	520.23	79.70	122.35	765.72	-133.01	-365.93	-1124.27	-9.14	0.55	-0.00	0.22
13	-83.77	-871.77	151.93	72.31	299.18	-338.49	0.00	0.00	0.00	0.70	-0.00	0.45
14	0.00	0.00	0.00	10.33	328.52	-226.46	-95.84	-563.55	103.45	0.79	-0.00	0.76
15	110.01	261.70	73.64	91.40	491.27	-106.81	-255.96	-724.71	-17.82	0.54	-0.00	0.22
16	201.55	787.60	59.93	150.45	1107.18	-133.63	-423.10	-1481.09	11.94	0.66	-0.00	0.25
17	306.47	1301.91	64.10	88.71	621.93	-71.26	-397.05	-1305.98	-21.69	0.53	-0.00	0.19
18	-28.43	-476.23	100.69	102.95	747.57	-334.96	-217.41	-795.97	57.09	0.72	-0.00	0.41

						Margaric acid						
1	0.00	0.00	0.00	0.00	0.00	0.00	-0.31	0.00	-0.09	0.42	0.00	0.10
2	-0.03	0.18	-0.02	0.00	0.00	0.00	0.00	0.00	0.00	0.06	-0.07	0.02
3	0.00	0.00	0.00	0.01	0.24	-0.41	0.00	0.00	0.00	0.22	-0.17	0.17
4	411.87	1762.29	59.90	0.00	0.00	0.00	-351.79	-1021.70	-51.79	0.36	-0.14	0.09
5	-25.15	-452.37	97.70	106.34	784.40	-333.92	-231.94	-849.47	60.32	0.36	-0.41	0.20
6	-10.58	-382.42	90.76	57.57	497.91	-331.20	-137.11	-571.91	61.73	0.78	-0.91	0.48
7	441.47	2060.96	59.04	0.00	0.00	0.00	-361.46	-1151.27	-50.91	0.71	-0.18	0.18
8	-78.36	-714.35	120.05	124.20	683.73	-298.38	-167.30	-539.78	20.69	0.65	-0.82	0.33
9	-64.90	-594.03	106.43	133.27	692.75	-235.83	-185.35	-556.61	6.77	0.93	-1.06	0.40
10	-47.02	-470.21	93.53	122.60	609.86	-188.05	-173.05	-498.33	-2.17	0.50	-0.54	0.20
11	249.52	1069.31	56.34	123.34	913.57	-97.21	-401.01	-1411.21	-1.74	0.36	-0.11	0.10
12	170.03	520.09	79.79	122.34	765.66	-133.00	-365.78	-1124.31	-9.05	0.20	-0.12	0.06
13	-84.10	-871.28	151.78	72.42	299.83	-338.56	0.00	0.00	0.00	0.96	-1.41	0.61
14	0.00	0.00	0.00	10.46	329.49	-227.17	-96.15	-563.28	103.22	1.93	-1.78	1.28
15	109.86	262.36	73.60	91.42	491.36	-106.80	-255.97	-724.49	-17.81	0.85	-0.65	0.27
16	201.52	787.68	59.94	150.46	1107.19	-133.62	-423.09	-1480.86	11.99	0.82	-0.31	0.24
17	306.45	1301.95	64.11	88.71	621.93	-71.26	-397.01	-1305.84	-21.64	0.61	-0.21	0.17
18	-28.52	-476.06	100.68	103.00	747.78	-334.93	-217.43	-795.80	57.10	0.76	-0.90	0.42
						Glyceryl-1,3-dilinoleate						
1	0.00	0.00	0.00	0.00	0.00	0.00	-0.28	-0.09	-0.08	0.34	0.05	0.10
2	-0.02	0.17	-0.02	0.00	0.00	0.00	0.00	0.00	0.00	0.05	-0.08	0.02
3	0.00	0.00	0.00	0.01	0.25	-0.38	0.00	0.00	0.00	0.18	-0.19	0.15
4	411.91	1762.29	59.91	0.00	0.00	0.00	-351.79	-1021.76	-51.79	0.28	-0.17	0.09
5	-25.13	-452.39	97.71	106.33	784.43	-333.93	-231.92	-849.51	60.33	0.26	-0.46	0.18
6	-10.53	-382.45	90.78	57.54	497.93	-331.20	-137.08	-571.95	61.74	0.57	-1.01	0.45
7	441.51	2060.99	59.05	0.00	0.00	0.00	-361.44	-1151.41	-50.90	0.57	-0.20	0.17
8	-78.29	-714.43	120.07	124.18	683.76	-298.40	-167.29	-539.83	20.70	0.46	-0.93	0.31
9	-64.79	-594.17	106.46	133.25	692.80	-235.85	-185.34	-556.70	6.77	0.66	-1.22	0.38
10	-46.96	-470.30	93.55	122.59	609.88	-188.06	-173.05	-498.38	-2.17	0.36	-0.62	0.19
11	249.53	1069.31	56.34	123.34	913.59	-97.21	-400.99	-1411.29	-1.74	0.28	-0.12	0.09

12	170.04	520.09	79.79	122.34	765.68	-133.00	-365.78	-1124.34	-9.04	0.15	-0.14	0.06
13	-83.97	-871.39	151.83	72.39	299.83	-338.56	0.00	0.00	0.00	0.67	-1.56	0.57
14	0.00	0.00	0.00	10.42	329.50	-227.05	-96.05	-563.35	103.28	1.48	-1.94	1.19
15	109.95	262.26	73.62	91.42	491.39	-106.81	-255.97	-724.60	-17.81	0.63	-0.76	0.26
16	201.55	787.68	59.95	150.46	1107.24	-133.63	-423.06	-1481.03	12.00	0.64	-0.35	0.23
17	306.48	1301.96	64.12	88.71	621.95	-71.26	-396.99	-1305.96	-21.63	0.48	-0.23	0.16
18	-28.46	-476.11	100.70	102.97	747.80	-334.94	-217.40	-795.87	57.12	0.55	-1.00	0.40
						Trilinolenin						
1	0.00	0.00	0.00	0.00	0.00	0.00	0.00	-0.41	-0.31	0.00	-0.09	0.42
2	-0.03	0.16	-0.02	0.00	0.00	0.00	0.00	0.00	0.00	0.00	0.00	0.07
3	0.00	0.00	0.00	-0.14	0.01	0.27	-0.42	0.00	0.00	0.00	0.00	0.23
4	411.89	1762.34	59.90	0.00	0.00	0.00	0.00	-1434.54	-351.82	-1021.76	-51.79	0.37
5	-25.15	-452.39	97.70	556.84	106.34	784.45	-333.94	-1031.21	-231.94	-849.52	60.32	0.38
6	-10.56	-382.45	90.76	224.32	57.58	497.98	-331.24	-654.23	-137.11	-571.96	61.73	0.82
7	441.50	2061.08	59.04	0.00	0.00	0.00	0.00	-1574.43	-361.49	-1151.38	-50.91	0.72
8	-78.35	-714.45	120.05	509.56	124.20	683.78	-298.42	-692.61	-167.31	-539.84	20.69	0.70
9	-64.89	-594.19	106.43	590.23	133.28	692.82	-235.87	-741.33	-185.38	-556.71	6.76	1.00
10	-47.02	-470.30	93.53	544.43	122.60	609.89	-188.07	-678.78	-173.06	-498.38	-2.17	0.54
11	249.53	1069.34	56.34	939.73	123.35	913.60	-97.21	-1828.71	-401.02	-1411.27	-1.75	0.37
12	170.03	520.09	79.79	755.01	122.34	765.68	-133.01	-1510.58	-365.79	-1124.35	-9.05	0.21
13	-84.07	-871.39	151.79	33.74	72.44	299.92	-338.61	0.00	0.00	0.00	0.00	1.03
14	0.00	0.00	0.00	112.97	10.48	329.73	-227.23	-562.80	-96.14	-563.36	103.23	1.97
15	109.87	262.30	73.60	476.02	91.43	491.41	-106.81	-1005.47	-256.01	-724.60	-17.82	0.90
16	201.53	787.72	59.94	1124.10	150.47	1107.27	-133.63	-1907.87	-423.14	-1481.01	11.98	0.83
17	306.47	1302.01	64.12	639.42	88.72	621.96	-71.26	-1737.63	-397.04	-1305.94	-21.64	0.62
18	-28.50	-476.12	100.68	515.87	103.00	747.85	-334.97	-965.67	-217.44	-795.89	57.10	0.81

Table D.10. Characteristics, nature, and sources of the solvents under study, updated from GSK Solvent Sustainability Guide and CHEM21 solvent guide.

Solvent	Incineration	Recycle	Biotreatment	VOC emissions	Health Hazard	Environmental Impact		Life Cycle Analysis	Ranking by default (CHEM21 solvent guide)	Bio-source, *i.e.*, obtained:
						Aqueous	Air			
Chloroform	3	9	5	3	4	7	5	6	Problematic	No bio-sources. Chloroform are obtained from chlorination of methane & chlorination of methyl chloride, produced by the reaction of methanol and hydrogen chloride, are the two common methods for commercial chloroform production (Deshon 1979).
Cyclohexane (CH)	10	6	5	4	10	3	5	7	Problematic	From lignin degradation compounds over $Ni/ZrO_2–SiO_2$ catalysts (Zhang et al. 2020). From oleic acid via either a six- or eight-step enzyme cascade involving hydration, oxidation, hydrolysis and decarboxylation, followed by ring-closing metathesis (Wu et al. 2019).
Ethanol (EtOH)	5	5	3	4	10	9	5	-	Recommended	From several feedstocks: beets, corn, molasses, potatoes and other starchy materials such as wheat, barley, oat and rice; or even from lignocellulosic materials such as agricultural wastes and woody materials (Rudlf et al. 2009).
Ethyl acetate (EtOAc)	5	6	5	4	10	9	5	6	Recommended	From esterification, acetaldehyde condensation, ethylene adduct and ethanol dehydrogenation. For all these processes, the primary feedstock is ethanol, which may be obtained from renewable raw materials by fermentation) (Riemenschneider 2000, Bomgardner 2016.
Isopropanol (IPA)	5	5	3	5	10	8	7	4	Recommended	From anaerobic bacteria (*Clostridia*) fermentation, which convert carbohydrate-containing (waste)streams into IPA, *via* chemical and enzymatic conversion. From the hydrogenolysis of glycerol (Zhu et al. 2012).
Methanol (MeOH)	4	7	3	3	4	10	7	9	Problematic	From methanotrophic bacteria *Methylosinus trichosporium* fermentation, which produce methanol by the oxidation of methane to methanol (Duan et al. 2011, Lee et al. 2004).
2-methyl-tetrahydrofuran (2-MeTHF)	6	5	3	4	4	7	4	4	Problematic	From bioconversion renewable resources, namely, cellulose, hemicelluloses, and lignin. These raw materials are convenient transformed into levulinic acid or furfural, and both can be converted into 2-MeTHF (Al-Shaal et al. 2014, Hu et al. 2015, Amenuvor et al. 2016).
Water (H_2O)	4	2	4	6	10	10	8	10	Recommended	-

Few Know Issues **Some Know Issues** **Major Know Issues**

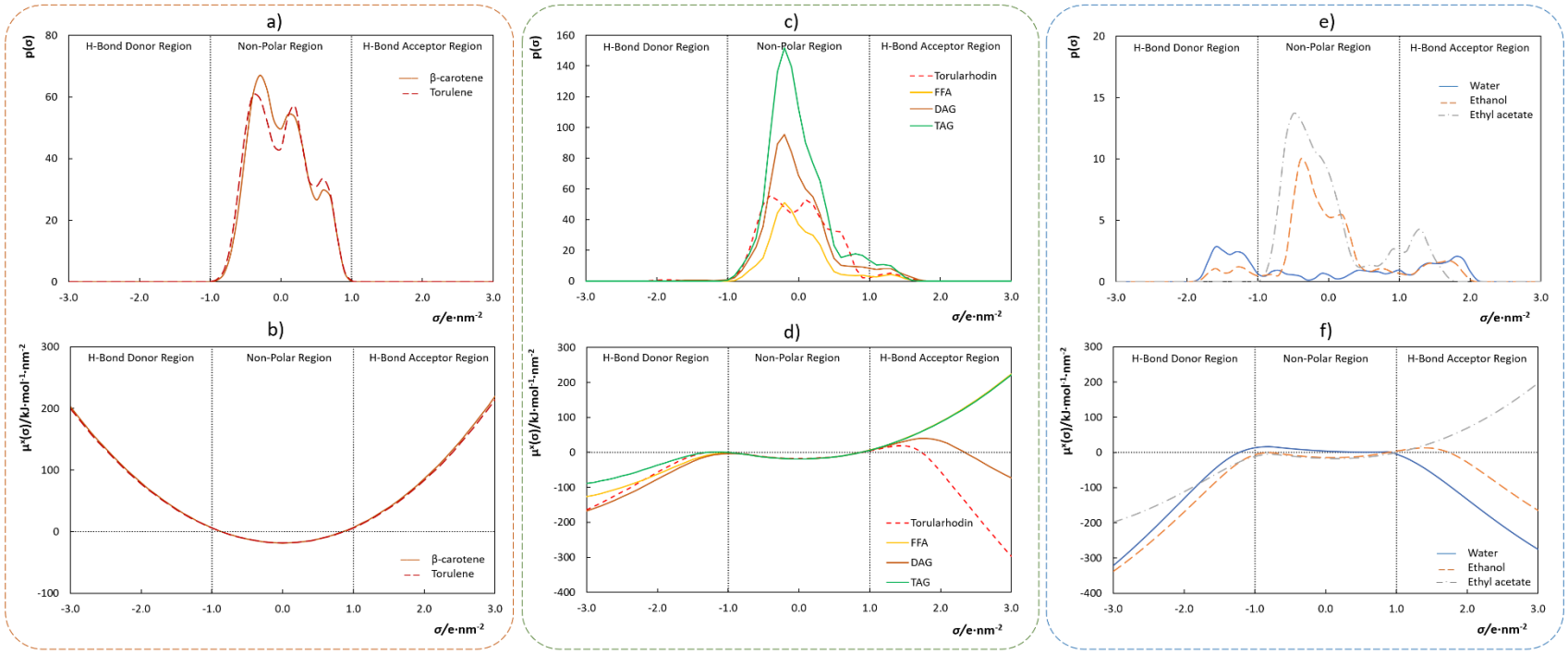

Figure D.1. Sigma profile (**a, c, e**) and potential (**b, d, f**) of solutes (β-carotene, torulene, torularhodin, FFA: free fatty acids (margaric acid), TAG: triglyceride (Trilinolenin) and DAG: diglyceride (Glyceryl-1,3-dilinoleate)) and solvents (EtOH, EtOAc and H_2O) at 298.15 K.

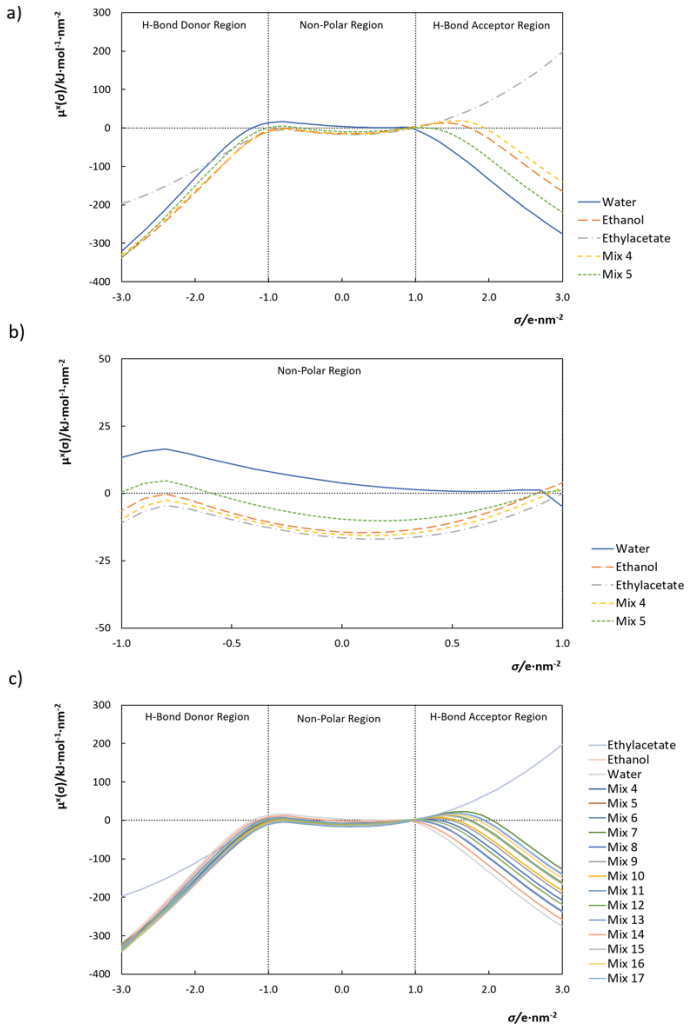

Figure D.2. Sigma potential of pure (EtOAc (A), EtOH (B) and H_2O (C)) and solvent mixtures (Mix 4 (D), Mix 5 (E), Mix 6 (F), Mix 7 (G), Mix 8 (H), Mix 9 (I), Mix 10 (J), Mix 11 (K), Mix 12 (L), Mix 13 (M), Mix 14 (N), Mix 15 (O), Mix 16 (P), Mix 17 (Q)) at 298.15 K. Different capital letters in brackets correspond to mixture points identified in the ternary phase diagram.

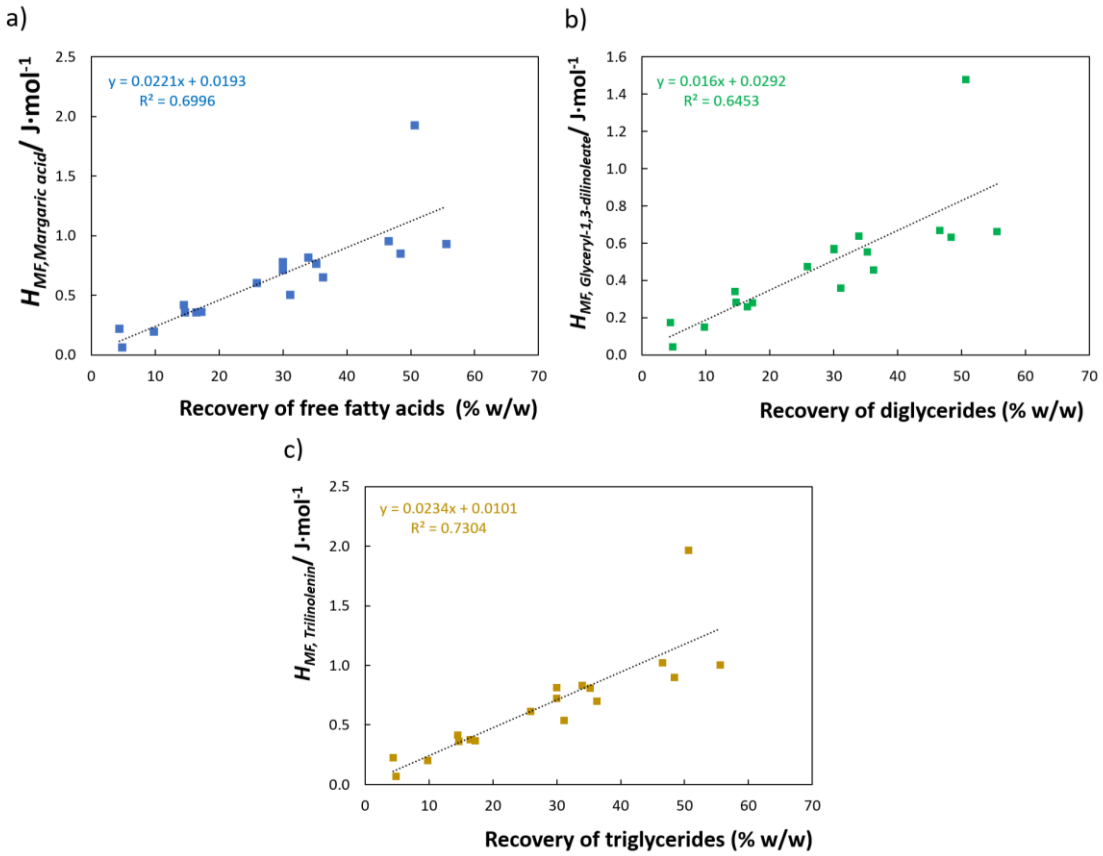

Figure D.3 Correlation plot between the interaction energies (X-axis) of solvents mixtures and the recoveries (% w/w) of a) (■) margaric acid, b) (■) glyceryl-1,3-dilinoleate and c) (■) trilinolein.

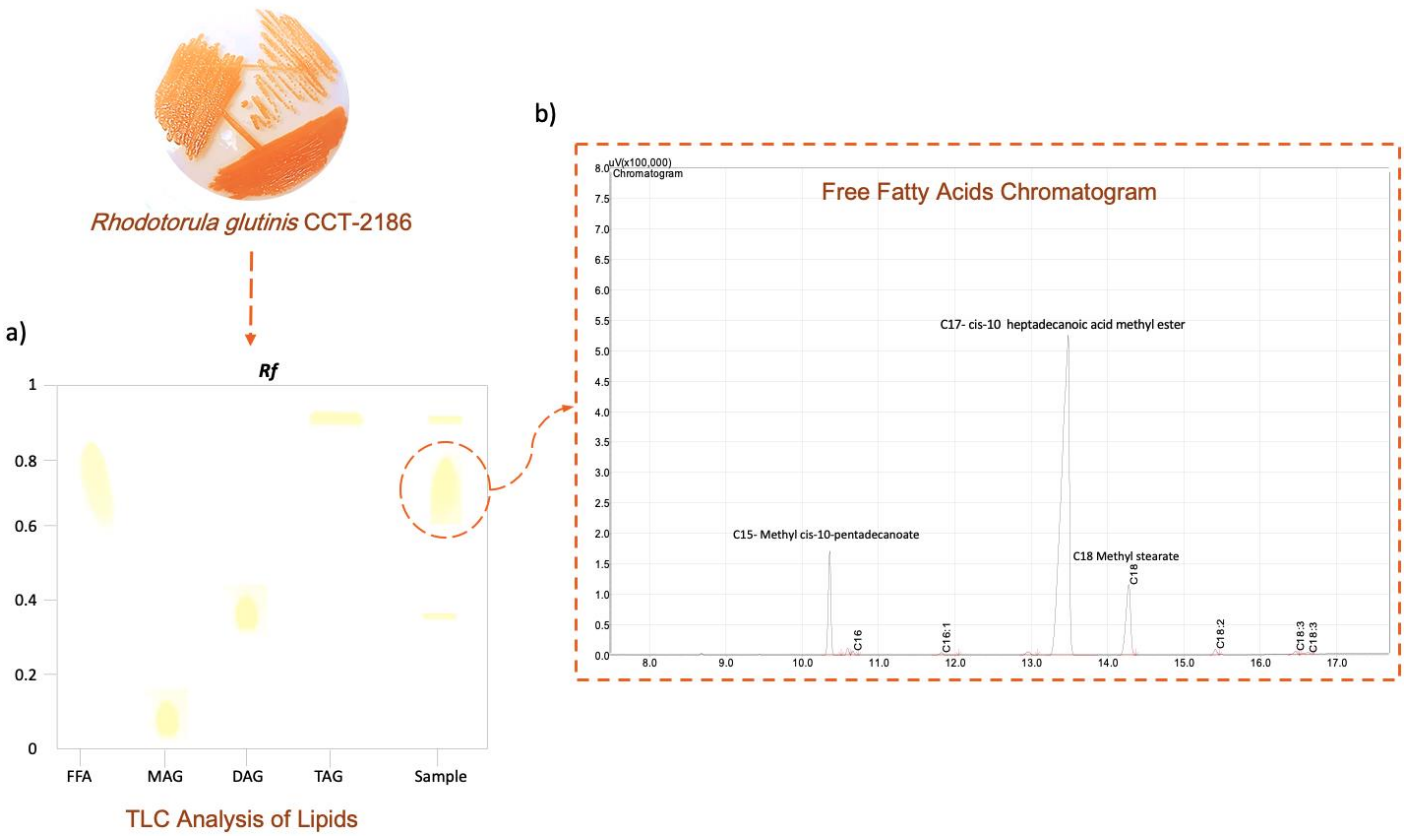

Figure D.4. a) TLC analysis of the lipid produced by *R. glutinis* CCT-2186. Symbols: FFA: free fatty acids (oleic acid), TAG: triglyceride (triolein), DAG: diglyceride (diolein), MAG: monoglyceride (monoolein). **b)** Gas chromatography profiles of the main fatty acid methyl esters (FAMEs) produced by *R. glutinis* CCT-2186.

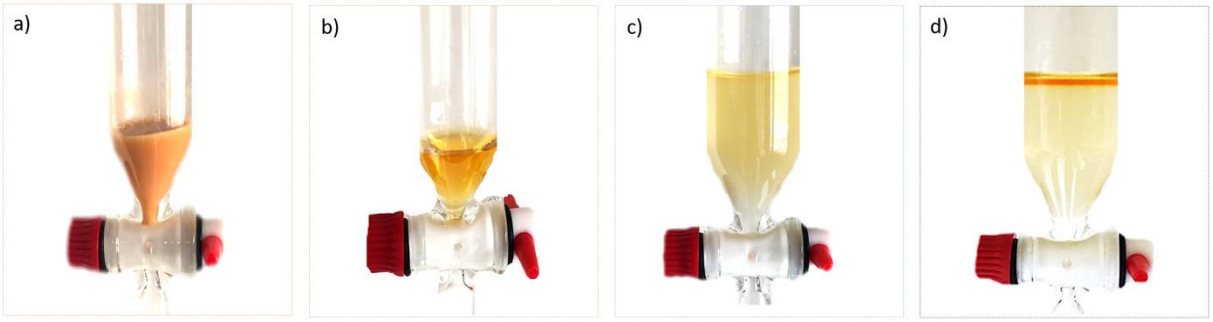

Figure D.5. Carotenoids and lipids polishing at a wet cell concentration of 0.2 g/mL after 1 h stirring (300 rpm) at 65 °C. **a-** *R. glutinis* wet biomass (1 g) in 5 mL of EtOAc/EtOH/H_2O solution (24/55/21% w/w/w). **b-** Initial carotenoids and lipids extracts in 5 mL of EtOAc/EtOH/H_2O solution. **c-** Carotenoids and lipids extracts with an additional of EtOAc (3 mL) and H_2O (10 mL). **d-** Biphasic-solution with a EtOAc-rich phase containing carotenoids (top phase) and an EtOH-aqueous-rich phase containing lipids (bottom phase).

References

Al-Shaal MG, Dzierbinski A, Palkovits R (2014) Solvent-free γ-valerolactone hydrogenation to 2-methyltetrahydrofuran catalysed by Ru/C: a reaction network analysis, Green Chem, 16(3), 1358.

Amenuvor G, Makhubela BCE, Darkwa J (2016), Efficient Solvent-Free Hydrogenation of Levulinic Acid to γ-Valerolactone by Pyrazolylphosphite and Pyrazolylphosphinite Ruthenium (II) Complexes, ACS Sustain Chem Eng, 2016, 4(11), 6010.

Bomgardner MM (2016), Chem. Eng. News, 94, 38–42.

Deshon HD (1979), Carbon tetrachloride, John Wiley & Sons, 5, 693-703.

Duan C, Luo M, Xing X (2011), High-rate conversion of methane to methanol by *Methylosinus trichosporium* OB_3b, BioresourTechnol, 102, 7349–53.

Hu X, Westerhof RJM, Wu I, Dong D, Li CZ (2015), Upgrading biomass-derived furans via acid-catalysis/hydrogenation: the remarkable difference between water and methanol as the solvent, Green Chem, 17(1), 219.

Lee SG, Goo JH, Kim HG, Oh JI, Kim YM, Kim SW (2004), Optimization of methanol biosynthesis from methane using *Methylosinus trichosporium* OB_3b Biotechnol Lett, 26, 947–50.

Lemos D, Dias AC, Gabarrell X and Arroja L (2013) Environmental assessment of an urban water system, J. Clean. Prod, 54, 157-165.

Myhre GD, Shindell D, Bréon FM, Collins W, Fuglestvedt J, Huang J, Koch D, Lamarque JF, Lee D, Mendoza B, Nakajima T, and H. Zhang (2013) Anthropogenic and natural radiative forcing. In Climate Change 2013: The Phys Sc. Basis., 659-740.

Riemenschneider W (2000), Esters, organic, in Ullmann's encyclopedia of industrial chemistry,Wiley-VCH, Weinheim.

Rudolf A, Karhumaa K, Hahn-Hägerdal B (2009), Ethanol Production from Traditional and Emerging Raw Materials, Yeast Biotechnology: Diversity and Applications, Springer, 489-513.

Wu S, Zhou Y, Gerngross D (2019) Chemo-enzymatic cascades to produce cycloalkenes from bio-based resources, Nat Commun, 10, 5060.

Zhang X, Wang T, Ma L, Zhang Q, Huanga X, Yu Y (2020), A review of conversion of lignocellulose biomass to liquid transport fuels by integrated refining strategies, Appl. Energy, 208, 106485.

Zhu S, Zhu Y, Hao S, Zheng H, Moa T, Li Y (2012), One-step hydrogenolysis of glycerol to biopropanols over Pt-$H_4SiW_{12}O_{40}/ZrO_2$ catalysts, Green Chem., 14, 2607–2616.